Targeted and High Relaxivity Contrast Agents

Dimitri Messeri

Department of Chemistry

University of Durham

A thesis submitted for the degree of Doctor of Philosophy

2001

Abstract

The peculiar magnetic properties of Gd(III) ion make it ideal for use as contrast agent (CA) for Magnetic Resonance Imaging (MRI). However, due to its high toxicity, gadolinium ions must be administered in the form of thermodynamically and kinetically stable complexes. The relatively high doses required and the low efficiency of the commercially available CA currently in use, have stimulated the search for new classes of such diagnostic compounds. In the first part of this work a new stable, high *relaxivity*, di-aqua gadolinium complex has been synthesized and its properties studied in detail. The presence of two water molecules in the coordination sphere of the complex increases its efficiency as a contrast agent. So far the failure to develop practicable di-hydrated systems has arisen mainly from the insufficient kinetic and thermodynamic stability associated with such complexes. In addition, each of the di-aqua complexes published in the literature have exhibited a high affinity towards the binding, either of endogenous anions (*e.g.* phosphate or carbonate) or of proteins, such as Human Serum Albumin (HSA). This binding contributes strongly to the decrease of the relaxivity of the complexes. In contrast, the anionic di-aqua complex herein described should be suitable as the basis of an MRI agent, because it possesses sufficient stability, with respect to acid or cation mediated dissociation pathways, has a fast rate of water exchange (30ns at 298K), a high relaxivity (12.3 $mM^{-1}s^{-1}$ at 20 MHz and 298K) and minimizes competing anion/protein binding. In the second part of this work new targeted contrast agents have been prepared and studied. In order to target specifically cancerous tissues, gadolinium chelates have been coupled to *folic acid,* which is overexpressed in certain types of cancerous cells. A tetra α-substituted DOTA derivative complex, has been chosen which for its optimal intrinsic relaxometric properties (*i.e.* faster water exchange, enhanced relaxivity). The affinity of its folate derivative for folate binding protein (FBP) has been investigated and compared to that of a non-specific protein (*i.e* HSA). The 83% enhancement in relaxivity in the presence of FBP clearly demonstrated that this receptor protein FBP is capable of recognizing this complex selectively.

Declaration

The work described herein was carried out in the Department of Chemistry, University of Durham and in the Dipartimento di Chimica Inorganica, Universita' degli Studi di Torino, between October 1998 and September 2001. All the work is my own unless otherwise stated and no part of it has been submitted for a degree at this or any other University.

Statement of Copyright

Acknowledgments

I would like to acknowledge the following people:

My supervisor Prof. David Parker, for all his support, help and enthusiasm in making this project.

All the people who have been working with me in the Wolfson Laboratory (CG27) in Durham. In particular Mark Lowe, for his advises and helps for the relaxivity measurements and for synthesizing some of the compounds I used and James Bruce for the luminescence studies. Thanks to Mark, Stefany, Gabriella, Suzy, Ofer, Linda, Rachel, Kanthy, Aileen, Simon and all the other I have missed for the nice time spent together.

Prof. Silvio Aime, Dr. Mauro Botta, Eliana Gianolio and all the people in the group in Turin for helping me during my short but intense visit.

Dr. Marc Port at Guerbet s.a. Paris, for the contribution of sample and financial founds.

COST D-18 for financing my visit in Turin.

Dr. Alan Kenwright, Ian McKeag and Julia Say for their help in setting up and running NMR experiments.

Finally I would like to express a special thank to Cinzia, whitout who I would have never achieved all of this.

Table of contents

Chapter One:

Introduction

1.1. Introduction

In the last decade there has been a great development of nuclear magnetic resonance imaging techniques for the diagnosis of diseases.[1-4] This has prompted the need for a new class of pharmaceuticals. Principally these drugs are administered to a patient in order to enhance the image contrast between normal and diseased tissue and to indicate the status of organ function or blood flow. Since the image intensity in these techniques depends on nuclear relaxation times, complexes of paramagnetic transition and lanthanide ions, which are able to decrease the relaxation times of nearby nuclei via dipolar interactions, have received the most attention as *contrast agents* (CA).[5, 6]

As a consequence of its own unique magnetic properties, the Gd^{3+} ion has become the most important paramagnetic ion used in nuclear magnetic resonance techniques, and since the approval of $[Gd(DTPA)H_2O]^{2-}$ (Magnevist) in 1988, it can be estimated that over 30 metric tons of gadolinium have been administered to millions of patients worldwide.[6] However, gadolinium complexes are not the only contrast agents nowadays used in clinical practice; for example another important class is represented by polysaccharide coated iron oxide particles.[5, 7]

1.2. Magnetic Resonance Imaging (MRI)

Magnetic resonance imaging is a powerful technique that is used to obtain images of body tissues and organs.[2-4, 8, 9] It is based on the detection of the NMR signals of water protons. Since the body is composed principally of water (more then 60 %), its protons are the most abundant and readily detected in vivo. Different kinds of tissues contain different amount of water, as showed in *Table 1.1*.

Tissue	*Water Content*	*Tissue*	*Water Content*
Brain	*71-84%*	*Kidney*	*81%*
Muscle	*79%*	*Teeth*	*10%*
Liver	*71%*	*Femur*	*12%*

***Table 1.1** – Water content of some tissue types.*[10]

Spatial information is obtained by imposing a linear gradient magnetic field across the sample. It is known that the *precessional Larmor frequency* of nuclei (ω_0) is field dependent according to the equation (1.1):

$$\omega_0 = \gamma B_0 \qquad (1.1)$$

where γ is the gyromagnetic ratio and B_0 the magnetic field. So if a gradient magnetic field is applied, protons in different spatial positions will resonate at different frequencies. Consequentially the resulting *free induction decay* (FID) will contain spatially encoded information. This "encoded" signal is Fourier transformed to give a one-dimensional projection of signal amplitude along a particular line through the subject. Images can be reconstructed repeating the scan. After each scan, the field gradient is rotated in the plane of interest, and a collection of one-dimensional images is obtained. Using adapted algorithms it is possible to reconstruct two-dimensional images. The equipment used in MRI is very similar to that used in the common NMR experiments. However since a gradient field has to be applied, an additional set of gradient coils is needed. In addition because of larger size sample, larger magnets are required.

The measured signal intensity depends on many factors, in particular on the values of the water relaxation times T_1 (the longitudinal or spin-lattice relaxation time) and T_2 (the transverse or spin-spin relaxation time), and on the nature of the pulse sequence used. For the most common spin-echo pulse sequences, the signal intensity (S.I.) is given by equation (1.2):[11]

$$S.I. = [H_2O]H_v(\exp(-\frac{T_E}{T_2})[1-\exp(\frac{T_R}{T_1})]) \qquad (1.2)$$

where $[H_2O]$ is the concentration of water protons in the volume element, H_v is a motion factor of the water proton, T_1 and T_2 are the longitudinal and transverse relaxation time respectively, T_E is the echo delay time and T_R is the pulse repetition rate. It is easy to see that reduction in the relaxation times gives opposite effects; a decrease in T_1 increases signal intensity, while a decrease in T_2 decreases it. Adjusting the T_E and T_R values with adapted pulse sequences, it is possible to weight the two effects (T_1 and T_2 weighted scan) appropriately.

Improvements in signal intensity can be achieved using paramagnetic compounds. The presence of one or more unpaired electrons in paramagnetic centres causes a strong decrease in both the water proton relaxation times T_1 and T_2. Otherwise the T_2 values of water in tissues are very short and they are not decreased appreciably by paramagnetic compounds at the concentration usually administred to the patients (ca. 0.1 mmol kg^{-1}). So the paramagnetic centre causes a perceptible decrease in T_1 only, and not in T_2, and this results in an enhancement of the signal intensity.[5, 6]

The value of relaxation times of water depends on its chemical and physical environment, so it is possible to discriminate between different tissue types. [5, 6] Moreover, cancerous tissue has shown to possess different values of T_1 compared to healthy tissue (as indicated in *Table 1.2)*, and this opens up the possibility for tumour diagnosis results.[12]

Tissue	*T_1 Cancerous (s)*	*T_1 Normal (s)*
Skin	*1.047*	*0.616*
Bone	*1.027*	*0.554*
Muscle	*1.413*	*1.023*
Breast	*1.080*	*0.367*
Liver	*0.832*	*0.570*

***Table 1.2** – Values of T_1 for water in a variety of tissues.*[12]

1.3. Relaxivity of metal complexes

The presence of a paramagnetic centre induces a decrease in the longitudinal and transverse relaxation times T_1 and T_2. Rather than referring to these parameters, it is common to refer to their inverse, $1/T_1$ (R_1) and $1/T_2$ (R_2), which represent respectively the longitudinal and the transverse relaxation rates of the solvent nuclei.

The diamagnetic and paramagnetic contributions to the relaxation rates are additive, and the observed solvent relaxation rate $R_{i\ obs}$, in the presence of a paramagnetic centre, is given by equation (1.3):[6]

$$R_{i\,obs} = (R_i)_d + (R_i)_p \quad i = 1,2 \qquad (1.3)$$

where $(R_i)_d$ is the diamagnetic solvent relaxation rates and $(R_i)_p$ is the additional paramagnetic contribution. In the absence of solute-solute interactions, a linear dependence between the solvent relaxation rates and the concentration of the paramagnetic centre is observed. So equation (1.3) can be written as:

$$(R_i)_{obs} = (R_i)_d + r_i[M] \qquad (1.4)$$

where r_i is the *relaxivity* measured in units of $M^{-1}s^{-1}$, or more commonly in $mM^{-1}s^{-1}$.

The relaxivity represents the enhancement of the water proton relaxation rate per unit concentration of contrast agent.[13] It indicates the ability of the paramagnetic complex to shorten the water relaxation rate. The presence of the paramagnetic centre causes a large fluctuating local magnetic field. The solvent nuclei around the paramagnetic metal, feeling this additional field, will relax more quickly. The local magnetic field falls off rapidly with the distance from the paramagnetic centre. So the relaxation mechanism will depend on how close the solvent nuclei are to the metal. Three classes of water molecules can be distinguished (*Figure 1.1*).

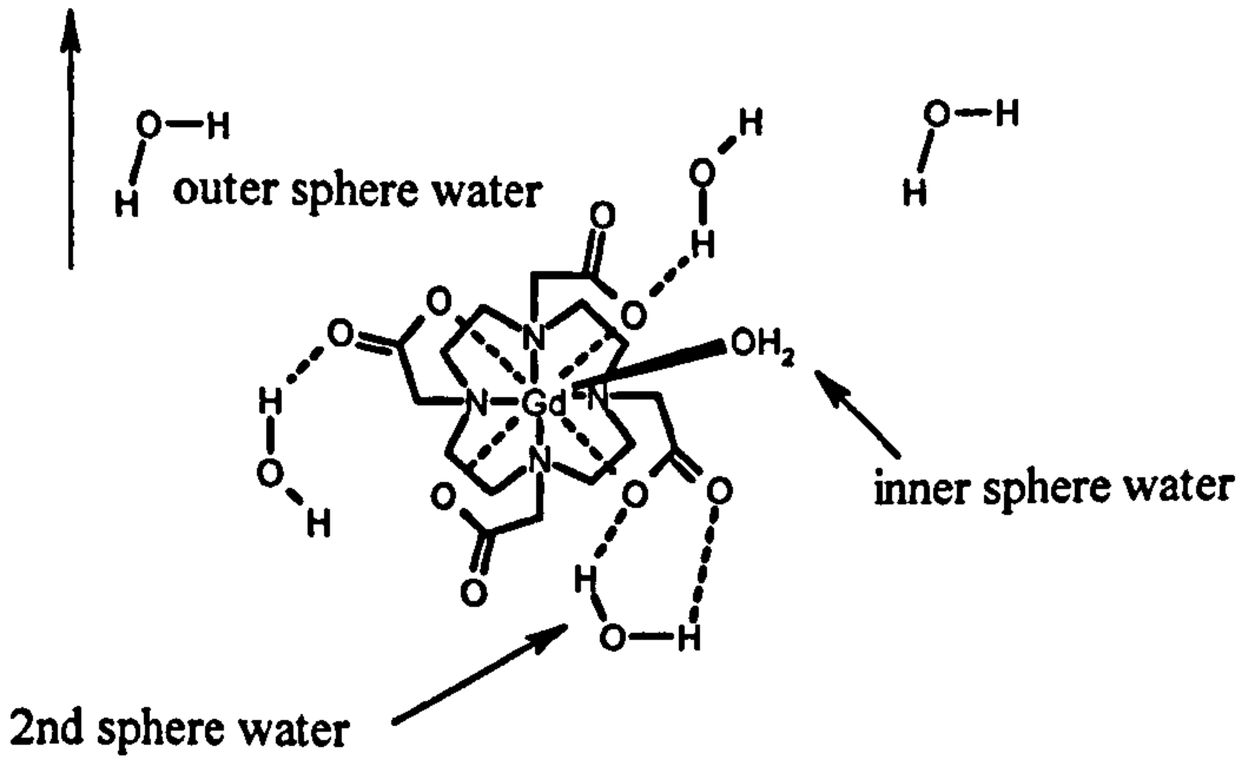

***Figure 1.1** – Three classes of solvent molecules.*

The first class is represented by water molecules bounded directly to the metal ion, in the primary cordination sphere. The solvent relaxation mechanism involving these molecules is called "*inner sphere relaxation*".

Water molecules in the second coordination sphere, which are bound via hydrogen bonding are considered as another class. The contribution from these molecules is difficult to treat separately, and usually it is not distinguished from water molecules, which closely diffuse outside the second sphere. The solvent relaxation

mechanism involving these two kinds of solvent molecules is generalised in the term of *"outer sphere relaxation"*.

Thus, the paramagnetic relaxation rate $(R_i)_p$ can be split into two contributions, one due to the water molecules in the inner sphere and the other due to unbound water molecules (equation 1.5):

$$(R_i)_p = (R_i)_{os} + (R_i)_{is} \qquad (1.5)$$

where i =1,2, and *os* and *is*, indicate outer sphere an inner sphere.

1.3.1. Inner sphere relaxation

Paramagnetic complexes with one or more directly bonded water molecules ($q \geq 1$) show higher relaxivity values than those completely saturated by the ligand (q=0).[6] Since the protons of coordinated water molecules are very close to the metal ion, they will relax very quickly. Moreover, due to the rapid exchange with the surrounding water molecules, a degree of relaxation will be "transferred" to bulk molecules, resulting in a highly efficient relaxation pathway. The contribution given by this mechanism to the longitudinal and transverse relaxation rates, is expressed by equations (1.6), (1.7) and (1.8):[14-16]

$$\frac{1}{T_1^{IS}} = \frac{[C]}{55.6} \frac{q}{T_{1M} + \tau_M} \qquad (1.6)$$

$$\frac{1}{T_2^{IS}} = \frac{q[C]}{55.6} \left[\frac{\tau_M^{-1} T_{2M}^{-1} \left(\tau_M^{-1} + T_{2M}^{-1}\right) + \Delta\omega_M^2}{\left(\tau_M^{-1} + T_{2M}^{-1}\right)^2 + \Delta\omega_M^2} \right] \qquad (1.7)$$

$$\Delta\omega_{obs}^{IS} = \frac{q[C]}{55.6} \left[\frac{\Delta\omega_M}{\tau_M^2 \left(T_{2M}^{-1} + \tau_M^{-1}\right) + \Delta\omega_M^2} \right] \qquad (1.8)$$

where IS stands for inner sphere, [C] is the concentration of the paramagnetic agent, q is the number of bound water nuclei per metal ion (*i.e.* the hydration number), τ_M is the residence lifetime of the bound solvent molecule, *M* refers to the solvent molecule in the

inner sphere, and $\Delta\omega$ is the chemical shift difference between the paramagnetic complex and a similar diamagnetic complex taken as reference.

The values of T_{iM} (*i=1,2*) can be calculated by the *Solomon-Bloembergen-Morgan* equations (1.9-1.15).[15-18]

$$\frac{1}{T_{iM}} = \frac{1}{T_i^{DD}} + \frac{1}{T_i^{SC}} \qquad i = 1,2 \tag{1.9}$$

$$\frac{1}{T_1^{DD}} = \frac{2}{5}\frac{\gamma_I^2 g^2 \mu_B^2 S(S+1)}{r^6}\left[\frac{3\tau_{c1}}{(1+\omega_I^2\tau_{c1}^2)} + \frac{7\tau_{c2}}{(1+\omega_S^2\tau_{c2}^2)}\right] \tag{1.10}$$

$$\frac{1}{T_1^{SC}} = \frac{2}{3}\frac{S(S+1)}{}(\frac{A}{\hbar})^2\left[\frac{\tau_{e2}}{(1+\omega_S^2\tau_{e2}^2)}\right] \tag{1.11}$$

$$\frac{1}{T_2^{DD}} = \frac{1}{15}\frac{\gamma_I^2 g^2 \mu_B^2 S(S+1)}{r^6}\left[\frac{3\tau_{c1}}{(1+\omega_I^2\tau_{c1}^2)} + \frac{13\tau_{c2}}{(1+\omega_S^2\tau_{c2}^2)} + 4\tau_{c1}\right] \tag{1.12}$$

$$\frac{1}{T_2^{SC}} = \frac{1}{3}S(S+1)(\frac{A}{\hbar})^2\left[\frac{\tau_{e2}}{(1+\omega_S^2\tau_{e2}^2)} + \tau_{e1}\right] \tag{1.13}$$

$$\frac{1}{\tau_{ci}} = \frac{1}{T_{ie}} + \frac{1}{\tau_M} + \frac{1}{\tau_R} \tag{1.14}$$

$$\frac{1}{\tau_{ei}} = \frac{1}{T_{ie}} + \frac{1}{\tau_M} \tag{1.15}$$

DD and SC refer to the two relaxation mechanisms operative for protons, *Dipole-Dipole* and *Scalar* or *Contact*. γ_I is the nuclear magnetogyric ratio, g is the electronic factor, μ_B is the Bohr magneton, *r* is the proton metal ion distance, ω_S and ω_I are the electron and nuclear Larmor procession frequencies, respectively, and A/h is the electron-nuclear hyperfine coupling constant. Both dipolar and scalar relaxation mechanisms are modulated by the correlation times τ_{ci} and τ_{ei} described by the equations (1.14) and (1.15). T_{1e} and T_{2e} (sometime refers as τ_{s1} and τ_{s2}) are respectively the longitudinal and the transverse electron spin relaxation times and τ_R is the rotational correlation time.

Equations (1.9-1.15) are field dependent, the electron Larmor frequency being related to the magnetic field through the gyromagnetic factor (equation 1.1). Also electronic spin relaxation rates are field dependent, due to a transient zero field splitting (ZFS) (equation 1.16):[6]

$$\frac{1}{T_{1e}} = B\left[\frac{1}{1+\omega_s^2\tau_v^2} + \frac{4}{1+4\omega_s^2\tau_v^2}\right] \qquad (1.16)$$

where B is a constant related to the magnitude of the transient ZFS and τ_v is the correlation time for the modulation of this ZFS.

The *inner sphere relaxivity* $1/T_1^{IS}$ depends on (equations 1.9-1.15) τ_m, τ_R, q, r, T_{1e} and T_{2e}. The influences of these variables on the relaxivity values can be investigated by measuring R_1 at different magnetic fields. The plot of the relaxivty versus the magnetic field results in a Nuclear Magnetic Relaxation Dispersion (NMRD) profile. The magnetic field is varied over a range corresponding to proton Larmor frequencies of 0.01 – 50 MHz. This can be achieved by using a field cycling spectrometer such as the one developed by Koenig and Brown.[19] In *Figure 1.2* the NMRD profiles of $[Gd(DTPA)]^{2-}$ (Magnevist) and $[Gd(DOTA)]^-$ (Dotarem) are shown.[5] These complexes have similar molecular weight and both have one water molecule coordinated (q=1).

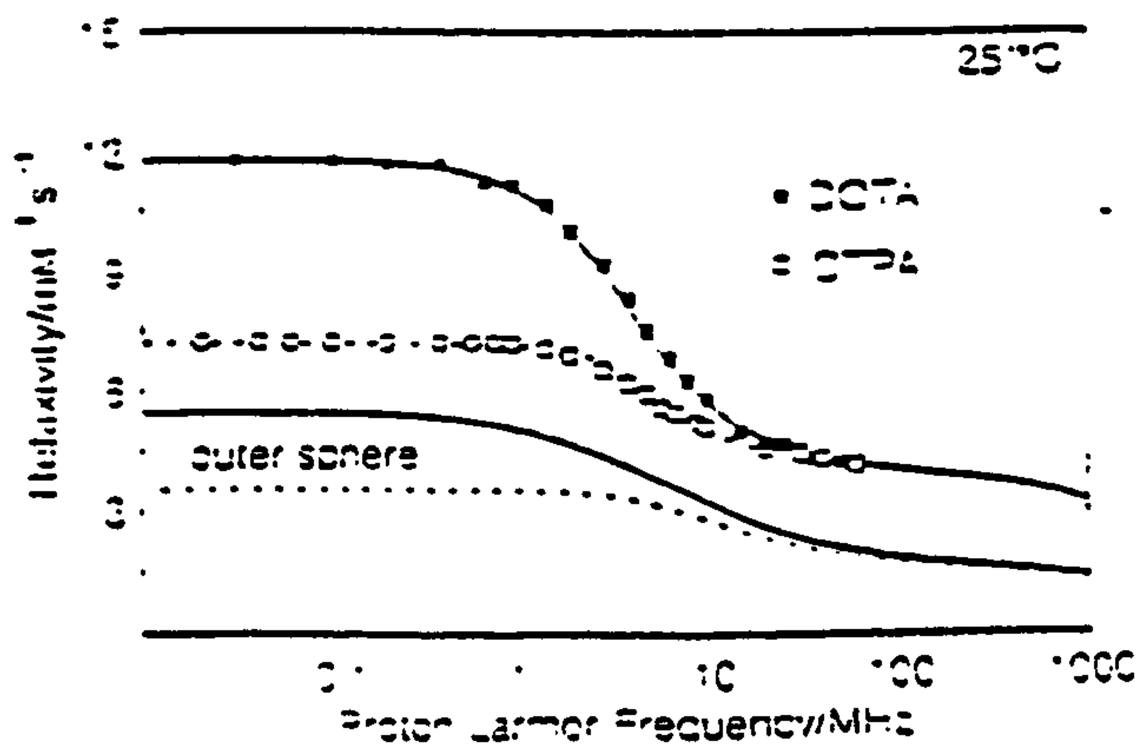

***Figure 1.2** – NMRD profile of $[Gd(DTPA)]^{2-}$ and $[Gd(DOTA)]^-$ at 298K.*

The profiles exhibit two different regions. In the first one (high field region) the two complexes show evidence of similar relaxivities. In the low field region a big difference is observed. At high field the effective correlation time τ_C is determined

mainly by τ_R, whilst at low field it is controlled principally by τ_S. Since τ_R depends mainly on the molecular dimensions of the complex, the similar high field behaviour may be rationalised. Furthermore, the differences in the τ_S values for the two complexes (τ_S=700 ps for $[Gd(DOTA)]^-$ and τ_S=80 ps for $[Gd(DTPA)]^{2-}$) explain the low field behaviour.

1.3.2. Outer Sphere relaxation

The outer sphere contribution to the overall relaxivity of a paramagnetic complex is difficult to quantify. Comparison of several $q = 0$ complexes, reveals that longer values of the longitudinal electronic relaxation times (T_{1e}) result in enhanced relaxivity.[5] The outer sphere relaxation arises from the translational diffusion of water molecules near the gadolinium complex. Water molecules and the complex are often treated as hard spheres and the relaxation rate is expressed by the equation (1.17):[20]

$$\left(\frac{1}{T_1}\right)_{os} = \left(\frac{32\pi}{405}\right)\gamma_I^2 g^2 \mu_B^2 S(S+1)\left(\frac{N_A}{1000}\right)\left(\frac{C}{dD}\right) f(T_{1e}, \tau_D, \omega_I, \omega_S) \quad (1.17)$$

where C is the concentration of the paramagnetic compound, N_A is the Avogadro's number, d is the distance of closest approach of the solvent molecule to the metal complex, and τ_D is the relative translational diffusion correlation time (equation 1.18):

$$\tau_D = \frac{d^2}{3(D_I + D_S)} \quad (1.18)$$

D_I and D_S indicate the diffusion coefficients of the water and the metal complex respectively. They can be estimated, assuming a motion of rigid spheres of ratio a in a medium of viscosity η according to equation 1.19.

$$D = \frac{kT}{6\pi a \eta} \quad (1.19)$$

1.4. Gadolinium (III) complexes as contrast agents for MRI

In order to enhance the MRI signal intensity, it has become routine practice to administer paramagnetic complexes to the patient, at a dose of about 0.1 mmol kg^{-1}.

The first paramagnetic agent was ferric chloride,[21] orally administrated in order to enhance the images of the gastrointestinal tract. Other compounds were later investigated, mostly based on iron (III),[22] manganese (II)[23] and particularly gadolinium (III).[24, 25] However, the first diagnostic imaging agent adopted in the medical protocol was $[GdDTPA(H_2O)]^{2-}$ (Magnevist) in 1988. Injected intravenously, it was used to enhance the images of the lesions caused by cerebral tumours.[26]

At the outset of this work, four extra cellular contrast agents currently in clinical use are the gadopentate dimetglumine injection (Magnevist, $[GdDTPA]^{2-}$) by Schering, godoterate meglumine injection (Dotarem, $[GdDOTA]^{-}$) by Guerbet, gadoteridol injection (ProHance, [GdHPDO3A]) by Squibb diagnostic Bracco, and gadodiamide injection (Omniscan, [GdDTPABMA] by Nycomed-Amersham (*Figure 1.3*).[27]

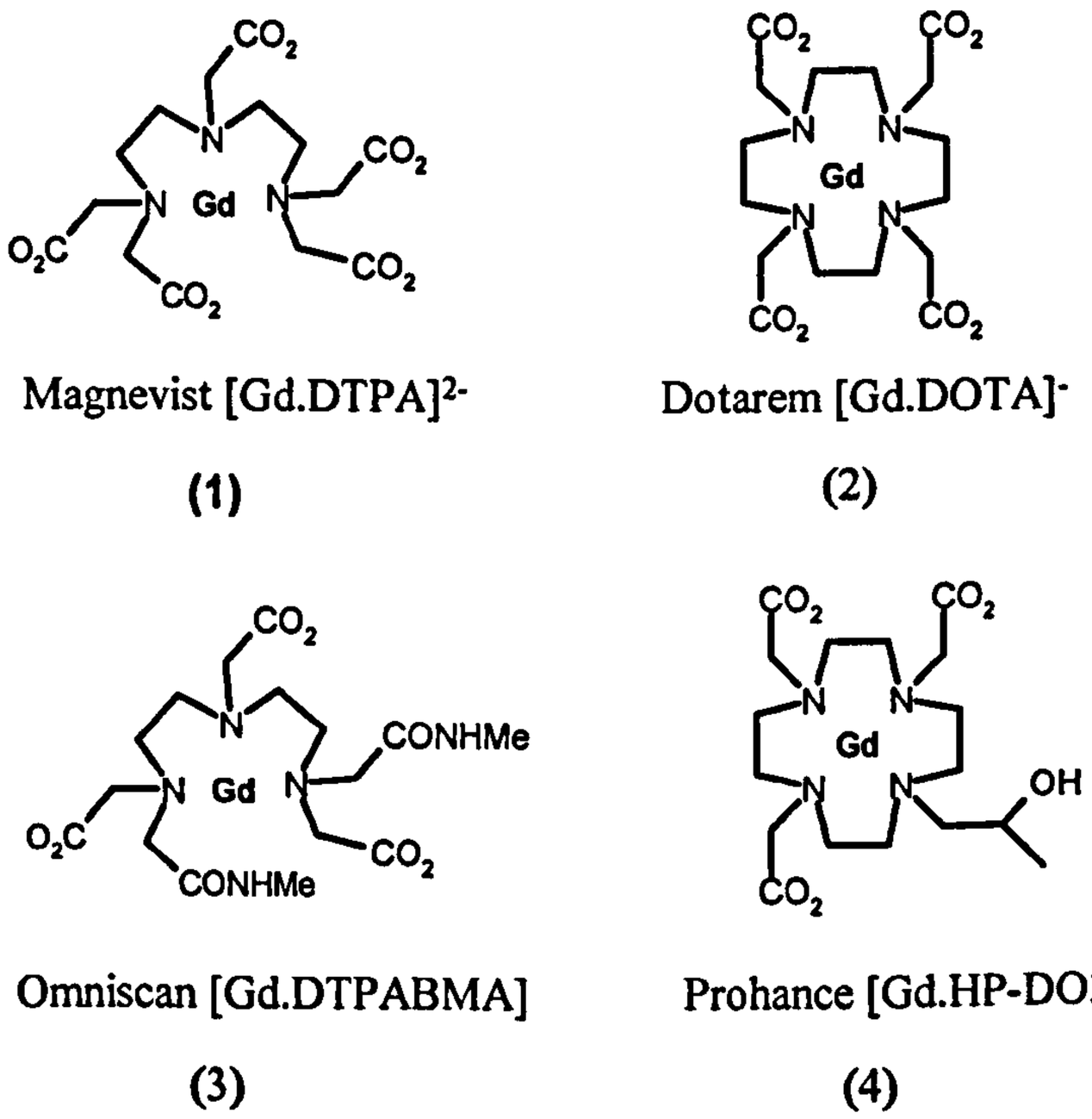

***Figure 1.3** – MRI contrast agents in clinical use.*

Gadolinium (III) ion has an electronic configuration with seven unpaired electrons, it has the highest spin quantum number (S=7/2) of any stable element in the periodic table. Unfortunately, it is a highly toxic aqua ion. Free gadolinium is known to

bind to serum proteins, eventually much of the released metal comes to reside in the bone, where it becomes tightly and irreversibly associated.[6] So, this paramagnetic ion must be administered in the form of a thermodynamically and kinetically stable complex, to reduce the possible release of the free ion in the body. Due to its large size, the Gd^{3+} ion, like all other lanthanides, tends to form complexes with high co-ordination number in aqueous media. Currently, all gadolinium (III) contrast agents used in MRI, are nine co-ordinate. A ligand occupies eight binding sites at the metal centres, whereas the ninth co-ordination site is occupied by a water molecule. The complexes can adopt two possible geometries, tricapped trigonal prism (TPP) or capped square antiprism (CSAP). However, the two geometries are closely related and sometimes a particular structure is well described by both.

Since Gd^{3+} is a hard metal ion, it prefers to coordinate hard σ-donors like nitrogen or oxygen, thus ligands with carboxylic or amine groups are indeed very common. Data accumulated over the past ten years indicate that all the chelates used in the commercially available products are remarkably stable with respect to dissociation in vivo,[6] assuring the first requirement for a contrast agent: its safety (*Table 1.3)*.

Ligand	*Log K_{GdL}*	*k_{obs} ($10^3 s^{-1}$)*
EDTA	*17.7*	*140000*
DTPA	*22.2*	*1.2*
DOTA	*25.3*	*0.021*
HPDO3A	*23.8*	*0.064*
DTPA-BMA	*16.85*	*>20*

***Table 1.3** – Stability constants and acid catalized dissociation constants at 25 ^0C.[6]*

Another important requirement of MRI contrast agents is represented by high water solubility. Since the amount of metal chelate required for a sufficient increment in image contrast is relatively high (0.1-0.3 mmol/kg total body weight), the concentration of the injected solution must be also high (typically 0.5 M).[6, 28] Thus, the metal chelates used as contrast agents must very soluble in water. For this reasons ligands that form non-ionic complexes with Gd^{3+} have been provided with hydrophilic groups as side chains or functional groups (*e.g.* alcoholic group in HP-DO3A).

The high concentration required also means high osmolality of the solutions injected, which may result in severe shocks in the patients.[6, 28] As is clear from the data given *Table 1.4*, the osmolality is particularly high for ionic metal chelates and thus neutral complexes may be preferred.

Ligand	*Osmol (kg^{-1})*
DTPA	*1.96*
DOTA	*1.35*
HPDO3A	*0.63*
DTPA-BMA	*0.65*
Blood plasma	*0.30*

***Table 1.4** – Osmolality measured in 0.5 M GdL solutions at 37 ^{0}C.* [6, 28]

1.5 How to improve the efficiency of MRI contrast agents

The first generation of gadolinium (III) MRI contrast agents is represented by low molecular weight chelates (*Figure 1.3*). Their low efficiency and the high dose required have prompted the need for new classes of these compounds. The development of improved contrast agents offers several advantages. Firstly the amount of contrast agent injected to the patients may be significantly reduced. As a consequence the pain deriving from osmotic shocks upon injection may be reduced. In addition the use of more efficient contrast agents would short the acquisition time required to record an image, with obvious economical and timesaving advantages.

Inspection of the equations (1-6)-(1-15), shows that in addition to the concentration of contrast agent, the number of bound water molecules (q) and a series of correlation times (τ_R, τ_M and τ_S) determine the inner sphere relaxivity of a paramagnetic complex. The challenge is to design new ligands capable of optimising these parameters and thus improving the relaxivity of the complexes. In particular the two variables, which can have an effect upon relaxivity and can be "adjusted" by the chemist are represented by the hydration number, q, and by the rotational correlation time, τ_R.

1.5.1 Polyhydrated contrast agents

A way to improve the relaxivity of low molecular weight contrast agents is to increase the hydration number q, as is clear from the equation (1.6). However, an increment in the number of water molecules bounded to the metal center has so far always been accompanied by a reduction in the thermodynamic stability, as well as in the kinetic inertness. Moreover, the possible formation of ternary adducts with endogenous anions, such as phosphate or carbonate, which can "replace" the inner sphere molecules and thus reduce the relaxivity, must be taken into account. In recent years many papers have been published on di- or tri-hydrated chelates, this aspect will be described in more detail in Chapter Two.

1.5.2. Macromolecular conjugates

Another way to improve the relaxivity of a gadolinium chelate can be achieved by "operating" on the rotational correlation time τ_R. For spherical rigid molecules it can be estimated using equation (1.20):[6]

$$\tau_R = \frac{4\pi a^3 \eta}{3kT} \qquad (1.20)$$

where a is the ratio of the sphere and η is the viscosity.

In theory τ_R can be increased in two ways, either by increasing the size of the complex, or by increasing the viscosity of the medium. However, the viscosity of extracellular fluid (the medium) cannot be changed, so the only practicable way consists in changing the size of the contrast agent. The most common approaches used to prepare macromolecular gadolinium contrast agents involve conjugation of functionalized chelates to polymers, dendrimers or biological molecules. Conjugation methods for linking chelates to macromolecules are well established in the literature.[29] Usually they involve functionalization of primary amines using acylation, alkylation, urea or thiourea formation and reductive amination. The majority of papers published using commercially available reagents, such as DTPA. Reaction of these reagents with a reactive primary amine on the macromolecule generates an amide bond using one of the DTPA carboxylates.

Polylysines (commercially available in a variety of molecular weight ranges) have been derivatized with gadolinium chelates.[6] The reactive ε-amino groups of the lysine backbone have been modified with acyclic and macrocyclic polyaminocarboxylate derivatives, such as the anhydride or the C-linked isothiocyanate (*Figure 1.4*) Conjugates containing up to seventy gadolinium chelates have been reported. The relaxivities of these compounds range from 15 to 20 $mM^{-1}s^{-1}$ at 20 MHz. These not particularly high values are a consequence of the flexible nature of the linear polymeric backbone, so that the motion of the paramagnetic ion is not efficiently coupled to that of the whole macromolecule.

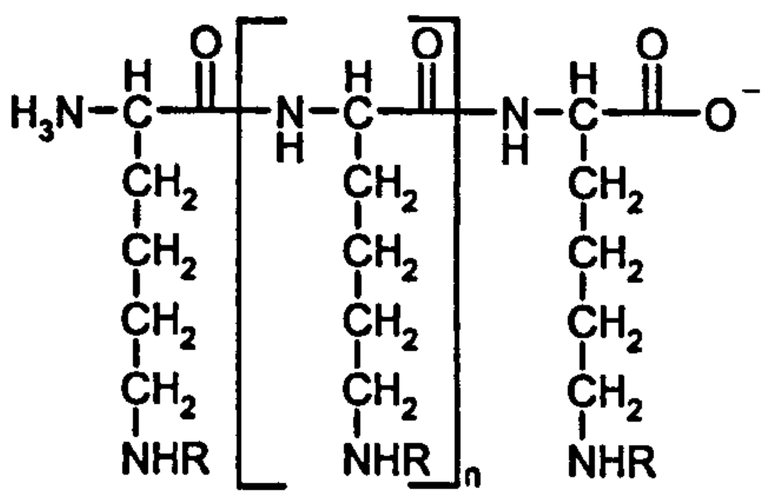

R:

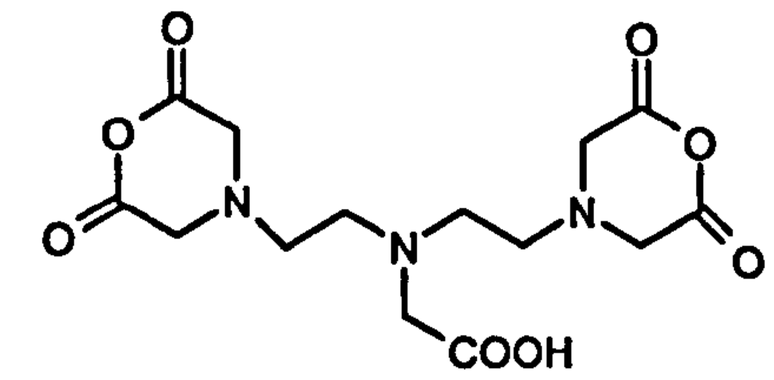

DTPA bisanhydride

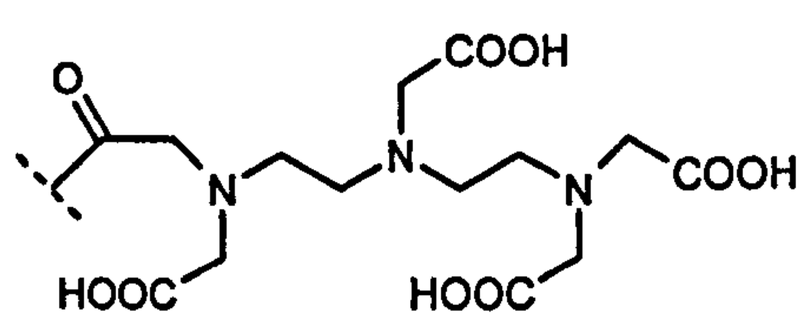

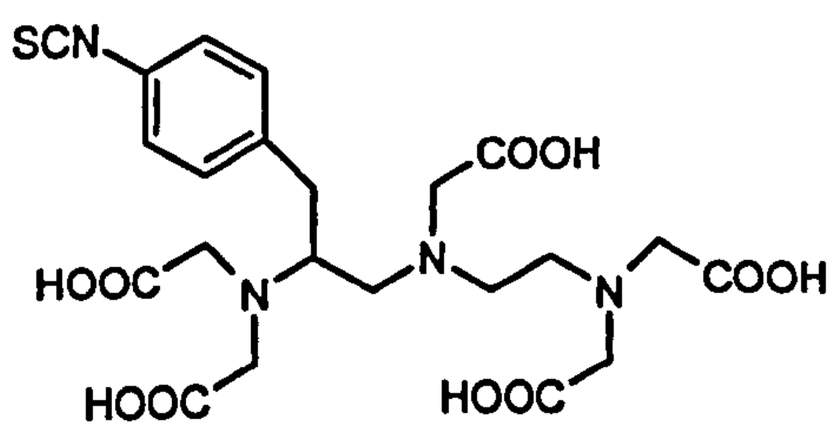

C-alkylated-p-isothiocyanate derivative

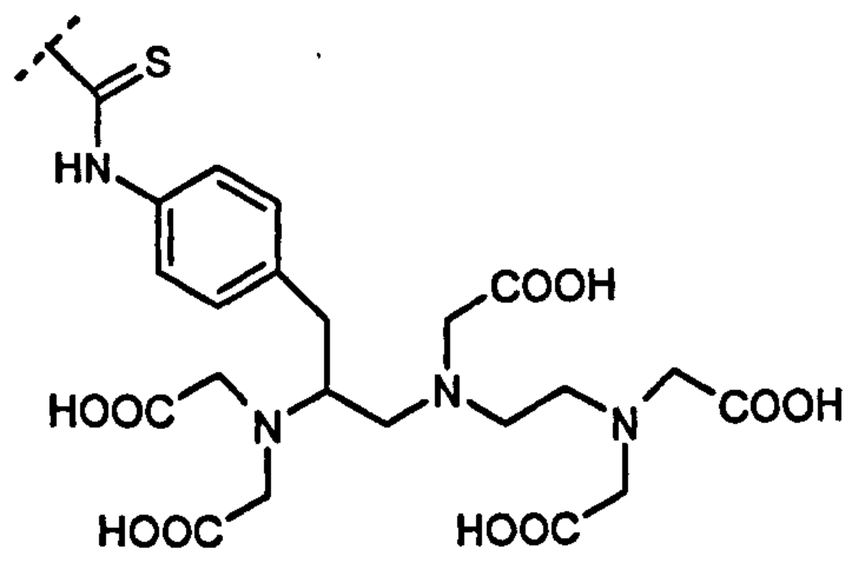

***Figure 1.4.** – Chemical structure of polylysine and representative chelate conjugates*

Dendrimers conjugates have been widely explored as potential new class of macromolecular MRI agents.[6] The potential advantage of such compounds is due to the fact that dendrimers, such as Starburst polyamidoamine (PAMAM), have uniform surface chemistry and minimal molecular weight distribution and shape variation. In

contrast to linear polymers, dendrimers have a relatively rigid structure and the overall tumbling of the molecule should contribute more efficiently to the rotational correlation time. However, the values found fall short of those expected, again as a result of poor motional coupling.

Gadolinium chelates have been coupled to natural polymers as well, such as proteins, polysaccharides and nucleic acids. For example, GdDTPA derivatives of human or bovine serum albumin (HSA or BSA) have been studied as blood pool agents in MR angiography, to image the blood flow in vessels, because of the high intravascular retention of these macromolecules.[6, 28]

1.5.3. Targeted contrast agents

The *extracellular* contrast agents, currently in clinical use, are non-specific in their biodistribution. The action of these agents derives from their diffusion throughout the extracellular fluid. The aim of the new generation of CA is strongly oriented to develop agents with high tissue and/or organ specificity. The idea is to develop CA able to detect malignant lesions and differentiate them from non-malignant ones. Conceptually, antibodies or other tissue specific molecules may be combined with gadolinium chelates to provide disease-specific MRI agents. Schematically they should be formed by three components, a Gd^{3+} complex, a spacer and a tissue-specific molecule or an antibody fragment (*Figure 1.5*).

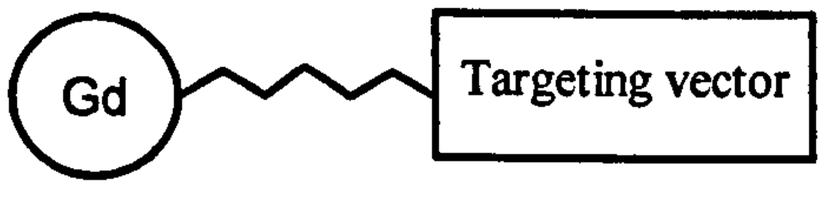

***Figure 1.5** – Schematic representation of a targeted contrast agent.*

Curtet and co-workers[30] have described the conjugation of polylysine-gadolinium chelates to anticarcinoembryonic antigen (CEA) monoclonal antibodies. *In vivo* studies conducted in nude mice grafted with human colorectal carcinoma LS 174T, showed that twenty-four hours after the injection (0.001 mmol/kg of gadolinium labelled immunoconjugate) the tumor uptake was 10-15% and the corresponding r_1 increase of 15-20% was observed.

Wu and co-workers[31] have reported the preparation of metal chelate-dendrimer-antibody constructs for use in imaging and radioimmunotherapy. Generation 2

polyamidoamine (PAMAM) dendrimers were modified by reaction with bifunctional DTPA or DOTA chelates followed by conjugation to monoclonal antibodies. While this work was primarily directed toward radioimmunotherapy, the approach was noted to be useful for gadolinium as well.

Wiener and co-workers[32] described the preparation of folate-conjugated MRI imaging agents using a dendrimer conjugation approach. They attached folic acid to a generation four ammonia core dendrimer, which was then reacted with an isothiocyanate DTPA derivative, to form the polymeric chelate *f-PAMAM-TU-DTPA*. It is accumulated in cells in a specific manner and it gave rise to an enhancement of the longitudinal relaxation rate of about 109%.

Among the possible choices in the *targeting vectors,* the vitamin folic acid has attracted considerable attention in the last years. This is because many human cancerous tissues (including breast, cervical, ovarian, colorectal, renal and nasopharyngeal) express higher concentrations of the protein receptor which binds folic acid,[33-35] compared to the healthy tissues. So folate-conjugated MRI agents represent a promising new approach to tumor targeting.

1.6. The vitamin folic acid

Folic acid (derived from the Latin *folium*-leaf) occurs in green leaves of many kinds, including grass. Mushrooms and yeast are other good sources, as well as a number of animal tissues such as liver and kidney. It was isolated for the first time from liver in 1943,[36] but its structure was completely elucidated only in 1948 by Stockstead.[37] Three moieties can be recognised in the molecule: pteridine, *p*-amino benzoyl acid and glutamic acid (*Figure 1.6*).

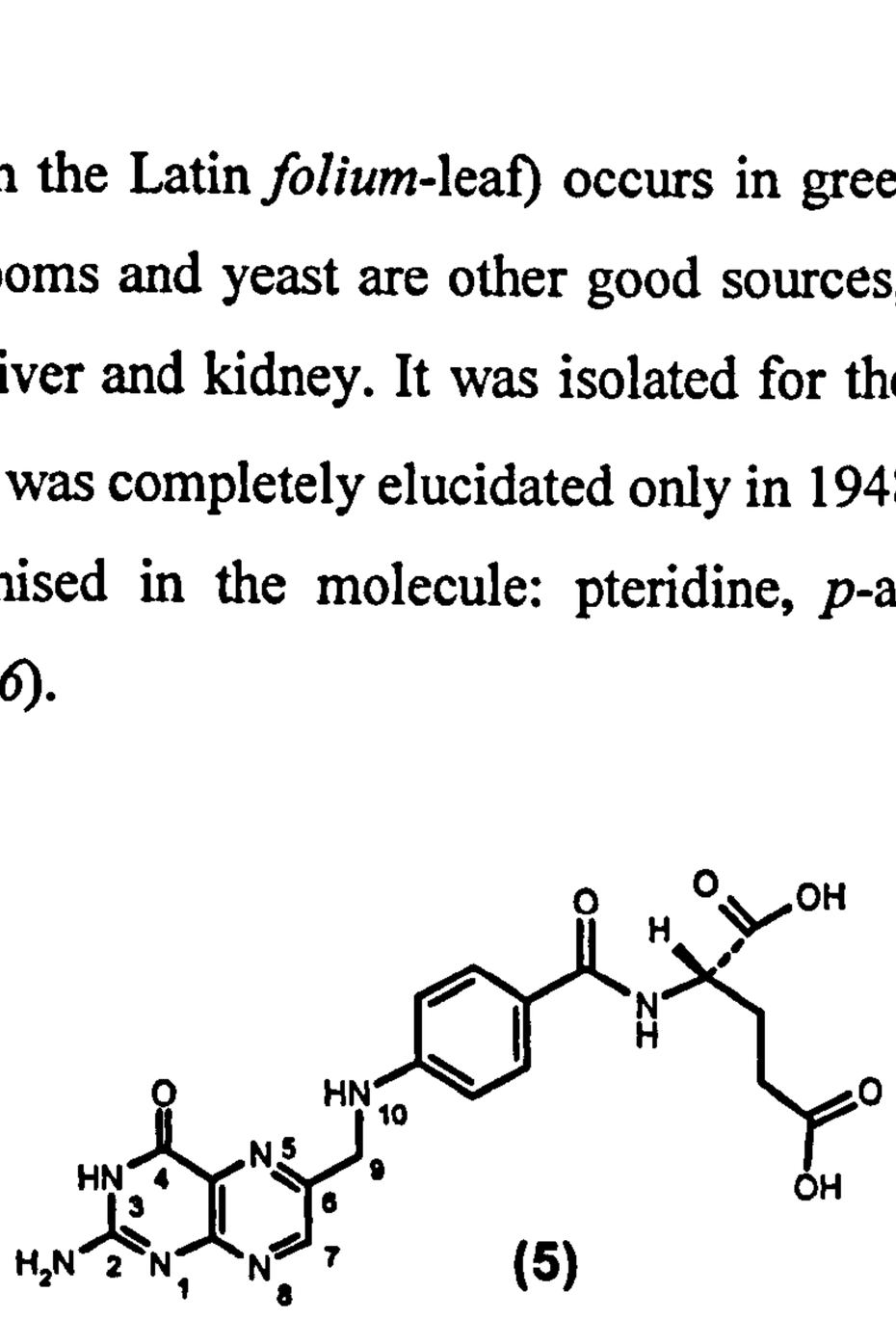

***Figure 1.6** – Folic acid structure.*

Folic acid (named also pteroylglutamic acid (PGA), folacin or vitamin B_c) crystallises from water in the form of yellow, spear shaped leaflets. The free acid is not highly soluble in water (10 mg/l at 0 ^{0}C; 500 mg/l at 100 ^{0}C), whereas the disodium salt presents a much higher solubility (15 g/l).

This vitamin comprises a large family of biologically active forms of folic acid. These differ in the oxidation state of the pteridine ring, in the number of glutamate residues or in the substitution at N^5 and N^{10}. Folates function as essential coenzymes, which involve the incorporation of a single carbon fragment, in the syntheses of purines, pyrimidines and certain amino acids. Folic acid and folates are absorbed from the diet primarily via the proximal portion of the small intestine. Following their absorption from the digestive system, dietary folates are rapidly reduced by dihydrofolate reductase and by other enzymes to tetrahydrofolic acid.

The cellular uptake of these compounds is assured by at least two independent transport mechanisms. Reduced folates are internalised via a carrier-mediated low affinity (K_m ~ 1-5 μM) anion transport system that is found in nearly all cells.[38] Folic acid and 5-methyl tetrahydrofolate can also enter the cells via a high affinity (K_D in the order of nanomolar) membrane bound folate binding protein (FBP) that is anchored to the cell membrane via a glycosylphosphatidylinositol (GPI) moiety. [39-42] Experiments conducted in MA104 cells,[43] have shown that 5-methyl tetrahydrofolate is taken up into the cell after binding to GPI-anchored FBP that has clustered in cell structures, known as caveolae.[44] The caveolae then seal the folate binding protein-folate complex off from the extracellular space and transport folate into the cell. Once inside, the folate dissociates from FBP and diffuses into the cytoplasm, where it is readily coupled to one or more glutamic acid residue, slowing diffusion out of the cell. The caveolae and FBP then migrate to the membrane surface for another round of folate uptake.

Human FBP exists in two major isoforms, the α and the β. They possess almost 70% amino acid sequence homology, but differ dramatically in their stereospecificity for folates species.[45] Healthy tissues usually express low to moderate amount of the β-form, whereas the α-FBP is generally overexpressed in a variety of carcinomas.[34]

These membrane proteins represent an interesting delivering system for pharmaceutical or diagnostic agents coupled to folic acid, because they can distinguish between normal and cancerous cells. FBP levels are low in many normal tissues, whereas they are high in many tumour cells. This difference allows selective

concentration of pharmaceutical or diagnostic agents in tumour cells compared to normal ones and thus facilitate treatment or visualisation of tumour cells.

1.7. Lanthanide ions

The paramagnetic Gd^{3+} ion has some spectroscopic limitations. For example, the ^1H NMR spectra cannot be recorded because its long electronic relaxation time causes a broadening of the NMR lines to such an extent that no peaks are observed. Moreover, fluorescence studies are not useful in case of gadolinium (III) compounds. The difference in energy between its ground state ($^8S_{7/2}$) and its first excited state ($^6P_{7/2}$) is too high. However, its neighbour ions Eu^{3+} and Tb^{3+} do not posses such limitations and having similar ionic radii, they can be used to elucidate the solution behaviour of the corresponding gadolinium species.

Measurements of the radiative rate constant for decay of the luminescent europium or terbium excited state in H_2O and D_2O allow an estimate of the complex hydration state, whereas the analysis of high resolution absorption and luminescence spectra can help in understanding the structure and symmetry of the complex in solution. Therefore, when examining the properties of a new gadolinium complex, it is usual practice to prepare also the analogous Tb and Eu complexes and study their photophysical and NMR properties in detail.

1.7.1. Electronic configurations and spectroscopic transitions

Luminescence in lanthanide (III) ions occurs through transitions between 4f states. Energy levels may be calculated by considering interelectronic repulsion, spin orbit coupling and the ligand field. For example, interelectronic repulsion splits the configurations $4f^6$ of Eu^{3+} and $4f^8$ of Tb^{3+} into $^{(2S+1)}\Gamma$ spectroscopic terms, where Γ = S, P, D, F when the quantum number L = 0, 1, 2, 3. The terms deriving from this electrostatic interaction are separated by about 10^4 cm^{-1}. Spin-orbit coupling then splits these terms into J states, which are typically separated by 10^3 cm^{-1}. There are 295 $^{(2S+1)}\Gamma_J$ spectroscopic levels for the $4f^6$ and $4f^8$ configurations. Their relative energies are predicted by Hund's rules. For example, for both Eu^{3+} and Tb^{3+} ions, the ^7F term is lowest in energy and the ground state levels are $^7F_6$ for Tb^{3+} and $^7F_0$ for Eu^{3+} (*Figure 1.7*).

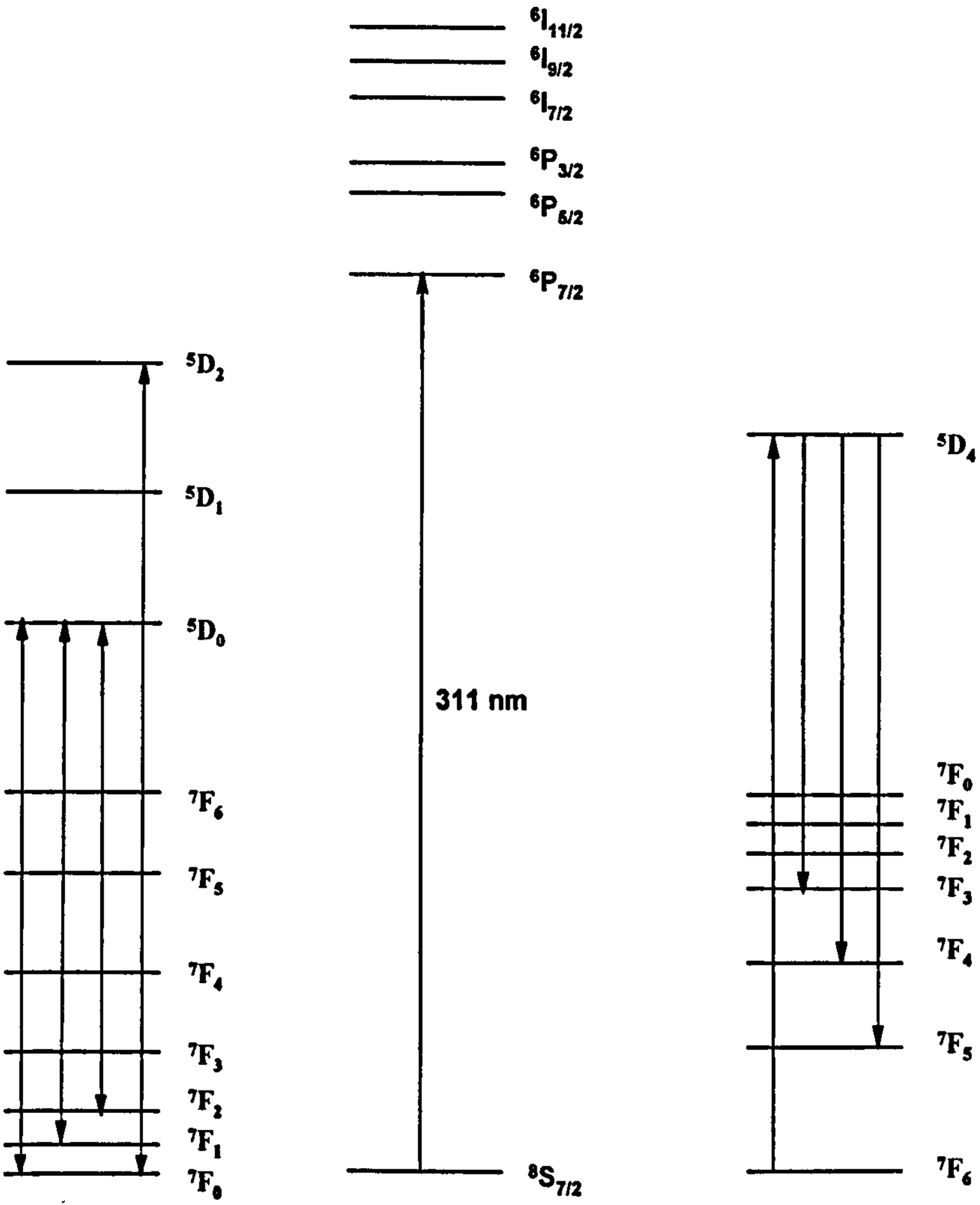

Figure 1.7 – Energy levels for Eu^{3+}, Gd^{3+} and Tb^{3+}.

Selection rules govern the various electronic transitions. In case of magnetic dipole allowed transitions these are: $\Delta S = 0$; $\Delta L = 0$; $\Delta J = 0, \pm 1$. In addition, a transition is only allowed if it conforms to the group theoretical rules, which are appropriate to the site symmetry of the lanthanide ion.

1.7.2. Luminescence from Eu^{3+} complexes

The investigation of the emission spectra of lanthanide complexes allow us to gain information about complex speciation, structure and the local symmetry. We will focus our attention mainly on the Eu^{3+} emission spectra, which have been recorded in this work. When the Eu^{3+} ion is excited from the $^7F_0$ ground state to a higher state, it undergoes radiationless decay to the long lived $^5D_0$ state, from which all luminescence

to the ^7F_J arises in solution. The strongest transitions occur between states with rather low J values, so that detailed interpretation is possible without the need for analysis of crystal field splitting. The $\Delta J = 0$ (580 nm), $\Delta J = 1$ (590 nm), $\Delta J = 2$ (618 nm) and $\Delta J = 4$ (700 nm) transitions are particularly interesting. The latter two (termed hypersensitive) have an intensity, which is very sensitive to the chemical environment. The origin of this hypersensitivity has not been fully clarified yet. However, the analysis of several examples suggests that the intensity of this band is lower for axially symmetric complexes and increases with the degree of polarisability of the donor atom type.[46] The magnetic dipole allowed transition $\Delta J = 1$ has an intensity, which varies relatively little from one coordination environment to another.[47] In addition, there are three transitions allowed in low symmetry, but only two if the complex possesses a C_3 or a C_4 axis. The highest energy emission band is for the formally forbidden $\Delta J = 0$ transition. Probing this transition requires high-resolution laser spectroscopy. Usually twisted square antiprismatic complexes exhibit lower intensity for this transition compared to the square antiprismatic isomer.

1.7.3. Hydration number

In the late seventies Horrocks developed a method for determining the hydration number *q* of the luminescence lanthanides europium and terbium.[48] Luminescence from excited Tb^{3+} and Eu^{3+} ions in solution is quenched by vibrational oscillators of water. The greater the number of water molecules bound to the metal centre, the more efficient is the quenching. Kropp and Windsor showed that the luminescence of Eu^{3+} and Tb^{3+} complexes was more intense in D_2O than in H_2O and that the luminescence lifetimes were about an order of magnitude longer in D_2O.[49, 50]

The luminescence lifetimes in H_2O and D_2O were measured for a series of europium and terbium complexes with a known number of bound water molecules. The plot of the hydration state *q* versus the difference in rate of lanthanide luminescence quenching (Δk) gave a straight line. Horrocks defined the slope of this line as the factor A, which reflected the sensitivity of a given lanthanide ion to vibrational quenching. The value of *q* can be estimated by using equation 1.21.

$$q = A\left(k_{H_2O} - k_{D_2O}\right) \quad (1.21)$$

where A is equal to 4.2 ms^{-1} for terbium complexes and equal to 1.05 ms^{-1} for europium complexes.

However, other energy matched exchangeable XH oscillators may also quench the excited state of lanthanide ions, including amide NH,[51, 52] amine NH[53, 54] and CH. [53, 55] These oscillators, in the context of complexes used in MRI, are more distant from the lanthanide centre and hence their quenching effect is less marked than the effect of directly bound OH oscillators. In addition the presence of unbound water molecules in the second sphere may contribute to the quenching. [53] As a consequence of these effects the equation (1.21) has been modified to account for the quenching effect of closely diffusing water molecules and the effect of other exchangeable XH oscillators (equation 1.22).

$$q = A\left[\left(k_{H_2O} - k_{D_2O}\right) - 0.25\right] \quad (1.22)$$

where A is equal to 1.2 for the europium complexes and 5 for terbium complexes.

1.8. Objectives of the work

The aim of this work is the development of new efficient contrast agents for MRI. In the first part of this thesis (Chapter Two) a new efficient di-hydrated complex is described. In the light of what has been discussed in the previous paragraphs, the relaxivity of a gadolinium complex may be improved by increasing the hydration number *q*. The gadolinium complex $[Gd\cdot\mathbf{8}]^{3-}$ (*Figure 1.8*) has been synthesised and fully characterised. Relaxometric studies revealed a significant high relaxivity, the highest measured for a complex of similar size so far, and a fast water exchange (τ_M=30 ns). In addition, it showed both a good thermodynamic stability and a kinetic inertness. In contrast to other dihydrated complexes published in literature, $[Gd\cdot\mathbf{8}]^{3-}$ does not bind endogenous anions (such as phosphate, carbonate, lactate or citrate) at physiological pH. These properties make it a promising candidate as contrast agent for MRI.

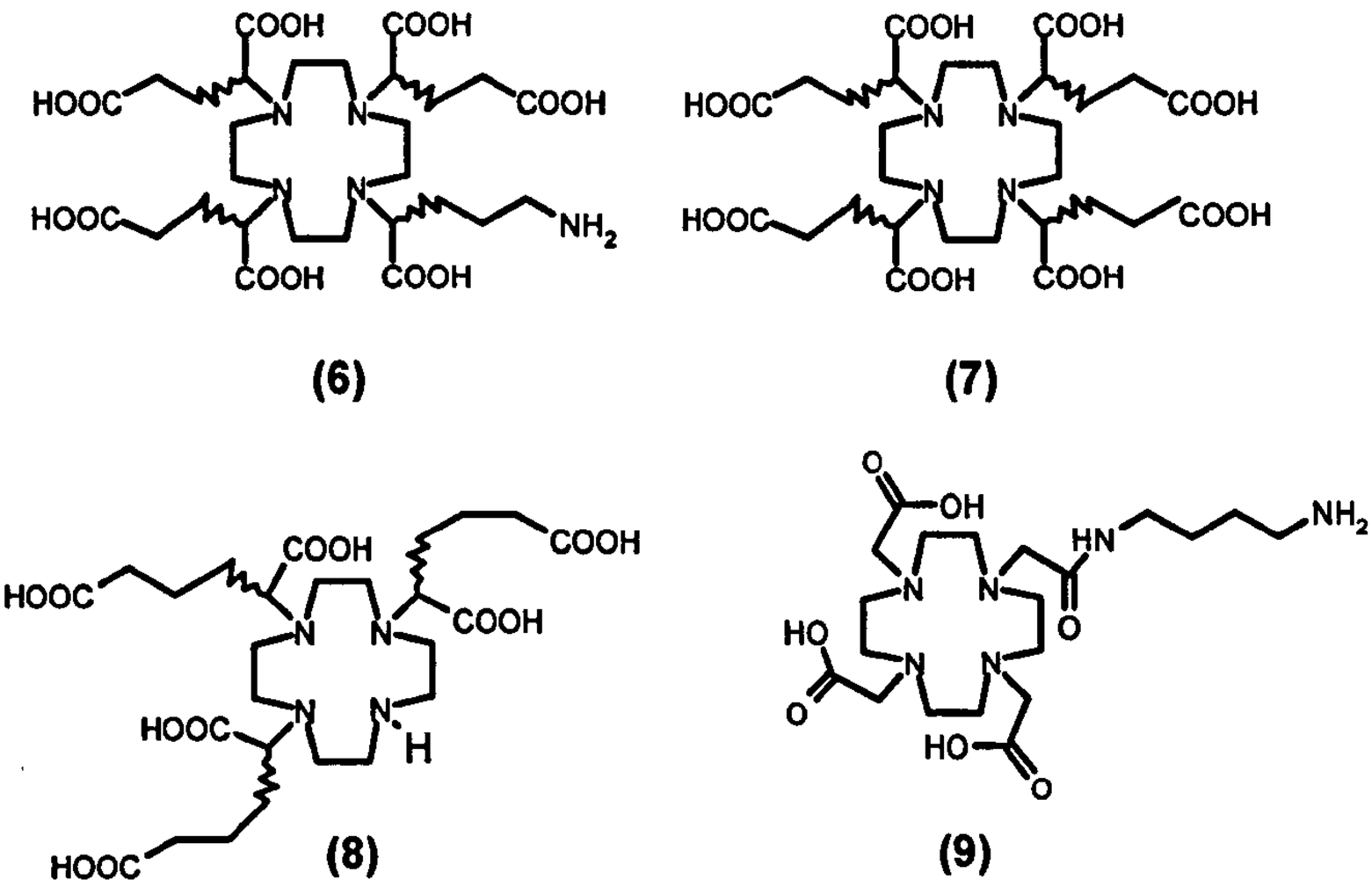

***Figure 1.8** – Ligands structures.*

In the second part of this work new targeting contrast agents have been developed. Gadolinium chelates have been coupled to the targeting vector folic acid. Since many human cancer cells have higher levels of FBP than normal ones[26], they will present higher amounts of folic acid. Binding a gadolinium (III) complex to folic acid allows the possibility of tumor targeting. Currently, the conjugation of folate derivatives is carried out through reactions between a carboxylic group of folic acid and an amino group of a particular substrate. This amide conjugation is achieved by using dehydrating agents, such as DCC or EDC. Practicable routes for the syntheses of a new folate conjugate have been developed, using the simple model complex [Gd·**9**]. However, the main idea of the project was the synthesis of folate conjugates of the anionic gadolinium complex $[Gd\cdot\mathbf{6}]^-$.

The choice of this structure can be explained as follows. Firstly, its amino arm provides the "binding site" for folic acid. Secondly, the three terminal carboxylic acid groups can be linked to high molecular weight compounds to improve the rotational correlation time τ_R, and thus the relaxivity of the complex. Finally, the four carboxylic groups together with the four nitrogens of the cycle constitute the donor atoms for the gadolinium (III) ion. In addition, the existence of eight different stereoisomers of the ligand **(6)** must be considered. They are determined by the configuration at each of the carbon stereogenic centres: *RRRR (SSSS)*, *RSSS (SRRR)* and the related diastereoisomers *RSRS (SRSR)* and *RRSS (SSRR)*. Previous studies have demonstrated that the exchange rate (τ_m) of water bonded to lanthanide ions (*e.g.* Eu and Yb) depends upon the nature and composition of the isomers of a given complex.[56, 57] In recent

work on lanthanide complexes of the ligand (**7**), it was shown that the water exchange rate was faster for the *RRRR* isomer (τ_m=71, 140 and 270 ns (298 K) for the (*RRRR*), (*RRRS*) and (*RSRS*) isomers respectively).[58] The (*RRRR*)-[Gd·**6**]$^-$ complex may therefore be expected to possess the shortest value of τ_m, and therefore will not limit the overall relaxivity to the same extent as the other isomers.

1.9. References

[1] Peters, J. A.; Huskens, J.; Raber, D. J. *Prog. NMR Spectrosc.* **1996**, *28*, 283.

[2] Koenig, S. H.; Brown, R. D. *Prog. NMR Spectrosc.* **1990**, *22*, 487.

[3] Kumar, K.; Tweedle, M. F. *J. Pure Appl. Chem.* **1993**, *65*, 515.

[4] Young, S. W. *Magnetic Resonance Imaging: Basic Principles*; Raven Press: New York, 1988.

[5] Aime, S.; Botta, M.; Fasano, M.; Terreno, E. *Chem. Soc. Rev.* **1998**, *27*.

[6] Caravan, P.; Ellison, J.; McMurry, T. J.; Lauffer, R. B. *Chem. Rev.* **1999**, *99*, 2293.

[7] Petersein, J.; Saini, S.; Weisslader, R. *MRI Clin. N. Am.* **1996**, *4*, 53.

[8] Stark, D. D.; Bradley, W. G. *Magnetic Resonance Imaging*; C. V. Mosby: New York, 1988.

[9] Edelman, R.; Warack, S. *New Eng. J. Med.* **1993**, *328*, 708.

[10] Diem, K.; Leutner, C. *Documenta Geigy Scientific Tables*; Gregory: Basel, 1970.

[11] Tweedle, M. F. In *Lanthanide Probes in Life, Chemical and Earth Sciences,* ; G. Bunzli and G. R. Choppin, Ed.; Elsevier: Amsterdam, 1989; Vol. 5.

[12] Damadian *Proc. Nat. Acad. Sci. USA* **1974**, *71*, 1471.

[13] Aime, S.; Batsanov, A. S.; Botta, M.; Howard, J. A. K.; Parker, D.; Senenayake, K.; William, J. A. G. *Inorg. Chem.* **1994**, *33*, 4696.

[14] Bertini, I.; Luchinat, C. *NMR of Paramagnetic Molecules in Biological Systems*; Benjamin-Cummings: Boston, 1986.

[15] Solomon, I. *Phys. Rev.* **1955**, *99*, 559.

[16] Bloembergen, N.; Morgan, L. O. *J. Chem. Phys.* **1961**, *34*, 842.

[17] Bloembergen, N.; Puccel, E. M.; Pound, R. V. *Phys. Rev.* **1948**, *73*, 697.

[18] Bloembergen, N. *J. Chem. Phys.* **1957**, *27*, 572.

[19] Koenig, S. H.; Brown, R. D. In *Relaxometry of Tissue in NMR Spectroscopy of Cells on Organisms,* ; R. M. Gupta, Ed.; CKC Press: Boca Raton, FL, 1987, pp 75.

[20] Freed, J. M. *J. Chem. Phys.* **1978,** *68,* 4034.

[21] Young, I. K.; Clarke, G. J.; Cailes, D. R. *Computed Tomography* **1981,** *5,* 534.

[22] Njornerud, A.; Oksendal, A. N. Presented at Cost D8 Meeting, Bergen, 1997

[23] Elizondo, G.; Fretz, C. J.; Stark, D. D.; Rockloge, S. M.; Quay, S. C.; Warah, D.; Tsung, Y. M. *Radiology* **1991,** 73.

[24] Schaffer, M.; Mayer, D.; Beoute, S. *Magn. Res. Med.* **1991,** *22,* 238.

[25] Weinman, M. J.; Schmitt, G. J. *Magn. Res. Med.* **1991,** *22,* 233.

[26] Carr, D. M.; Brown, J.; Bydder, G. M.; Weinman, M. J.; Speck, U.; Thomas, D. J.; Young, I. R. *Lancet* **1984,** *1,* 484.

[27] Hasso, A. N.; Stark, D. D. *J. Magn. Res. Imag.* **1993,** 135.

[28] Merbach, A. E.; Toth, E. *The Chemistry of Contrast Agents in Medical Magnetic Resonance Imaging*; Wiley: New York, 2001.

[29] Brinkley, M. *Bioconj. Chem.* **1992,** *3,* 2.

[30] Curtet, C.; Maton, F.; Havet, T.; Slinkin, M.; Mishra, A.; Chetal, J. F.; Muller, R. N. *Invest. Radiol.* **1998,** *33,* 752.

[31] Wu, C.; Brechbiel, M. W.; Kozak, R. W.; Gansow, O. *Biorg. Med. Chem. Lett.* **1994,** *4,* 449.

[32] Weiner, E. C.; Konda, S.; Shadron, A.; Brechbiel, M.; Gansow, O. *Invest. Radiol.* **1997,** *32,* 748.

[33] Franklin, W. A.; Wantub, M.; Edwards, D.; Christiensen, K. *Int. J. Cancer* **1994,** *8,* 89.

[34] Ross, J. F.; Chonduri, P. K.; Rotman, M. *Cancer* **1994,** *73,* 2432.

[35] Wang, S.; Luo, J.; Lantrip, D. A.; Waters, D. J.; Mathias, C. J.; Green, M. A.; Fucks, P. L.; Low, P. S. *Bioconj. Chem.* **1997,** *8,* 673.

[36] Pfiffner, J. J.; Binkley, S. B.; Bloom, E. S.; Brown, O. D.; Bird, A. D.; Emmet, A. J. *Science* **1943,** *97,* 404.

[37] Stockstead, E. L. K.; Hutchings, Y.; Subbarow, S. *J. Am. Chem. Soc.* **1948,** *70,* 3.

[38] Kisliuk, R. L. In *Folate Antagonists as Therapeutic Agents,* ; F. Sirotnack, J. J. Burcall, W. D. Emsinger and J. A. Montgomery, Ed.; Academic Press: Orlando, 1984.

[39] Kane, M. A.; Waxman, S. *Lab. Invest.* **1989,** *60,* 737.

[40] Henderson, G. B. *Ann. Rev. Nutr.* **1990**, *10*, 319.

[41] Ratnam, M.; Marquardt, H.; Duhring, J. L.; Freisheim, J. H. *Biochemistry* **1989**, *28*, 8249.

[42] Sadasivan, E.; Rothenberg, S. P. *J. Biol. Chem.* **1989**, *264*, 5806.

[43] Kamen, B. A.; Schmith, A. K.; Anderson, R. G. W. *J. Clin. Invest.* **1991**, *87*, 1442.

[44] Leamon, C. P.; Low, P. S. *Biochem. J.* **1993**, *291*, 855.

[45] Wang, X.; Schen, F.; Freisheim, J. H.; Gentry, L. E.; Ratnam, M. *Biochem. Pharmacol.* **1992**, *9*, 1898.

[46] Bryden, C. C.; Reilley, C. N. *Anal. Chem.* **1982**, *54*, 610.

[47] Bunzli, J.-C. G.; Choppin, G. R. *Lanthanide Probes in Life, Chemical and Earth Sciences*; Elsevier: AMsterdam, 1989.

[48] Horrocks, W.; Schmidt, G. R.; Sudnick, D. R.; Kittrell, C.; Pernheim, R. A. *J. Am. Chem. Soc.* **1977**, *99*, 2378.

[49] Kropp, J. L.; Windsor, M. W. *J. Chem. Phys.* **1963**, *39*, 2769.

[50] Kropp, J. L.; Windsor, M. W. *J. Chem. Phys.* **1965**, *42*, 1599.

[51] Parker, D.; Williams, J. A. G. *J. Chem. Soc., Perkin Trans. 2* **1995**, 1305.

[52] Dickins, R. S.; Parker, D.; De Sousa, A. S.; Williams, J. A. G. *J. Chem. Soc., Chem. Comm.* **1996**.

[53] Beeby, A.; Clarkson, I. M.; Dickins, R. S.; Faulkner, S.; Parker, D.; Royle, L.; De Sousa, A. S.; Williams, J. A. G.; Woods, M. *J. Chem. Soc., Perkin Trans. 2* **1999**, 493.

[54] Wang, Z.; Chopping, G. R.; Bernardo, P. D.; Zanonato, P. L.; Portonova, R.; Tolazzi, M. *J. Chem. Soc., Dalton Trans.* **1993**, 2791.

[55] Hemilla, I.; Mukkala, V. H. *J. Fluoresc.* **1995**, *5*, 159.

[56] Aime, S.; Barge, A.; Botta, M.; Parker, D.; De Sousa, A. S. *Angew. Chem. Int. Ed. Engl.* **1998**, *37*, 2673.

[57] Aime, S.; Barge, A.; Bruce, J. I.; Botta, M.; Howard, J. A. K.; Moloney, J. M.; Parker, D.; De Sousa, A. S.; Woods, M. *J. Am. Chem. Soc.* **1999**, *121*, 5672.

[58] Woods, M.; Aime, S.; Botta, M.; Howard, J. A. K.; Moloney, J. M.; Navet, M.; Parker, D.; Port, M.; Rousseaux, O. *J. Am. Chem. Soc.* **2000**, *122*, 9781.

Chapter Two:

A Stable New High Relaxivity Di-Aqua Contrast Agent.

2.1. Introduction

The relatively high doses required and the low efficiency of the commercially available MRI contrast agents, have prompted the search for new classes of these diagnostic compounds.

As we have seen in Chapter One, the efficiency of a contrast agent can be improved by increasing the hydration number *q*. However, high hydration numbers reduce both the kinetic and thermodynamic stability of the complex with respect to dissociation, limiting the choice to di-hydrated (*q*=2) or tri-hydrated (*q=3*) species. Another disadvantage of these systems is that they are more likely to bind endogenous anions, such as phosphate or carbonate, displacing one or more of the water molecules and hence lowering the relaxivity.

Heptadentate ligands are most appropriate for formation of *q=2* complexes, because they should allow the coordination of two water molecules in the inner sphere of the metal. Moreover, heptadentate-based gadolinium complexes should present a relatively fast water exchange rate, with respect to analogous complexes based on octadentate ligands, giving an additional improvement. For these reasons, in the last few years, the interest in di-hydrated complexes has increasingly grown.

Xu and co-workers[1] reported the syntheses and characterization of [Gd-TREN-Me-3,2,-HOPO] **(10)** (*Figure 2.1)*, a complex with relatively high relaxivity (10 mM^{-1} s^{-1}), apparently good stability but poor water solubility (less then 0.1 mM at pH = 7.0). To further exploit the properties of this ligand, a number of functionalized derivatives have been synthesized, mainly to improve the solubility. Cohen and coworkers[2] synthesized and characterized three new complexes [GdTREN-Me-3,2-HOPOSAM] **(11)**, [GdTREN-Me-3,2-HOPOTAM]$^-$ **(12)** and [GdTREN-Me-3,2-HOPOIAM] **(13)**, by replacing one of the hydroxypyridinone groups of **(10)** with moieties able to "tune" properties, such as denticity, charge, solubility and stability of the resulting complex. These ligands bind the metal in a hexadentate fashion, allowing for coordination of at least two inner sphere water molecules. The relaxivity values, although smaller then the parent compound [Gd-TREN-Me-3,2-HOPO] **(10)**, were higher than those of all the currently available commercial contrast agents (8.8 mM^{-1} s^{-1} for TAM **(12)**, 7.2 mM^{-1} s^{-1} for SAM **(11)** and 7.7 mM^{-1} s^{-1} for IAM **(13)** at 20 MHz and 25^{0}C).

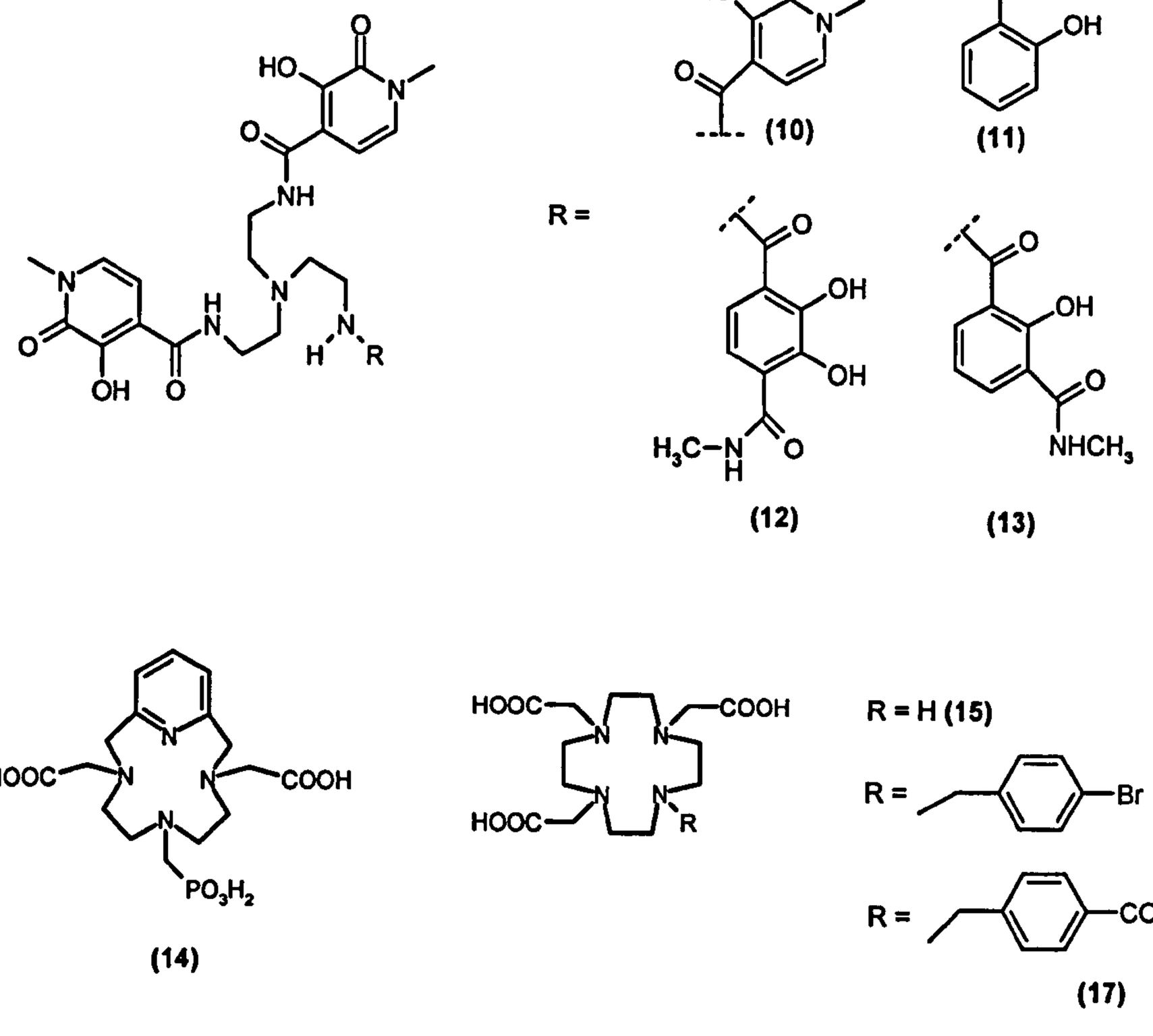

***Figure 2.1** – Ligands forming di-aqua complexes with Gd^{3+}.*

Recently Aime and coworkers[3] have reported the syntheses of a new ligand based on a pyridine containing macrocycle, bearing two acetate and one methylenephosphonate arms (PCP2A) **(14)**. The interest around this complex was mainly due to its high stability (Log K_{GdL} = 23.4). In addition, it has a good value of relaxivity (8.3 mM^{-1} s^{-1}) for a complex of this size. This can be explained by considering the additional contribution from water molecules in the second sphere, arising from the ability of the phosphonate group to form hydrogen bonds.

The neutral [GdDO3A] **(15)** was one of the first $q = 2$ systems to be investigated. It does not present either a particularly high value of relaxivity (6.0 mM^{-1} s^{-1}, 20 MHz, 298 K) nor a fast water exchange rate (τ_M = 160 ns).[4, 5] However, it has been frequently functionalized and several examples of DO3A-like complexes have been reported in the literature.

Aime and coworkers[6] have synthesized two derivatives, which bear either a p-bromo benzyl **(16)** or a p-phosphonatomethylbenzanilido **(17)** substituent, with the aim of promoting further interaction with macromolecular substrates. They both exhibit a higher relaxivity (7.9 mM^{-1} s^{-1} and 10.7 mM^{-1} s^{-1} respectively) than the parent DO3A complex.

In this work the complexes of the ligands shown in *Figure 2.2* have been investigated and compared to the analogous monohydrated complexes based on the corresponding octadentate ligands. It has previously been established that lanthanide complexes of DO3MA **(18)** possess a high kinetic and thermodynamic stability (Log K_{GdL} = 25.3).[7] This forms a suitable starting point for an investigation of complexes, which are designed to resist anion or protein binding. Accordingly the complexes of the ligands **(8)** and **(19)** (*Figure 2.2*) have been considered, as the pendant carboxylate groups are expected to inhibit anion binding by electrostatic repulsion. The study has been limited to complexes with two or three methylene groups in the chain because longer hydrocarbon chains reduce the water solubility. Being heptadentate ligands, in their lanthanide complexes they should coordinate two water molecules. An additional improvement in the relaxivity may be expected from a second sphere contribution, since the three remote carboxylate arms can form hydrogen bonds with bulk water molecules. Moreover, the three terminal carboxylic acid groups provide sites for covalent linkage to high molecular weight compounds. By increasing the molecular weight of the complex an increment in the rotational correlation time, τ_R and hence in the relaxivity should be expected.

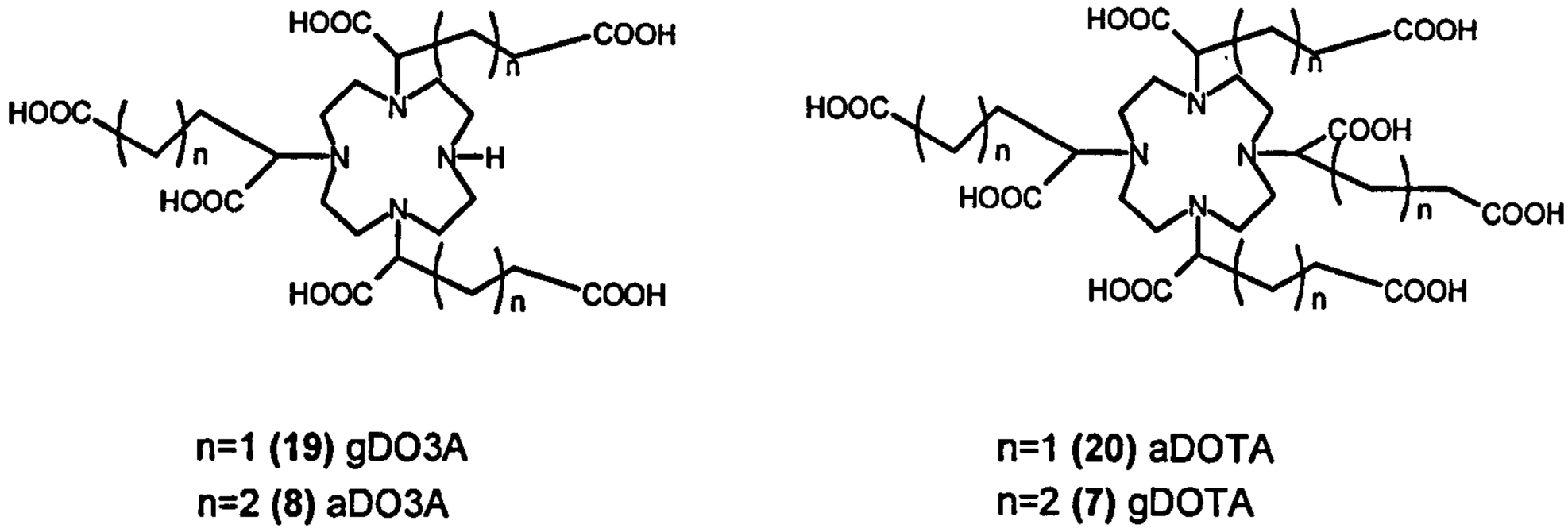

Figure 2.2 – Ligands investigated.

2.2. Strategies of syntheses

The europium (III) and gadolinium (III) complexes of the ligand aDO3A (8) were synthesized according to scheme below (*Figure 2.3*).

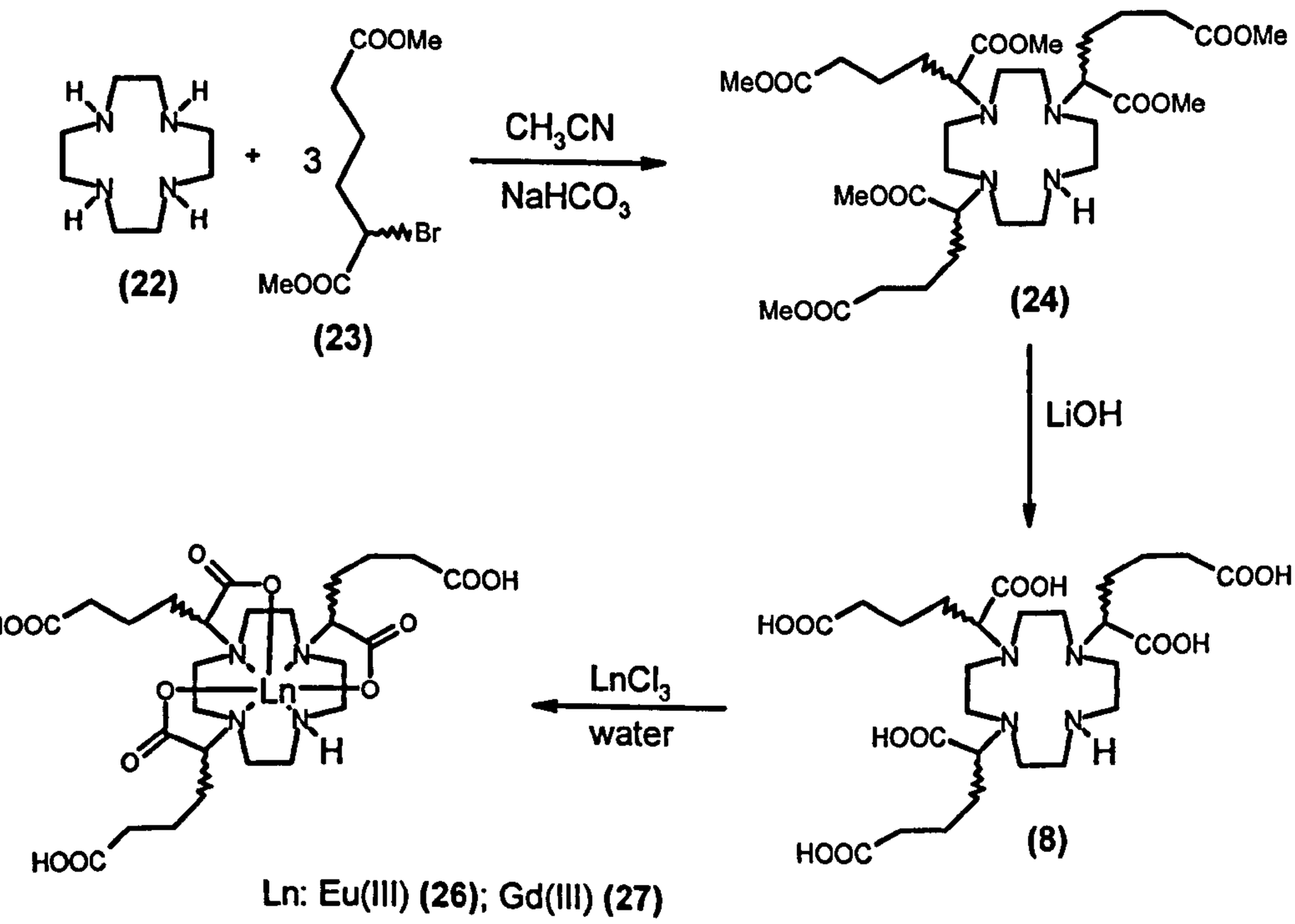

Figure 2.3 – Synthesis of Ln (III) complexes of aDO3A (8).

The alkylation of the cyclen **(22)** was achieved using racemic 2-bromo dimethyl adipate **(23)** with sodium hydrogen carbonate as base. Each nitrogen in the macrocycle cyclen exhibits a different pK_a. Although the exact value depends on the N-substituent, they are typically around 3, 5, 10 and 13.[8] The reactivity of the four nitrogens is different and in theory can be modulated by the choice of the base. The use of a strong base increases the rate of the reaction, but reduces the selectivity yielding a high amount of the tetra-alkylated derivative. On the other hand by using a weak base it should be possible to improve the selectivity, by slowing the reaction rate. According to the procedure followed by Pillai for the syntheses of DO3A derivatives, sodium hydrogen carbonate was used as the base.[9] Even though the reaction was not complete after four days and some tetra and di-alkylated derivatives were present in the crude, the tri-alkylated compound **(24)** was isolated in a reasonable yield (33%), following chromatographic purification.

The β-elimination of the bromo compound **(23)** competes with the S_{N2} reaction and contributes to reduce the final yield (*Figure 2.4*). The formation of the alkene **(23a)** was detected by ESMS. When a strong excess of base was used, the amount of alkene increased. An excess of base equal to 2.9 equivalents of cyclen was found to be the best compromise.

The tri-alkylated cyclen derivative **(24)** was isolated as a mixture of the RRR (SSS), RSR (SRS) and SSR (RRS) isomers after purification over silica gel, eluting with ammonia solution in tetrahydrofuran in the presence of methanol and dichloromethane.

The methyl esters were efficiently hydrolysed in a 1 M lithium hydroxide solution at 90^0C. The progress of the reaction was followed by ^{1}H NMR. Small portions of the reacting solution were collected over time, evaporated, dried and dissolved in D_2O. The disappearance of the methyl resonances between 3.65 and 3.75 ppm was checked and reaction was found to be complete after 24 hours. The crude solid was purified through a strong cationic exchange resin, eluting with a 12% ammonia solution; the pure ligand was collected in the form of its ammonium salt.

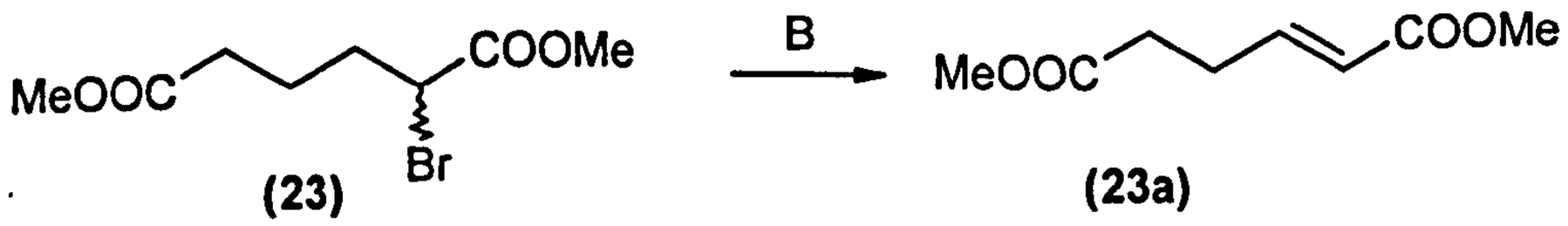

(23) **(23a)**

***Figure 2.4** – Competitive β-elimination.*

The gadolinium (III) and the europium (III) complexes of aDO3A **(8)** were synthesized from a water/methanol mixture (1:1; v/v) at pH 5.5. Due to the insolubility in methanol, the complexes precipitated as soon as they formed. They were isolated by filtration at the end of the reaction. The formation of the complexes was followed by ESMS, which showed the complete disappearance of the ligand after 24 hours.

The ^{1}H NMR spectrum of the isolated Eu (III) complex showed the predominance (*ca* 50%) of one isomer. However, it was not separated from the minor isomers present. In the absence of a crystal structure it is hard to understand which of the possible three diastereoisomers (RRR, RSR, RRS) is the most abundant, although for the analogous C_4-symmetric complexes, the RRR (SSS) ligand and complex were found to be least soluble in water.

The gadolinium and the europium complexes of gDO3A **(19)**, aDOTA **(20)** and gDOTA **(7)** were synthesized by Dr. Mark Lowe and Dr. Ofer Reany in the group.

2.3. Structure studies in solution

Contrast agents function in an aqueous environment, so it is important to study the properties and structure in solution. The determination of the hydration number q and the understanding of which isomer is the most abundant in solution are fundamental issues to understand the biophysical properties of the complex. Unfortunately the gadolinium (III) ion has some spectroscopic "limitations". Its remarkably long electronic relaxation time, which makes it most suitable for use as a contrast agent in MRI, has the effect of broadening NMR spectra lines to such an extent that *e.g.* ^{1}H NMR spectra of gadolinium complexes may not be recorded.

In addition the Gd(III) ion is not useful in fluorescence studies. The difference in energy between its ground state ($^{8}S_{7/2}$) and its first excited state ($^{6}P_{7/2}$) is quite high. The emission from the excited state occurs at 311 nm. However, its neighbors ions Eu(III) and Tb (III), do not posses such limitations and since they have similar ionic radii, they can be used as valid models to allow a good estimation of the properties of the gadolinium complexes in solution.

2.3.1. ^1H NMR studies

Further information about the nature of complex solution structure can be obtained by ^1H NMR studies. Derivatives of DO3A are heptadentate ligands and the resulting complexes can adopt three different coordination geometries; a pseudo-square antiprism, a pseudo twisted square antiprism and mono-capped octahedron, as indicated in *Figure 2.5*. These geometries can easily interconvert by arm rotation or ring inversion.

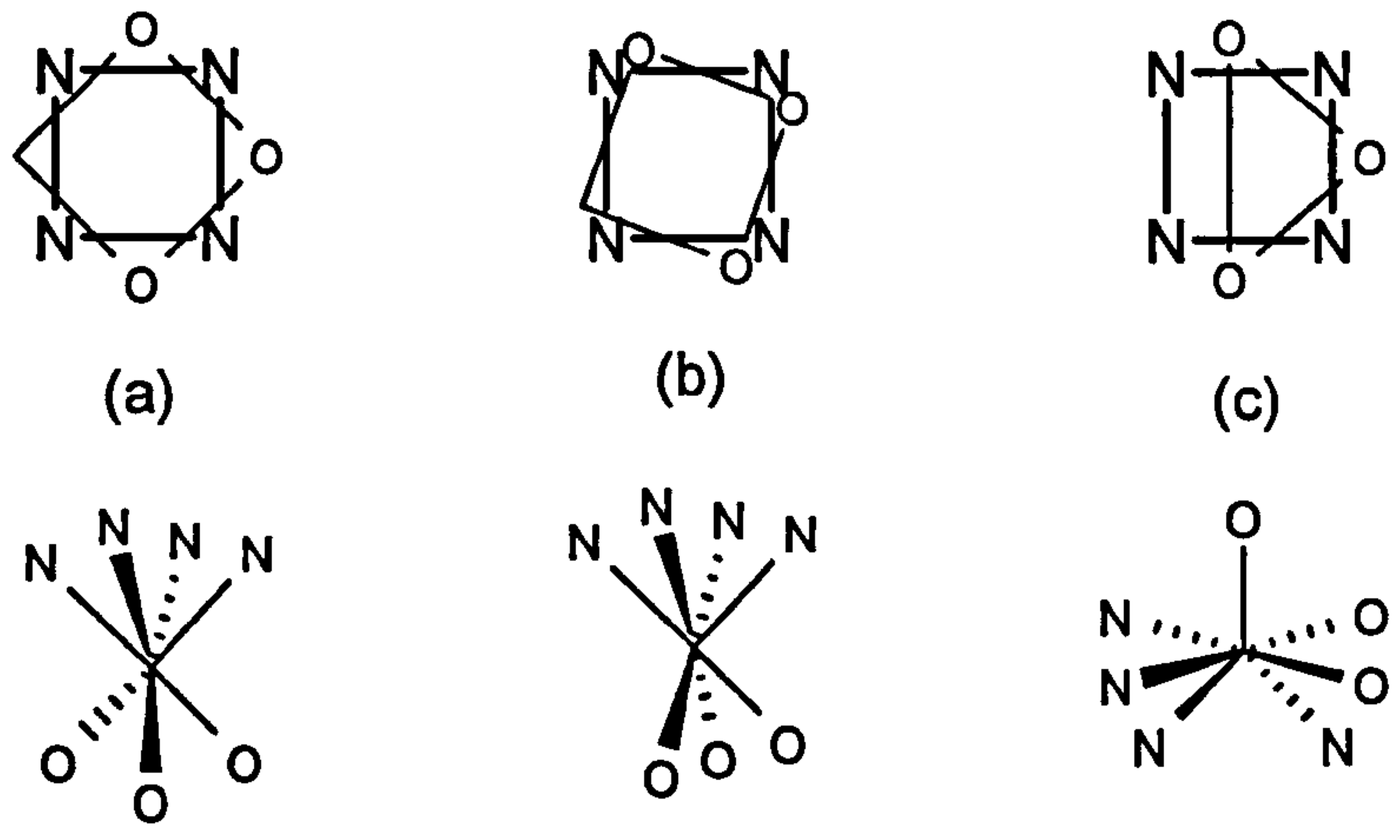

***Figure 2.5** – Co-ordination geometries adopted by DO3A-like lanthanide complexes. (a) pseudo square antiprism, (b) pseudo twisted antiprism and (c) mono-capped octahedron.*

^1H NMR analyses can detect the presence of different coordination isomers in solution and their time-averaged symmetry. Previous studies on C_4-symmetric analogous complexes **(7)**, have demonstrated that two major diastereoisomers are present in solution,[10] whose relative proportion is a function of the lanthanide ion, temperature and solvent. These two isomers, a regular monocapped square antiprismatic (M) and a twisted square antiprismatic (m), are characterized by different dipolar shifts. The complexes of the former series usually possess the bigger paramagnetic shifts for a given resonance. Particularly useful is the analysis of the most shifted axial ring proton. This resonates at around 30-50 ppm in the case of 9-coordinate square antiprismatic Eu (III) complexes and at around 20 ppm for related 9-coordinated twisted square antiprismatic complexes.

Analysis of the ^1H NMR spectra of the (RRRR)- (RRRS)- and (RSRS)-$[Eu{\cdot}7]^-$ complexes provided evidence for the presence of two major isomeric species in a relative

ratio (M/m) of 1:4, 2:1 and 4:1 respectively.[10] For the (RRSS)-[Eu·7]$^-$ only one isomer (M) was detected in solution.

The ^{1}H NMR spectrum of [EuaDO3A]$^{3-}$ recorded in D_2O solution at pD = 7.0 (*Figure 2.6*) shows a prevalence (*c.a.* 50%) of one isomeric species, which possesses modest paramagnetic shifts (*c.a.* 20 ppm).

Accordingly to what has been observed for the parent C_4-symmetric analogues complexes **(7)**,[10] it is reasonable to think that the major isomer in solution may be the RRR (SSS). However, in the absence of an X-ray crystal structure no definitive conclusion can be made.

Recently, it has been demonstrated that the rate of the water exchange at the lanthanide ions is dependent upon the nature and composition of the isomers of a given complex.[10] Thus, for example τ_M for [Eu·7]$^-$ was equal to 68, 140 and 270 ns (298 K) for the RRRR, RRRS and RSRS respectively. However, it can be anticipated, that in the case of the di-hydrated [EuaDO3A]$^{3-}$ a faster water exchange should be expected and thus the isomeric composition may not affect significantly the water exchange rate.

The ^{1}H NMR spectrum of [EuaDO3A]$^{3-}$ was recorded over time, in order to ascertain the stability of the complex in D_2O solution at pD = 7.0. The spectrum did not change after several weeks, confirming that no significant dissociation had occurred. Moreover, since the spectra look identical with respect to the isomer composition, no isomer interconversion took place.

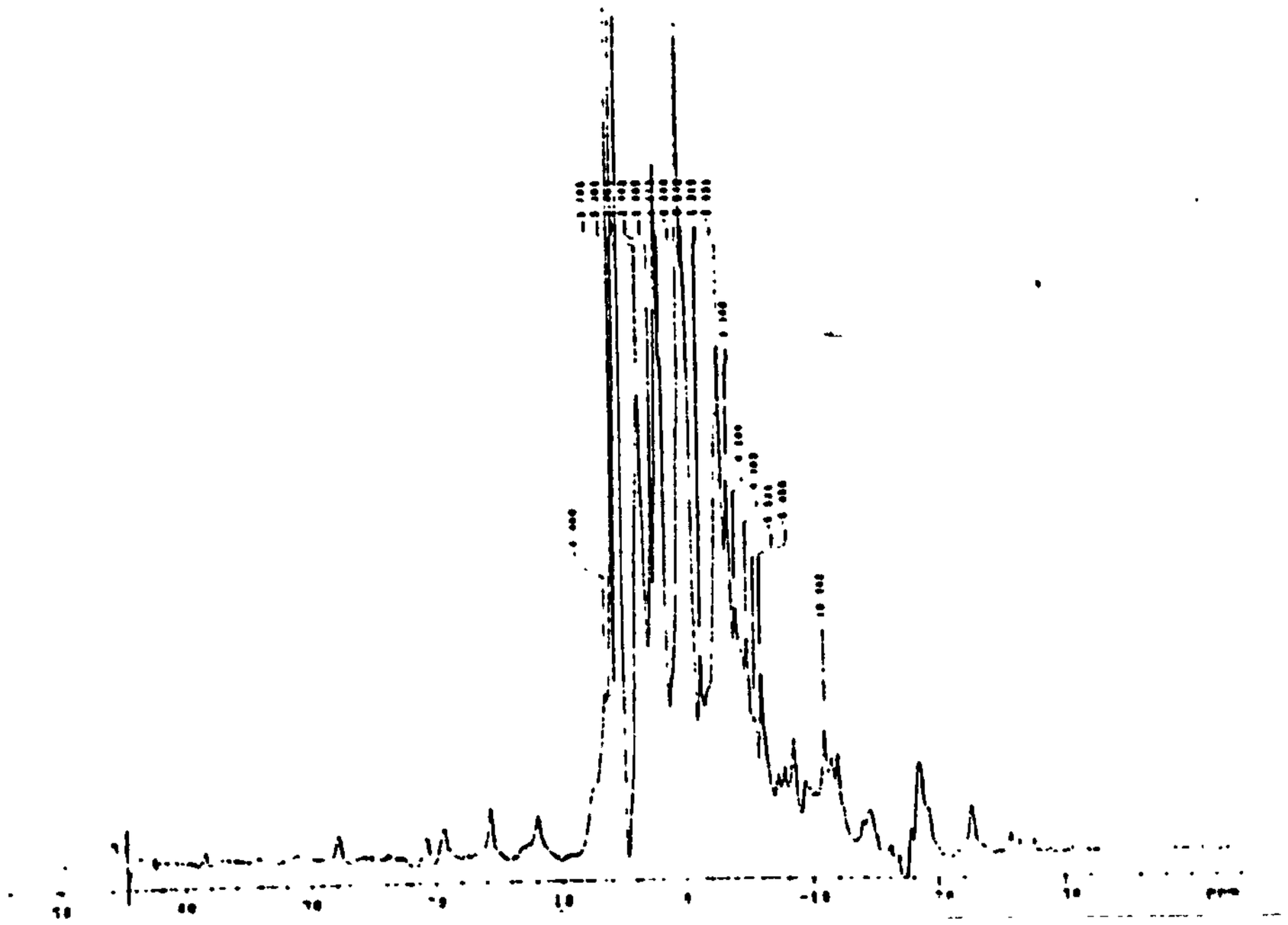

Figure 2.6 – ^1H NMR spectrum of $[EuaDO3A]^{3-}$ (200 MHz, in D_2O, pD = 7.0).

2.3.2. Emission spectra

The emission spectra of lanthanide ions are particularly sensitive to the ligand field effect. Each transition observed in the spectra is informative of the structure. The spectra of $[EuaDO3A]^{3-}$, $[EugDO3A]^{3-}$ and $[EuaDOTA]^{-}$ were recorded following direct excitation at 397 nm (293 K) in water at pH 7.20 (*Figure 2.7*).

(a)

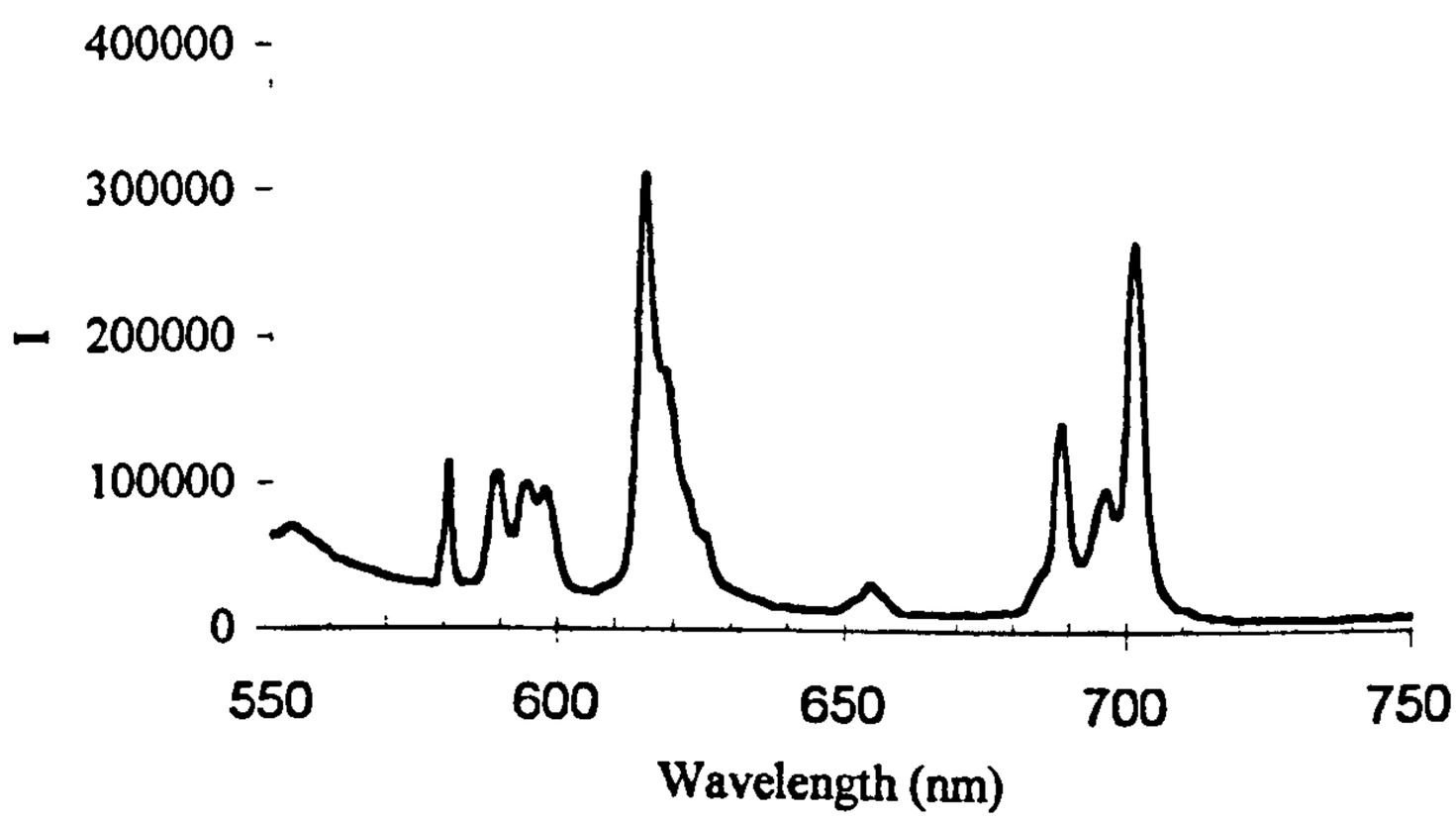

(b)

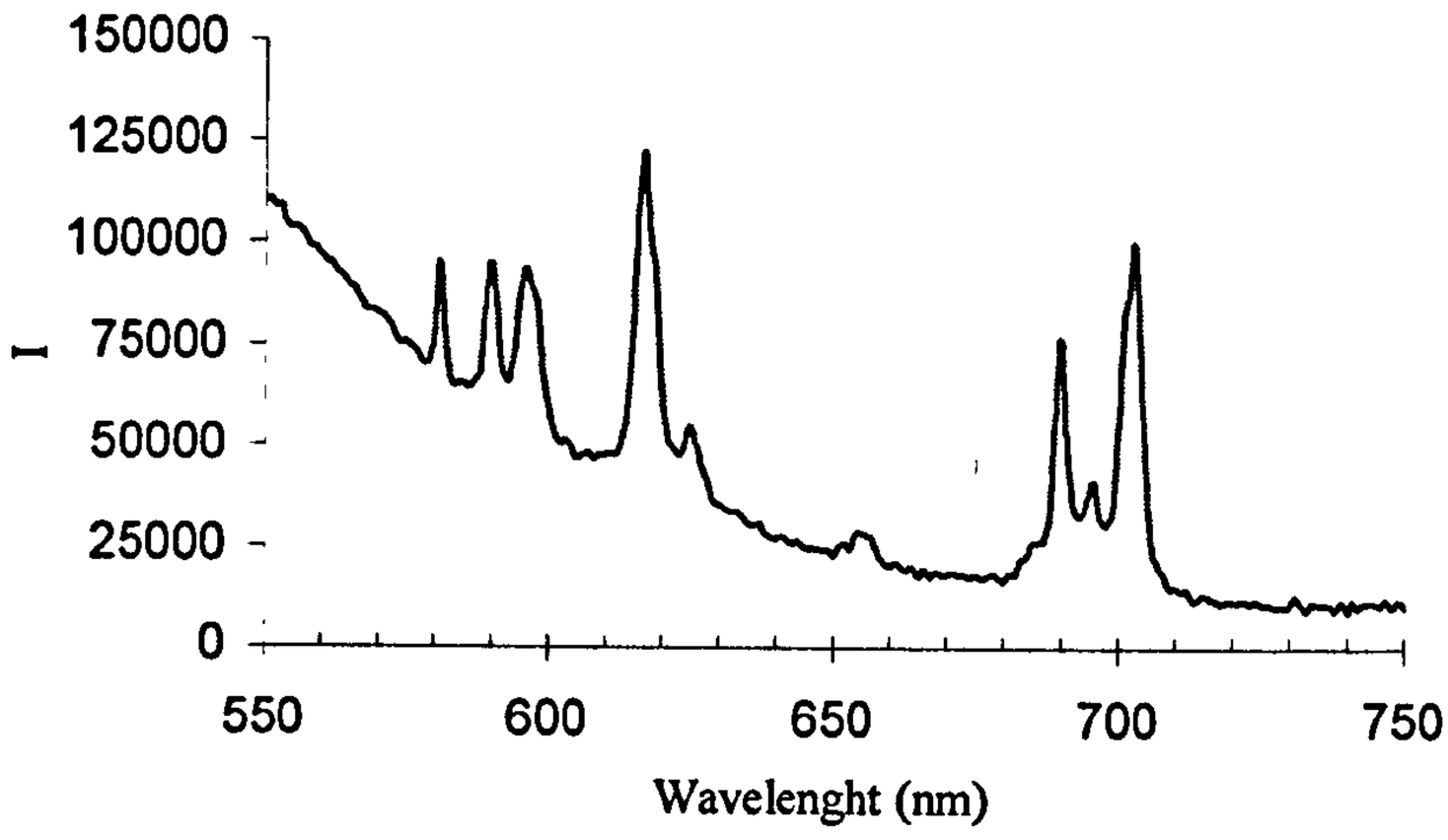

(c)

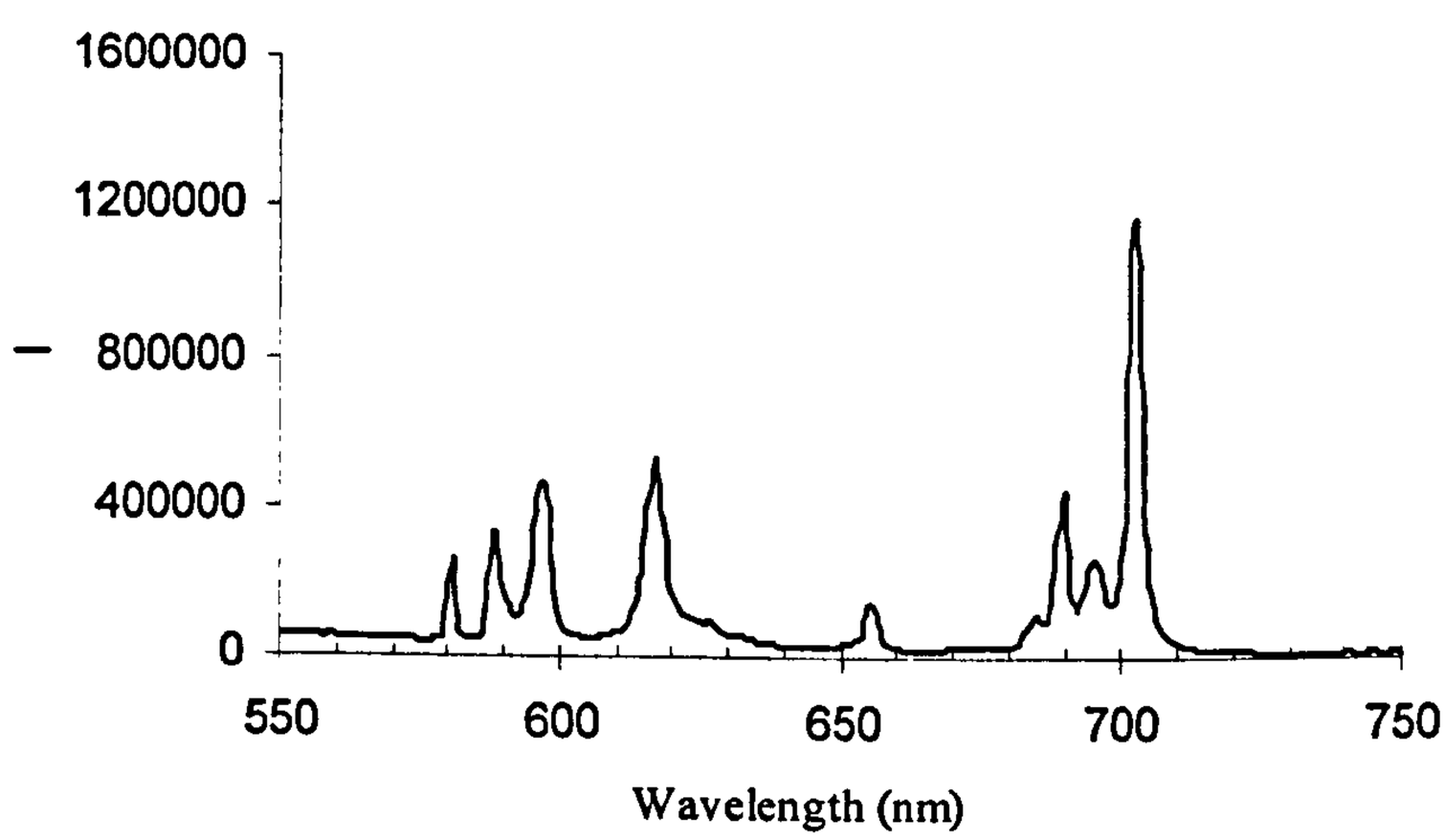

Figure 2.7 – Emission spectra in H_2O at pH =7.20 of: (a) $[EuaDO3A]^{3-}$, (b) $[EugDO3A]^{3-}$ and (c) [EuaDOTA].

The intensity of the "hypersensitive" ΔJ=2 (618 nm) transition is particular sensitive to the chemical environment. The analysis of a great number of Eu^{3+} complexes suggests that the intensity is lower for axially symmetric complexes, is sensitive to the polarizability of the axial donor and increases by lowering symmetry.[11] In addition, the number of bands in this transition is strongly determined by the site symmetry. The higher the symmetry the

lower the number of bands is observed. This is confirmed by looking at the spectra of the more symmetric [EuaDOTA]$^-$, in which the intensity ratio $\Delta J=2/\Delta J=1$ is about one and the less symmetric tri-substituted analogous $[EuaDO3A]^{3-}$, in which the intensity ratio $\Delta J=2/\Delta J=1$ is about three. However, $[EugDO3A]^{3-}$ shows a lower intensity than expected for this transition, with an intensity ratio $\Delta J=2/\Delta J=1$ approximately equal to two.

The intensity of the magnetic-dipole allowed $\Delta J=1$ (590 nm) transition does not change very much with coordination environment. However two or three bands can be observed depending on the symmetry of the complex. In complexes of low symmetry, three transitions are allowed, whereas for complexes with a C_3 or C_4 axis, only two transitions are permitted.[12] Again this observation is satisfied in the case of [EuaDOTA]$^-$, $[EugDOTA]^{3-}$ (two bands) and $[EuaDO3A]^{3-}$ (three bands), but apparently not in the case of $[EugDO3A]^{3-}$ (two bands). The spectra differ also in the form of the $\Delta J=4$ transition manifold.

The chemical environment around the metal ion must be different in $[EuaDO3A]^{3-}$and $[EugDO3A]^{3-}$, i.e. they possess different structures in solution. The total emission spectrum of $[EuaDO3A]^{3-}$ closely resembles that of [EuDO3A] (q = 1.8), whereas the spectrum of the analogue $[EugDO3A]^{3-}$ does not. A reasonable explanation for these differences can be found by considering the formation of an intra-molecular bond between one remote carboxylate group and the metal centre. This would result in a stable seven-membered ring in the case of $[EugDO3A]^{3-}$, which is much less likely in the case of $[EuaDO3A]^{3-}$, where an 8-ring chelate is required.

2.3.3. Hydration number q

Although solid-state X-ray structures can indicate the hydration number, it can be different in solution. For this reason a method for the determination of q in solution is needed. One method consists in measuring the luminescence lifetimes of Eu(III) or Tb(III) complexes in H_2O and D_2O solutions (see Chapter One). Using the empirical equation (2.1) it is possible to calculate the q value, with an uncertainly of ± 0.2.

$$q = A\left[\left(k_{H_2O} - k_{D_2O}\right) - \Delta k_{corr}\right] \qquad (2.1)$$

The constant A is equal to 1.2 and 5 in the case of europium and terbium respectively, whereas the parameter Δk_{corr} (0.25 ms^{-1} for Eu and 0.06 ms^{-1} for Tb) takes into account the effect of unbound water molecules for relatively hydrophilic complexes.

The values of the rate constants for the depopulation of the excited states of $[EuaDO3A]^{3-}$ and $[EugDO3A]^{3-}$ and the derived hydration number, *q*, are shown in *Table 2.1*.

Complex	K_{H2O} $(ms)^{-1}$	k_{D2O} $(ms)^{-1}$	q
$[EuaDO3A]^{3-}$	3.06	0.99	2.2 ± 0.2
$[EugDO3A]^{3-}$	2.51	1.20	1.2 ± 0.2

***Table 2.1** – Rate constants for the depopulation of excited states and calculated q values (295 K, 1mM complex solution at pH = 7.20).*

This method gives an estimation of the hydration number, associated with an error of about 20%. According to the data shown in *Table 2.1*, $[EuaDO3A]^{3-}$ possesses two water molecules in the inner sphere, as expected, whereas $[EugDO3A]^{3-}$ has just one. Thus in $[EugDO3A]^{3-}$ the ligand behaves as if it was octadentate. It is reasonable to suppose that, the eighth binding site is provided by a remote carboxylate group, which forms a stable seven-membered ring, as shown in *Figure 2.8*.

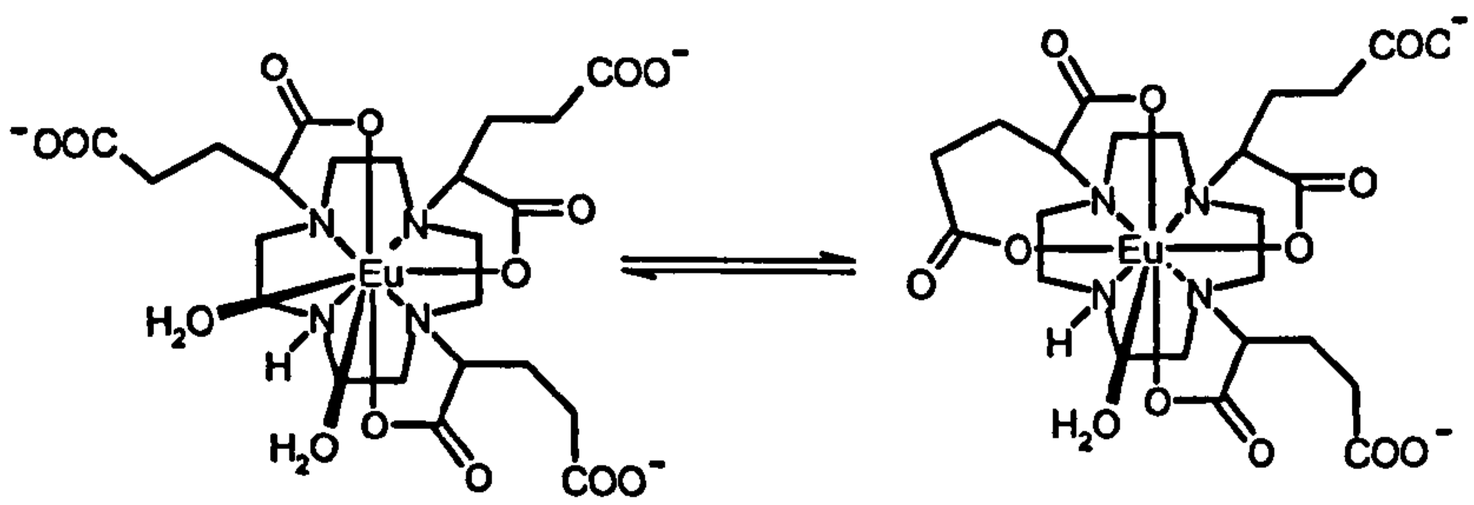

***Figure 2.8** – Intra-molecular carboxylate binding in $[EugDO3A]^{3-}$.*

The stability of the seven membered ring drives the equilibrium towards the right so that the monohydrated *q=1* species predominates in solution. On the other hand, in the case

of $[EuaDO3A]^{3-}$ intra-molecular carboxylate ligation gives a less stable eight-membered ring. This is disfavoured both entropically and enthalpically, as a result of ring strain.

Intramolecular (7-ring) carboxylate ligation can be confirmed by fluorescence studies. According to the equilibrium shown in *Figure 2.8*, when the remote carboxylate binds intra-molecularly to the metal centre, it displaces a water molecule. The displacement of co-ordinated water molecules in lanthanide complexes can be signalled by an increase in the lifetime of the lanthanide excited state and the emission intensity.

Emission spectra of $[EuaDO3A]^{3-}$ and $[EugDO3A]^{3-}$ have been recorded at different pH in a 0.1 M sodium chloride solution to maintain the ionic strength constant. The relative emission intensity (I/I_0) at 618 nm of two analogue europium complexes was plotted as function of pH (*Figure 2.9*).

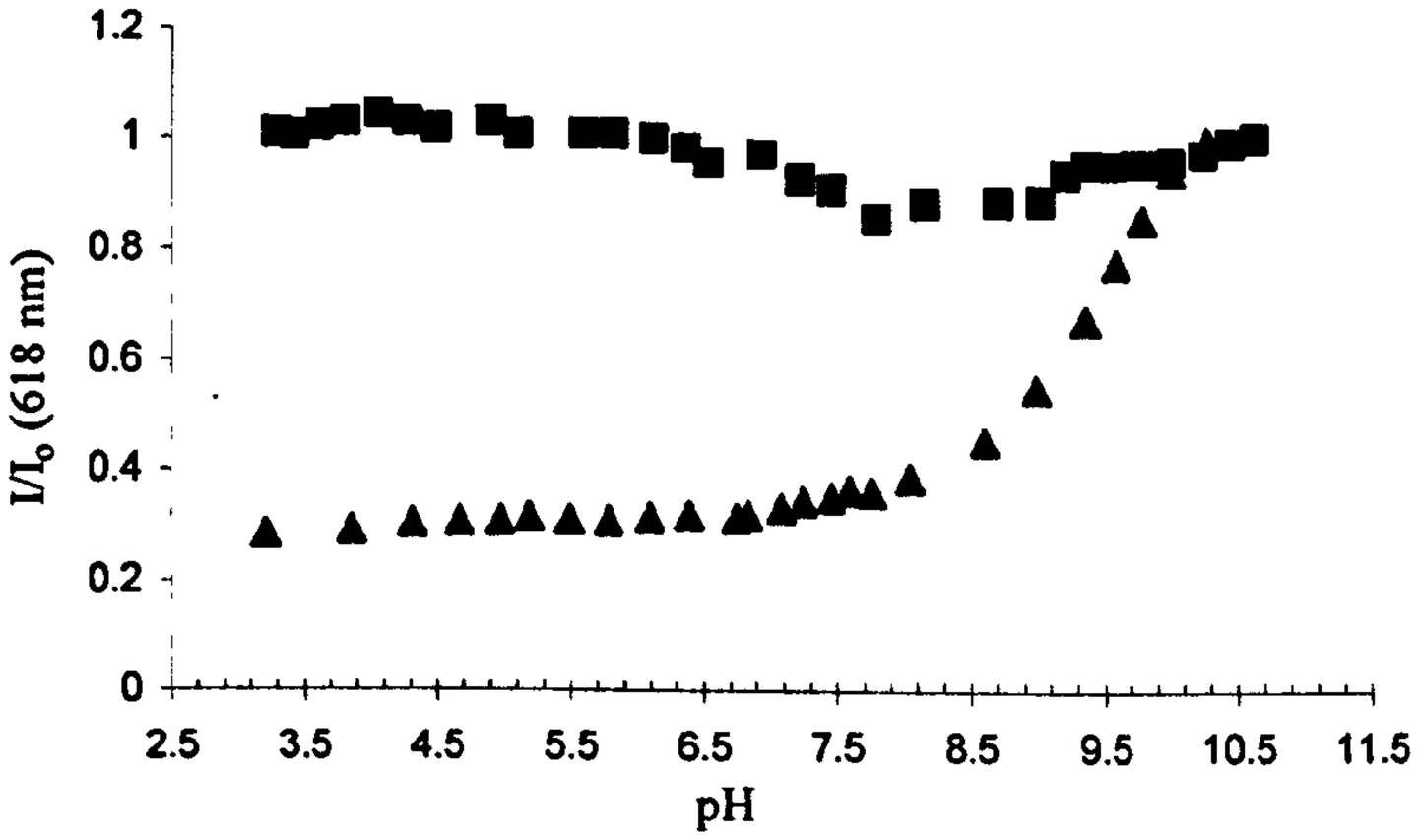

***Figure 2. 9** – Relative emission intensity (I/I_0) as function of pH in NaCl 0.1 M (λ_{exc}=397 nm, λ_{em}=618 nm, 295 K, [EuL] 1mM) for $[EuaDO3A]^{3-}$ (triangles) and $[EugDO3A]^{3-}$ (squares).*

The increment observed beyond pH 8.0 in the case of $[EuaDO3A]^{3-}$ is associated with the binding of carbonate deriving from the atmospheric carbon dioxide. The concentration of HCO_3^- falls from *c.a.* 90% at pH 8.9 to less than 2% at pH 4.9. Accordingly, the effective concentration of HCO_3^- in solution is determined by the pH of the solution and above pH 9.0 significant amount of CO_3^{2-} are present (pK_a = 10.2 at 298 K). Carbonate binding has been proven in several related studies, especially with cationic complexes where electrostatic attraction favors complex formation.[13] However, upon the same conditions

$[EugDO3A]^{3-}$ shows a quite different behaviour. The relative emission intensity does not change appreciably over the whole range of pH investigated, suggesting a lesser carbonate binding affinity. Binding of dissolved carbonate is inhibited by the intra-molecular binding of the remote carboxylate. However, a closer look to the profile reveals slight changes between pH 6.5 and 9.0. This suggests competition between the intra-molecular carboxylate arm ligation and the inter-molecular carbonate binding at the metal center. Because of the low concentration of carbonate dissolved in solution, the equilibrium is strongly shifted towards the intramolecular species.

2.4 Anion binding studies

Contrast agents operate in an environment in which ions, such as carbonate (30 mM), phosphate (0.9 mM), citrate (0.13 mM) and lactate (2.3 mM) are present. If they bind the metal centre, displacing one or both the water molecules, the efficiency of the contrast agent will decrease. So it is important to study the anion binding properties of such systems. The displacement of water molecules by coordinating anions can be detected by an increment in the emission intensity. It is well known that OH oscillators, as in bound water molecules, are the most effective quenchers of the luminescence of lanthanide ions.[14] If they are displaced by anions, the quenching effect is reduced and the emission intensity is increased. Emission spectra of $[EuaDO3A]^{3-}$ and $[EugDO3A]^{3-}$ have been recorded at different pH in an anion containing solution that simulates an extra-cellular environment and the relative emission intensity (I/I_0) at 618 nm was plotted as function of pH (*Figure 2.10).*

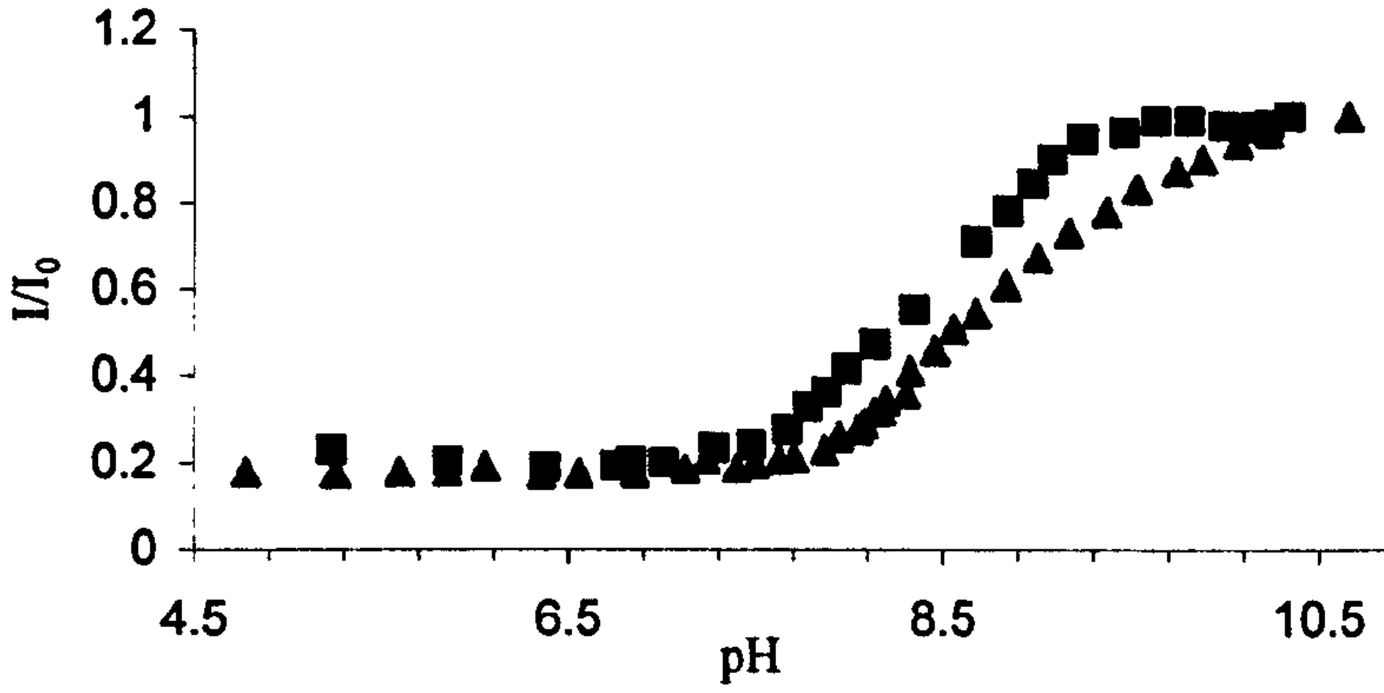

***Figure 2.10** – Relative emission intensity (I/I_0) of $[EuaDO3A]^{3-}$ (squares) and $[EugDO3A]^{3-}$ (triangles) as function of pH. (λ_{exc}=397 nm, λ_{em}=618 nm, 295 K, H_2O, 30 mM $NaHCO_3$, 100 mM NaCl, 0.9 mM NaH_2PO_4, 2.3 mM lactate and 0.13 mM citrate).*

Both complexes undergo an increment in the relative emission intensity beyond pH 7.5, suggesting the displacement of water molecules by anions. The equilibrium shown in *Figure 2.11* helps to rationalize the above experimental profiles.

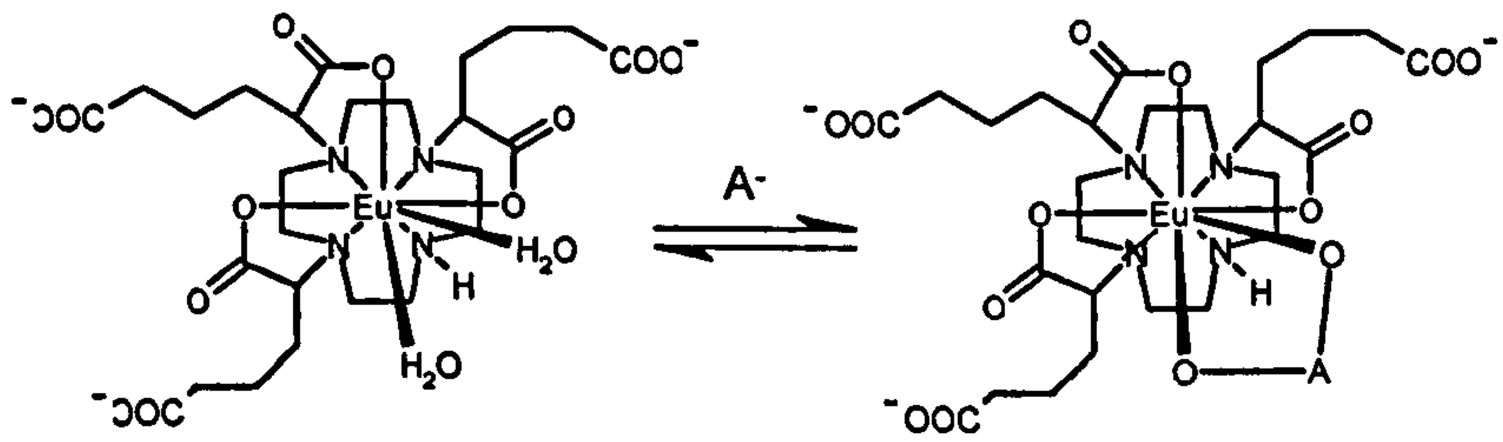

***Figure 2.11** – Formation of the ternary adduct complex-anion.*

The pH response of $[EugDO3A]^{3-}$ exhibits a change towards higher pH, suggesting a lesser anion binding affinity, compared to $[EuaDO3A]^{3-}$. Again, this behaviour supports the formation of an intramolecular binding process, discussed above.

In the case of $[EugDO3A]^{3-}$, both the remote carboxylate and the anions in solution (possibly carbonate) "compete" for binding to the metal centre. It is only a consequence of the large excess of carbonate (30 times more concentrated than the europium complex) that the equilibrium is strongly shifted toward the formation of the ternary adduct at higher pH.

In order to unequivocally prove which anion is bound to the europium centre, emission spectra in single anion containing solutions at different pH have been recorded. In lactate (2.3 mM), phosphate (0.9 mM) and citrate (0.13 mM) solutions, the emission spectra did not show any variation with pH, indicating the absence of binding. The spectra recorded in phosphate solution are shown in *Figure 2.12*, as example. However, in carbonate solution (30 mM) significant changes were observed on higher pH (*Figure 2.12)*. The intensity of the hypersensitive $\Delta J = 2$ transition increases by about three times from pH 4.5 to pH 10.0. Significant changes are observed in the $\Delta J = 1$ transition, which shows three bands at acidic and neutral pH, but just two major bands at alkaline pH.

Taken together these emission spectra strongly suggest that it is indeed the carbonate anion, which is responsible for displacing the water molecules at higher pH and it forms the ternary adduct.

In conclusion, these experiments suggest that the complexes investigated are likely to bind anions (particularly carbonate) in an extra-cellular environment. However, at physiological pH, the extent of inter-molecular anion binding is less then 5% and should not affect significantly the efficiency of these systems as contrast agents.

Moreover, this series of experiments clearly exclude $[GdgDO3A]^{3-}$ as a possible *q=2* MRI contrast agent candidate. The length of its hydrocarbon chain promotes intramolecular carboxylate ligation, which then represents the eight co-ordination site for the metal center. The resulting complex is octadentate with just one water molecule in the inner sphere. On the other hand $[GdaDO3A]^{3-}$ possesses two water molecules in the inner sphere, which are "retained" at physiological pH in an extra-cellular-like environment, because the anion binding is suppressed by electrostatic repulsion.

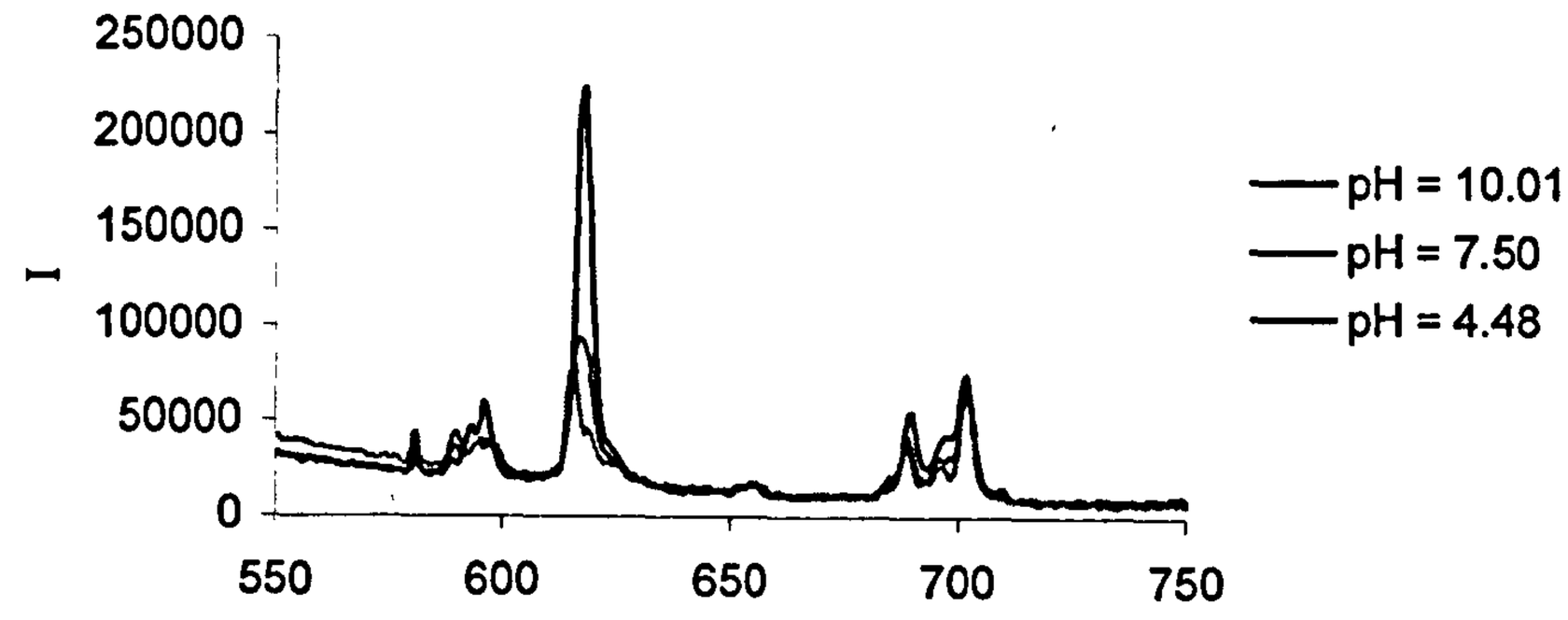

***Figure 2.12** – Emission spectra in single anions containing solution ($NaHCO_3$ 30 mM at the top and NaH_2PO_4 0.9 mM at the bottom).*

2.5 Stability of the complexes

At clinical doses of about 0.1 $mM^{-1}kg^{-1}$, Gd^{3+} complexes used as contrast agents for MRI are not toxic, although individually their components, the metal ion and the free ligand, usually are. The Gd^{3+} aqua ion can inhibit neuromuscular transmission by blocking calcium channels[15,16] and may be deposited as insoluble salts in skeleton, liver and spleen.[17] Animal studies have demonstrated a long-term retention of gadolinium in the body,[18-20] with a build up in the skeleton and the liver.For these reasons the complexes used as CA's must be very stable and the determination of their thermodynamic and kinetic stability becomes an important issue.

A preliminary study was conducted following the stability of $[EuaDO3A]^{3-}$ by ^1H NMR. The ^1H NMR spectrum of $[EuaDO3A]^{3-}$ was recorded over time in D_2O solution at

pD = 6.80. No variation was observed over a period of several weeks, suggesting a "good" stability of this complex in aqueous solution.

However, an *in-vivo* environment is a more complicated one. Endogenous extracellular ions such as Cu^{2+}, $Ca^{2+}$and especially Zn^{2+} can compete with Gd^{3+}, expelling it from the complex through a transmetallation process. Among these ions Cu^{2+} is present in small concentration in the blood (1-10 μmol/L)[21] and it is usually tightly bound, whereas Ca^{2+} has a relatively low affinity for this kind of organic ligands.[22] On the other hand, Zn^{2+} may be present in the blood at relatively high concentration (55-125 μmol/L) and can form stable complexes with these ligands. So it becomes "potentially dangerous", because it can displace the Gd^{3+}ion.

It is indeed important to study the stability of gadolinium complexes in the presence of zinc. A relaxometric method proposed by Laurent and co-workers has been followed.[23] The technique is based on the measurement of the evolution of the paramagnetic water proton longitudinal relaxation rate (R_{1p}) of a buffered solution (phosphate buffer pH = 7.0) containing equimolar amounts of the gadolinium complex and zinc chloride. If transmetallation occurs the diamagnetic zinc ion will displace gadolinium, which then precipitates in the form of its insoluble phosphate salt (equations 2.2–2.4). This will result in a reduction of the observed water proton relaxation rate.

$$LigGd^{(n)-} \rightarrow Lig^{(n+3)-} + Gd^{3+} \qquad (2.2)$$

$$Lig^{(n+3)-} + Zn^{2+} \rightarrow LigZn^{(n+1)-} \qquad (2.3)$$

$$Gd^{3+} + PO_4^{3-} \rightarrow Gd(PO_4)_{ins.} \qquad (2.4)$$

In *Figure 2.13* is shown a plot of the relative water proton longitudinal relaxation rates ($R_{1p}(t)/ R_{1p}(0)$) as function of time in the case of $[GdaDO3A]^{3-}$, $[GdgDO3A]^{3-}$ and $[GdaDOTA]^{-}$.

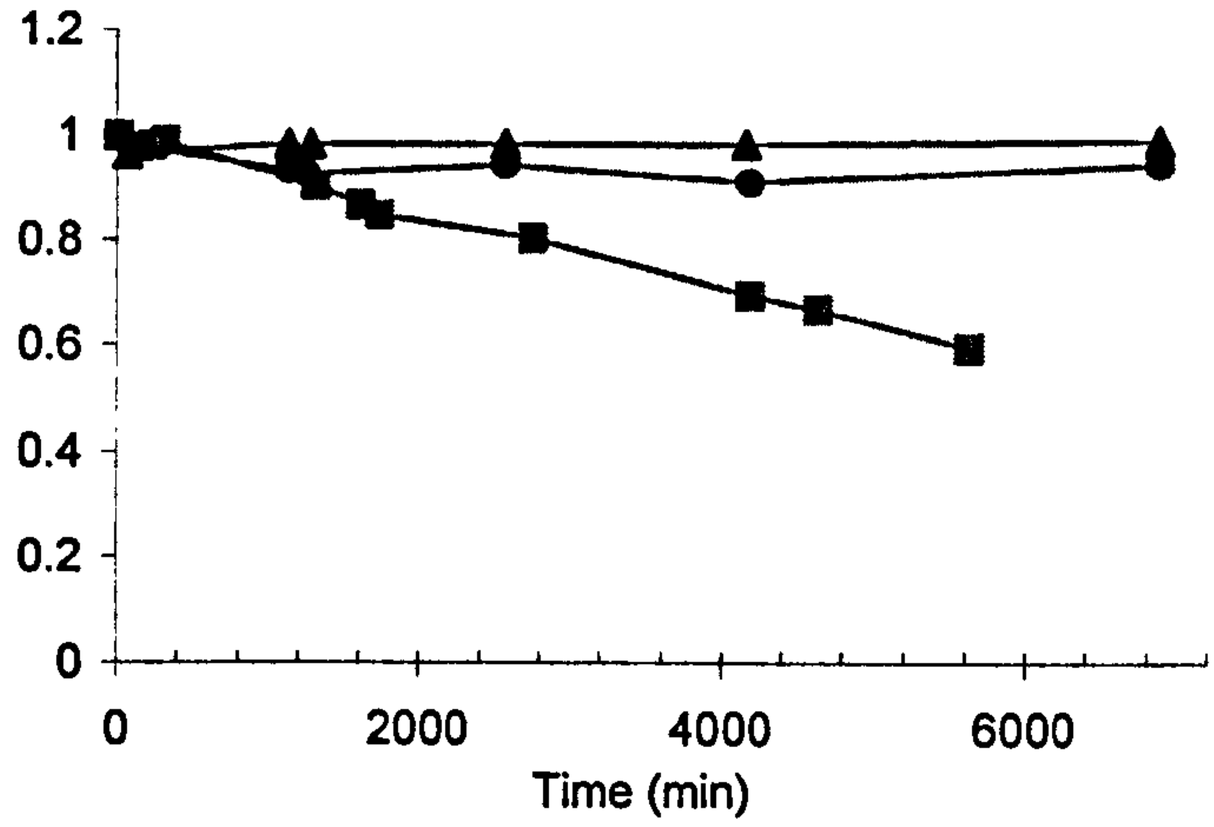

***Figure 2.13** – Relative longitudinal relaxation rates as function of time at 65 MHz and 293 K for [GdaDO3A]$^{3-}$ (squares), [GdgDO3A]$^{3-}$ (circles) and [GdDOTA]$^{-}$ (triangles).*

Laurent and co-workers[23] arbitrarily defined a kinetic index (*K.I.*), which is the time required to reach 80% of the initial $R_{1p}(t)/ R_{1p}(0)$ value and a thermodynamic index (*T.I.*), which is the $R_{1p}(t)/ R_{1p}(0)$ value measured after three days (4320 min). These parameters are shown in *Table 2.2* for [GdaDO3A]$^{3-}$, [GdgDO3A]$^{3-}$ and [GdaDOTA]$^{-}$ in comparison with three commercially available contrast agents.

Complex	T.I.	K.I.
[GdaDO3A]$^{3-}$	0.70	2760
[GdgDO3A]$^{3-}$	0.97	∞
[GdaDOTA]$^{-}$	0.99	∞
[GdHPDO3A]	0.99	∞
[GdDTPA]$^{2-}$[23]	0.49	260
[GdDOTA]$^{-}$[23]	0.99	∞

***Table 2.2** – K.I. and T.I. index measured at 65 MHz and 293 K.*

The thermodynamic indexes indicate that more than 98% of the paramagnetic relaxation rate is retained for the monohydrated macrocyclic complexes [GdDOTA]$^{-}$

(Dotarem), [GdHPDO3A] (Omniscan) (known for their high thermodynamic stability), $[GdaDOTA]^-$ and $[GdgDO3A]^{3-}$. The complex $[GdaDO3A]^{3-}$ retains less than 70% of the initial value, suggesting a less thermodynamic stability. However, it is higher than the *T.I.* measured for the acyclic complex $[GdDTPA]^{2-}$ (Magnevist), which has been used commercially since 1988.

By looking at the kinetic indexes (KI), the same sort of conclusions can be drawn. $[GdDOTA]^-$ (Dotarem), [GdHPDO3A] (Omniscan), $[GdaDOTA]^-$ and $[GdgDO3A]^{3-}$ all show excellent kinetic stability, they practically do not undergo transmetallation. The di-hydrated $[GdaDO3A]^{3-}$ instead exhibits a KI value of 2760, but this is more than ten times larger than the one measured for Magnevist.

2.6. Relaxometric studies

2.6.1. Relaxivity

The efficiency of a contrast agent is usually expressed in term of *relaxivity*. As we have seen in Chapter One, it represents the enhancement of the water relaxation rate per unit of concentration and it is usually expressed in $mM^{-1}s^{-1}$.

The observed longitudinal relaxation rate can be divided into a diamagnetic and a paramagnetic contribution, due to the presence of the paramagnetic species. The latter one, in absence of solute-solute interaction, has a linear dependence with the concentration of complex as shown in equation (2.5), (2.6) and (2.7).

$$R_{1obs} = R_{1d} + R_{1p} \qquad (2.5)$$

$$R_{1p} = r_{1p}[GdL] \qquad (2.6)$$

$$R_{1obs} = R_{1d} + r_{1p}[GdL] \qquad (2.7)$$

A plot of the observed longitudinal water relaxation rate R_{1obs} as function of the concentration of the complex results in a straight line, in which the slope represents the relaxivity (r_{1p}), as shown in *Figure 2.14* for $[GdaDO3A]^{3-}$ (H_2O; pH = 7.20; 65 MHz; 293K)

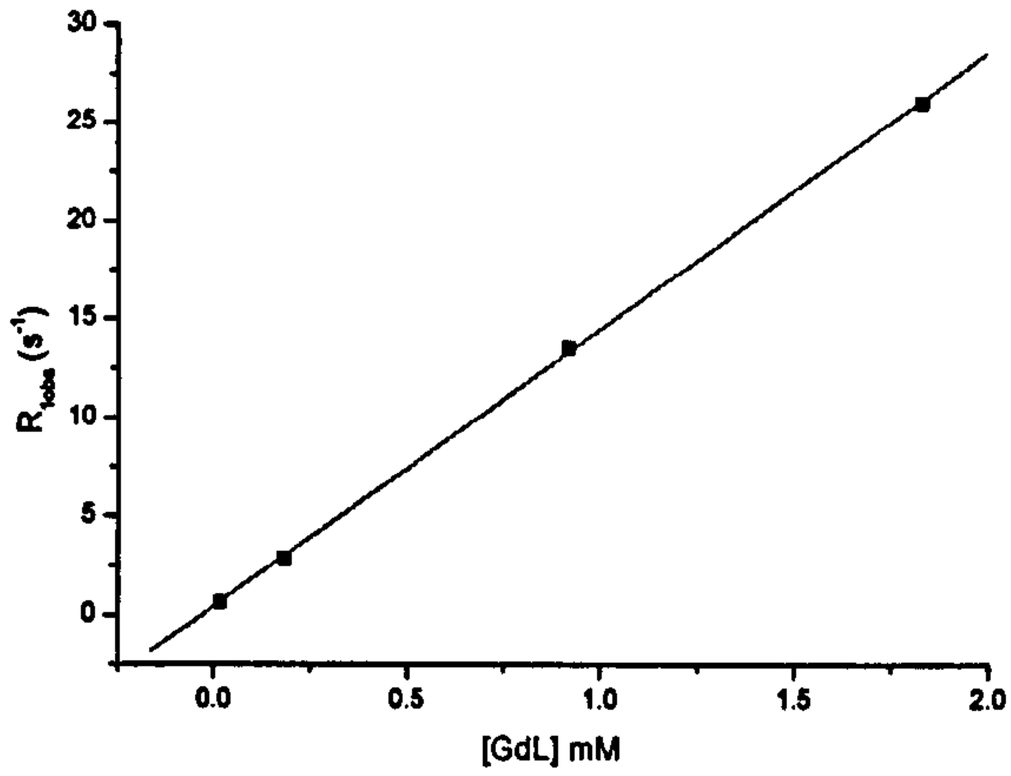

Figure 2.14– *Observed longitudinal relaxation rate (R_{1obs}) as function of the concentration of complex (H_2O at pH =7.20, 65 MHz, 293 K).*

The calculated value in water (13.9 $mM^{-1}s^{-1}$) is significantly higher then those reported for gadolinium complexes of similar size and based on heptadentate ligands.[4] These values are reported in *Table 2.3* in comparison with the values calculated under the same conditions in an anionic background and in human serum.

Complex	r_{1p} ($mM^{-1}s^{-1}$) Water	r_{1p} ($mM^{-1}s^{-1}$) Anionic bkg	r_{1p} ($mM^{-1}s^{-1}$) Human Serum
$[GdaDO3A]^{3-}$	13.9	10.6	11.6
$[GdgDO3A]^{3-}$	6.4	4.8	7.1
$[GdaDOTA]^{-}$	8.9		11.9
$[GdgDOTA]^{-}$	8.8		11.1
$[GdDO3A]$ *4	6.0		
$[GdPCP2A]^{*}$ 4	8.3		
$[GdaDO3A]^{3-*}$	12.3		

Table 2.3 *– Relaxivity in water at pH =7.20, 65 MHz and 293K. *At 20 MHz and 298K.*

The relaxivities measured at 65 MHz and 293 K (13.9 $mM^{-1}s^{-1}$) is about 12% higher than the one measured at 20 MHz and 298 K (12.3 $mM^{-1}s^{-1}$). This difference is mainly attributed to the temperature change. In fact, relaxivity tends to increase at lower temperatures for low molecular weight chelates. This is a consequence of slower tumbling

rates. [4] On the other hand, the difference in magnetic field (from 65 to 20 MHz) does not influence significantly the relaxivity, as it lies in the flat region of the NMRD profile (see *Figure 2.18*).

The comparison between the relaxivity of $[GdaDO3A]^{3-}$ and its monohydrated analogue $[GdaDOTA]^{-}$ highlights the contribution of the additional water molecule, which brings an increment close to 40% in water solutions. The surprisingly high magnitude of this parameter could derive, however from an additional outer or second sphere contribution. The three remote carboxylate arms can "trap" water molecules in the second sphere by forming hydrogen bonds. This is known to occur with ligands bearing phosphate groups, such as [GdPCP2A].[3] However, the effect exhibited by $[GdaDO3A]^{3-}$ is remarkably higher.

In addition, these data confirm the different behaviour of $[GdaDO3A]^{3-}$ and $[GdgDO3A]^{3-}$. The latter one being a monohydrated complex (as discussed in the previous paragraphs) exhibits a much lower relaxivity both in water and in human serum.

In order to explore more deeply the properties of these complexes, the relaxivity was measured as function of pH. The pH dependence of relaxivity in water for $[GdaDOTA]^{-}$ (65 MHz and 293 K) and $[GdaDO3A]^{3-}$ (20 MHz and 298 K) is shown below (*Figure 2.15*).

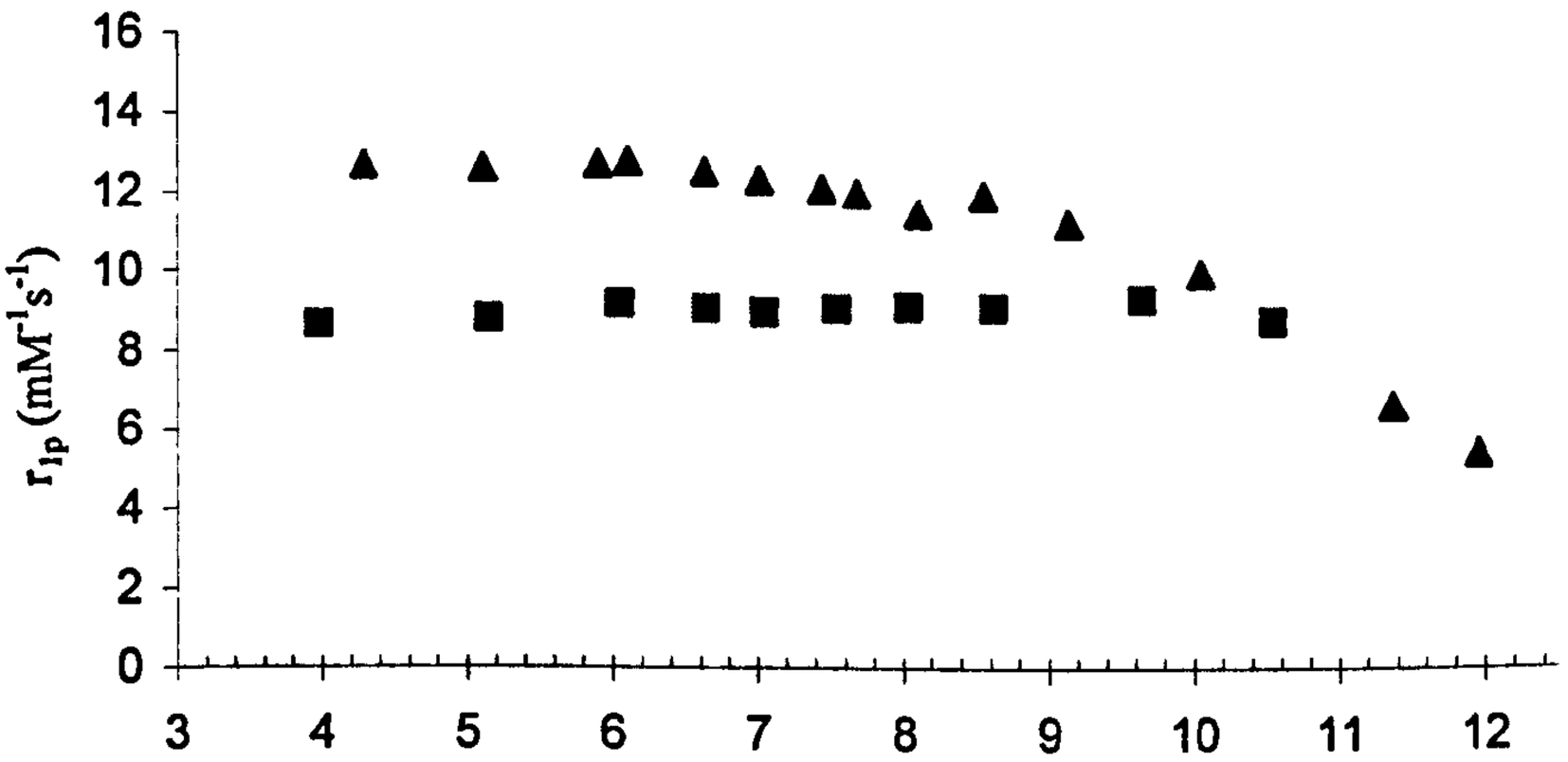

***Figure 2.15** – Relaxivity as function of pH for $[GdaDO3A]^{3-}$ (65 MHz; 293 K; triangles) and $[GdaDOTA]^{-}$ (20 MHz; 298 K; squares).*

The decrement observed over pH 8.5, in the case of the $q=2$ complex is due to the binding of dissolved carbonate deriving from the atmospheric carbon dioxide. As it has

been demonstrated previously by luminescence studies on the Eu (III) analogue complex, binding the metal centre, the carbonate anion displaces the two water molecules, reducing the relaxivity.

On the other hand, the octadentate q=1 $[GdaDOTA]^-$ does not show any appreciable variations in relaxivity over the whole range of pH investigated, because of its lower anion binding affinity.

How can *in-vivo* concentration of carbonate (30 mM) influence the relaxivity (*i.e* the efficiency) of $[GdaDO3A]^{3-}$? In order to answer this question, the relaxivity was measured as function of pH in anionic background (*i.e.* the simulated extra-cellular solution) and in human serum (*Figure 2.16*).

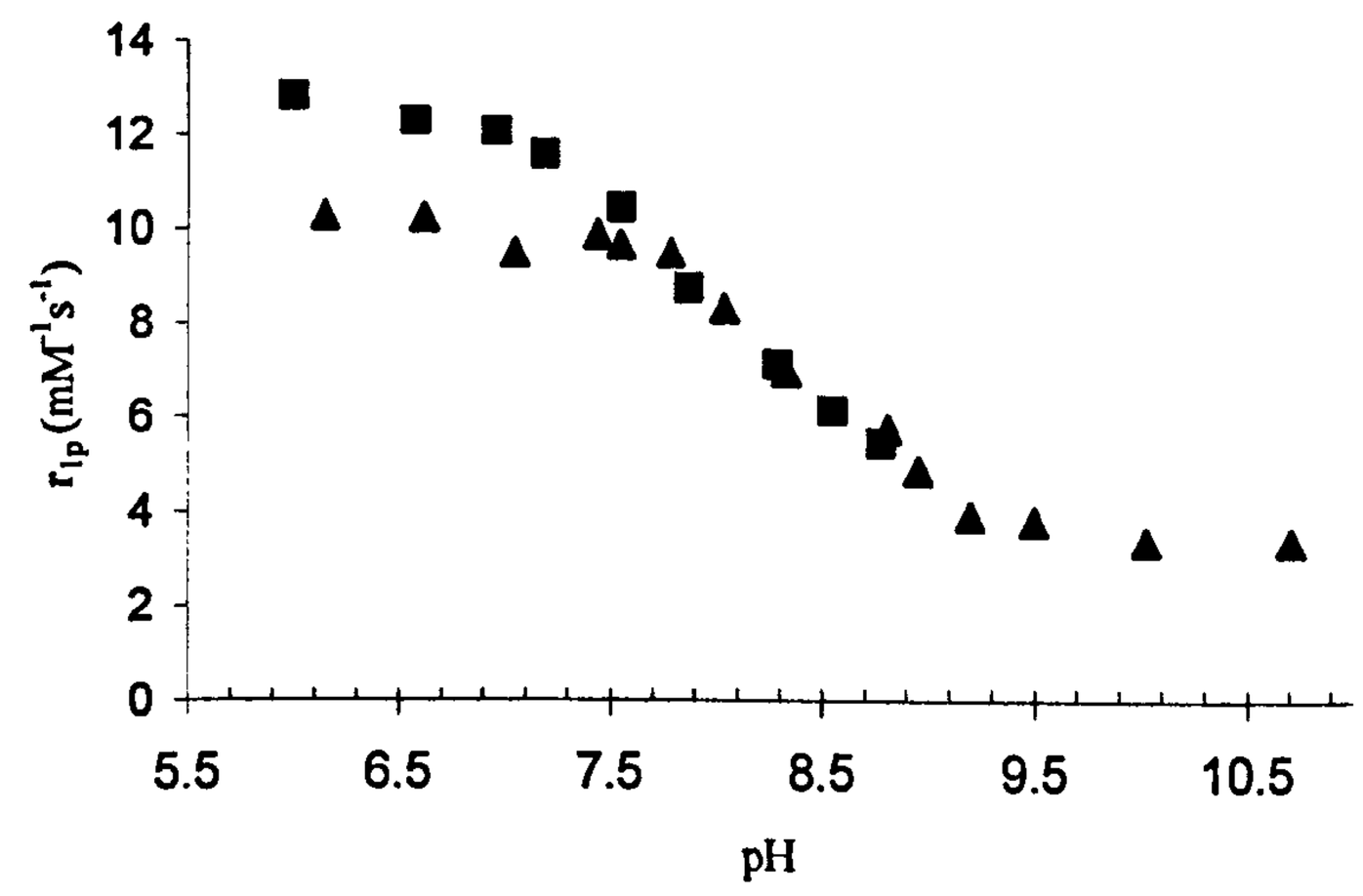

***Figure 2.16** – Relaxivity vs pH of $[GdaDO3A]^{3-}$ at 65 MHz, 293 K in human serum (squares) and anionic background (triangulars).*

The profile in anion solution shows a decrement in relaxivity above pH 8.0, which then reaches a minimum value close to 3 $mM^{-1}s^{-1}$ at pH 9.5, corresponding to a pure outer sphere contribution. The equilibrium shown in *Figure 2.11* helps to understand this experimental behaviour. Again the carbonate anion displaces the two water molecules reducing the relaxivity of the complex. The system clearly changes from being a q=2 complex in acidic and neutral media to a *q=0* species at alkaline pH. However, at physiological pH the complex still possesses two water molecules in the inner sphere and thus the relaxivity remains close to its highest value. So the efficiency of $[GdaDO3A]^{3-}$ as

contrast agent for MRI is not affected significantly by the presence of *in-vivo* concentration (30 mM) of carbonate.

The curve in human serum can be explained by the same sort of considerations.

It should be noted at this point that defining relaxivity in terms of $mM^{-1}s^{-1}$ in protein solution (such as human serum) can be misleading. High concentrations of protein are dissolved in serum (*i.e.* Human Serum Albumin HSA 0.6 mM). Usually at the concentrations used more than 20% of the volume is occupied by protein and hence less than 80% by water. The molar concentration of 1 mmol of Gd^{3+} complex in a litre of serum is 1 mM, but the molal concentration would be 1.25 mmolal, so the reported relaxivity is overestimated by 25%. For these reasons the relaxivities quoted in human serum have been corrected by the same percentage.

The slightly higher values observed in human serum may now be ascribed to an increment in the micro-viscosity of the medium, which increases the rotational correlation time τ_M, slowing the tumbling in solution and thus increasing the relaxivity. An important point to be noticed is that at physiological pH the high relaxivity of $[GdaDO3A]^{3-}$ measured in water, is "retained" in human serum, indicating suppression of protein/anion binding. Such features render this complex extremely attractive as a contrast agent for MRI.

The comparison between the pH dependence of the relaxivity for $[GdaDO3A]^{3-}$ and the relative emission intensity of the analogous europium complex is shown in *Figure 2.17*. The nice correlation reveals a near mirror image relationship. Such behaviour is consistent with the idea that increases in r_{1p} are directly proportional to changes in the hydration state *q*, while the Eu emission intensity decreases in direct proportion.

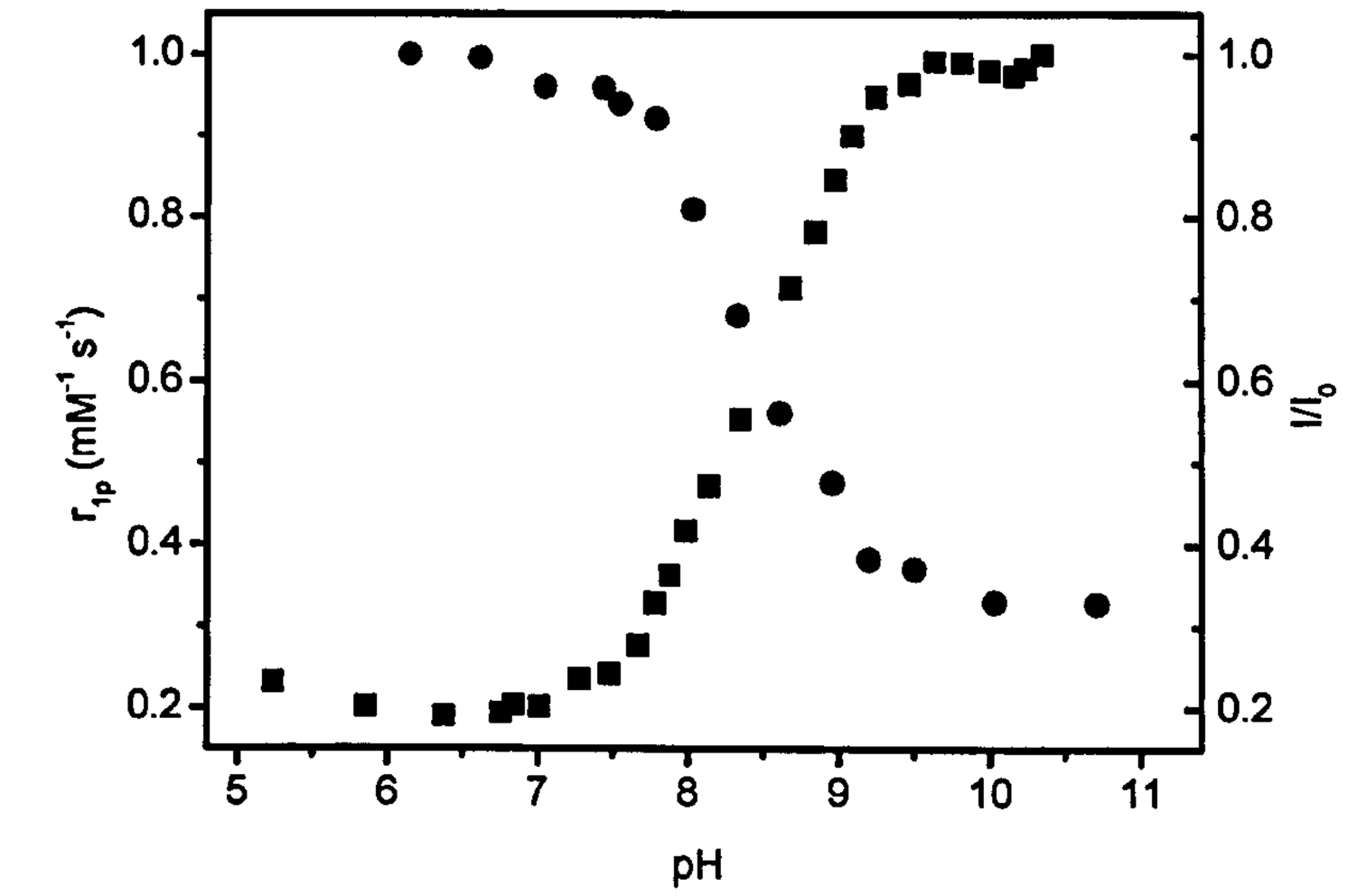

***Figure 2.17** – Comparison between the pH dependence of the relaxivity of $[GdaDO3A]^{3-}$ on the left and the relative emission intensity of the analogue $[EuaDO3A]^{3-}$ on the right.*

2.6.2. NMRD profiles

To characterize the different contributions to the observed relaxivity NMRD profiles, over an extended range of frequencies at 25 ^{0}C, were measured for $[GdaDO3A]^{3-}$, $[GdgDO3A]^{3-}$ and $[GdaDOTA]^{-}$ (*Figure 2.18*).

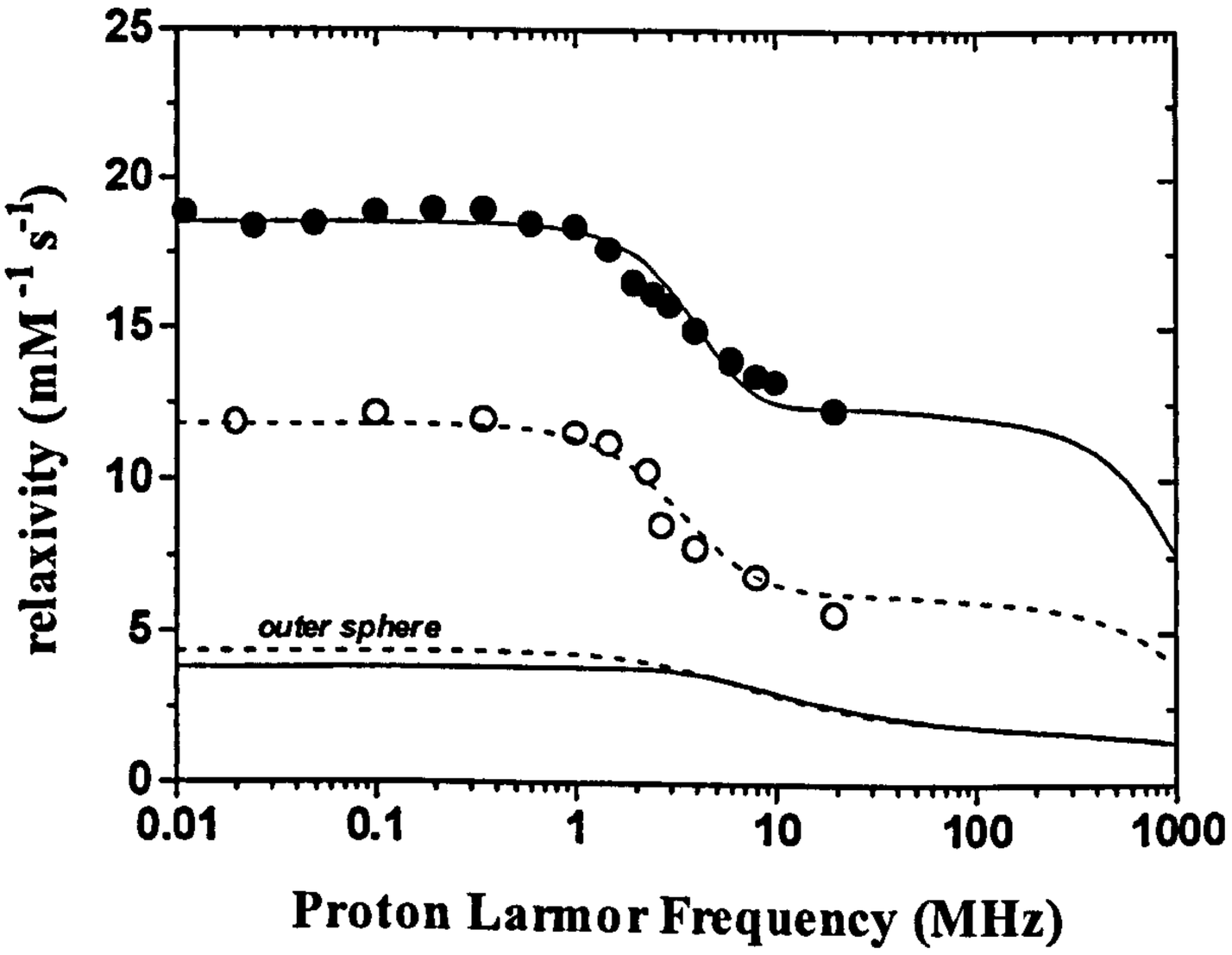

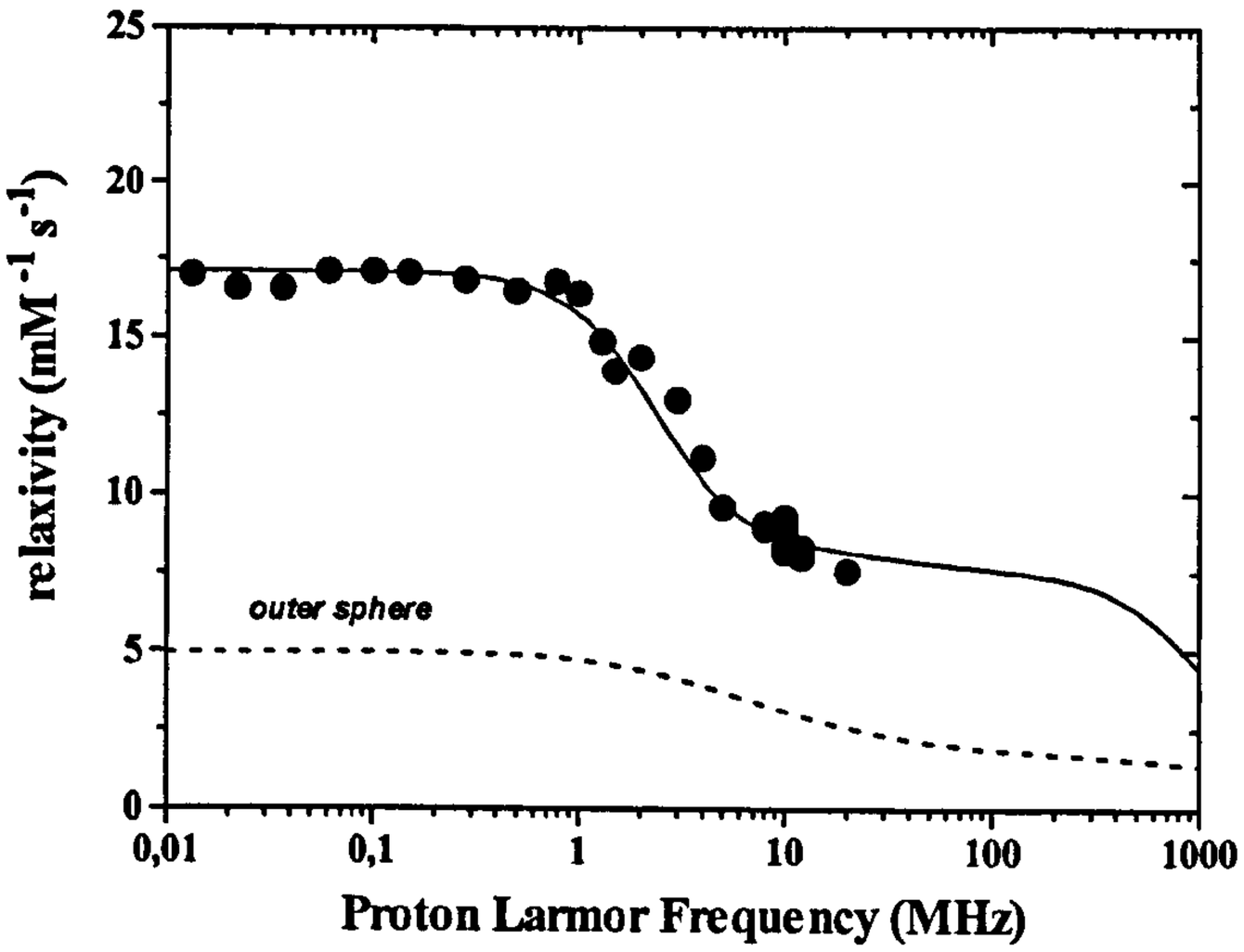

Figure 2.18 *– NMRD profiles in water solution at pH = 7.0 and 298 K for $[GdaDO3A]^{3-}$ (black circles) $[GdgDO3A]^{3-}$ (white circles) at the top and for $[GdaDOTA]^{-}$ (black circles) at the bottom.*

The curves were fitted to the equations for inner and outer sphere paramagnetic relaxation (see Chapter One) to give the parameters listed in *Table 2.4*. The dashed lines in *Figure 2.18* represent the outer sphere water contribution.

Complex	Δ^2 (s^{-2})/10^{-19}	τ_V (ps)	τ_R (ps)
$[GdaDO3A]^{3-}$	2.75	31	130
$[GdgDO3A]^{3-}$	3.14	16	130
$[GdgDOTA]^{-}$	2.30	10	116
$[GdaDOTA]^{-}$	1.23	20	154

Table 2.4 *– Best fitting parameters determined by analyses of NMRD profiles.*

In the analyses a reasonable choice was made for *r* (2.98 Å), the distance between the metal centre and closed water molecules, based on known values of similar complexes. The parameters *a* (distance of the closest approach of diffusing water) and D (diffusion coefficient) were fixed to typical values of 3.8 Å and $2.24 \cdot 10^{-5}$ cm^2s^{-1} respectively, whereas

q was considered as two in the case of $[GdaDO3A]^{3-}$ and as one in the case of $[GdgDO3A]^{3-}$ and $[GdaDOTA]^{-}$, as has been measured by luminescence studies.

The comparison of these profiles highlights the different behaviour for the two analogous DO3A derivatives, which differ in the number of water molecules in the inner sphere.

The calculated rotational correlation times τ_R are in the expected range for complexes of similar molecular volume.[4]

The profiles depend only slightly on the actual value of the water residence lifetime τ_M, which then cannot be determined with sufficient accuracy by the fitting process.

An independent assessment of this important parameter can be obtained by variable-temperature proton-decoupled ^{17}O NMR measurements of the water nuclear transverse relaxation rate. The quadrupolar ^{17}O nucleus is NMR active and when it is co-ordinated to a paramagnetic ion (*i.e.* Gd^{3+}) its relaxation time is shortened. If the exchange of the bound water is sufficiently fast, then the effect will be transferred to the bulk water. Decrements in the transverse relaxation times T_2 bring broadening in the linewidth of the signal arising from the bound oxygen. By measuring the effect of the temperature on the linewidth of an ^{17}O enriched solution containing the paramagnetic complex and correcting it for the natural linewidth, a profile of the paramagnetic transverse relaxation rate (R_{2p}) can be obtained. Since the relaxation rate is dependent on the contribution from coordinated water molecules, it is also dependent on τ_M.

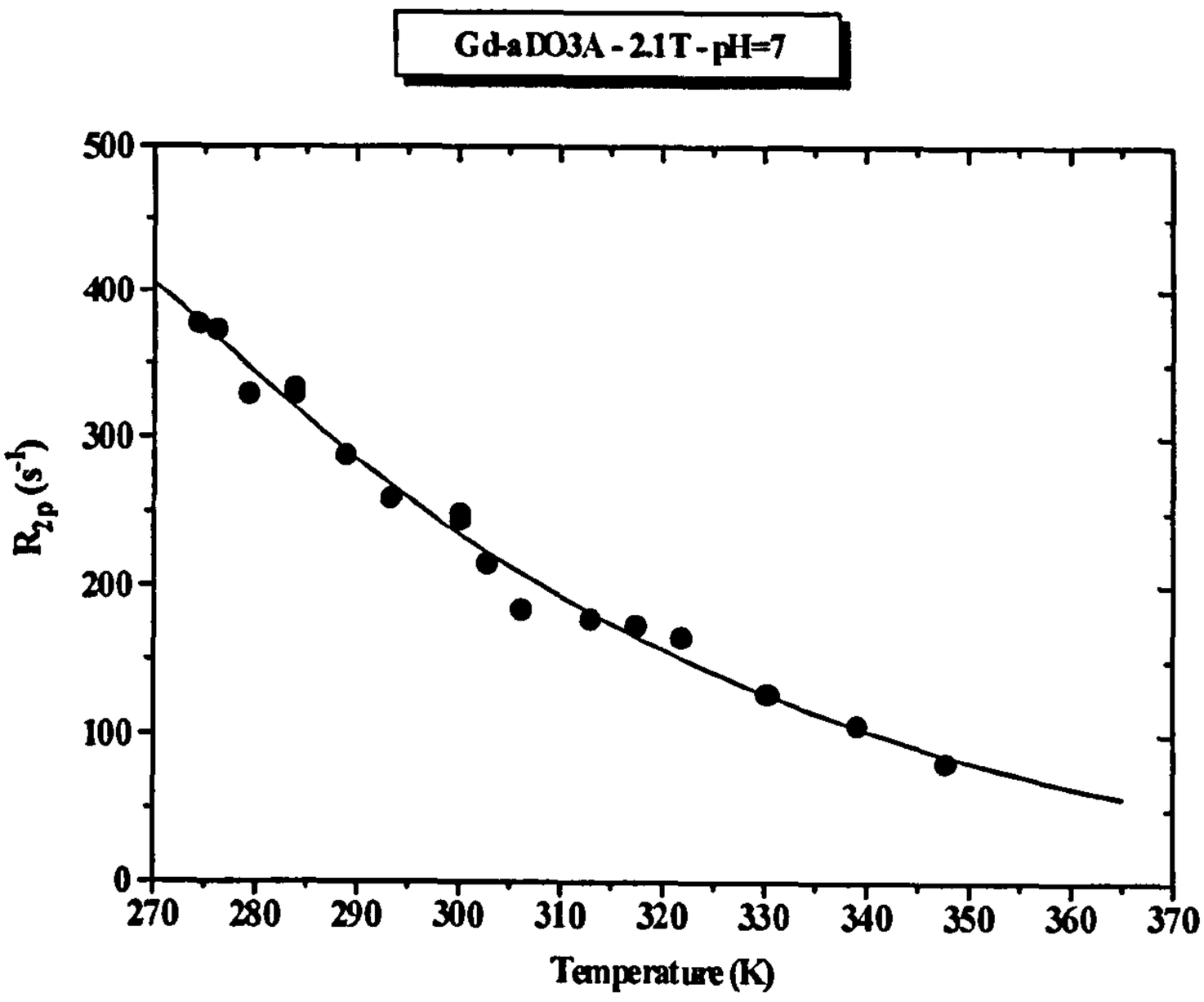

Figure 2.19 – R_{2p} as function of temperature at 90 MHz and pH=7.0.

The measured variation of R_{2p} as a function of temperature at 90 MHz in ^{17}O enriched solution at pH 7.0 for $[GdaDO3A]^{3-}$ (*c.a.* 10 mM) is shown in *Figure 2.19*. The curve was fitted to the Swift-Connick equations.[24-26] In the analysis, a standard value for the hyperfine coupling constant A/h ($-3.8 \cdot 10^6$ rad s^{-1}) was used, whereas the values obtained from the NMRD profiles for Δ^2 and τ_V were considered. The calculated values of the water exchange lifetimes at 298 K are reported in *Table 2.5* and compared to those of other *q=2* complexes published in the literature.[5] The analysis of these data clearly indicates that the water molecules in $[GdaDO3A]^{3-}$ exchange very rapidly with the bulk solution and this certainly contributes to the high value of relaxivity measured. For example, [GdDO3A], which has q = 1.8 and r_{1p}= 6.04 $mM^{-1}s^{-1}$ (20 MHz and 298 K) exhibits a τ_M more than five times bigger than this system.[5] These differences could be due to a structuring effect of the remote carboxylate groups on the nature of the second sphere of hydration.

Complex	$[GdaDO3A]^{3-}$	$[GdgDO3A]^{3-}$	$[GdaDOTA]^{-}$	[GdDO3A]	[GdPCP2A]
τ_M *(ns)*	30	230	200	160	68

***Table 2.5** – Water exchange rates calculated at 298 K and pH = 7.0.*[5]

2.7 High molecular weight contrast agents

The conjugation of low molecular weight chelates to macromolecules changes their biophysical and pharmacological properties. Firstly, high molecular weight conjugates, tumbling more slowly in solution, increase the rotation correlation time τ_R and hence improve the relaxivity. Secondly, these molecules are retained in the vascular spaces longer, because of their molecular size and thus facilitate imaging of the blood vassels (Angiography).

In developing new high MW complexes it is important first to find small chelates which display optimal values of q, τ_M and τ_S, because the amplification effect associated with the formation of the macromolecular adduct strictly depends on the relaxometric properties of the free complex.

The fast water exchange rate and the minimization of anion/protein binding of $[GdaDO3A]^{3-}$, suggest that it could be used as a potential candidate for high MW conjugates. With such a short water exchange lifetime, in fact, it should be possible to obtain high relaxivity values because the rotational correlation time of the complex will be drastically elongated upon the formation of a macromolecular adduct.

The gadolinium complexes of aDO3A and for comparison of aDOTA have been coupled to the hydrophilic amine **(28)** to yield the high molecular weight derivatives [GdaDO3A-AG] **(29)** (MW = 4093.9) and $[GdaDOTA-AG]^{-}$ **(31)** (MW = 5350.6) respectively, according to the schemes in *Figures* 2.*20* and 2.*21*.

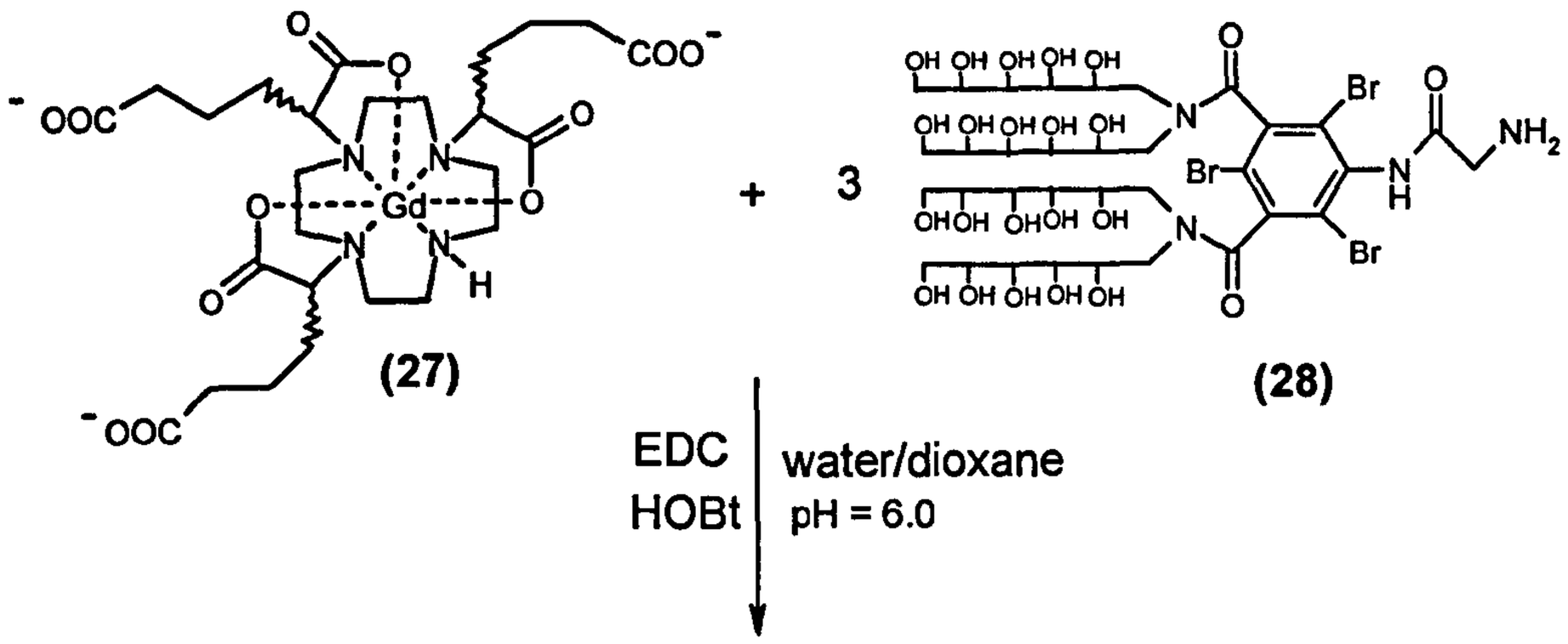

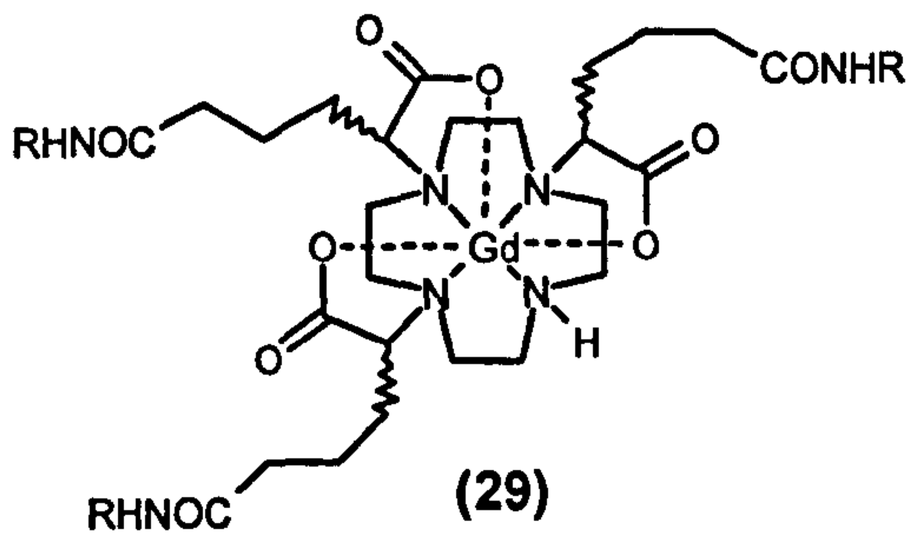

Figure 2.20 – Synthesis of [GdaDO3A-AG] (29).

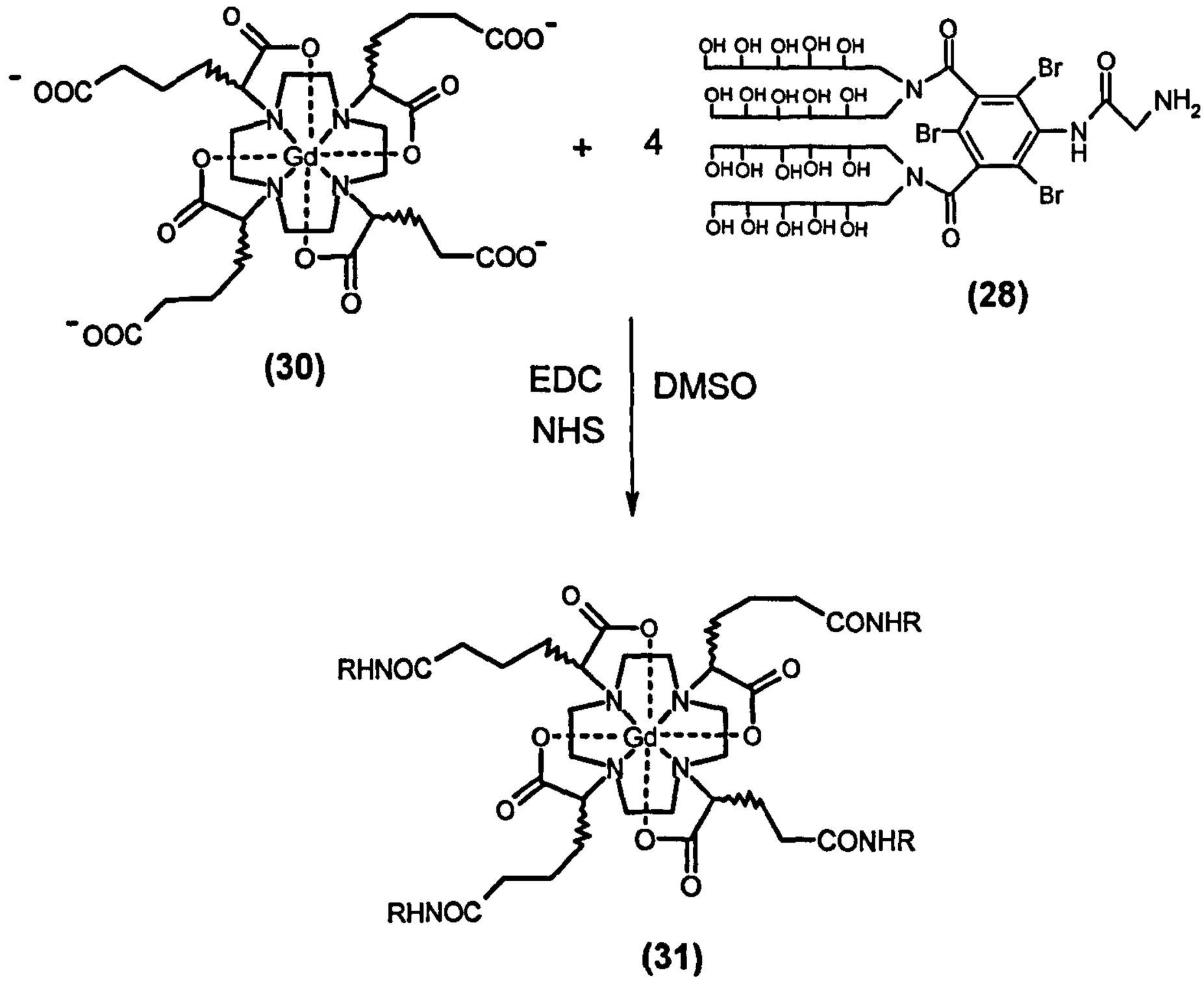

Figure 2.21 – Synthesis of [GdaDOTA-AG]⁻ (31).

The amine **(28)** was kindly provided by Guerbet s.a. (Paris).

The crude compounds were purified using gel exclusion chromatography (Sephadex G-25), which allows the complete elimination of the unreacted starting amine **(28)**. ESMS and UV-vis spectroscopy were used to characterize the final compounds.

The relaxivities measured in water were 27.7 $mM^{-1}s^{-1}$ for [GdaDO3A-AG] **(29)** and 23.4 $mM^{-1}s^{-1}$ in the case of the monohydrated analogue $[GdaDOTA\text{-}AG]^-$ **(31)** (65 MHz, 293 K in water pH =7.20). However, these high values of relaxivities are not "retained" in human serum. [GdaDO3A-AG] **(29)** exhibits in fact a much lower relaxivity in this medium (15.5 $mM^{-1}s^{-1}$). Consideration of the structure reveals that the complex is now neutral. The formation of three amide bonds has removed the three negative charges. So the high molecular weight complex is now more likely to bind endogenous anions, such as carbonate, phosphate or lactate compared to the parent low molecular weight species, because of a reduction in the electrostatic repulsion. In order to understand better the properties of the complex, the relaxivity was measured in water, in an anionic background solution and in human serum as function of pH (65 MHz, 293 K), as shown in *Figure 2.22*.

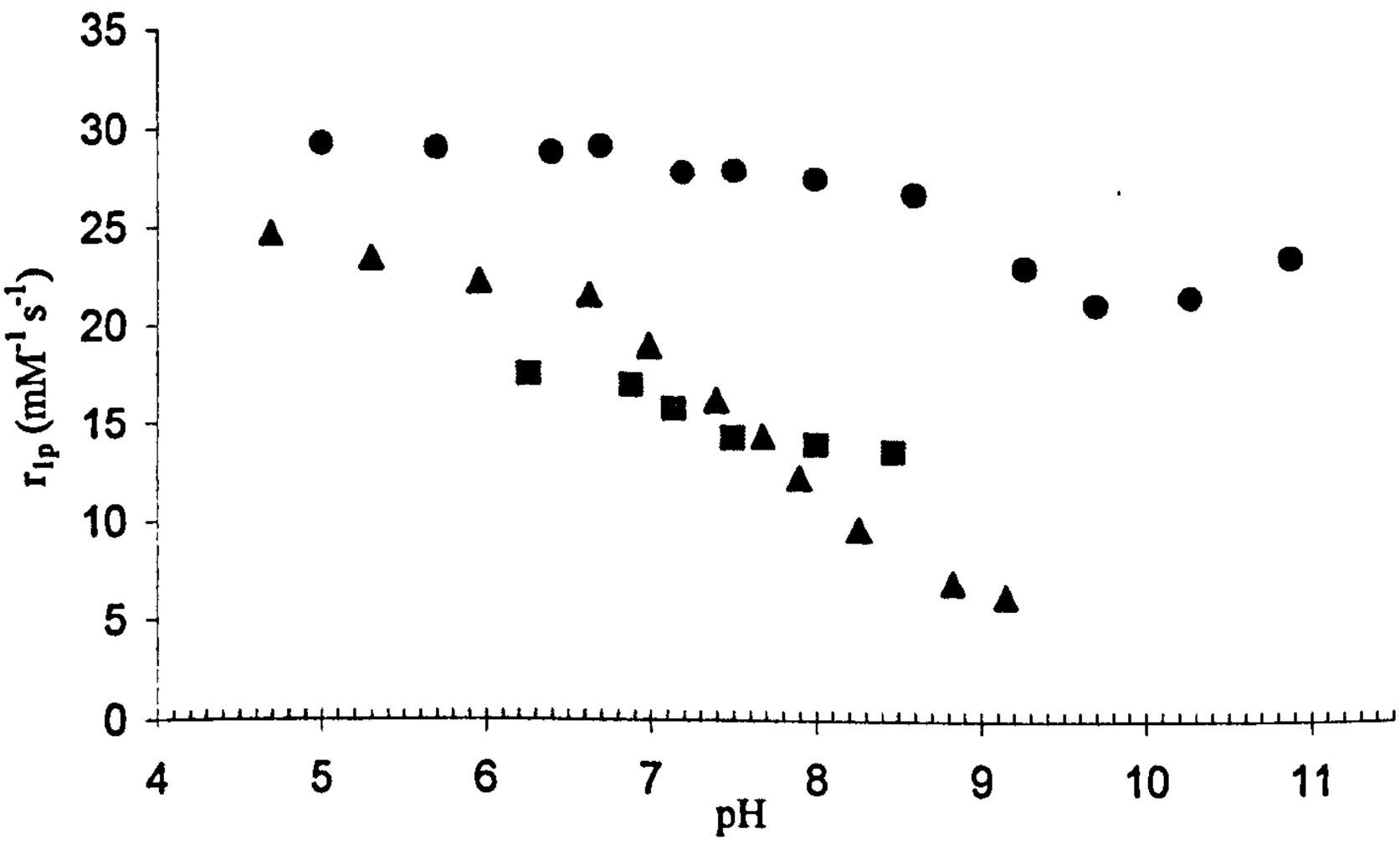

***Figure 2.22** – Relaxivity of [GdaDO3A-AG] (29) as function of pH in aerated water (circles), anionic background (triangles) and human serum (squares) at 65 MHz, 293 K.*

The profile in water reveals a decrement in relaxivity beyond pH 8.5, possibly due to the dissolved carbonate binding deriving from atmospheric carbon dioxide, which displaces water molecules in the inner sphere, reducing the relaxivity. The increment observed beyond pH 10.0 may be associated with fast prototropic exchange of the amide NH proton, as has been suggested for related tetra-amide complexes.[Amin, 1994 #63; Aime, 1999 #62; Peters, 1996 #64; Aime, 1998 #65]

The profile in the anionic background (*i.e.* the simulating extra-cellular environment) shows a remarkable reduction in relaxivity above pH 6.5, which suggests a strong anion binding affinity. Meanwhile, the relaxivities over the whole range of pH investigated are lower than those observed in pure water. Possibly, carbonate is not the only anion involved in the binding and other species (lactate or phosphate) may participate to the formation of a ternary adduct. For example, at pH 4.9 the concentration of HCO_3^- is less than 2%, but the relaxivity in anion solution is about 20% lower than in pure water. This reduction cannot be attributed just to the binding of carbonate and thus other anions, such as phosphate or lactate must be involved. However, in the absence of luminescence studies on the analogous europium complex, no definitive conclusion can be drawn.

The profile in human serum can be explained by the same sort of considerations. The relaxivities were corrected for volume changes, as discussed previously and the small differences are in part due the changing in the micro-viscosity of the medium. In addition, the behaviour observed in human serum, suggests that [GdaDO3A-AG] **(29)** does not bind any proteins contained in serum, *e.g.* human serum albumin (HSA). This was confirmed by a simple experiment. To a solution of complex in the anionic background at pH = 7.20 (r_{1p} = 17.6 $mM^{-1}s^{-1}$) HSA was added (0.6 mM). The relaxivity of the resulting solution did not change, confirming that the serum proteins do not bind the high molecular weight complex.

The NMRD profiles of [GdaDO3A-AG] **(29)** and [GdaDOTA-AG]$^-$ **(31)** were recorded over an extended range of frequencies at 25^{0}C (*Figure 2.23*).

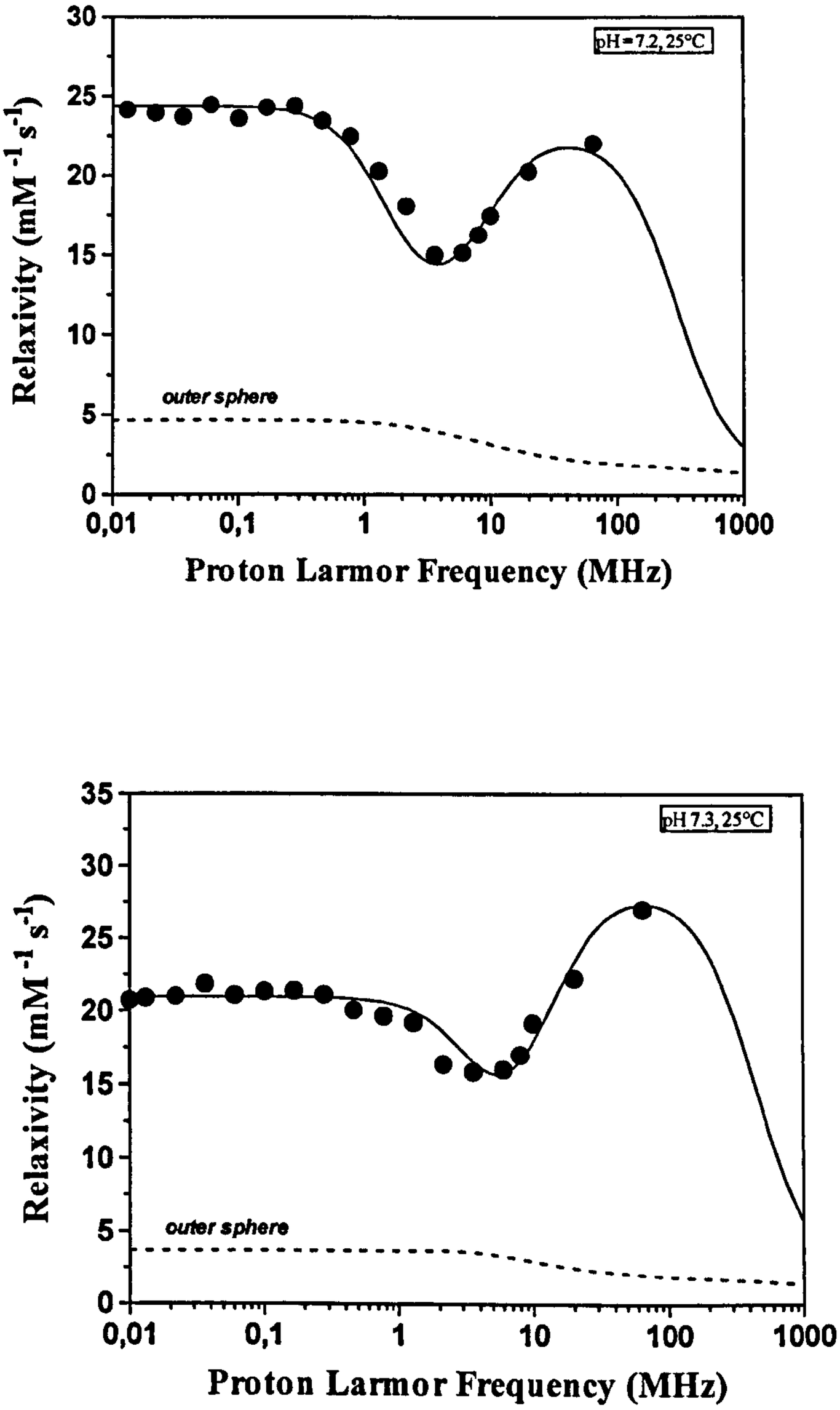

***Figure 2.23** – NMRD profiles recorded at 298 K for [GdaDOTA-AG]$^-$ **(31)** (at the top) and [GdaDO3A-AG] **(29)**.*

The curves were fitted to the equations for the inner and outer sphere paramagnetic relaxation (Chapter One) to give the parameters reported in *Table 2.6*.

Complex	Δ^2 (s^{-2})/10^{-19}	τ_V (ps)	τ_R (ps)	τ_M (ns)
[GdaDO3A-AG] **(29)**	3.54	27	368	(100)
[GdaDOTA-AG]$^-$ **(31)**	1.20	30	585	(100)

***Table 2.6** - Best fitting parameters determined by analyses of NMRD profiles.*

The high field region of the profile (5-50 MHz) is particularly important, because in clinical imaging the fields used are typically between 20 and 60 MHz. For small chelates this region is mainly controlled by τ_R. The characteristic "hill" observed in the case of high molecular weight compound indicates a larger τ_R value. The low field region, however, is most influenced by the value of Δ^2 (electronic spin relaxation time at zero field). The factors, which govern this parameter, are still not fully understood. However, some generalizations can be drawn. [4] DOTA-like chelates, with high symmetry, have smaller values of Δ^2. Practically this results in a higher low field relaxivity. This is confirmed by looking at the NMRD profiles in *Figure 2.23*. [GdaDOTA-AG]$^-$ **(31)**, which has a smaller value of Δ^2, exhibits a higher relaxivity at low fields (0.01-0.1 MHz), compared to [GdaDO3A-AG] **(29)**, which has a higher Δ^2 value.

As has already been pointed out, the profiles are only slightly dependent on the actual value of the water residence lifetime τ_M, which then cannot be determined with sufficient accuracy by the fitting procedure. We were not able to record variable-temperature proton-decoupled ^{17}O NMR measurements of the water transverse relaxation rates. So the values of τ_M reported in *Table 2.6* are not significant.

2.8. Conclusion

The drawbacks encountered in developing *q=2* systems are mainly due to their poor thermodynamic and kinetic stability, with respect to dissociation of the free gadolinium ion. Moreover, these complexes are more likely to bind endogenous anions, such as carbonate, phosphate or lactate, displacing water molecules in the inner sphere and reducing the relaxivity. For these reasons, despite the high relaxivity measured in water for some of the di-hydrated complexes published in the literature so far, none of them seem to possess all the characteristics needed for an effective contrast agent.[1-3, 5, 6]

$[GdaDO3A]^{3-}$ represents instead a promising candidate as a contrast agent for MRI. It possesses the highest value of relaxivity so far measured for a *q=2* complex in water. More importantly, its high relaxivity is retained in human serum, because the binding of endogenous anions (*e.g.* HCO_3^-/CO_2^{-2}) or proteins (HSA) is suppressed by electrostatic repulsion. In addition, this complex seems to be sufficiently stable, showing a kinetic inertness ten times higher than $[GdDTPA]^{2-}$ (Magnevist) which has been in commercial use since 1988.

In conclusion, $[GdaDO3A]^{3-}$ is the first *q=2* gadolinium complex that is likely to be suitable as contrast agent for MRI. Moreover, due to its fast water exchange rate and the minimisation of the anion/protein binding, it is an attractive candidate for high molecular conjugates.

A high molecular weight derivative has been synthesised and characterized. However, despite its high relaxivity in water at physiological pH (27.7 $mM^{-1}s^{-1}$), it is not able to retain the high value in human serum (15.6 $mM^{-1}s^{-1}$), because of its high affinity for anion binding. For these reasons, despite the substantial differences in molecular size of the low and high molecular weight parent complex, their relaxivities in human serum at physiological pH differ by just 20%. Thus $[GdaDO3A]^{3-}$ is a very good system in itself. However, the promising high relaxivity of [GdaDO3A-AG] measured in water, renders this complex an interesting one. The aim is to modify opportunely its structure in order to reduce or suppress the anion binding and thus retain the high relaxivity even in an in-vivo environment. This could be a feature of a complex possessing a negatively charged phospholirate linkage, in place of the carboxylate moiety.

2.9. References

[1] Xu, J.; Franklin, S. J.; Whisenhunt, D. W. J.; Raymond, K. N. *J. Am. Chem. Soc.* **1995**, *117*, 7245.

[2] Cohen, S. M.; Xu, J.; Radkov, E.; Raymond, K. N.; Botta, M.; Barge, A.; Aime, S. *Inorg. Chem.* **2000**, *39*, 5747.

[3] Aime, S.; Botta, M.; Frullano, L.; Geninatti Crich, S.; Giovenzana, G.; Pagliarin, R.; Palmisano, G.; Riccardi Sirtori, F.; Sisti, M. *J. Med. Chem.* **2000**, *43*, 4017.

[4] Caravan, P.; Ellison, J.; McMurry, T. J.; Lauffer, R. B. *Chem. Rev.* **1999**, *99*, 2293.

[5] Aime, S.; Botta, M.; Geninatti Crich, S.; Giovenzana, G.; Pagliarin, R.; Sisti, M.; Terreno, E. *Magn. Res. Chem.* **1998**, *36*, 200.

[6] Aime, S.; Gianolio, E.; Terreno, E.; Giovenzana, G.; Pagliarin, R.; Sisti, M.; Palmisano, G.; Botta, M.; Lowe, M. P.; Parker, D. *J. Biol. Inorg. Chem.* **2000**, *5*, 488.

[7] Kang, S. I.; Ranganathan, J. E.; Emswiler, K.; Kumar, J. Z.; Gougoutas, M. F.; Malley, M. F.; Tweedle, M. F. *Inorg. Chem.* **1993**, *32*, 2912.

[8] Kumar, K.; Tianzhu, J.; Xiangyun, W.; Desreux, J. F.; Tweedle, M. F. *Inorg. Chem.* **1994**, *33*, 3823.

[9] Pillai, R.; Fan, H.; Ranganathan, R. S. *Abstr. Pap. Am. Chem. Soc.* **1996**, 359.

[10] Woods, M.; Aime, S.; Botta, M.; Howard, J. A. K.; Moloney, J. M.; Navet, M.; Parker, D.; Port, M.; Rousseaux, O. *J. Am. Chem. Soc.* **2000**, *122*, 9781.

[11] Bryden, C. C.; Reilley, C. N. *Anal. Chem.* **1982**, *54*, 610.

[12] Bunzli, J.-C. G.; Choppin, G. R. *Lanthanide Probes in Life, Chemical and Earth Sciences*; Elsevier: Amsterdam, 1989.

[13] Bruce, J. I.; Dickins, R. S.; Govenlock, L. J.; Gunnlaugsson, T.; Lopinski, S.; Lowe, M. P.; Parker, D.; Peacock, R. D.; Perry, J. J. B.; Aime, S.; Botta, M. *J. Am. Chem. Soc.* **2000**, *122*, 9674.

[14] Beeby, A.; Clarkson, I. M.; Dickins, R. S.; Faulkner, S.; Parker, D.; Royle, L.; De Sousa, A. S.; Williams, J. A. G.; Woods, M. *J. Chem. Soc., Perkin Trans. 2* **1999**, 493.

[15] Biagi, B. A.; Enyeart, J. J. *Am. J. Physiol.* **1990**, *259*, 515.

[16] Molgo, J.; Pozo, E. D.; Banos, J. E. *J. Pharmacol.* **1991**, *104*, 133.

[17] Rochlage, S. M.; Worah, D.; Kim, S. H. *Magn. Res. Med.* **1991**, *22*, 216.

[18] Kasokat, T.; Urich, K. *Drug Res.* **1992**, *42*, 869.

[19] Wedeking, P.; Kumar, K.; Tweedle, M. F. *Magn. Res. Imag.* **1992**, *10*, 641.

[20] Wedeking, P.; Kumar, K.; Tweedle, M. F. *Invest. Radiol.* **1995**, *30*, 372.

[21] Chacheris, W. P.; Quay, S. C.; Rochlage, S. M. *Magn. Res. Imag.* **1990**, *8*, 467.

[22] Tweedle, M. F.; Hagan, J. J.; Kumar, K. *Magn. Res. Imag.* **1991**, *9*, 409.

[23] Laurent, S.; Elst, L.; Copoix, F.; Muller, R. L. *Invest. Radiol.* **2001**, *36*, 115.

[24] Swift, T.; Connick, R. E. *J. Chem. Phys.* **1962**, *37*, 307.

[25] Aime, S.; Botta, M.; Fasano, M. *Chem. Eur. J.* **1997**, *3*, 1499.

[26] Swift, T. J.; Connick, R. E. *J. Chem. Phys.* **1964**, *41*, 2553.

[27] Amin, S.; Morrow, J. R.; Lake, C. H.; Churchill, M. R. *Angew. Chem. Int. Ed. Engl.* **1994**, *33*, 773.

[28] Aime, S.; Barge, A.; Botta, M.; Clarkson, I. M.; Howard, J. A. K.; Moloney, J. M.; Parker, D.; De Sousa, A. S. *J. Am. Chem. Soc.* **1999**, *121*, 761.

[29] Peters, J. A.; Huskens, J.; Rabe, D. J. *Prog. NMR Spectrosc.* **1996**, *28*, 283.

[30] Aime, S.; Botta, M.; Fasano, M.; Terreno, E. *Chem. Soc. Rev.* **1998**, *27*.

[1] Xu, J.; Franklin, S. J.; Whisenhunt, D. W. J.; Raymond, K. N. *J. Am. Chem. Soc.* **1995**, *117*, 7245.

[2] Cohen, S. M.; Xu, J.; Radkov, E.; Raymond, K. N.; Botta, M.; Barge, A.; Aime, S. *Inorg. Chem.* **2000**, *39*, 5747.

[3] Aime, S.; Botta, M.; Frullano, L.; Geninatti Crich, S.; Giovenzana, G.; Pagliarin, R.; Palmisano, G.; Riccardi Sirtori, F.; Sisti, M. *J. Med. Chem.* **2000**, *43*, 4017.

[4] Caravan, P.; Ellison, J.; McMurry, T. J.; Lauffer, R. B. *Chem. Rev.* **1999**, *99*, 2293.

[5] Aime, S.; Botta, M.; Geninatti Crich, S.; Giovenzana, G.; Pagliarin, R.; Sisti, M.; Terreno, E. *Magn. Res. Chem.* **1998**, *36*, 200.

[6] Aime, S.; Gianolio, E.; Terreno, E.; Giovenzana, G.; Pagliarin, R.; Sisti, M.; Palmisano, G.; Botta, M.; Lowe, M. P.; Parker, D. *J. Biol. Inorg. Chem.* **2000**, *5*, 488.

[7] Kang, S. I.; Ranganathan, J. E.; Emswiler, K.; Kumar, J. Z.; Gougoutas, M. F.; Malley, M. F.; Tweedle, M. F. *Inorg. Chem.* **1993**, *32*, 2912.

[8] Kumar, K.; Tianzhu, J.; Xiangyun, W.; Desreux, J. F.; Tweedle, M. F. *Inorg. Chem.* **1994**, *33*, 3823.

[9] Pillai, R.; Fan, H.; Ranganathan, R. S. *Abstr. Pap. Am. Chem. Soc.* **1996**, 359.

[10] Woods, M.; Aime, S.; Botta, M.; Howard, J. A. K.; Moloney, J. M.; Navet, M.; Parker, D.; Port, M.; Rousseaux, O. *J. Am. Chem. Soc.* **2000**, *122*, 9781.

[11] Bryden, C. C.; Reilley, C. N. *Anal. Chem.* **1982**, *54*, 610.

[12] Bunzli, J.-C. G.; Choppin, G. R. *Lanthanide Probes in Life, Chemical and Earth Sciences*; Elsevier: AMsterdam, 1989.

[13] Bruce, J. I.; Dickins, R. S.; Govenlock, L. J.; Gunnlaugsson, T.; Lopinski, S.; Lowe, M. P.; Parker, D.; Peacock, R. D.; Perry, J. J. B.; Aime, S.; Botta, M. *J. Am. Chem. Soc.* **2000**, *122*, 9674.

[14] Beeby, A.; Clarkson, I. M.; Dickins, R. S.; Faulkner, S.; Parker, D.; Royle, L.; De Sousa, A. S.; Williams, J. A. G.; Woods, M. *J. Chem. Soc., Perkin Trans. 2* **1999**, 493.

[15] Biagi, B. A.; Enyeart, J. J. *Am. J. Physiol.* **1990**, *259*, 515.

[16] Molgo, J.; Pozo, E. D.; Banos, J. E. *J. Pharmacol.* **1991**, *104*, 133.

[17] Rochlage, S. M.; Worah, D.; Kim, S. H. *Magn. Res. Med.* **1991**, *22*, 216.

[18] Kasokat, T.; Urich, K. *Drug Res.* **1992**, *42*, 869.

[19] Wedeking, P.; Kumar, K.; Tweedle, M. F. *Magn. Res. Imag.* **1992**, *10*, 641.

[20] Wedeking, P.; Kumar, K.; Tweedle, M. F. *Invest. Radiol.* **1995**, *30*, 372.

[21] Chacheris, W. P.; Quay, S. C.; Rochlage, S. M. *Magn. Res. Imag.* **1990**, *8*, 467.

[22] Tweedle, M. F.; Hagan, J. J.; Kumar, K. *Magn. Res. Imag.* **1991**, *9*, 409.

[23] Laurent, S.; Elst, L.; Copoix, F.; Muller, R. L. *Invest. Radiol.* **2001**, *36*, 115.

[24] Swift, T.; Connick, R. E. *J. Chem. Phys.* **1962**, *37*, 307.

[25] Aime, S.; Botta, M.; Fasano, M. *Chem. Eur. J.* **1997**, *3*, 1499.

[26] Swift, T. J.; Connick, R. E. *J. Chem. Phys.* **1964**, *41*, 2553.

Chapter Three:

Regioselective Protection of Folic Acid

3.1. Introduction

The majority of contrast agents currently in clinical use are small chelates that remain in the extracellular fluids and show little specificity in their biodistribution, being excreted rapidly via the kidneys.[1] A new generation of these diagnostic agents is being developed as specifically targeted contrast agents, which can selectively enhance the MRI signal intensity in particular tissue types. As discussed in Chapter One, this can be achieved by linking a targeting vector to a gadolinium complex. The vector used in this work is the vitamin folic acid **(5)** (*Figure 3.1*).

Folic acid and its related compounds are required for the survival and growth of eukaryotic cells. They are involved in the biosynthesis of purine and certain amino acids. They enter the cell via a family of transport proteins, the Folate Binding Proteins (FBP).[2 3] Cancerous cells overexpress FBP's and as a consequence folate species.[4-6] The conjugation of a gadolinium complex to folate derivatives enhances the cellular uptake of the diagnostic agents and permits a selective targeting of unhealthy cells, as seen in Chapter One. The aim is to bind via amide bond formation, a gadolinium chelate, which possesses a pendant amino group, to a carboxylic group of folic acid with control over regiochemistry.

It has been demonstrated, that when folate species are covalently linked to a molecule via their α or γ carboxylic groups, the affinity for the cell surface receptors change appreciably compared to the free folate.[7-9]

In developing a method to enhance transmembrane transport of exogenous molecules, Low and coworkers[10] coupled folic acid to a variety of exogenous molecules including, peptides, nucleic acids, analgesics, antihypertensive agents, antiviral agents, plasmids and diagnostic agents. The synthetic methods proposed by the authors were not regioselective, and mixtures of either the α- or the γ-regioisomers were obtained. The distinction between the two isomers of DF-folates, for example (*e.g.* those where deferoxamine is coupled to the folate moiety through the α- or the γ-carboxyl group of folate) was based on their competition with free folate for the cell surface FBP. It was found that the α-conjugate was unable to compete with free folate.

Wang and coworkers[11, 12] studied the uptake of ^{67}Ga-deferoxamine-folate into KB tumor cells (a human nasopharyngeal epidermal carcinoma cell line that overexpresses the FBP) as a potential radiopharmaceutical. The compound showed a low, non-specific

binding. In a second paper the authors reported[13] the preparation of FITC-EDA-folate derivatives containing a fluorescein moiety (FITC) linked to folate via either the α- or the γ- carboxylate group. The two isomers were incubated with KB cells. The γ isomer showed half maximal binding to KB cells, but the α isomer had virtually no affinity for the cell surface receptors.

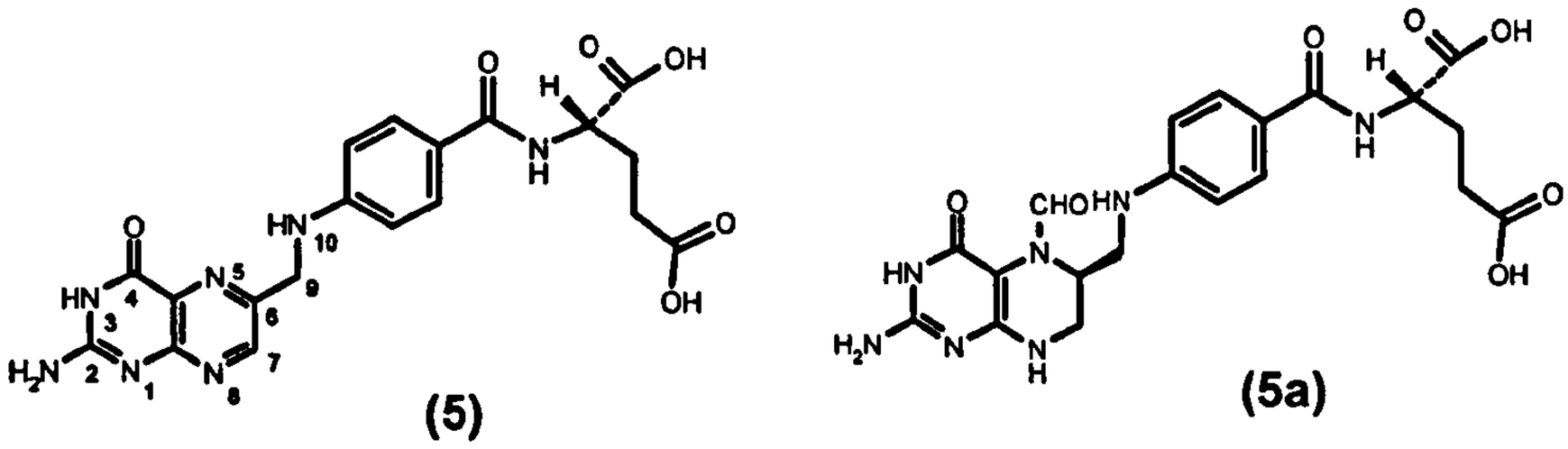

***Figure 3.1** - Structure of folic acid (5) and folinic acid (5a).*

In a recent patent published by Bracco,[14] the inventors proposed regiospecific synthesis of the folate conjugates of several gadolinium complexes. Both the α and the γ isomers were synthesized and their ability to bind to FBP in tumor cells was compared *in-vitro*. In contradiction to the results published by Wang and coworkers[13] the α isomer conjugates bound to FBP to the same extent as the γ one in a variety of in vitro studies. Moreover, the bis derivative (functionalized on both the α and γ groups) was also able to bind to FBP. In addition, the urinary clearance of the α-isomers from the body was significantly and unexpectedly higher than that observed for the corresponding γ-isomers.

These studies confirmed the different behaviour showed by folate derivatives, which are covalently bound through the α-carboxylate compared to those, which are linked through the γ position. It is then important to synthesize both the α- and γ-folate derivatives and study their characteristics separately.

The synthesis, characterization and relaxometric studies of folate conjugates of different gadolinium chelates are presented in Chapter Four. In the present one we focus on the development of new methods to regioselectively protect folic acid.

3.2. Regioselective protection of Folic Acid

In order to bind selectively a gadolinium chelate to folic acid (or folate derivatives) through one carboxylic group, the protection of the other acid group is required.

In the structure of folic acid, a glutamate moiety can be recognized. Synthetic methods that allow the selective protection of one carboxylate of glutamic acid are well known and have been widely used in peptide chemistry. Some of them can be applied to folic acid. However, this vitamin is rather difficult to handle, mainly due to its poor solubility. In addition, side reactions can take place at the other functional groups present in the molecule. Finally, folate derivatives are light and air sensitive and appropriate precautions must be considered. For each of these reasons, modifications of the conventional methods used for glutamic acid have been developed.

3.2.1. Method A: Use of alkylating agents

Nefkens and co workers had earlier found a practicable route for the regioselective esterification of N-substituted glutamate derivatives.[15] The two carboxylic groups (α and γ) of these molecules present a difference in pK_a (in the order of 0.4), the α groups having lower values. So in the presence of one equivalent of a base, the α groups will be preferentially deprotonated. The reaction with an alkylating agent occurred in a selective derivatization and α-esters were obtained in good yield, after purification over silica gel.

A similar procedure was later adopted by Fitzhugh and coworkers for [(6S)-5 formyl-5,6,7,8-tetrahydropteroyl]mono L-glutamic acid, folinic acid, **(5a)**, (*Figure 3.1*) to give the corresponding α-benzyl ester in reasonable yield (30%).

In this work, similar conditions have been adopted to synthesize both the α- and the γ-benzyl monoesters of folic acid, according to the scheme in *Figure 3.2*.

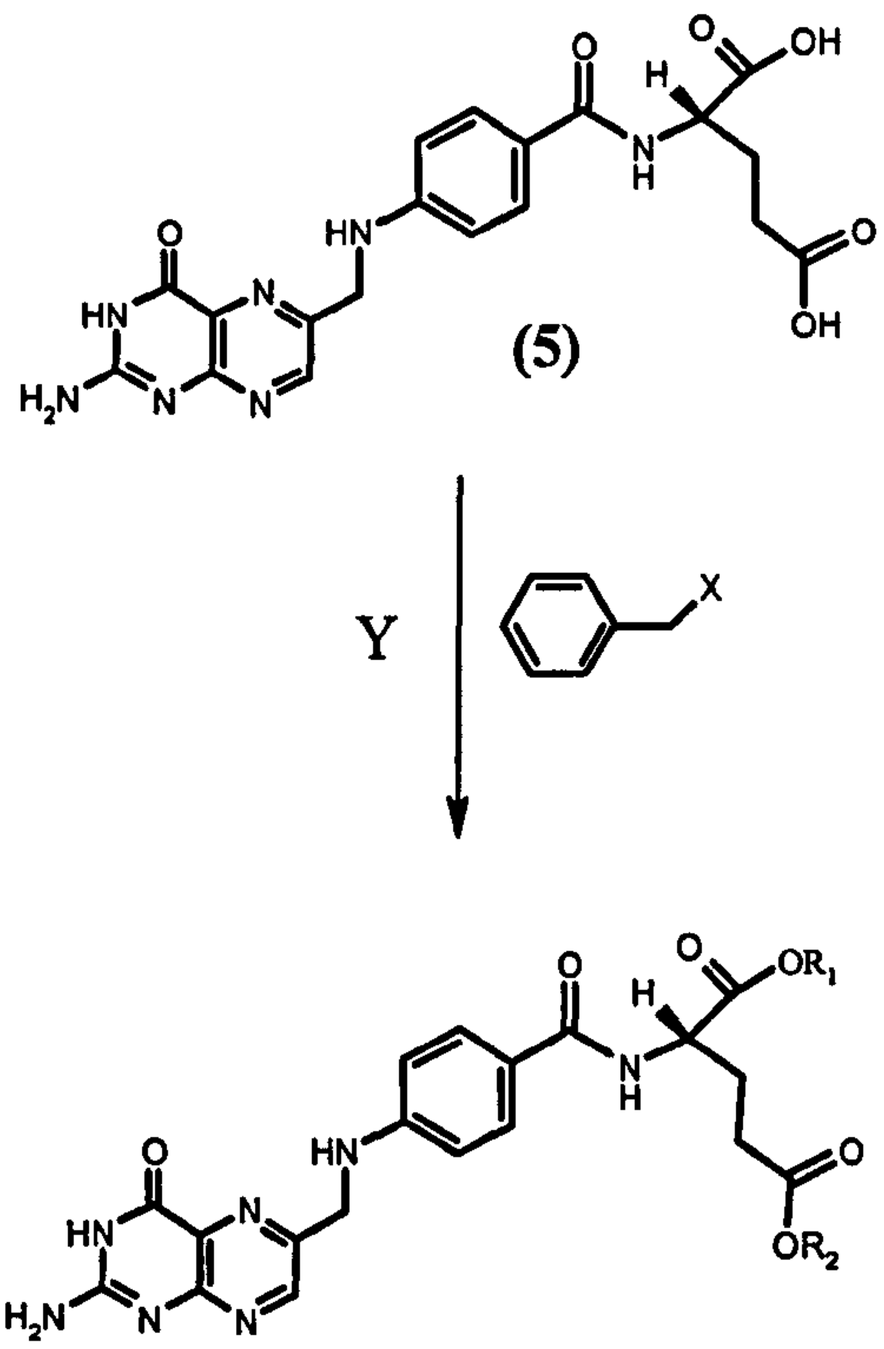

***Figure 3.2** – Regioselective O-benzylation of folic acid. Method A: X=Br, $Y=Cs_2CO_3$. Method B: X=OH, $Y=HBF_4$.*

Due to the poor solubility of folate species, the reaction was carried out in DMSO, according to the procedure followed by Rosowsky and coworkers[16] for the syntheses of several diesters of folinic acid. Caesium carbonate was used as base, whereas benzyl bromide was employed as alkylating agent. Since folic acid and its derivatives are light and air sensitive, the reaction was carried out under an inert atmosphere and in the dark. The progress of the reaction was followed by analytical reverse phase HPLC. The formation of a mixture of the two mono-benzyl esters α and γ **(32a-b)** was observed in ratio 4:1 (t_r = 21.1 and 22.1 min), in addition to the diester **(32c)** (t_r = 28.9 min) and unreacted folic acid (t_r =14.8 min). The crude material, which was precipitated by adding acetonitrile, was purified by reverse phase semi preparative HPLC, using a mixture of acetonitrile-water as

eluent. Trifluoroacetic acid (TFA) was added to water in small concentration (0.1 %), in order to improve the separation.

The chemical purity of each fraction was confirmed by the use of analytical HPLC. The first fraction (t_r = 14.8 min) was demonstrated to be unreacted folic acid by the presence of a single peak (m/z = 441) in the ESMS spectrum. Moreover, the ^{1}H NMR spectrum perfectly resembled the spectrum of the commercially available vitamin.

The ESMS analysis (m/z = 621) of the last fraction (t_r = 28.9 min) clearly indicated the presence of the diester. In addition, the ^{1}H NMR spectrum revealed two singlets (5.08 and 5.14 ppm) in a ratio 1:1, corresponding to the benzylic protons (OCH_2Ph). The integral values agreed with the diester structure.

Pure mono-benzyl esters were obtained collecting the fractions at t_r = 21.1 and 22.1 min. The ESMS analysis of these fractions was consistent with the presence of the monobenzyl ester, α or γ (m/z = 530). In order to understand which isomer corresponds to the two peaks in HPLC, detailed ^{1}H NMR analysis were made. In the case of the less retained monoester, the shifting to lower field of the proton H_α demonstrated (by analogy with reported literature values on related compounds[13]) that the esterification most probably occurred at the α carboxylic group. Moreover, the two benzylic protons ($O\underline{CH_2}Ph$) gave rise to a singlet at 5.09 ppm. The more retained monoester gave rise to a two proton singlets for the benzylic protons ($O\underline{CH_2}Ph$) at 5.04 ppm and the presence of an unshifted signal for the singlet assigned to the H_α methine proton at 4.35 ppm is consistent with the presence of the benzyl ester in the γ-position.

Despite the simplicity of this reaction, a mixture of the two regioisomers was obtained, which is difficult to separate. Silica gel chromatography can be used to remove unreacted folic acid and the diester. However, all the attempts made to separate the two isomers using column chromatography failed. Semipreparative reverse phase HPLC is indeed the only practicable way to successfully purify the mixture. Improvement in the separation can be achieved by changing the eluent composition. However, this method is extremely expensive and it does not readily satisfy the need of reasonable amounts of pure compounds (*i.e.* of the order of 100-500 mg).

3.2.2. Method B: Use of tetrafluoroboric acid as catalyst

Albert and co-workers[17] found a simple and high yield way to synthesize β-aspartates and γ-glutamates, using tetrafluoroboric acid as catalyst.

The same conditions were adapted for the benzyl esterification of folic acid, as shown in *Figure 3.2*. A mixture of α and γ monobenzyl ester **(32a,b)**, dibenzyl ester **(32c)** and unreacted folic acid was obtained, as confirmed by analytical reverse phase HPLC. Under these conditions, the major product was the diester, with benzyl alcohol used as both the reagent and the solvent for the reaction. Moreover, the ratio between the α and γ isomers was inverted compared to the method A (α/γ = 0.5). So the catalyst tetrafluoroboric acid favours the γ-benzyl esterification. It was suggested that the boron coordinates both the nitrogen of the α amino group and the oxygen of the α carboxylate of the glutamate moiety leaving the γ-carboxylate group free to react, as shown in *Figure 3.3*.

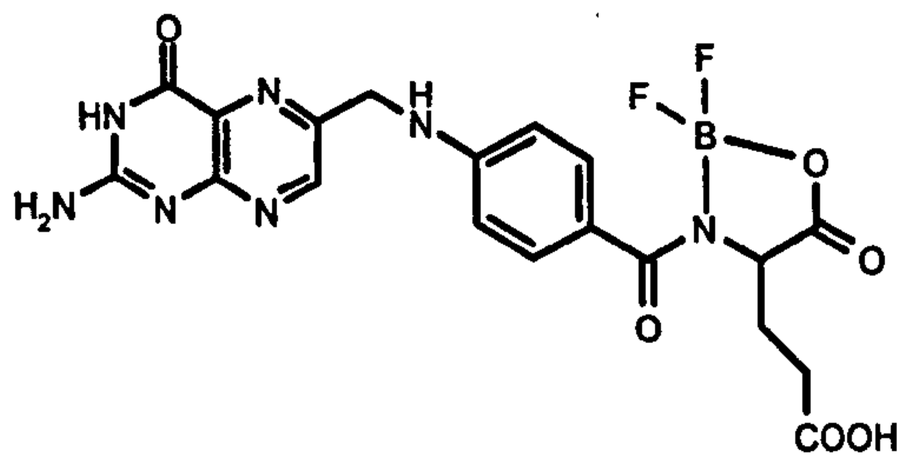

***Figure 3.3** – Schematic representation of the possible intermediate in the reaction catalized by tetrafluoroboric acid.*

The purification of the crude material was achieved by reverse phase semipreparative HPLC, as in method A. The fractions collected were analyzed by ESMS and ^{1}H NMR as discussed previously.

This procedure is complementary to method A. Here the γ isomer is synthesized in higher amounts compared to the α one. However, the purification of the crude material remains problematic. Small amounts of pure monoesters were obtained (10-20 mg), but the procedure is affected by the same limitations seen in Method A.

3.2.3. Method C: Enzymatic hydrolysis

Enzymes are nowadays widely used in organic syntheses, because they can catalyze efficiently and specifically a wide range of types of reactions, usually avoiding difficult separation procedures. Monoesters of N-protected α-aminoacid can be obtained by enzymatic hydrolyses of the corresponding diesters. For example, Alkalase from *B.licheniformis* was used for the regioselective hydrolyses of dibenzyl ester of N-unprotected aspartic and glutamic acid by Chen and coworkers.[18] Miyazawa and coworkers[19] have instead used several microbial proteases (*e.g.* from *Bacillus, Aspergillus, Rhizopus* and *Penicillium* species) to catalyze the regioselective hydrolysis of diesters (the dimethyl, diethyl or diisopropyl esters) of N-benzyloxycarbonylated α-aminocarboxylic acid (glutamic, aspartic, α-aminoadipic or α-aminosuberic acid) to produce γ- or ω-monoesters.

In this work a modified procedure has been applied to the di-esters (dimethyl and dibenzyl) of folic acid, as shown in *Figure 3.4*.

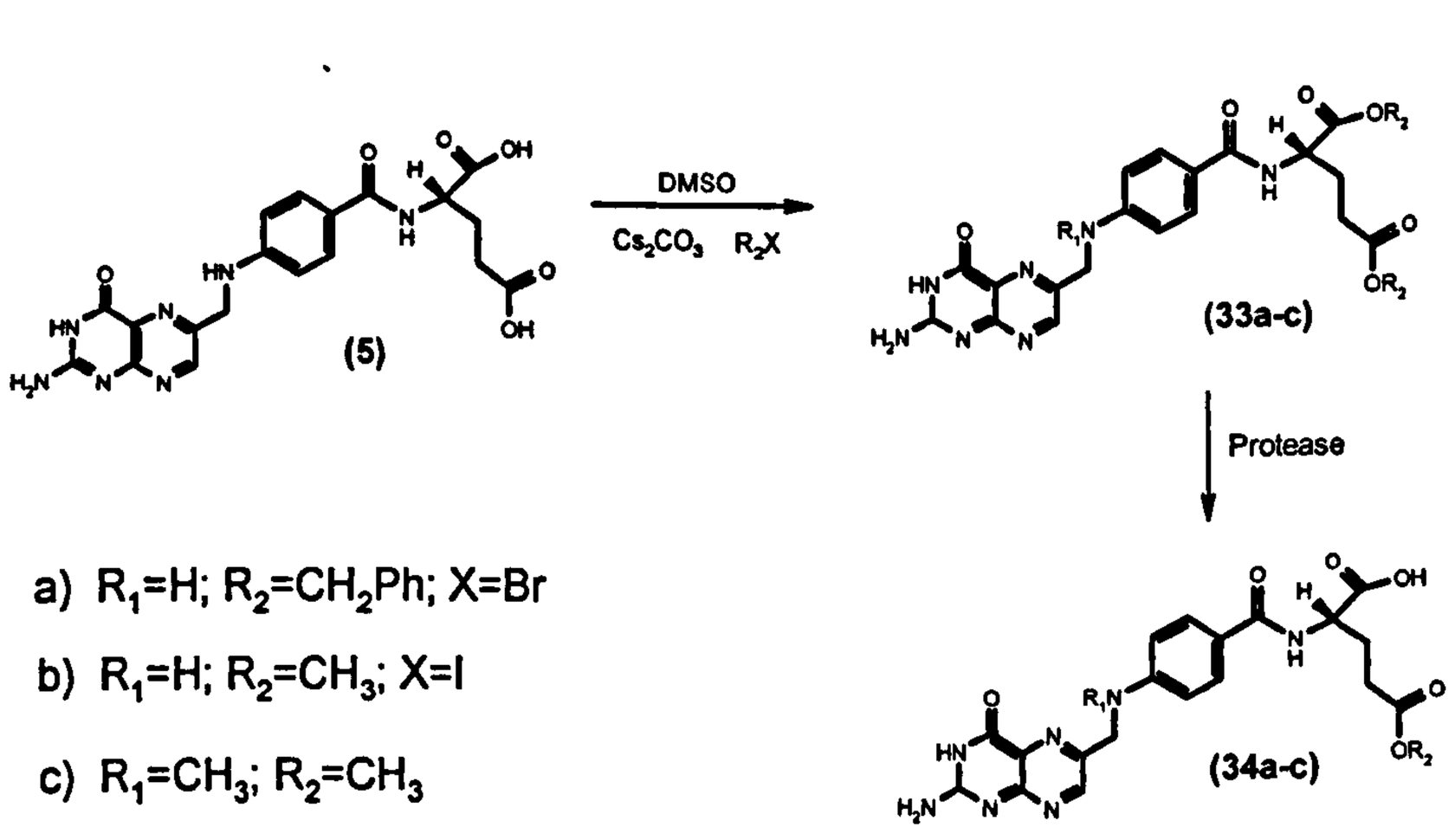

***Figure 3.4** – Enzymatic hydrolyses of diesters of folic acid.*

As Miyazawa and co-workers have demonstred,[19] the alcohol moiety of the esters has little influence on the regioselectivity of the hydrolysis, mediated by each of the microbial proteases examined. The choice of the starting diester is mainly dependent upon its solubility and availability.

The dibenzyl ester of folic acid **(33a)** was synthesized using two equivalent of benzyl bromide and caesium carbonate as base in DMSO, as shown in *Figure 3.4*. The crude was easily purified over silica gel and the pure compound fully characterized. When a similar procedure was repeated for the syntheses of the dimethyl ester **(33b)**, using methyl iodide as the alkylating agent, a more complex mixture was obtained. This contained both the dimethyl ester **(33b)** and the dimethyl ester N^{10}-methylated **(33c)**, as confirmed by ESMS (m/z = 468 and 482) and by ^{1}H NMR, which showed the presence of a singlet at 3.22 ppm. All attempts made to separate the two compounds using silica gel chromatography failed. This problem was not encountered in the synthesis of the dibenzyl ester, possibly because of the steric hindrance associated with alkylation of the bulkier benzyl group, inhibiting therefore alkylation at nitrogen.

The dimethyl ester of folic acid **(33b)** was therefore synthesized following another, simpler strategy. By simply refluxing folic acid in methanol in the presence of catalytic amount of hydrochloric acid, the dimethyl ester was obtained in quantitative yield. The reaction did not require any further purification and the pure diester was simply precipitated from the solution by adding ethyl acetate. ESMS, ^{1}H NMR and elemental analysis confirmed the formation of the dimethyl ester.

The enzymatic hydrolyses of the diesters were carried out in a mixture of phosphate buffer pH = 7.0 and DMSO, using *Protease* (from *Rhizopus species*) according to the procedure proposed by Miyazawa and co-workers.[19] The use of a co-solvent in enzymatic reaction can increase the rate of the reaction, mainly by an improvement in the solubility. However, high amount of non-aqueous solvents could dramatically reduce the activity of the enzyme. Different ratios were tried and the progress of the reactions was followed by analytical reverse phase HPLC. The ratio of phosphate buffer pH=7.0/DMSO 8:2 (v/v) was found to be the best compromise between solubility and reaction rate, for the dimethyl ester substrate. The unreacted di-methyl ester and the enzyme were removed by centrifugation and the γ-monoester **(34b)** was precipitated by acidification of the solution (to pH 3.5). No further purification was required and analytically pure γ-methyl ester of folic acid **(34b)** was obtained in reasonable yield (64%). Due to the lower solubility of the dibenzyl ester, higher amounts of DMSO were needed. At a ratio of phosphate buffer pH=7.0/DMSO 1:1 (v/v), in which the starting material was reasonably soluble, the reaction did not seem to progress.

Compared to the non-enzymatic procedures, previously discussed, this method does not suffers from low yields, tedious manipulation, difficult separations and high costs and can be applied on a reasonably high scale (0.5–1.0 g). In addition, the γ-methyl ester **(34b)** represents a good starting material to obtain the α isomer. A possible strategy involves synthesizing the γ-tert-butyl-α-methyl diester followed by selective cleavage of the methyl group by mild alkaline hydrolyses (pH = 9.0).

3.2.4. Others procedures

Another common procedure used to protect selectively the α carboxylic group of glutamic or aspartic acid is represented by the use of metal cations, such as $Zn^{2+}$and Cu^{2+}. These cations coordinate both the α-N or the amide carbonyl group and the α-carboxylic group of the glutamic moiety, leaving the γ-carboxylate free to react, as shown in *Figure 3.6*.

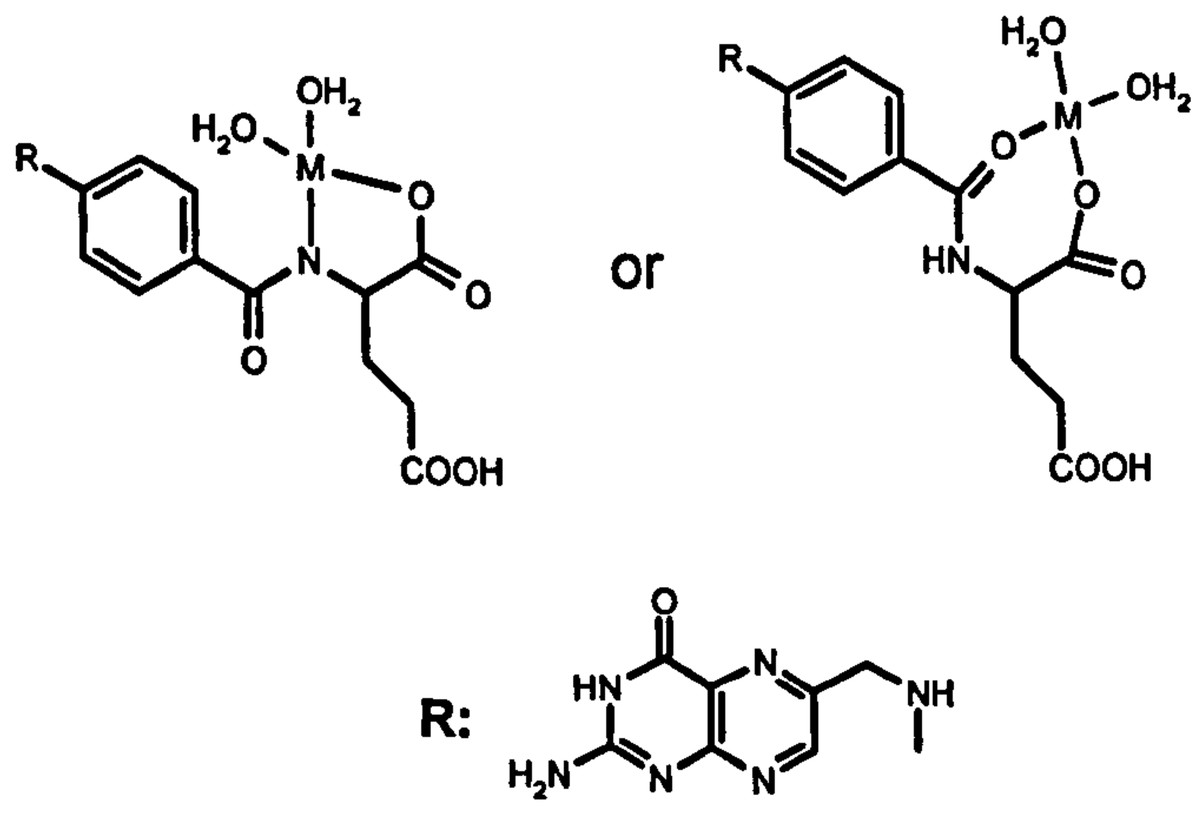

***Figure 3.6** – Schematic representation of possible structures in the protection of the α- position by using metal cations, M=Zn^{2+}, Cu^{2+}.*

This method has been applied to folic acid itself. However, two major problems are believed to have resulted in its failure. First, the nitrogens N^5 and the oxygen of the pteridine moiety and the para-amino group can coordinate the metal ions, as shown in *Figure 3.7*. Secondly, in the presence of high concentration of metal ions (such as Cu^{2+} or Zn^{2+}), insoluble folate salts precipite.

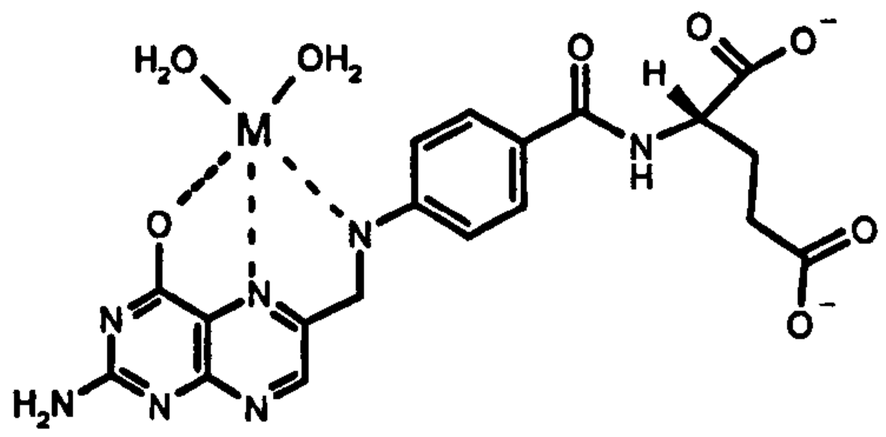

Figure 3.7 – Alternative sites of metal ion complexation of folic acid.

3.3. A different approach: the pteroic acid route

A completely different approach to bind a gadolinium chelate regioselectively to folic acid has been developed. The target molecule we want to synthesize is schematically shown in *Figure 3.8*. The disconnections indicated would reduce the synthesis to two major steps, which would involve amide bond formation between the moiety A (pteroic acid), B (glutamic acid) and C (gadolinium chelate). A similar procedure has been described by Bracco[14] for the synthesis of several gadolinium conjugates.

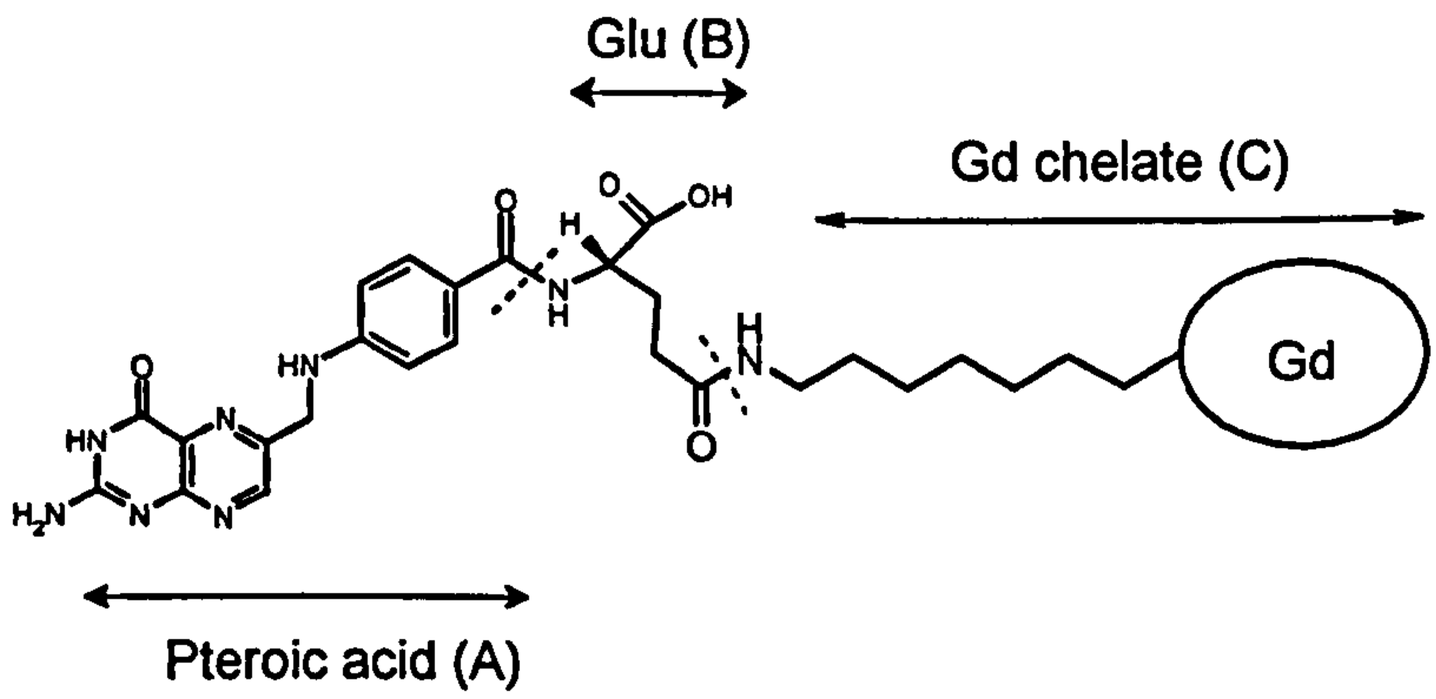

Figure 3.8 – Target molecules.

The route developed in this work independently (and prior to the appearance of the Bracco patent[14]) consists of the coupling of the two moieties C and B, followed by the conjugation to the moiety (A). To avoid side reactions, with consequent formation of oligomers, the amino group and one carboxylate group in glutamic acid must be protected. The N-protected mono-esters of glutamic acid **(35a)** and **(35b)** (*Figure 3.9*) were selected

to consitute moiety (B), because they are commercially available, cheap and allow the synthesis of both the α and γ derivatives. Pteroic acid (A) is commercially available too, but is quite expensive. However, several synthetic procedures for its preparation have been described in the literature.[20-22]

This synthetic approach is described more in detail in the next Chapter and in the experimental section (Chapter Five).

The reverse approach, in which A is first coupled to B and then to C is not practicable. In fact, the first step would require the use of a diester (*e.g.* dimethyl, dibenzyl) of glutamic acid to avoid intermolecular reaction between molecules of glutamic acid, which would then result in the syntheses of a diester of folic acid.

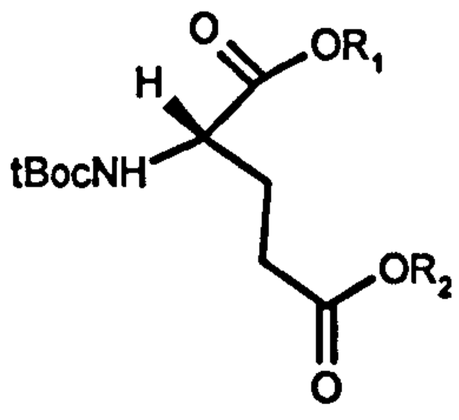

a) R_1= Bn; R_2 = H

b) R_1= H; R_2 = Bn

(35a-b)

***Figure 3.9** – N-tBoc monesters of Glu, used as moiety (B).*

3.4. Discussion

The conventional synthetic methods used for the regioselective protection of glutamic or aspartic acid cannot be successfully applied to folic acid. Its poor solubility, the presence of several functional groups and its light and air sensitivity render it difficult to handle. Mixtures of the α and γ isomers can be purified only by using reverse phase semipreparative HPLC, a very expensive method of low efficiency. However, a simple and high yield method has been developed. By using the enzyme Protease, the γ methyl ester of folic acid **(34b)** can be synthesized regioselectively from the corresponding diester, avoiding tedious purification procedures. The monoester thus synthesized can be directly coupled to a gadolinium chelate.

An alternative multistep approach has been developed too. In this case a gadolinium chelate is firstly coupled to an N-protected glutamate monoester and then, following deprotection of the amino group of the gluatmic moiety, it is coupled to pteroic acid. This method presents the advantage of using commercially available starting materials to synthesise each of the isomers on a practicable 50-100 mg scale.

3.5. References

[1] Caravan, P.; Ellison, J.; McMurry, T. J.; Lauffer, R. B. *Chem. Rev.* **1999**, *99*, 2293.

[2] Kane, M. A.; Waxman, S. *Lab. Invest.* **1989**, *60*, 737.

[3] Henderson, G. B. *Ann. Rev. Nutr.* **1990**, *10*, 319.

[4] Franklin, W. A.; Wantub, M.; Edwards, D.; Christiensen, K. *Int. J. Cancer* **1994**, *8*, 89.

[5] Mantovani, L. T.; Miotti, S.; Menard, S.; Canevari, S. *Eur. J. Cancer* **1994**, *30A*, 363.

[6] Ross, J. F.; Chonduri, P. K.; Rotman, M. *Cancer* **1994**, *73*, 2432.

[7] McHugh, M.; Cheng, Y. C. *J. Biol. Chem.* **1979**, *254*, 11312.

[8] Anthony, A. C.; Kane, M. A.; Portillo, R. M.; Ellwood, P. C.; Kallhouse, J. F. *J. Biol. Chem.* **1985**, *260*, 14911.

[9] Kamen, B. A.; Capdevila, A. *Proc. Nat. Acad. Sci. USA* **1986**, *83*, 5983.

[10] Low, P. S. US 5,416,016, 1997.

[11] Wang, S.; Lee, R. J.; Mathias, C. J.; Green, M. A.; Low, P. S. *Bioconj. Chem.* **1996**, *7*, 56.

[12] Mathias, C. J.; Wang, S.; Lee, R. J.; Waters, D. J.; Low, P. S.; Green, M. A. *J. Nucl. Med.* **1996**, *37*, 1003.

[13] Wang, S.; Luo, J.; Lantrip, D. A.; Waters, D. J.; Mathias, C. J.; Green, M. A.; Fucks, P. L.; Low, P. S. *Bioconj. Chem.* **1997**, *8*, 673.

[14] Wedeking, P. W.; Wager, R. E.; Arunachalam, T.; Ramalingam, K.; Linder, K. E.; Ranganathan, R. S.; Nunn, A. D.; Raju, N.; Tweedle, M. F. WO 99/59640, 1999.

[15] Nefkens, G. H. L.; Nivard, R. J. F. *Recl. Trav. Chim. Pais-Bas* **1964**, *83*, 199.

[16] Rosowsky, A.; Yu, C. S. In *Chemistry and Biology of Pteridines,* ; R. L. Kisliuk and G. M. Brown, Ed.; Elsevier North Holland: New York, 1978.

[17] Albert, R.; Danklmaier, J.; Honig, H.; Kandolf, H. *Synthesis* **1987**, *7*, 635.

[18] Chen, S. T.; Wang, K. T. *Synthesis* **1987**, 581.

[19] Miyazawa, T.; Ogura, M.; Nakayo, S.; Yamada, T. *Biotech. Tech.* **1998**, *12*, 431.

[20] Temple, C. J.; Rose, J. D.; Montgomery, J. A. *J. Org. Chem.* **1981**, *46*, 3666.

[21] Martinelli, J. E.; Chaykovsky, M.; Kisliuk, R. L.; Gaumont, Y.; Gittelman, G. *J. Med. Chem.* **1979**, *22*, 869.

[22] Goldman, P.; Levy, C. C. *Proc. Nat. Acad. Sci. USA* **1967**, *58*, 1299.

Chapter Four:

Folate Targeted Contrast Agents.

4.1. Introduction

Folic acid has been regioselectively linked to the gadolinium complexes of the ligands **(9)** and **(6)** (*Figure 4.1*), prepared following the procedures described in Chapter Three. Each ligand contained a pendant primary amine, which represents the site of conjugation to folic acid.

The monoamide [Gd·**9**] is a monohydrated complex ($q=1$), for which a long water exchange time should be expected. As has been demonstrated for several amide derivatives of DOTA, the replacement of one carboxylate group by an amide moiety reduces the water exchange rate of the gadolinium complex by a factor of between three and four.[1-4] The long value of τ_M in [Gd·**9**] is likely to limit the overall relaxivity of its folate conjugates. Nevertheless, [Gd·**9**] was considered to be a good model system with which to develop practicable synthetic routes to couple a gadolinium chelate to folic acid, as well as to test the affinity of folate conjugates for Folate Binding Protein (FBP).

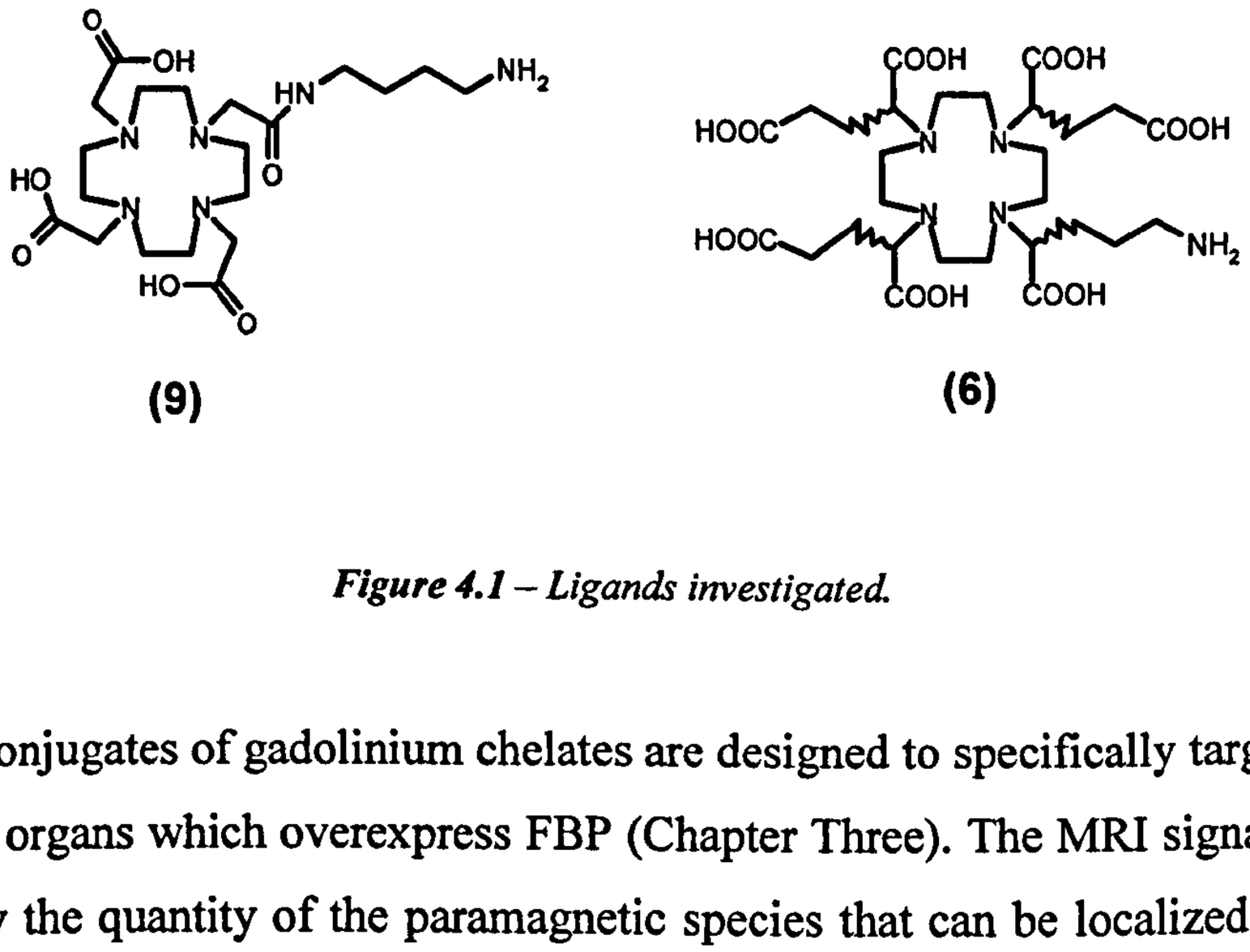

***Figure 4.1** – Ligands investigated.*

Folate conjugates of gadolinium chelates are designed to specifically target cancerous tissues and/or organs which overexpress FBP (Chapter Three). The MRI signal intensity is determined by the quantity of the paramagnetic species that can be localized in the target tissue, which in turn is limited by the amount of FBP present. Low relaxivity chelates, when used as the basis for such folate targeting contrast agents, would require high doses to bring sufficient reduction in the T_1 relaxation time. The desired increment in signal intensity could be achieved either by attaching multimeric gadolinium chelates to a single folate residue, or by the use of enhanced relaxivity chelates.[5]

The anionic complex [Gd·**6**]$^-$ has been chosen as an example of a complex that should provide higher intrinsic signal intensity. The enhanced relaxivity arises mainly from its faster water exchange rate. It is structurally similar to [Gd·**7**]$^-$, having replaced a carboxylate with a primary amine group. The *RRRR*-isomer of [Gd·**7**]$^-$, which contains the highest proportion of the twisted antiprismatic (m) isomer in solution, showed the fastest water exchange (τ_M = 68 ns; 298 K) compared to the other diastereoisomers.[6] So the *RRRR*-α substituted derivatives of DOTA should be preferred, because their water exchange rates are likely to be sufficiently fast as not to limit the overall relaxivity of the derived higher molecular weight conjugates. An additional enhancement in relaxivity may also arise from the increase in the rotational correlation time, τ_R. The ligand **(6)** has been designed with three remote carboxylate groups, which provide linkage points for high molecular weight compounds, such as the amine **(28)** (kindly provided by Guerbet s.a.). Another advantage of using [Gd·**6**]$^-$ as base for targeting contrast agents is related to its charge. Negatively charged chelates may interact more strongly with the binding sites of proteins,[4] compared to neutral complexes, and then may be carried more efficiently into the cells. For all these reasons [Gd·**6**]$^-$ represents a promising candidate upon which to develop folate targeting contrast agents.

4.2. Synthesis of [Gd·9] and its folate derivatives

4.2.1. Synthesis of [Ln·9]

The gadolinium and the europium complexes of the ligand **(9)** were synthesized according to the scheme outlined in *Figure 4.2*.

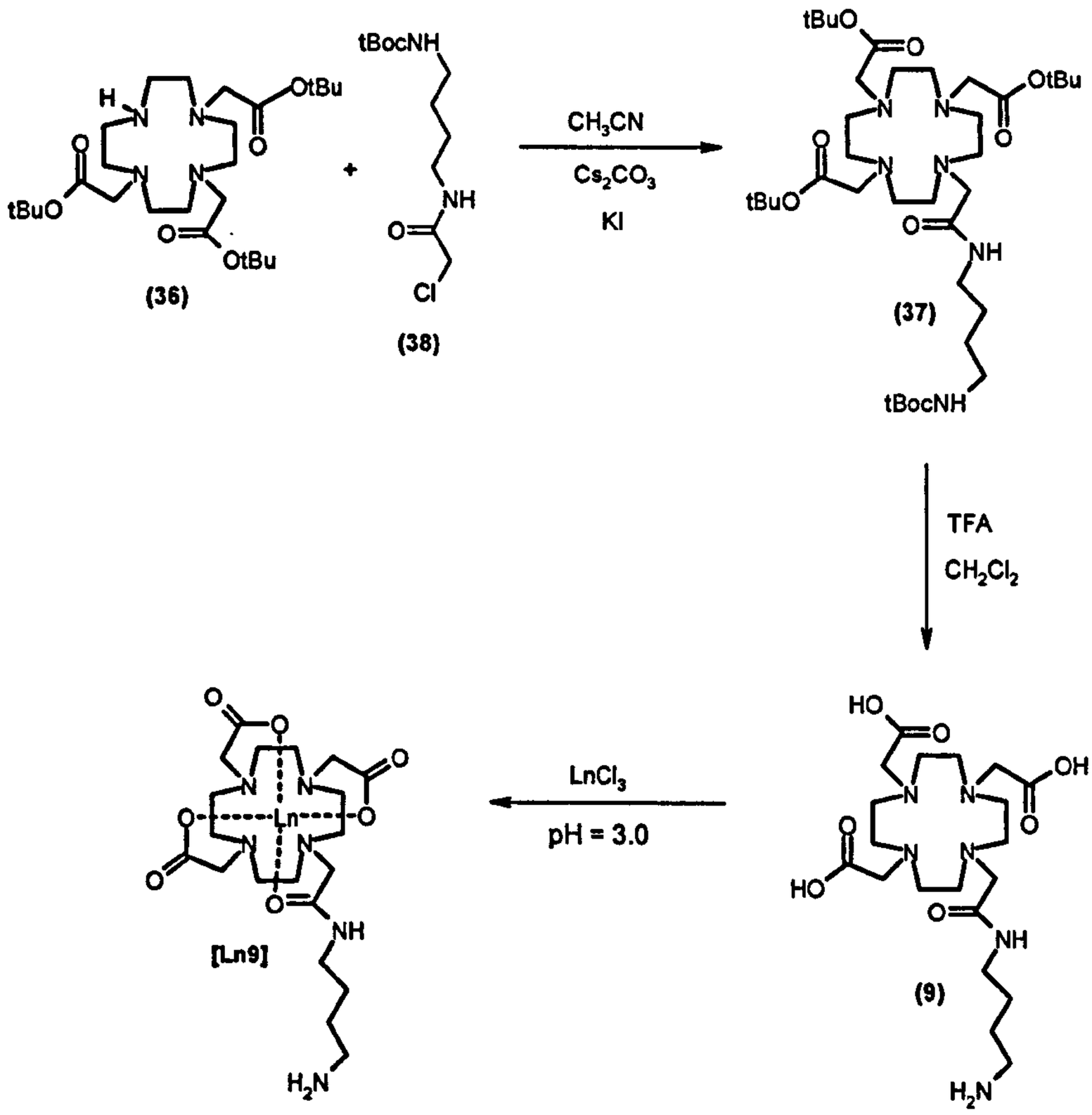

***Figure 4.2** – Synthesis of [Ln·9] Ln = Eu^{3+} and Gd^{3+}.*

The N-alkylation of DO3A^{t}Bu **(36)** was effectued using the chloroamide **(38)** in the presence of caesium carbonate as base. All the attempts made in acetonitrile solution were accompanied by rather low yields (< 30%) and no appreciable improvements were obtained by increasing either the temperature or the reaction time. However, the addition of small quantity of potassium iodide to the stirring solution resulted in a significant increase in the final yield. Nucleophilic substitution of the chlorine by iodide gave the intermediate α-iodoamide in which the iodide is a leaving group leading to a speeding up of the reaction rate. The progress of the reaction was followed by TLC and ESMS, which indicated the completion of the reaction after 18 hours. The triester **(37)** was isolated in high yield (~80%) after purification over silica gel.

The cleavage of both the carbamate and the t-butyl esters was carried out using trifluoroacetic acid in DCM at room temperature. The reaction was followed by TLC and by ^{1}H NMR. Small portions of the reacting solution were collected over time, evaporated and dissolved in $CDCl_3$. The disappearance of the t-butyl and t-Boc resonances at 1.44 and 1.64 ppm respectively was checked and the reaction was found to be complete after 18

hours. The free ligand **(9)** was extracted from aqueous solution and isolated in the form of the trifluoroacetate salt.

The europium complex was synthesized from water solution. Its formation was followed by ^{1}H NMR, which showed the disappearance of the free ligand after 24 hours. The reaction was repeated in the case of the analogous gadolinium chelate. Purification was achieved by passing the crude material through a strong anionic exchange resin, which yielded the complexes in the form of the free amine.

The pendant α-chloroamide **(38)** was synthesized starting from the commercially available 1,4-diamino butane **(39)** (*Figure 4.3*). Slow addition of a dioxane solution of $(BOC)_2O$ to an excess of 1,4 diamine, resulted in a mixture of mono- and di-protected amine. The "unwanted" N,N bis-t-Boc compound was removed by filtration in water/dioxane, and the mono-protected amine **(40)** was finally isolated in low yield (15%). Its free amino group was then coupled to chloroacetic acid **(41)**, previously activated by using the conventional coupling agents (EDC and NHS) to yield the chloroamide **(38)**.

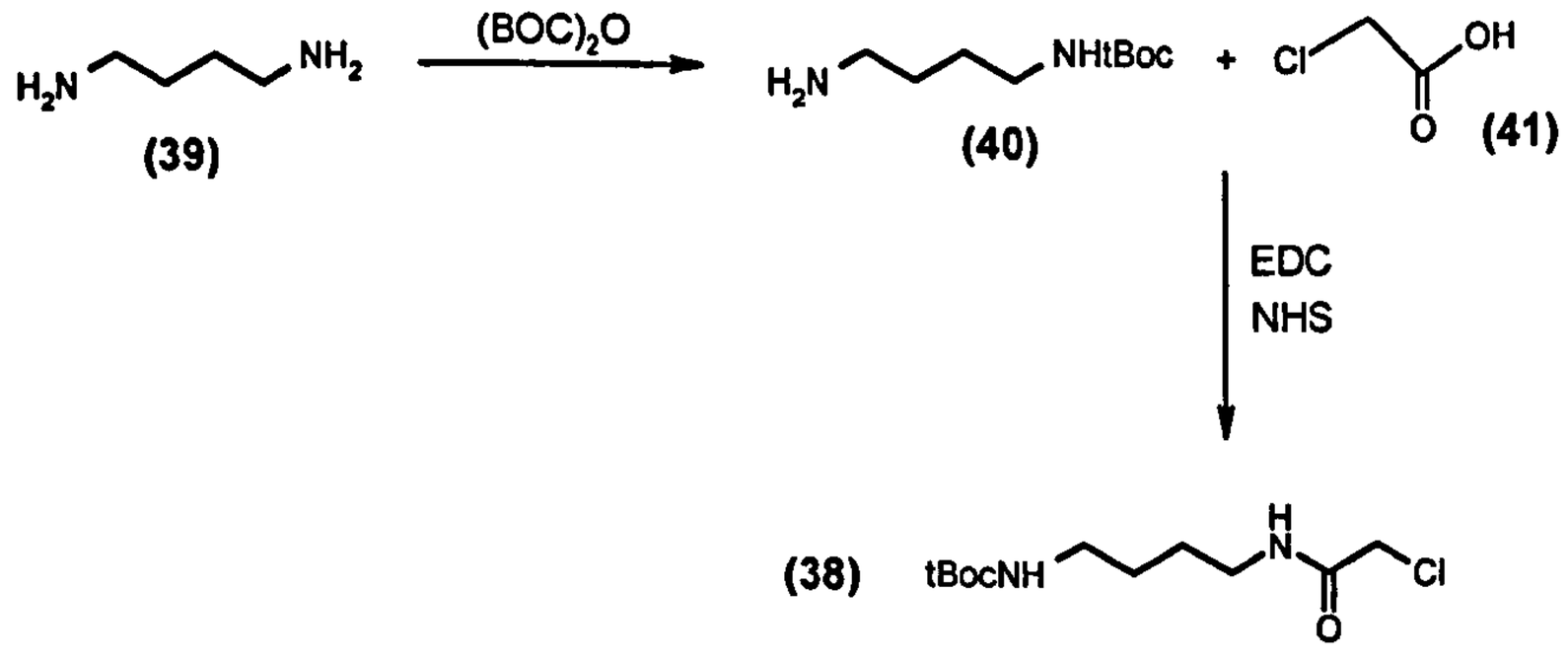

***Figure 4.3** – Synthesis of N-(N-t-butoxycarbonyl-1,4-diaminobutyl)-2-chloro acetamide **(38)**.*

4.2.2. Synthesis of the [Gd·9]-γ-folate conjugate

The folate γ-conjugate of **[Gd·9]** was synthesized according to the pathway outlined in *Figure 4.4*.

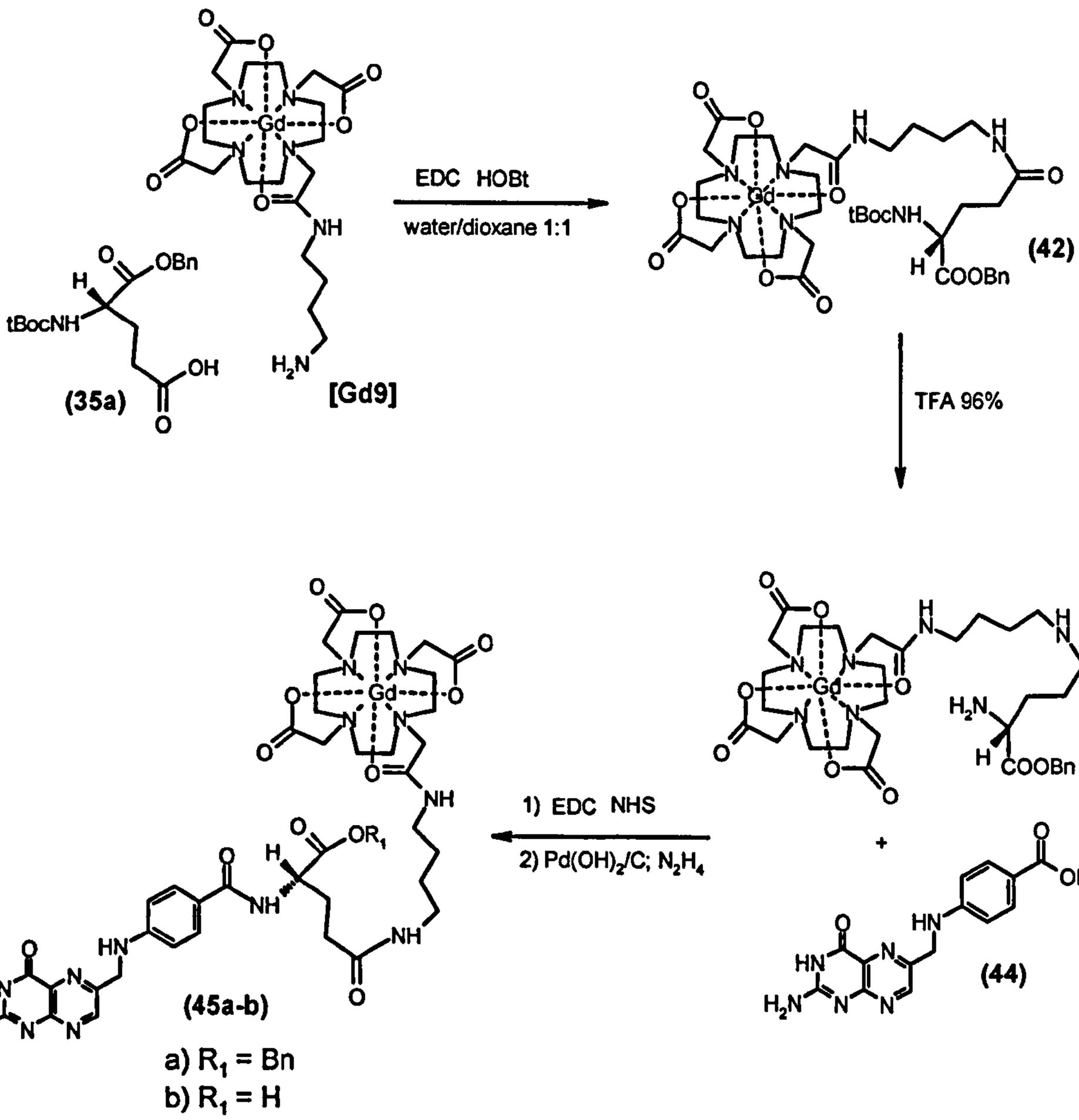

***Figure 4.4** – Synthesis of the [Gd9]-γ-folate conjugate.*

Following the approach described in Chapter Three, the gadolinium chelate [Gd·**9**] was first coupled to the commercially available α-benzyl-N-^{t}Bocglutamate **(35a)**. The free γ-carboxylate was activated using EDC and HOBt in a water/dioxane mixture 1:1 (v/v) maintaining the pH constantly at 6.0. The resulting activated ester was reacted *in situ* with [Gd·**9**]. Formation of the amide **(42)** was monitored and confirmed both by ESMS (m/z = 971) and HPLC (t_r = 16.5 min) and purification of the crude material was achieved by chromatography over alumina. The cleavage of the ^{t}Boc protecting group was performed in acidic solution, using trifluoroacetic acid. Under such strongly acidic conditions the gadolinium chelate could undergo decomplexation. However, due to its high thermodynamic and kinetic stability and to the short time required for the reaction (few minutes), no free ligand was detected either by ESMS nor by TLC and the compound **(43)**

was isolated in quantitative yield in the form of its TFA salt. The corresponding free amine, obtained passing the salt through a strong anionic exchange resin, was then coupled to pteroic acid **(44)**.

Harvison and coworkers,[7] in synthesizing a series of γ-substituted folic acid analogues have used N^{10}-trifluoroacetyl pteroic acid instead of pteroic acid because of its higher solubility. However, the presence of the electron withdrawing N^{10}-trifluoroacetyl group, may reduce the nucleophilicity of the para carboxylate, resulting in incomplete formation of the activated ester. Moreover, the additional step required to synthesize the trifluoroacetyl derivative is characterized by a low yield and separation problems, whereas pteroic acid is commercially available even though expensive. However, different synthetic procedures have been published in the literature for the preparation of pteroic acid. For example, it can be obtained by treating folic acid with acetic anhydride in acetic acid to give the acetylated azlactone, which is then cleaved under mild basic condition to yield pteroic acid.[8] Alternatively, it can be obtained enzymatically from folic acid using carboxypeptidase G.[9, 10] For these reasons pteroic acid itself was preferred in this work.

Attempts to further optimize the yields of the coupling reaction, between pteroic acid and the gadolinium chelate **(43)**, by varing the reaction conditions (*i.e.* time, temperature and reagent concentration) were made.[11] Typically pteroic acid was activated in DMSO (c = 6-15 mM) in the presence of a dehydrating agent (DCC, EDC) and a coupling adjuvant (NHS, HOBt) at a temperature between 0 ^{0}C and 25 ^{0}C for a period of time between 3 and 24 hours. The activated ester, which was detected by ESMS, was then reacted *in situ* to the gadolinium chelate **(43)** in the presence of a base, such as triethylamine. Temperatures of between 25 ^{0}C and 50 ^{0}C and reaction times between 12 and 48 hours were compared. The formation of the amide **(45a)** was followed by ESMS (m/z = 1141) and HPLC (t_r = 13.8 min). The best conditions found are detailed in the experimental section (Chapter Five). The crude material was precipitated by adding organic solvents (ethyl acetate or acetonitrile). Unreacted pteroic acid co-precipitated as well. All attempts made to purify the mixture, either by silica gel or reverse phase chromatography or by gel filtration, failed because of the poor solubility of the compounds. The unreacted pteroic acid was therefore not removed completely and the mixture was used directly in the next step.

Deprotection of the α carboxylate (*i.e.* as its benzyl ester) was first performed in a diluted sodium hydroxide solution (pH = 9.0). The hydrolysis of the benzyl group was

followed by HPLC and ESMS, which showed the completion of the reaction after 20 hours. However, this method cannot be applied in this case because racemization at the chiral centre (the α-carbon) occurs, as it shown in *Figure 4.5*. This was confirmed by measuring the optical rotation $[\alpha]_D^{20}$ over time, in sodium hydroxide solution (pH=9.0). Starting from an initial value of + 14.6 (c = 0.4 g/100 ml in NaOH 0.02 M),[12] the optical rotation gradually decreased to 0^0 after one hour, when racemization was complete.

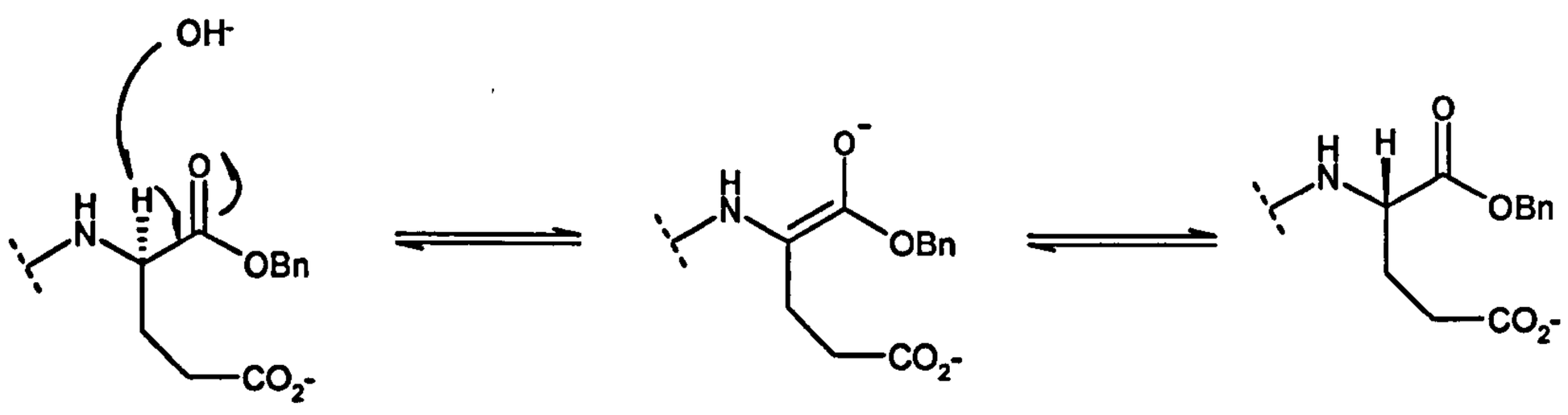

***Figure 4.5** – Racemization at the α-carbon in basic aqueous solution.*

An alternative method of deprotection was required. Previous attempts made on the α-benzyl ester of folic acid in DMF/water mixture, using H_2 or ammonium formate in presence of palladium over carbon as catalyst failed, maybe because of the low solubility of the starting materials in these solvents. The use of DMSO, in which folate derivatives are more soluble, could also poison the catalyst, reducing its activity. However, when α-O-debenzylation was performed in the presence of N_2H_4, using palladium hydroxide over carbon in DMSO solution, the reaction worked successfully in quantitative yield. The catalyst was removed over celite, and the crude material precipitated by adding organic solvents (ethyl acetate or acetonitrile). Pteroic acid, deriving from the previous step, was separated at this stage by silica gel chromatography to yield the pure [Gd·**9**]-γ-folate.

An alternative method of purification, which exploits the different masses of the compounds to be separated (MW **(45b)** = 1051 and MW **(44)** = 311), is represented by gel filtration. It was successfully performed on a small scale (10-20 mg), by using Sephadex G-25 and water as eluent.

The synthetic procedure described in this paragraph could be repeated for the synthesis of the α-[Gd·**9**]-*folate*, using γ-benzyl-N-^{t}Boc-glutamate **(35b)** as starting material. However, a different approach was followed in the end as discussed below.

4.2.3. Synthesis of the [Gd·9]-α-folate conjugate

The [Gd·9]-α-folate was synthesized according to the scheme in *Figure 4.6*.

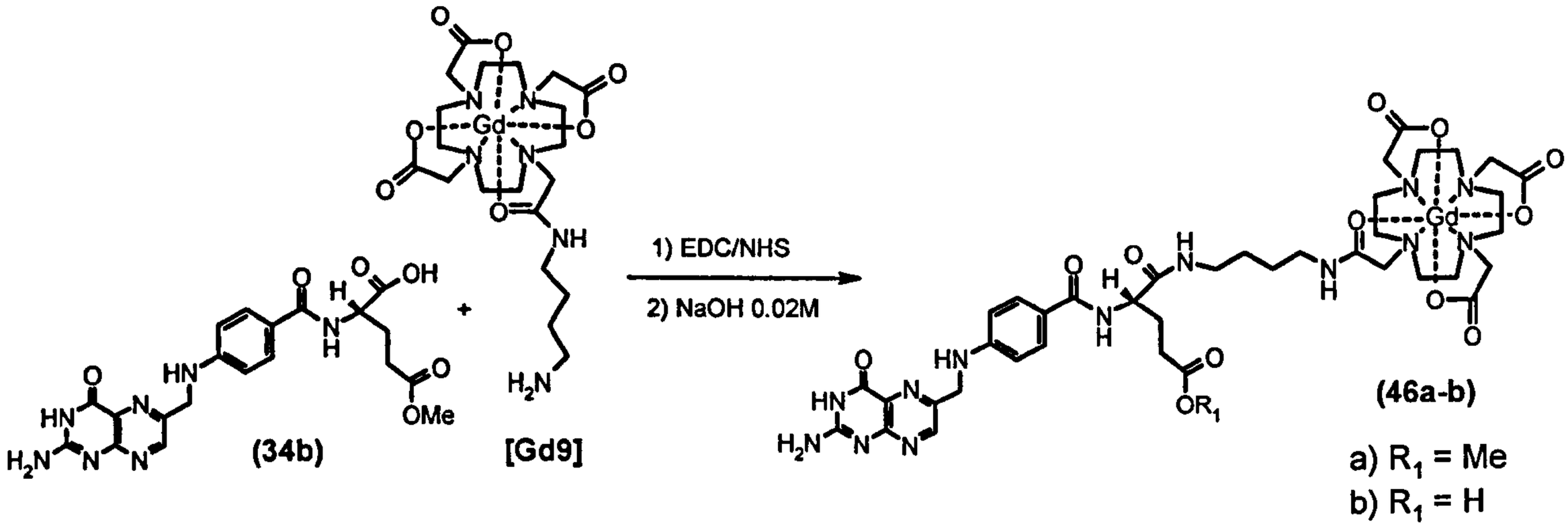

***Figure 4.6** – Synthesis of the [Gd·9]-α-folate conjugate.*

In order to optimize the coupling reaction conditions, the γ-methyl ester of folic acid **(34b)** was first reacted with the simple and cheap amine, hexylamine. The α carboxylate was activated using different dehydrating agents (EDC, DCC) and coupling adjuvants (NHS, HOBt) in DMSO solution at temperature between 0 ^{0}C and 25 ^{0}C. The resulting activated ester, which was detected by ESMS, was then reacted *in situ* with hexylamine at temperature between 25 ^{0}C and 50 ^{0}C for a period of time between 12 and 48 hours. The formation of the amide was followed by ESMS, HPLC and ^{1}H NMR. The best conditions found for this "model reaction" were repeated in the coupling of the monoamide complex [Gd·9] (see Chapter Five) and the [Gd·9]- α-folate was obtained in modest but satisfactory yield (33%), after purification over silica gel.

Cleavage of the γ-methyl ester in **(46a)** was easily achieved in sodium hydroxide solution 0.02 M (pH = 9.0). Racemization at the α-carbon is less likely to occur in this case, because the pK_a of the hydrogen in an α position to an amide is higher than the pK_a of the α-hydrogen in an ester. The mild alkaline hydrolysis was followed by ESMS and HPLC and was found to be complete in 24 hours.

This procedure could be repeated for the synthesis of the [Gd·9]-γ-folate. The α-ester of folic acid required in this case could be synthesized as discussed in Chapter Three.

4.2.4. Synthesis of the [Gd·9]$_2$-α,γ-folate conjugate

The MRI signal intensity depends on the amount of paramagnetic species that can be localized in the target tissue. In the case of folate targeted contrast agents this is limited by the amount of FBP present in the target tissue. As already discussed, a possible way to increase the signal intensity consists in using multimeric gadolinium chelates.[5] However, the main interest in the dimer [Gd·**9**]$_2$ -α,γ-folate relates to a study of its affinity for FBP. It represents a reference point to allow a comparison with the binding affinity of its mono-folate analogues.

For these reasons [Gd·**9**]$_2$ -α,γ-folate has been synthesized according to the sequence shown in *Figure 4.7*. Folic acid was directly coupled to two equivalents of the monoamide complex **[Gd·9]**, using the same conditions discussed in the previous paragraph. The dimeric chelate was isolated in satisfactory yield (32%) after purification over silica gel.

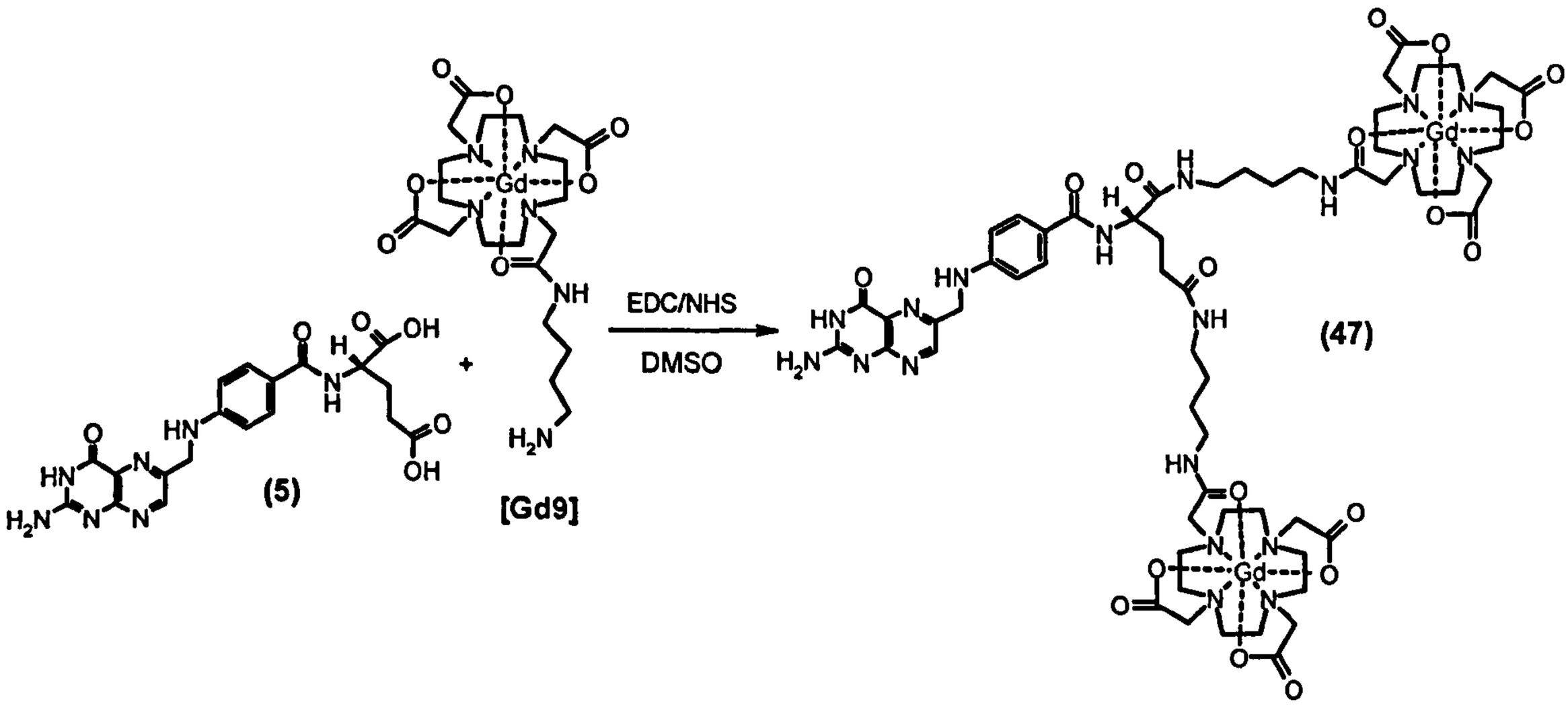

***Figure 4.7** – Synthesis of the [Gd·9]$_2$-α,γ-folate conjugate.*

4.3. Synthesis of [Gd·6]⁻ and its folate derivatives

4.3.1. Synthesis of [Ln·6]⁻

Syntheses of tetra-alkylated derivatives of cyclen, such as (22b), may be obtained following two different strategies (*Figure 4.8*).

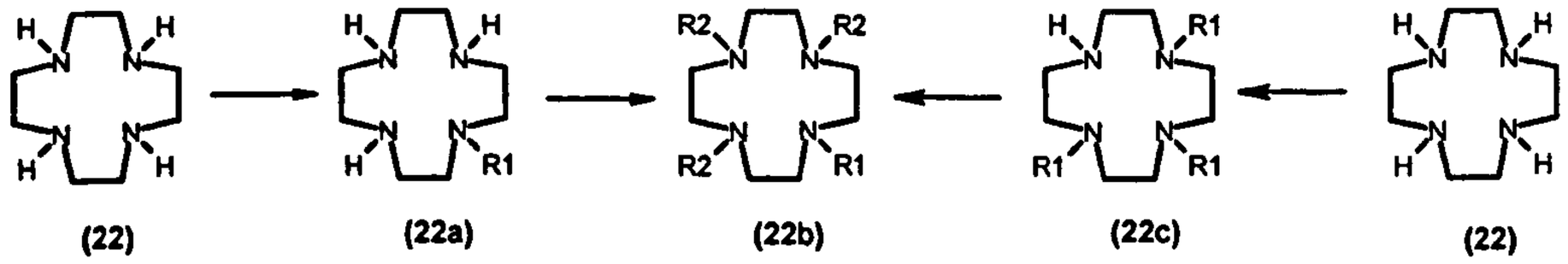

***Figure 4.8** – Different approaches to synthesize tetra-alkylated cyclen derivatives.*

In the first route, the mono-alkylated compound **(22a)** may be synthesized first. In this case a preliminary protection of the other three nitrogens may be required, because of the difficulties in a selective mono-alkylation step. Molybdenum hexacarbonyl in dibutyl ether can be used for this purpose.[13] The metal coordinates three nitrogens of the ring, leaving the fourth free to react with the alkylating agent. The removal of the molybdenum complex requires oxidation in air and acidic hydrolysis. The three remaining nitrogens may then be further alkylated to yield **(22b)**. In a second approach, the tri-alkylated derivative **(22c)** may be synthesized first. In order to alkylate selectively three of the four nitrogens, a preliminary mono-protection of the amine group is, in theory, required. Several methods for the mono-protection of cyclen have been published in the literature. For example, Atkins and coworkers[14] developed a procedure, which involved the formation of 1,4,7,10-tetraazacyclo[5.5.1.0]tridecane **(22d)** (*Figure 4.9*), followed by its hydrolysis to yield the 1-formyl monoprotected cyclen **(22e)**. The remaining three free nitrogens can undergo further alkylation under standard conditions, before the protecting group is removed.

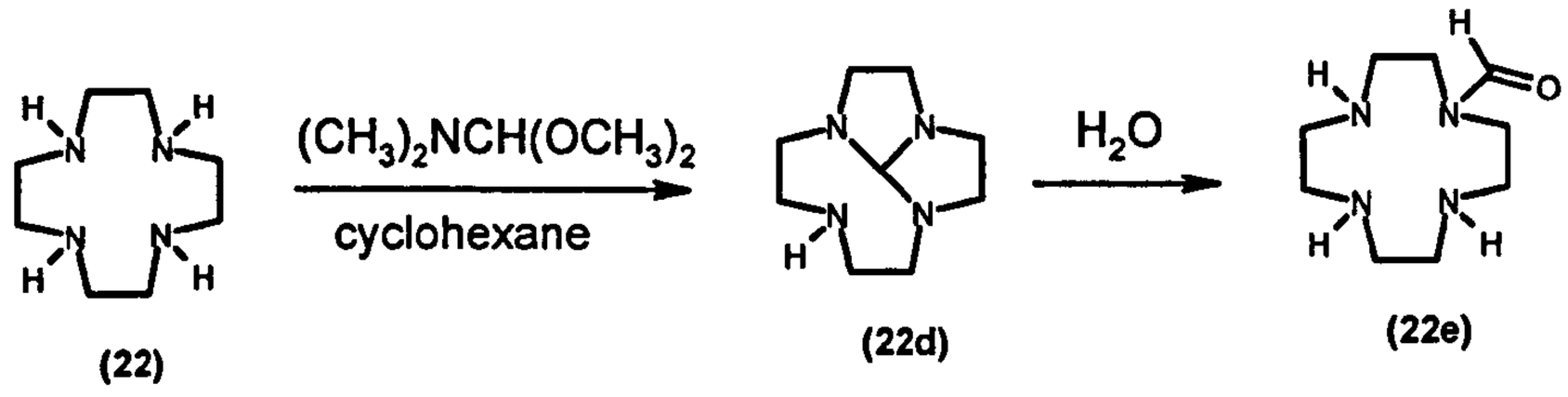

***Figure 4.9** – Example of mono-protection of cyclen.*

However, it has also been demonstrated that cyclen can be selectively alkylated three or four times depending on the nature of the base employed (Chapter Two). This represents an easy one step route to synthesize tri-alkylated derivatives of cyclen. Although further purification is required, the yields of these reactions are generally good (~ 35%). Once the tri-alkylated derivative **(22c)** is made, the fourth nitrogen can be easily alkylated.

This approach has been chosen in the present work, as shown in *Figure 4.10*.

The tri-alkylated compound **(49)** was synthesized according to the procedure employed for the analogous adipate derivative **(24)** (Chapter Two). The use of racemic dimethyl-α-bromoglutarate **(48)** ($NaHCO_3/CH_3CN$) led to formation of a mixture of diastereoisomers. Alkylation of the fourth nitrogen was achieved by using the racemic methyl α-bromo-N-benzoyl-5-amino valerate **(50)**, in the presence of caesium carbonate as base. The reaction was followed by TLC, which showed the disappearance of the starting tri-alkylated material after three days. The compound **(51)** was isolated in high yield (~80%) after purification over silica gel.

Cleavage of the methyl ester groups was achieved in lithium hydroxide solution. The hydrolysis was followed by ^1H NMR, which showed disappearance of the methyl proton resonances between 3.60 and 3.75 ppm after 24 hours. The benzoyl amide group, which is stable in strong alkaline conditions, was then subsequentially removed under strongly acidic conditions. Again the amide hydrolysis step, performed in 6 M hydrochloric acid solution, was followed by ^1H NMR. The aromatic proton resonances at 7.45 ppm and 7.80 ppm were checked and the reaction was found to be complete after 24 hours. The ligand (6) was isolated in the form of the free amine after purification through a strong cationic exchange resin (Dowex 50W), eluting with 12% ammonia solution.

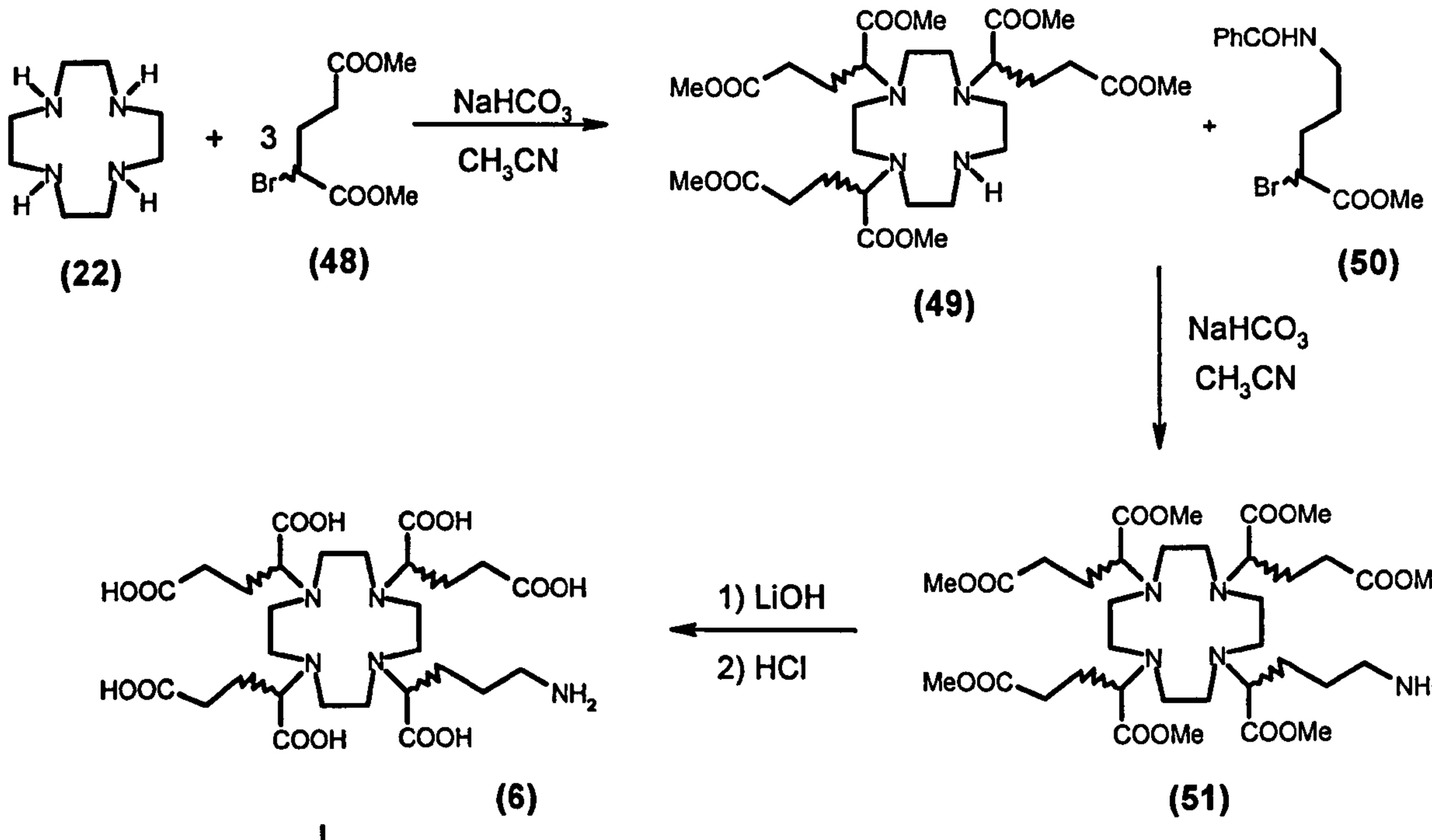

Figure 4.10 – Synthesis of [Ln·6]⁻ Ln = Eu^{3+} and Gd^{3+}.

Both the europium and gadolinium complexes were synthesized in aqueous solution at pH 5.5. The complexation reaction was followed by ESMS and, in case of europium, by ^{1}H NMR as well. Both complexes were recrystallized from acidic aqueous solution (pH = 3.0), and were isolated as a mixture of diastereoisomers. No further separation of the isomers was attempted.

4.3.2. Synthesis of methyl α-bromo-N-benzoyl-5-amino-valerate (50)

The methyl ester of α-bromo-N-benzoyl-5-amino-valerate **(50)** was synthesized starting from the commercially available 5-amino valeric acid **(52)** (*Figure 4.11*). The amino group was protected using a benzoyl protecting group, to give high stability to hydrolysis. Standard conditions (benzoyl chloride in water/THF solution at pH between 8-10) worked successfully and gave the desired compound **(53)** in good yield (88%).

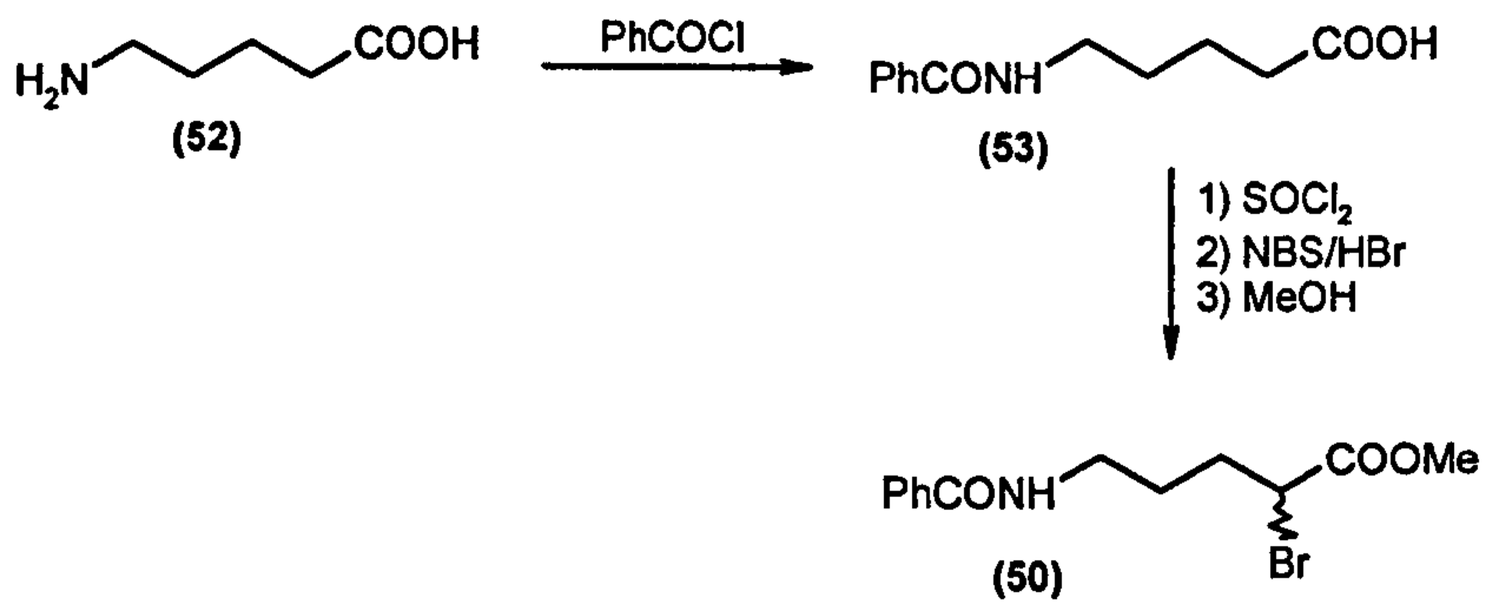

***Figure 4.11** – Synthesis ofmethyl α-bromo-N-benzoyl-5-amino valerate (50).*

A first attempt to α-brominate the N-benzoyl-5-amino valeric acid **(53)** was made via the classical Hell-Volhard-Zelinsky approach,[15-19] in which the carboxylic acid was treated with free bromine in presence of a catalyst, such as red phosphorus. However, this procedure was characterized by low yields (<20%). The strenuous experimental conditions (high temperature and extended reaction times) resulted in partial hydrolysis of the amide group. N-Bromosuccinimide (NBS) is known to α-brominate a variety of acyl chlorides (formed *in situ* by the reaction of thionyl chloride with carboxylic acid) in good yields.[20] NBS was chosen as the brominating agent, not only because is easy to handle, but also because it α-brominates more efficiently than molecular bromine, requiring lower temperatures and reaction times. Under these milder conditions, the extent of the amide hydrolysis was significantly reduced, resulting in a higher final yield. The methyl esterification was easily achieved by treating the corresponding acyl chloride with methanol. Pure compound was obtained after purification over silica gel.

4.3.3. Synthesis of the [Gd·6]⁻ -α-folate conjugate

The three remote carboxylic groups in [Gd·**6**]⁻ must be protected before coupling folate derivatives, in order to avoid intra or intermolecular reactions involving the complex itself. Surprisingly, methyl esterification was successfully achieved suspending the complex [Gd·**6**]⁻ in methanol, in presence of catalytic amounts of hydrochloric acid (*Figure 4.12)*. The reaction was followed by TLC and ESMS and was found to be complete within an hour. Purification was achieved by a column chromatography, over alumina.

Direct coupling of the tri-ester complex **(54)** to the γ-methyl ester of folic acid should result in the formation of the corresponding folate α-derivative. However, all attempts made in DMSO and using the same conditions for the monoamide complex [Gd·**9**] (*Paragraph 4.2.2*) failed. The steric hindrance associated with coupling to the secondary carboxylic acid and/or the short hydrocarbon amine chain may be responsible for the failure of this reaction. A possible solution could be found by introducing a spacer, between the complex and the folate moiety. This approach, however, has not been followed in this work.

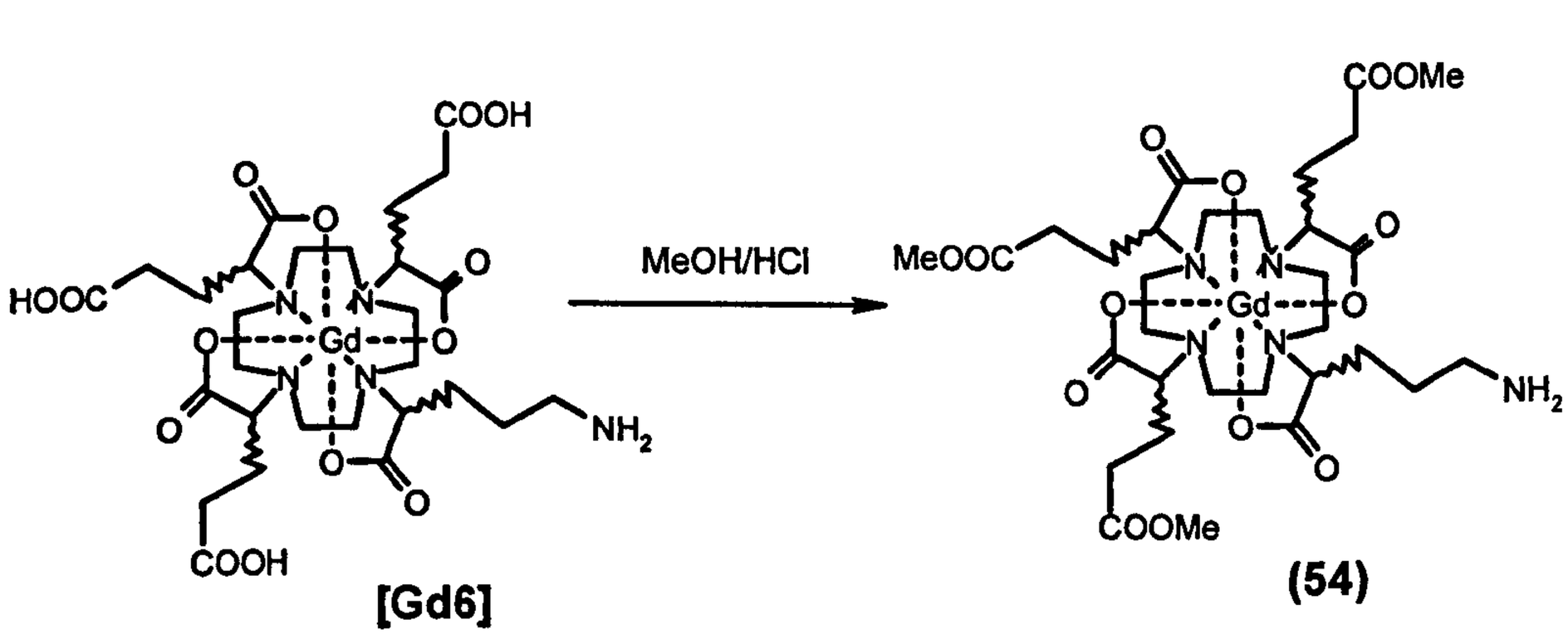

***Figure 4.12** – Methyl esterification of the remote carboxylate in [Gd·6]⁻.*

4.3.4. Synthesis of the [Gd·6]-γ-folate conjugate

The failure of the previous reaction can be turned to advantage in the syntheses of the folate γ-derivative of [Gd·**6**]⁻. In theory, by reacting folic acid itself with the tri-methyl complex **(54)**, the γ position may react selectively, because of the steric problems mentioned below.

Therefore the mixture of α and γ benzyl esters of folic acid (ratio 4:1) previously synthesized was used as the starting material. It was reacted with the tri-ester gadolinium complex **(54)** in DMSO, using the usual conditions (*Figure 4.13*). The reaction was followed by ESMS, which revealed the formation of the amide **(56a)** (m/z = 1385) after 24 hours. More importantly, HPLC indicated the presence of one isomer, confirming that the α-carboxylate did not react. The crude compound was purified over silica gel to yield the [Gd·6]-γ-folate in satisfactory yield (44%). The hydrolysis of the three methyl and of the α-benzyl esters was easily achieved in sodium hydroxide solution (pH = 9.0).

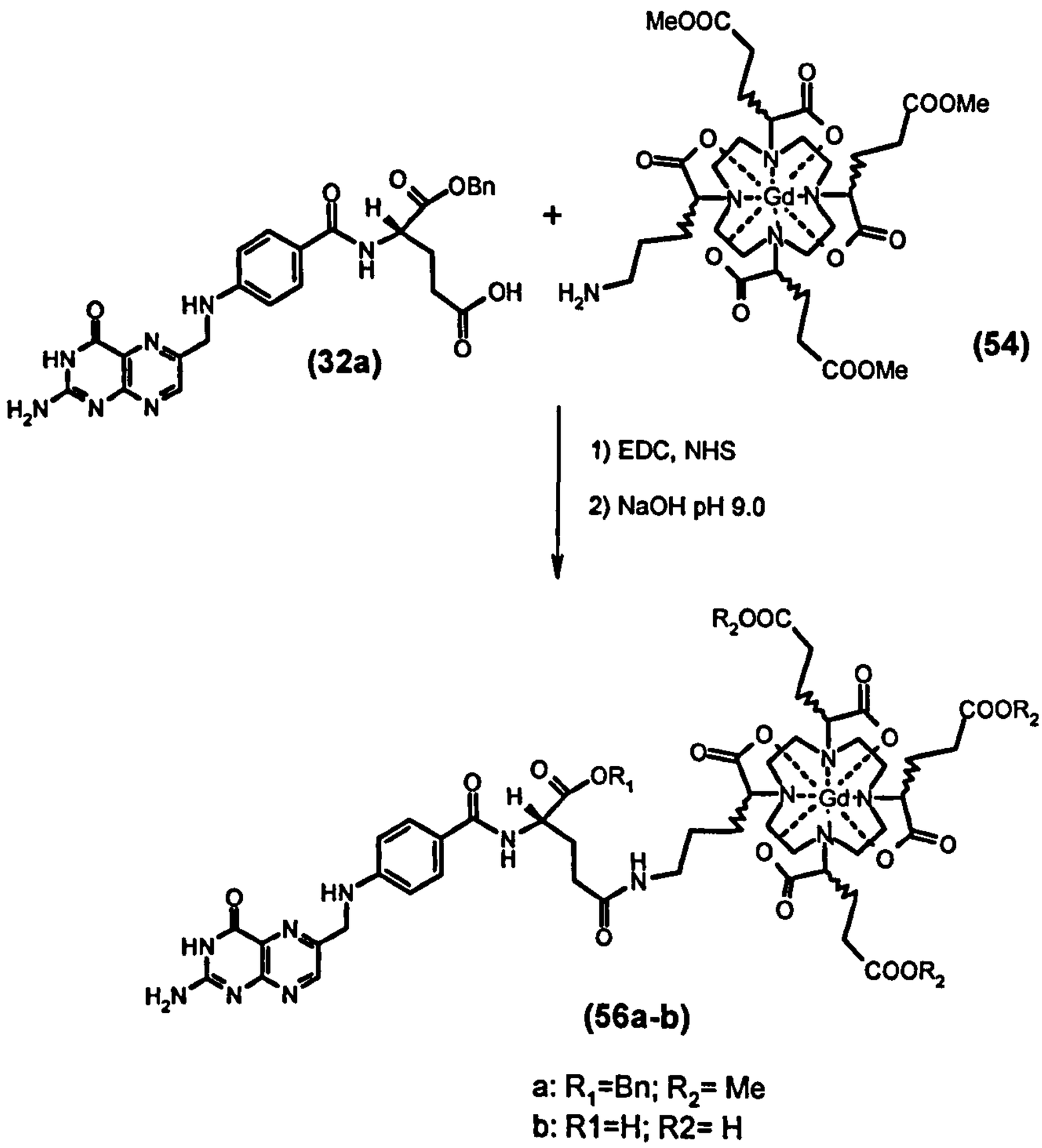

***Figure 4.13** – Synthesis of the [Gd·6]-γ-folate conjugate.*

4.4. Solution structures of Europium (III) complexes

The emission spectrum of the complex [Eu·9] has been recorded in water solution (pH = 7.50), following direct excitation at 397 nm (*Figure 4.14)*. The analysis of the $\Delta J = 1$ (~ 590 nm) transitions are particularly interesting. The intensity of this magnetic-dipole transition varies very little from one co-ordination environment to another.[21] However, two or three transitions are allowed depending on the complex symmetry. For example, the emission spectrum of $[EuDOTA]^-$ (recorded under the same conditions) presents two overlapping pairs of bands, related to the square antiprismatic (M) isomer and a weaker set related to the twisted square antiprismatic (m) isomer in a ratio 4:1. A similar shape and ratio of the $\Delta J = 1$ transition bands was observed in the emission spectra of [Eu·9], suggesting that the square antiprismatic (M) isomer is predominant in solution.

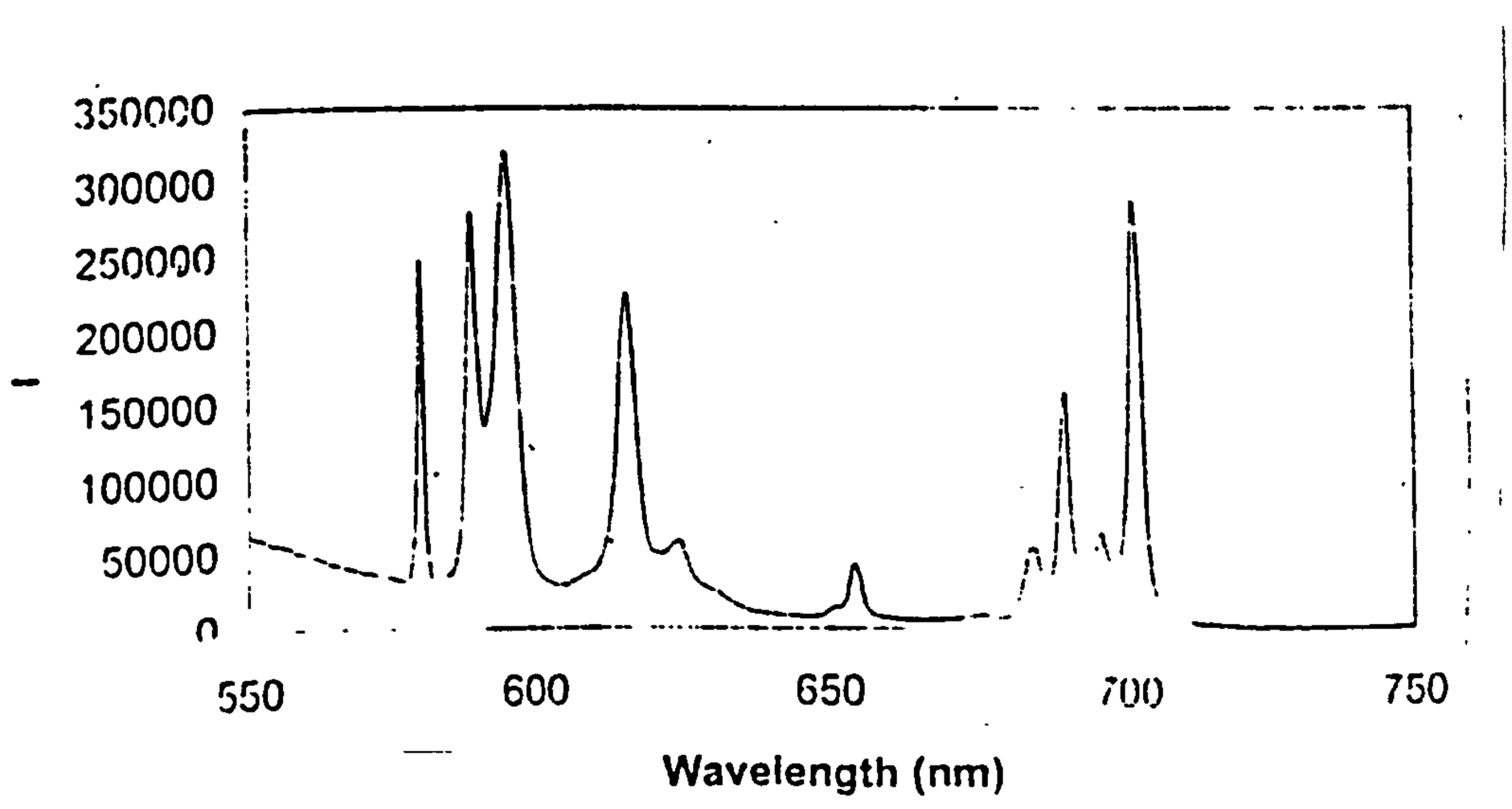

Figure 4.14 – Emission spectrum of [Eu·9] in H_2O at pH = 7.20.

The ^1H NMR spectrum of [Eu·9] was recorded in D_2O at pD=7.0. As previously demonstrated for $[EuDOTA]^-$ two major isomers are present in solution,[22-25] which can be distinguished by observing the resonances of the most shifted axial ring protons (30-50 ppm for the square antiprismatic isomer (M) and about 20 ppm for the twisted square

antiprismatic isomer (m)). The four singlets, observed for the axial ring protons between 30 and 37 ppm are similar to those reported for other monoamide derivatives of DOTA,[26] and suggest the prevalence of the square antiprismatic isomer (M), a result which is consistent with the emission spectra.

The ^1H NMR spectrum of [Eu·**6**]$^-$ was recorded in D_2O at pD = 7.0 and it clearly evidenced the presence of all the eight stereoisomers.

The hydration number *q* has been evaluated by measuring the luminescence lifetimes of the europium complex in H_2O and in D_2O solutions (Chapter Two). The empirical equation (1.22) has been used to calculate the hydration number, however an additional correcting parameter Δ'_{corr} has been considered to take into account the quenching effect of the closest amide NH oscillator (0.08 ms^{-1}).[27] The values for the rate constants for the depopulation of the exctited states of the [Eu·**9**] and the [Eu·**6**]$^-$ and the derived hydration numbers *q* are reported in *Table 4.1*. Both the monamide complex, [Eu·**9**], and the anionic complex, [Eu·**6**]$^-$, possess one water molecule in the inner sphere as expected.

Complex	k_{H2O} $(ms)^{-1}$	k_{D2O} $(ms)^{-1}$	q
[Eu·**9**]	1.55	0.41	0.97 ± 0.2
[Eu·**6**]$^-$	1.58	0.45	0.96 ± 0.2

***Table 4.1** – Rate constants for the depopulation of the excited states of [Eu**9**], [Eu·**6**]$^-$ and the derived q value.*

4.5. Relaxometric studies

4.5.1. Relaxivity of [Gd·9] and its folate derivatives

The relaxivity of the monoamide complex [Gd·**9**] and its folate derivatives has been measured at 65 MHz and 293 K in water, in an anionic background (*i.e.* a simulated extracellular anion environment) and in human serum (*Table 4.2*).

Complex	r_{1p} (water)	r_{1p} (anionic bkg)	r_{1p} (human serum)
[Gd·9]	5.3	5.2	
[Gd·9]-α-Folate	7.0	5.7	7.1
[Gd·9]-γ-Folate	6.8	5.6	7.0
$[Gd·9]_2$-α,γ-Folate	14.9	14.8	13.6

Table 4.2 – Relaxivity ($mM^{-1}s^{-1}$) at 65 MHz, 293 K and pH = 7.20.

The free amino complex [Gd·9] exhibits a relaxivity in water (5.3 $mM^{-1}s^{-1}$) similar to the values found for related DOTA monoamide derivatives.[5] The absence of change in the anionic background suggests that no binding of endogenous anions (such as, carbonate, phosphate, lactate and citrate) has occurred at the metal center.

The α and the γ-[Gd·9] folates exhibit practically identical relaxivity, as expected for complexes of the same molecular weight and which are structurally very similar. For both complexes the relaxivity measured in the anionic background was about 20% lower than the value measured in water. This decrement is unlikely to be related to the binding of any of the anions present in solution. Instead, it could be due to a partial reduction of the second and outer sphere contribution, arising from the presence of the folate moiety.

Anelli and coworkers[28] have reported a series of monoamide derivatives of DOTA, used in hepatobiliarity X-ray contrast imaging, in which the amino group is linked to an iodinated aryl ring. They found a two to three-fold increment in the relaxivity in human serum compared to the values in water solution. This significant difference was due to the strong binding of such gadolinium chelates to Human Serum Albumin (HSA) present in serum.

In case of the [Gd·9] folate derivatives, no such increment was found. The relaxivity in human serum was practically identical to the value in water, indicating little or no binding to HSA.

The $[Gd·9]_2$-α,γ-folate shows a relaxivity of 14.9 $mM^{-1}s^{-1}$ (7.5 $mM^{-1}s^{-1}$ per gadolinium), which is not so different from the relaxivity of the mono-folate analogues. A plot of r_{1p} versus molecular weight, for a series of monomeric and multimeric gadolinium chelates, is shown in *Figure 4.15*, whereas *Table 4.3* reports the parameters plotted.[5]

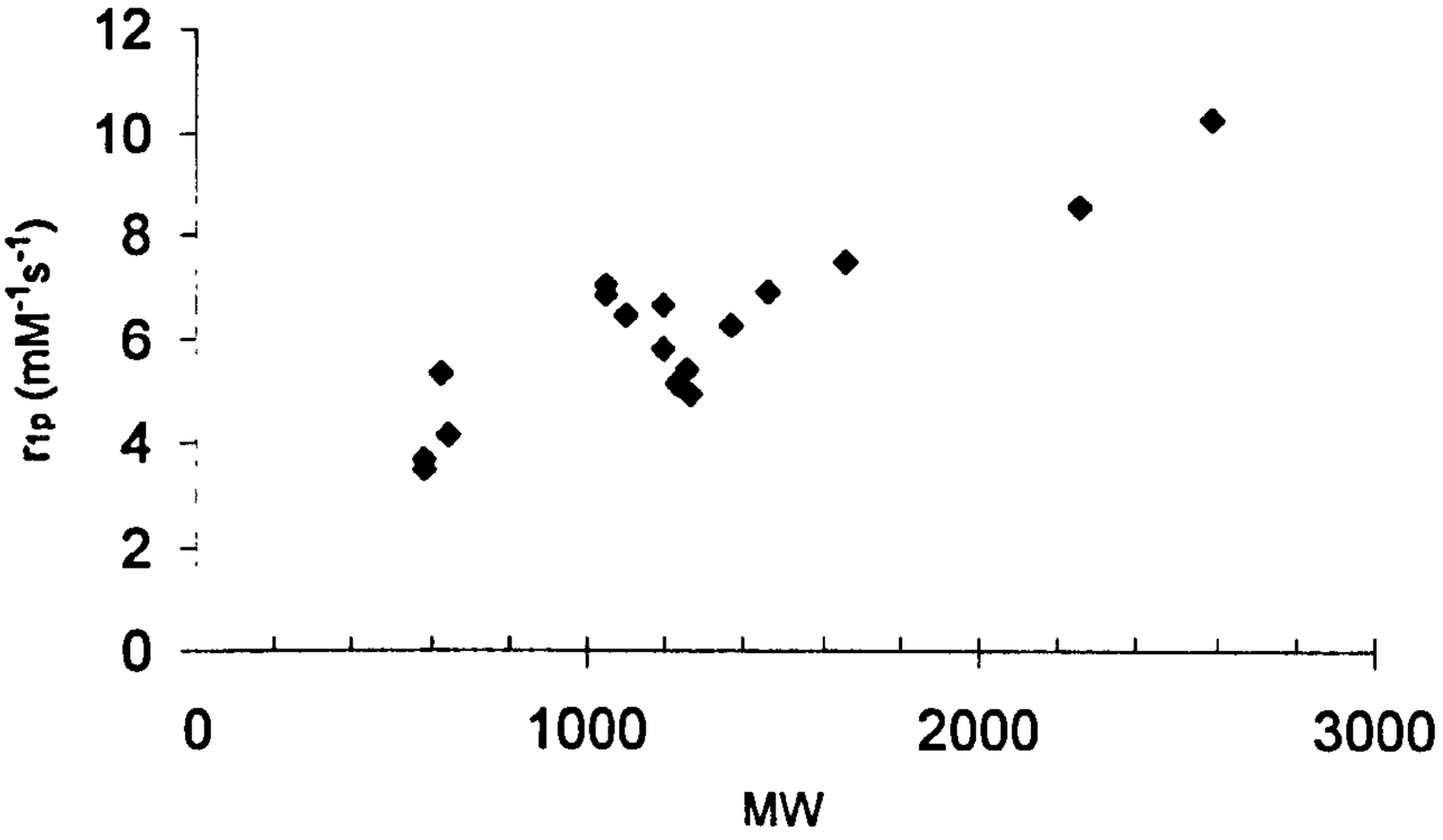

***Figure 4.15** – Plot of relaxivity versus MW for a series of multimeric and monomeric chelates.*

Ligand	MW	r_{1p}	Ligand	MW	r_{1p}
[Gd·4]	588	3.7	$[GdDO3A]_2$L9 **(64)**	1469	6.9
[GdDO3AMA] **(18)**	585	3.5	$[GdDO3A]_2$L6 **(60)**	1202	5.8
[Gd·65]	647	4.1	$[GdDO3A]_2$L7 **(62)**	1264	4.9
$[GdDO3A]_2$L2 **(57)**	1231	5.1	[Gd·9]	631	5.3
$[GdDO3A]_2$L5 **(61)**	1257	5.4	α-[Gd·9]-Folate	1051	7.0
$[GdDO3A]_2$L3 **(59)**	1103	6.4	γ-[Gd·9]-Folate	1051	6.8
$[GdDO3A]_2$L4 **(58)**	1201	6.6	α-γ-$[Gd·9]_2$-Folate	1663	7.5
$[GdDO3A]_2$L8 **(63)**	1367	6.2	$[GdDO3A]_3$L2	2259	8.5

***Table 4.3** – Relaxivity and molecular weight for a series of monomeric and multimeric Gd chelates.*[5]

The structures of the ligands reported are shown in *Figure 4.16*. The plot indicates that relaxivity generally increases with the molecular weight (*i.e.* the rotational correlation time τ_R) of the complex. However, the relationship is not always linear. Rigidity plays an important role in determining the relaxivity of multimeric gadolinium complexes. For example, $[GdDO3A]_2$L4 **(58)** and $[GdDO3A]_2$L5 **(61)** posses identical chelate structure and almost the same molecular weight. However, the first complex, having a less flexible linker, exhibits the higher relaxivity (6.6 $mM^{-1}s^{-1}$) compared to the second one (5.4 $mM^{-1}s^{-}$

[1]). Similarly, the flexibility of the linker between the two chelates in $[Gd\cdot\mathbf{9}]_2$-α,γ-folate explains the "limited" increment in relaxivity.

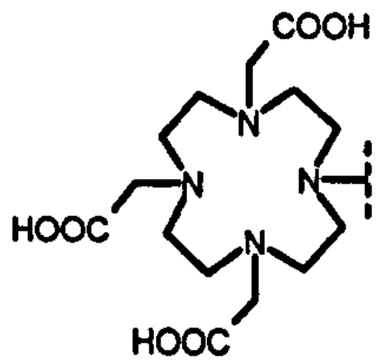

DO3A (**4**)

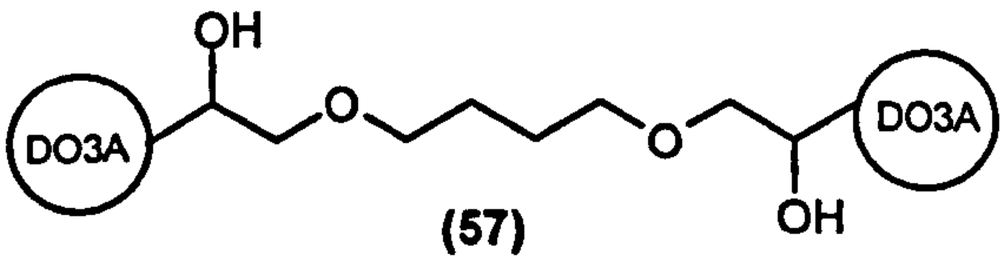

(57)

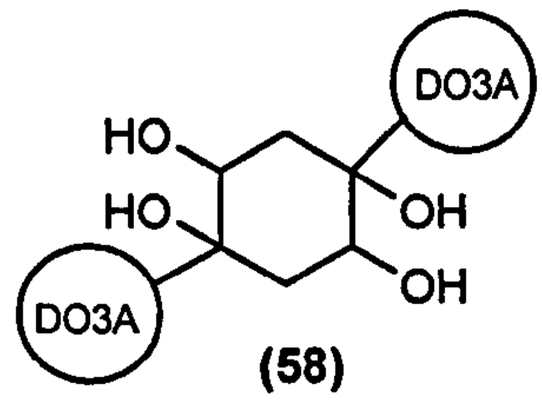

(58)

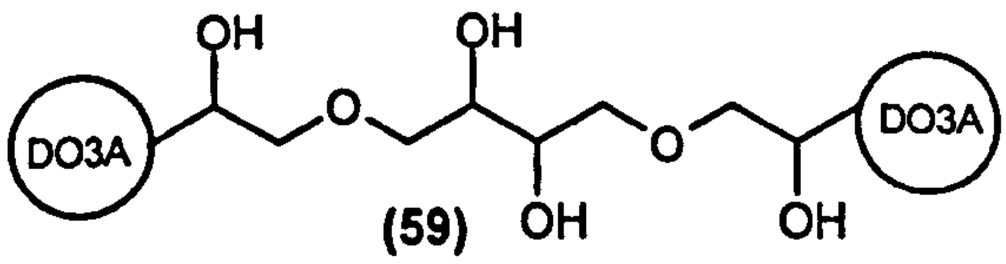

(59)

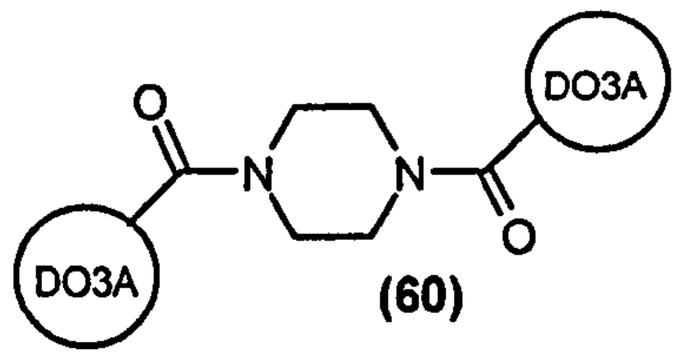

(60)

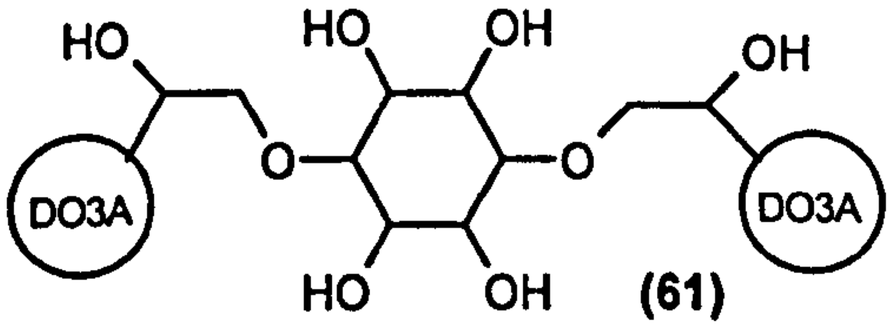

(61)

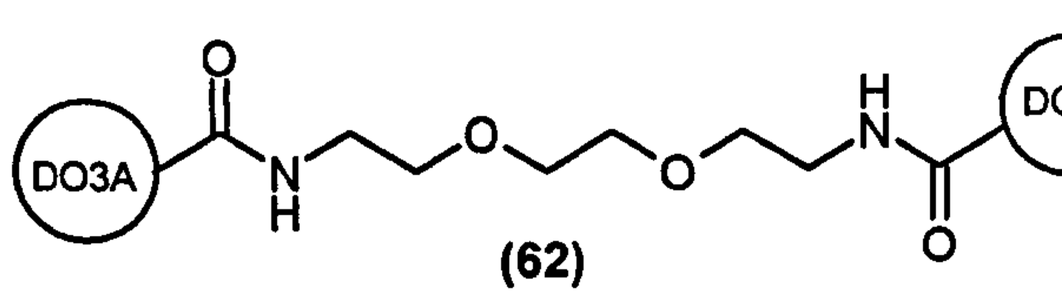

(62)

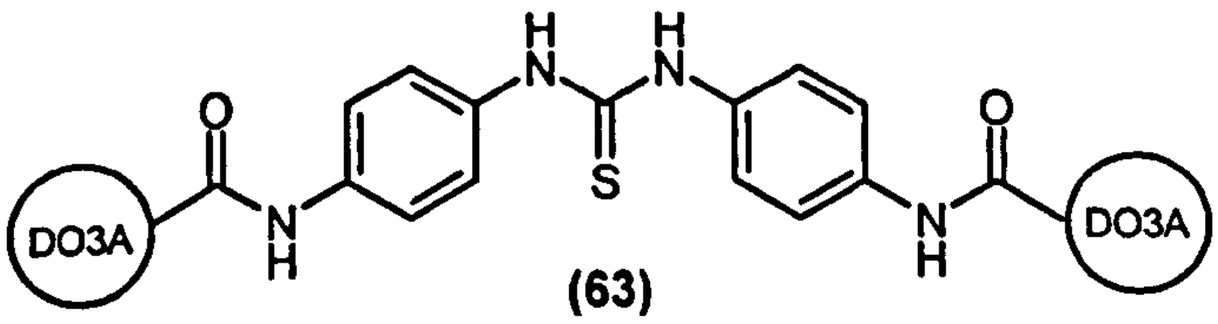

(63)

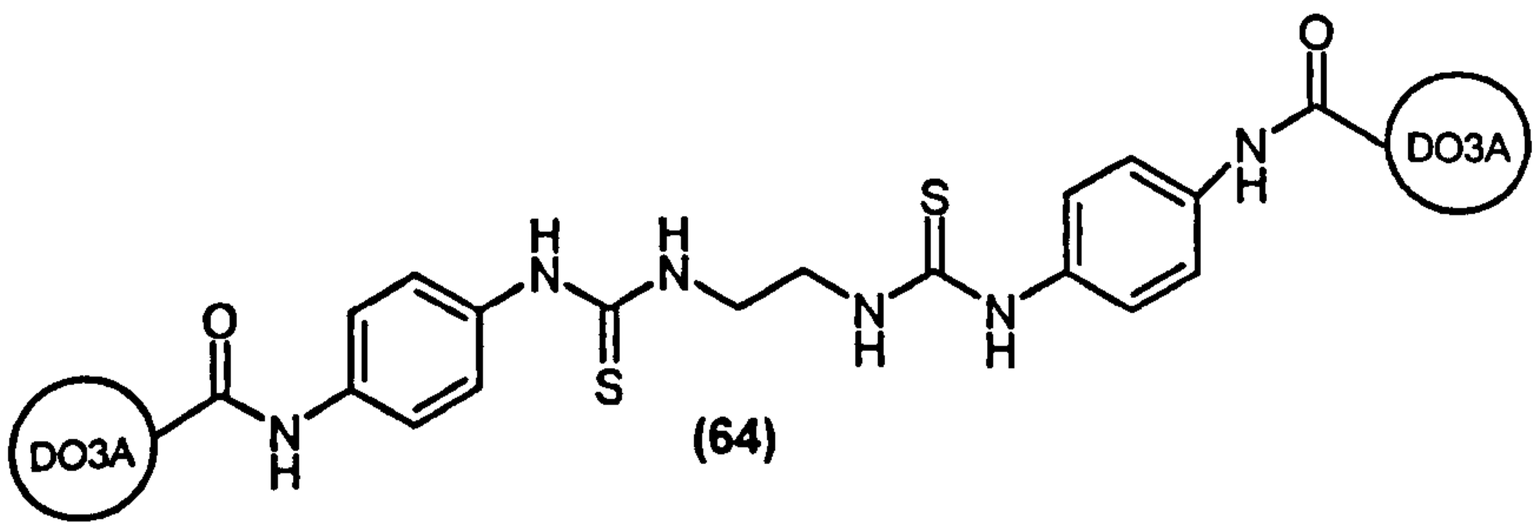

(64)

***Figure 4.16** – Structures of the multimeric ligands reported in Table 4.3.*

In order to explore more deeply the properties of these complexes, the relaxivity was measured as function of pH. The pH dependence of relaxivity (at 20 MHz, 298 K in water at pH = 7.0) for [Gd·**9**]-α-folate and [Gd·**9**]$_2$-α,γ-folate is shown in *Figure 4.17*.

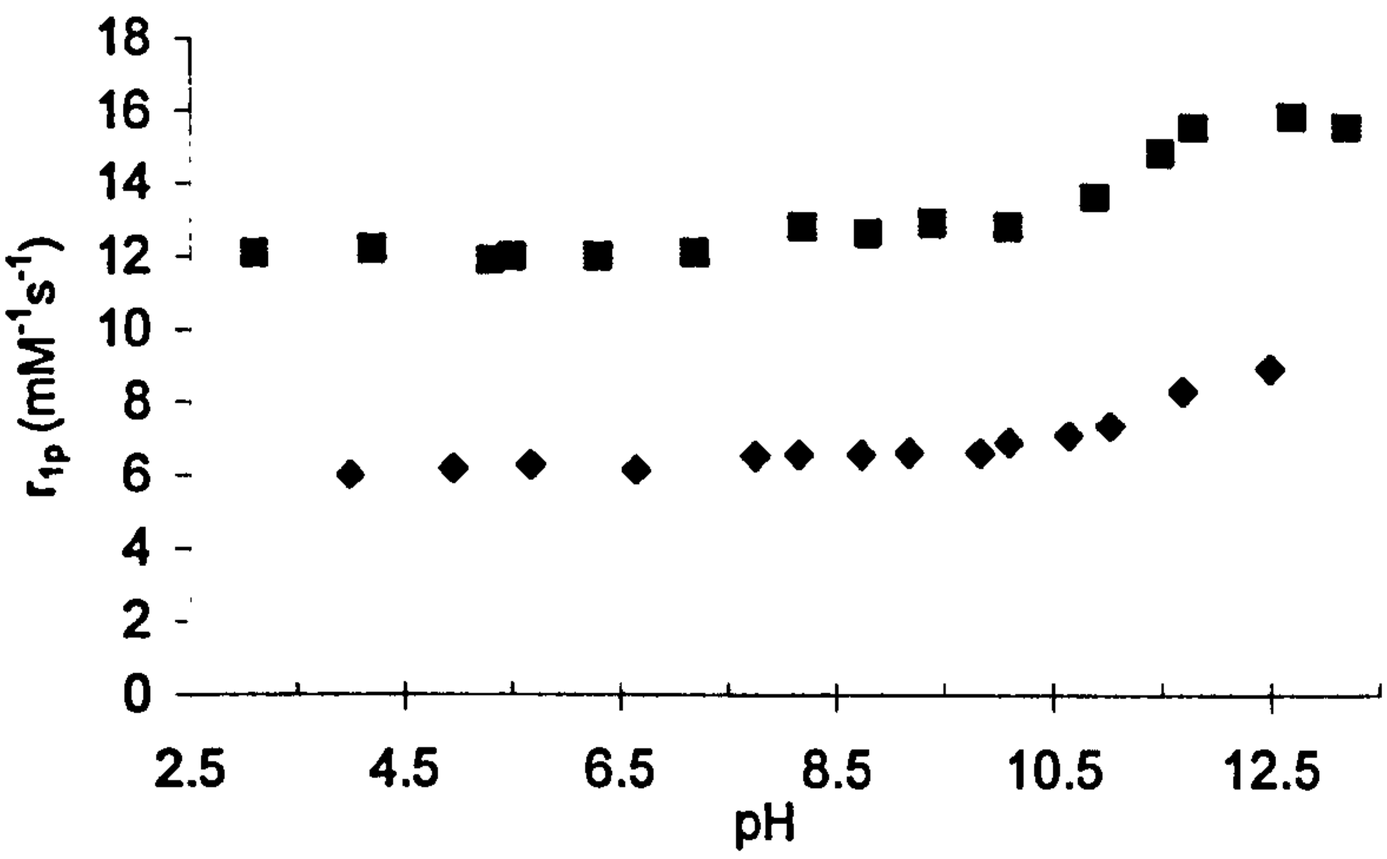

***Figure 4.17** – pH dependence of relaxivity for [Gd·9]-α-folate (diamonds) and [Gd·9]$_2$-α,γ-folate (squares)*

In both cases the relaxivity remains constant in the range between pH 3.0 and 8.0, then it shows an increase above pH 8.0. A base catalyzed prototropic exchange, involving deprotonation of the co-ordinated amide NH, accounts for such a variation.[29]

4.5.2. NMRD profiles of the [Gd·9] folate conjugates

In order to characterize the different contributions to the observed relaxivity, NMRD profiles over an extended range of frequencies at 25 ^{0}C were measured for [Gd·**9**]-α-folate and [Gd·**9**]$_2$-α,γ-folate (*Figure 4.18*).

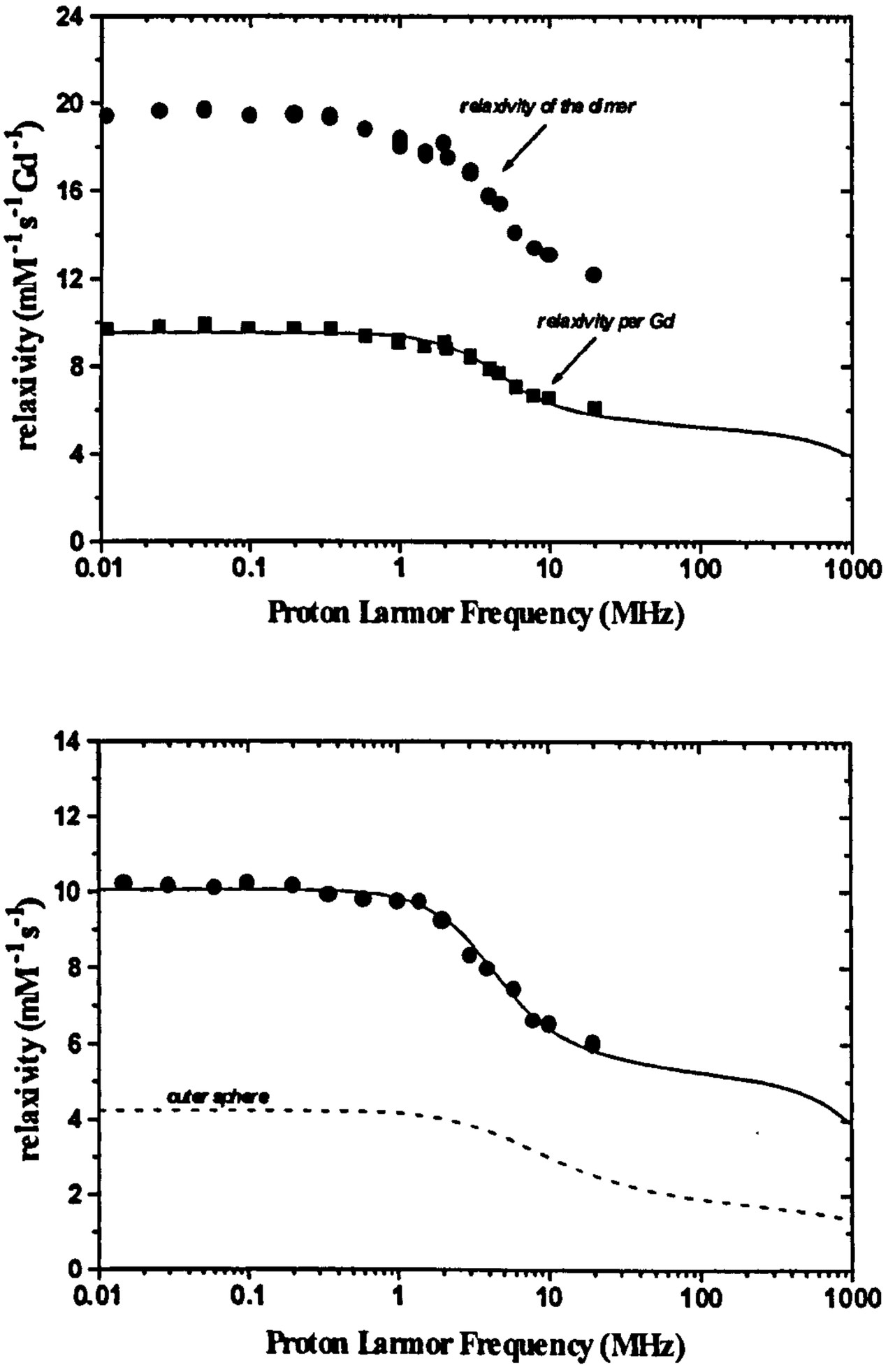

Figure 4.18 – NMRD profiles for α-γ-[Gd·9]$_2$-folate (upper) and α-[Gd·9]-folate (298 K), showing the fit to the experimental data .

The NMRD profile of the [Gd·9]-γ-folate has not been recorded. However, it should not be different from that recorded for the α-isomer.

The curves were fitted to the equations for inner and outer sphere paramagnetic relaxation (see Chapter One) to give the parameters listed in *Table 4.4*.

Complex	Δ^2 (s^{-2})/10^{-19}	τ_V (ps)	τ_R (ps)
[Gd·9]-α-folate	2.44	23	100
$[Gd·9]_2$ -α,γ-folate	2.94	23	100
$[GdDO3A]_2$L7 **(62)**	2.10	15	106
$[GdDO3A]_2$L6 **(60)**	1.70	19	171

***Table 4.4** – Best fitting parameters determined by analyses of NMRD profiles.*

In the analyses a reasonable choice was made for *r* (2.98 Å), the distance between the metal center and closed water molecule, based on known values of similar complexes. The parameters *a* (distance of the closest approach of diffusing water) and D (diffusion coefficient) were fixed to typical values of 3.8 Å and $2.24 \cdot 10^{-5}$ cm^2s^{-1} respectively, whereas *q* was considered one, as had been measured by luminescence studies.

The rotational correlation times τ_R calculated from the profiles are identical for the two complexes [Gd·**9**]-α-folate and $[Gd·\mathbf{9}]_2$-α,γ-folate (100 ps), despite the significant difference in molecular weight. On the other hand, $[GdDO3A]_2$L7 **(62)** and $[GdDO3A]_2$L6 **(60)** (*Table 4.4)* exhibit different rotational correlation times, despite their similar masses.

The absence of a linear relationship between τ_R and the molecular weight, predicted by the Debye formula (equation 1.20), can be explained in terms of the internal flexibility of the molecules. The rotational correlation time as evaluated experimentally, corresponds to the rotational motion of the Gd-coordinated water O (or H) vectors and it does not represent the correlation time for the whole molecule. This motion, which determines proton relaxivity, can be considerably faster than the motion of the whole molecule, which is instead related to the molecular mass.

In the case of $[Gd·\mathbf{9}]_2$-α,γ-folate, the two chelates are separated by a flexible "linker" and then are free to rotate independently each other. Their rotation is faster than the tumbling of the whole molecule. So the increment of about 40 % in molecular weight is not accompanied by a corresponding increment in τ_R and thus in the relaxivity. On the other hand, the less flexible linker present in $[GdDO3A]_2$L6 **(60)** accounts for the significant increment in τ_M and thus in relaxivity, compared to the $[GdDO3A]_2$L7 **(62)**, which possesses similar mass, but a more flexible linker.

As already pointed out, the profiles are only slightly dependent on the actual value of the water residence lifetime τ_M, which then cannot be determined with sufficient accuracy

by fitting procedures. As discussed in Chapter Two, τ_M can be measured independently by variable temperature proton decoupled ^{17}O NMR measurements of the water nuclear transverse relaxation rate. The measured variation of R_{2p} as function of T at 90 MHz in ^{17}O enriched solution at pH 7.0 for [Gd·**9**]-α-folate (*c.a.* 10 mM) is shown in *Figure 4.19*.

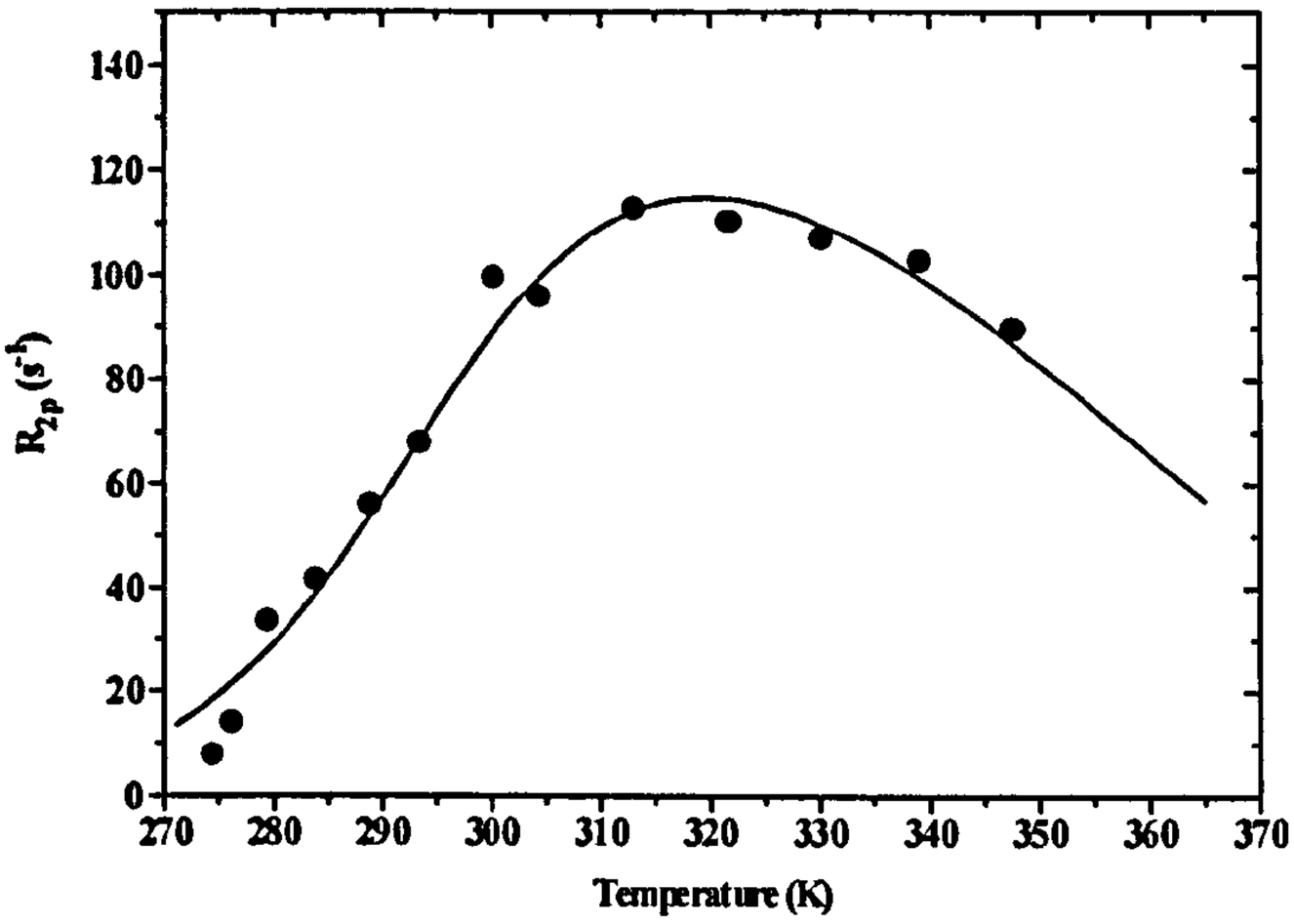

Figure 4.19 *– R_{2p} as function of temperature for [Gd·9]-α-folate (90 MHz; pH 7.0) showing the fit to the experimental data.*

The curve was fitted to the Swift-Connick equation.[30-32] In the analysis a standard value for the hyperfine coupling constant A/h ($-3.8 \cdot 10^6$ rad s^{-1}) was used, whereas the values obtained from the NMRD profile for Δ^2 and τ_V were considered. The calculated value of the water exchange lifetimes at 298 K are reported in *Table 4.5* and compared to those published for similar complexes.[5]

Complex	[Gd·9]- α-folate	$[Gd \cdot 9]_2$ α,γ-folate	$[GdDOTA]^-$	$[GdDO3A]_2$L7 **(62)**
τ_M (ns)	850	(850)	244	714

Table 4.5 *– Water exchange lifetime τ_M at 298 K.*

As discussed previously, the presence of an amide carbonyl as a coordinating donor, reduces the water exchange rate of the gadolinium complex by a factor between three and four.[1-3] This is clearly shown by the difference observed between $[GdDOTA]^-$ and the monoamide derivative [Gd·9]-α-folate, which shows a shorter water exchange rate.

In a dissociatively activated water exchange process, which is usually the case for octadentate gadolinium chelates, the bound water molecule must "depart" from the inner sphere, before the subsequent arrival of a second molecule. The corresponding eight co-ordinate transition state structure plays a crucial role. The more unstable it is the higher the activation energy needed for its formation. An amide group is usually considered to be less strongly bound to the metal center than a carboxylate. This may result in a higher energy transition state, which makes more difficult for the inner sphere water molecule to leave, and thus results in a higher value of τ_M.

Recently it has been demonstrated by NMR and luminescence studies that the rate of water exchange at the metal center depends on the nature and relative abundance of the isomers present in solution.[22, 33, 34] For example, the water exchange lifetime at 298 K for the tetraamides **(66a-c)** (*Figure 4.20)* is the order of 160 μs for the major square antiprismatic isomer (M) and about fifty times faster for the isomeric twisted square antiprismatic (m). The prevalence of the square antiprismatic (M) isomer, detected by NMR and luminescence studies is consistent with relatively long value of τ_M measured for both the [Gd·9]-α-folate and the $[Gd·9]_2$-α,γ-folate.

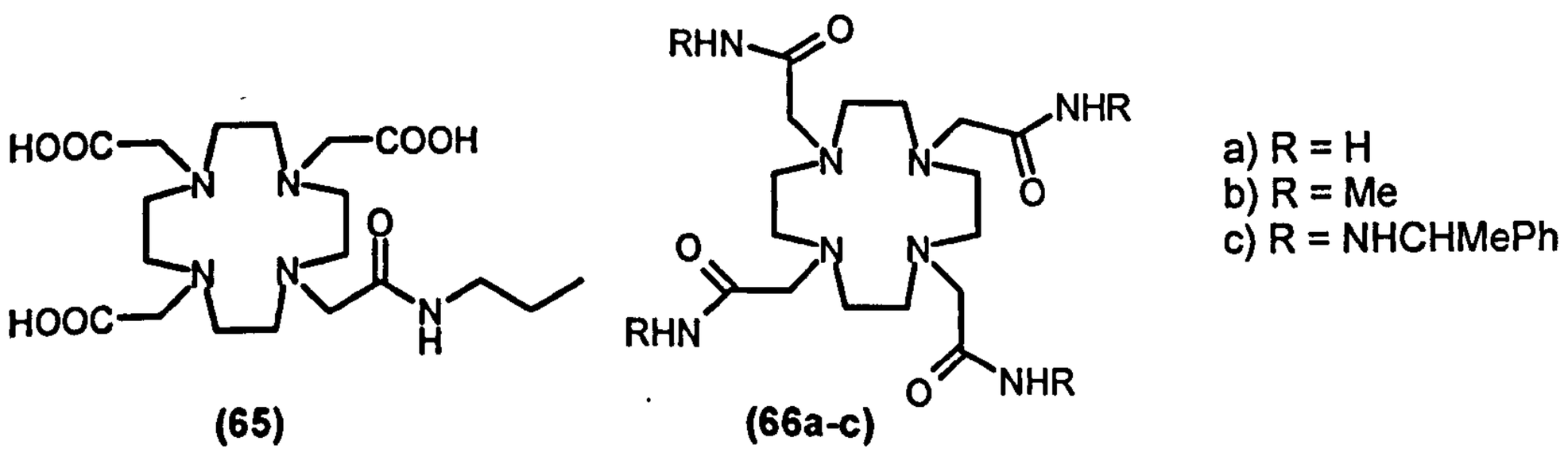

***Figure 4.20** – Mono and tetraamide ligands.*

4.5.3 *Relaxivity of the [Gd·6]⁻ and its folate conjugates.*

The relaxivity of [Gd·6]⁻ and its γ-folate derivative was measured at 65 MHz and 293 K in water, in an anionic background solution and in human serum (*Table 4.6*).

Complex	r_{1p} (water)	R_{1p} (anionic bkg)	r_{1p} (human serum)
[Gd·6]⁻	8.5	7.4	9.6
[Gd·6]⁻ γ-folate	9.5	8.8	11.1
RRRR-[GdgDOTA]⁻	8.7		(11.1)

Table 4.6 – Relaxivities (in $mM^{-1}s^{-1}$) at 65 MHz, 293 K and pH = 7.20.

Both the anionic complex [Gd·**6**]⁻ and the analogous complex [GdgDOTA]⁻, due to their similar structure and molecular volume, exhibit almost identical relaxivities in water solution. The [Gd·**6**]⁻-γ-folate shows instead a higher relaxivity, which is related to the increased molecular weight. In the anion solution, both [Gd·**6**]⁻ and the [Gd·**6**]⁻γ-folate show a decrease in relaxivity of about 15%. This reduction is very unlikely to be due to the binding of anions to the metal centre, because of the electrostatic repulsion. However, it may be explained by the partial lost of the second or outer sphere contribution.

The higher relaxivities measured in human serum are a consequence of either the increased micro-viscosity of the medium or the formation of weak adducts with proteins present in serum (*e.g.* serum albumin).

4.6. Interaction with proteins

The interaction of gadolinium chelates with proteins has been widely investigated in recent years.[4] The main interest, from the MRI point of view is determined by the expectation that paramagnetic macromolecular complexes should lead to a marked enhancement of the relaxation rate of tissue protons. The large molecular size of the protein-complex adducts results in a slowing down of the molecular motion (τ_R) and thus in an increase of the relaxivity.

In the case of the folate conjugates of the gadolinium complexes prepared in the present work, the study of the interaction with specific proteins (*e.g.* FBP) must be considered, because the delivering of these compounds into the target tissues or organs depends on the extent of such an interaction.

The three most important techniques that are used to determine the protein binding of metal chelates are represented by equilibrium dialysis,[35] ultrafiltration[35] and proton relaxation enhancement (PRE).[36] The first two are separation methods, in which a membrane or a filter is used to allow separation of free and bound complex with subsequent analysis of the unbound substrate. The long time required and the possible interference of the membrane on the binding equilibrium represent the main drawbacks of such methods.

The proton relaxation enhancement (PRE) method does not include a separation step. The extent of the binding between a protein and a substrate is exploited by the detection of the enhancement in the observed water proton relaxation rate (R_{1obs}). This method is widely used in the field of MRI contrast agents, and it has also been used in the present work. The experimental procedure consists in carrying out a titration, in which the observed water proton relaxation rate is measured as a function of the concentration of added protein. In aqueous solution, the substrate (S) and the protein (P) reach the equilibrium (equation 4.1), regulated by the association constant K_A (equation 4.2):

$$S + P \leftrightarrow SP \qquad (4.1)$$

$$K_A = \frac{[S-P]}{[S]\cdot[nP]} \qquad (4.2)$$

in which [nP] represents the concentration of the equivalent and independent binding sites on the protein. The longitudinal water proton relaxation rate (R_{1obs}) is given by the sum of the contributions arising from the unbound and the bound species, as well as the diamagnetic contribution of the protein itself (R_{1Pr}) (equation 4.3):

$$R_{1ob} = \left(r_1[S] + r_1^b[SP]\right)1000 + R_{1Pr} \qquad (4.3)$$

where r_1 and r_1^b represent the millimolar relaxivities of the unbound and bound substrate respectively. The combination of the equations (4.3) and (4.2) allows the calculation of the binding parameters, K_A and n, from the observed relaxation rate (equation 4.4):

$$R_{1obs} = \frac{(K_A S_T + nK_A P_T + 1) - \sqrt{(K_A S_T + nK_A P_T + 1)^2 - 4K_A^2 S_T n P_T}}{2K_A} - (r_1^P - r_1 + r_1 S_T)1000 + R_{1Pr} \quad (4.4)$$

By fitting the experimental curve to equation (4.4), a good estimate of the relaxivity of the substrate bound to the protein (r_1^b) may be obtained. However, the determination of the association constant (K_A) and of the number of interaction sites on the protein (n) is not accurate by this experiment, especially when the affinity constant is small. A more accurate evaluation of these parameters may be obtained by another experiment, in which a fixed concentration of protein is titrated with the paramagnetic compound.[4]

The non-covalent interactions between the folate conjugate complexes, [Gd·9]-α-folate and [Gd·6]$^-$-γ-folate and serum albumin were investigated first. These proteins are highly concentrated in the blood (*ca.* 50 g dm^{-3}) and their interaction with several gadolinium chelates has been widely investigated.[4, 37] It has been demonstrated that chelates bearing hydrophobic residues as well as negative charges are more likely to bind to these proteins.[38]

The [Gd·9]-α-folate was titrated with human serum albumin (HSA), in phosphate buffered solution at pH = 7.0 and 25 ^{0}C (*Figure 4.21*).

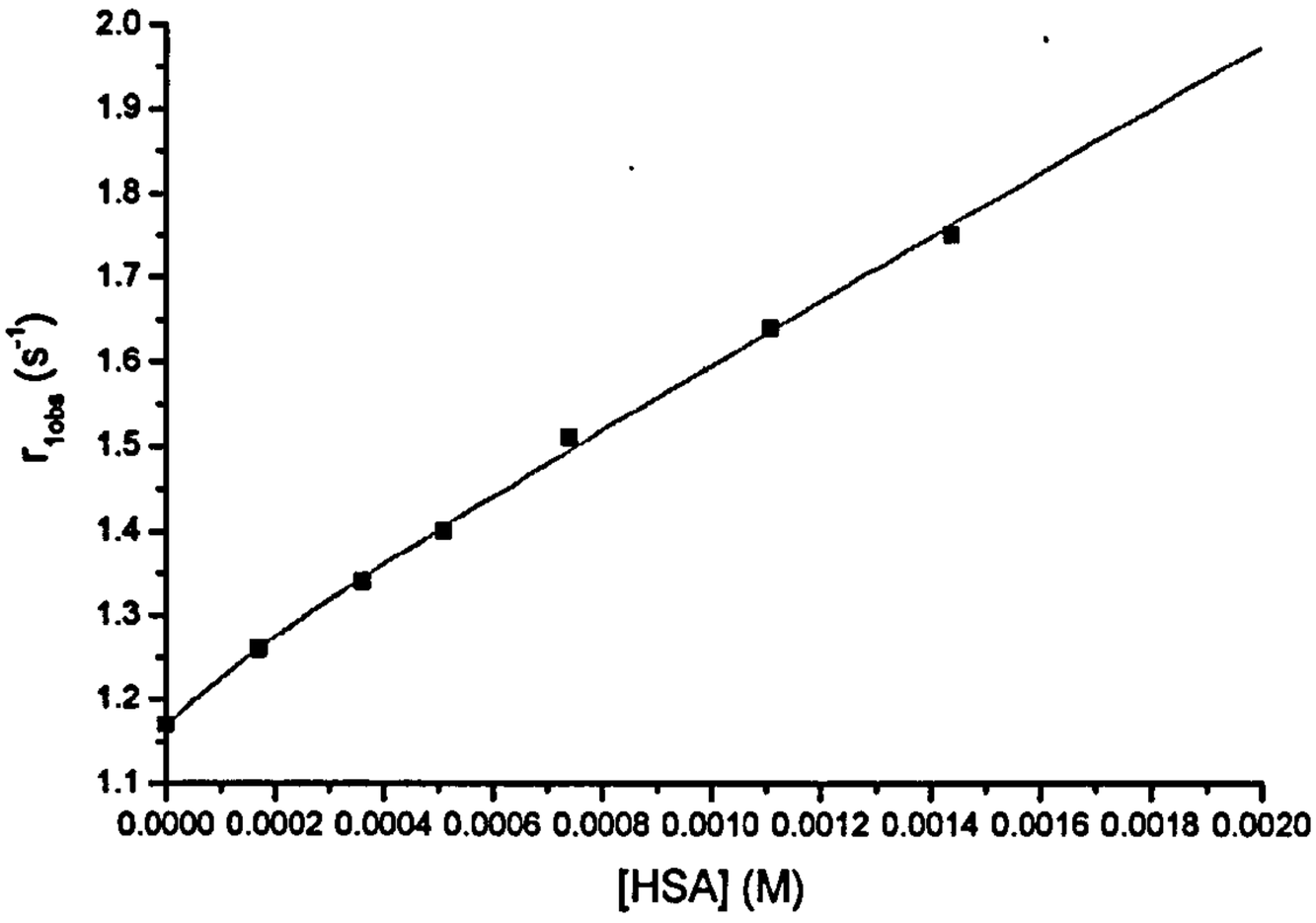

***Figure 4.21** – PRE titration of [Gd·9]-α-folate with Human Serum Albumin (HSA) at 20 MHz, 298 K in 50 mM phosphate buffer solution pH = 7.0, [GdL] = 0.125 mM.*

The binding curve was fitted to equation (4.4) and the calculated parameters were compared to those reported for related complexes (*Table 4.7*).

Complex	r_1^b ($mM^{-1}s^{-1}$)	K_A (M^{-1})
[Gd·**9**]-α-folate	6.3	$(9 \cdot 10^2)$
[GdDOTA(BOM)] **(67)**		$< 1 \cdot 10^2$
Cis-[GdDOTA$(BOM)_2$] **(68)**	35.2	$3.2 \cdot 10^2$
Trans-[GdDOTA$(BOM)_2$] **(69)**	44.2	$3.6 \cdot 10^2$
[GdDOTA$(BOM)_3$] **(70)**	53.2	$9.2 \cdot 10^4$

***Table 4.7** – Calculated values of r_1^b and K_A.*[39]

In the series of the DOTA$(BOM)_n$ complexes (*Figure 4.22*), the introduction of β-benzyloxy-α-propionic hydrophobic residues favours the formation of the macromolecular adduct with HSA.[39] This is clear from the increment in both r_1^b and in the association constant, K_A. In particular the tri-substituted [GdDOTA$(BOM)_3$] **(70)** shows the largest values, suggesting a higher affinity for this complex.

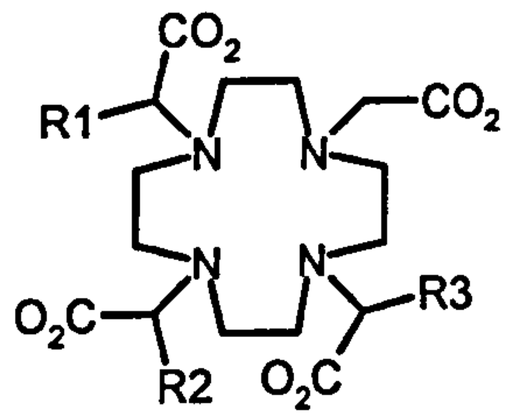

DOTA(BOM) **(67)** : R1=R3=H; R2=BOM

cis-DOTA(BOM)$_2$ **(68)** : R1=H; R2=R3=BOM

trans-DOTA(BOM)$_2$ **(69)** : R2=H; R1=R3=BOM

DOTA(BOM)$_3$ **(70)** : R1=R2=R3=BOM

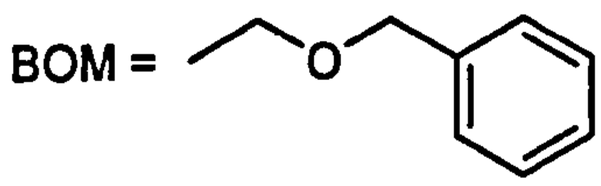

***Figure 4.22** – Structures of the series of DOTA(BOM)$_n$*

The monoamide [Gd·**9**]-α-folate complex does not show any appreciable change in relaxivity from the unbound chelates (r_1 = 6.5 $mM^{-1}s^{-1}$at 20 MHz) to the protein adduct (r_1^b = 6.3 $mM^{-1}s^{-1}$ at 20 MHz). This suggests that the [Gd·**9**]-α-folate does not interact with the protein HSA, as predicted by observing the relaxivity in human serum, compared to water. Similarly, the anionic complex [Gd·**6**]$^-$-γ-folate was titrated with bovine serum albumin (BSA) in phosphate buffered solution at pH 7.20 (*Figure 4.23)*. The observed PRE enhancement was not significant, suggesting again a very weak interaction between the protein and the complex. The presence of a negative charge, which usually improves the interaction with serum albumins, does not have any significant effect in this case.

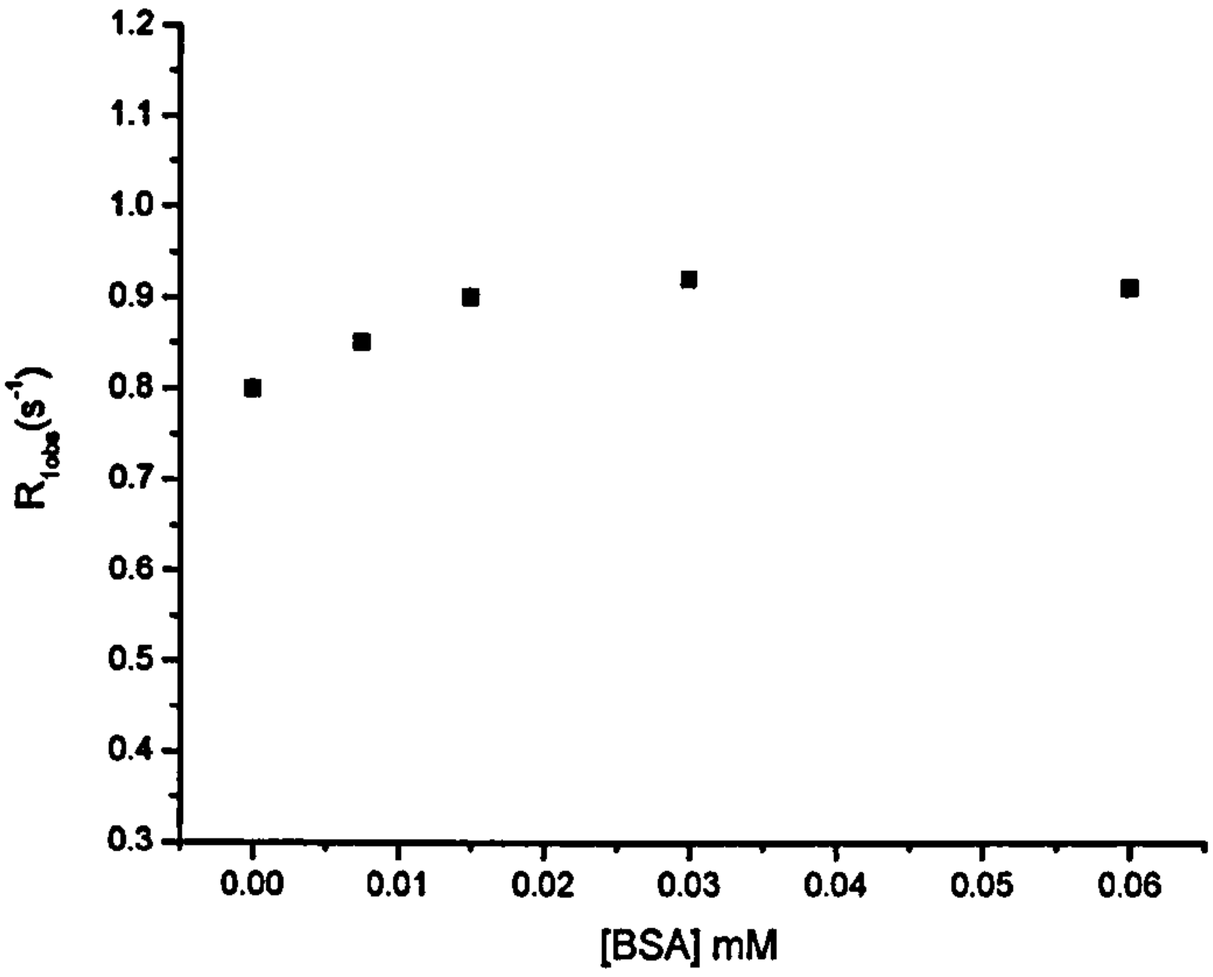

Figure 4.23 *– PRE titration of [Gd·6]⁻ -γ-folate (c = 0.06 mM) with bovine serum albumin (BSA) in 50 mM phosphate buffered solution pH = 7.0 at 298 K and 65 MHz.*

As already discussed the study of the specific interaction of the gadolinium complex conjugates with folate binding proteins (FBP) represents an important aim of this project. The two isomers [Gd·9] α- and γ-folate were separately titrated with FBP, in phosphate buffered solution at pH = 7.0 (*Figure 4.24*).

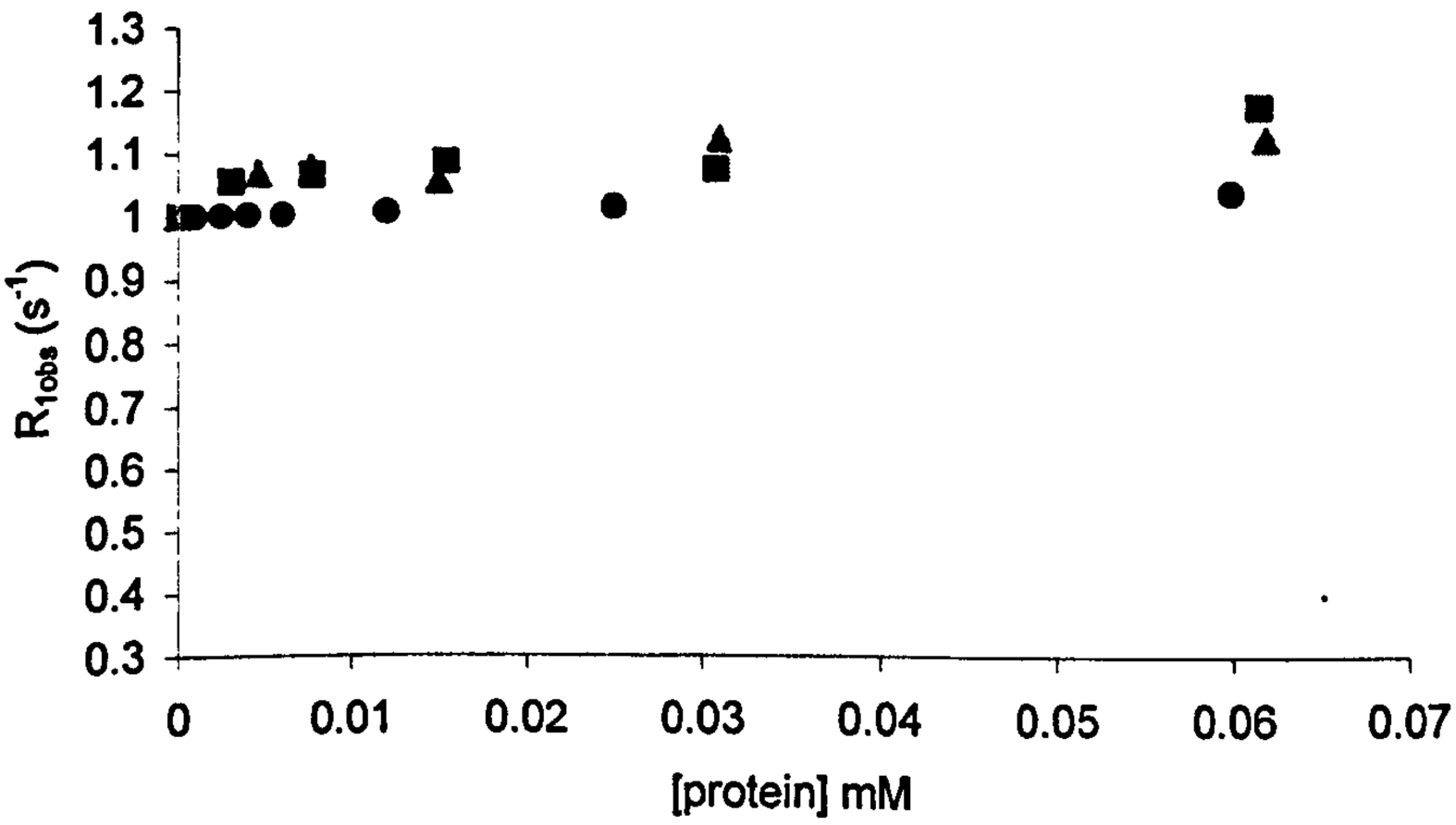

Figure 4.24 *– PRE titration of [Gd·9]-γ-folate (triangles) and [Gd·9]-α-folate (squares) with FBP, and of [Gd·9]-α-folate (circles) with HAS as control, in phosphate buffer solution pH = 7.0, 65 MHz, 293 K.*

The plot reveals only minor differences between the two isomers. In addition, the observed PRE measured in the presence of FBP is not significantly higher than that observed in the case of HSA, which does not experience any interaction with the complex [Gd·**9**]-α-folate (see below). These results clearly show that neither the α- nor the γ-isomer interact specifically with folate binding proteins. However, we must consider that the enhancement in the longitudinal proton relaxation rate and thus in relaxivity arising from the lengthening of τ_R (*i.e.* binding of proteins) can only be fully exploited if the water exchange lifetime and the electronic relaxation time have optimal values. These parameters depend mainly on the properties of the complex, rather than on the structure of the binding site of the protein. The very long water exchange time (850 ns) of the [Gd·**9**]-α-folate may be the limiting factor that prevents higher relaxation rates from being obtained.

In order to understand more deeply the affinity of these complexes for the cell surface folate receptors, *in-vitro* cell uptake experiments have been carried out on both the α- and γ-monoisomer and on the α-γ-bis derivative. These experiments are currently *en route* at Guerbet s.a., but no details can be drawn because of confidentiality reasons.

Finally, the anionic [Gd·**6**]$^-$-γ-folate complex was titrated with FBP, using the same conditions (*Figure 4.25*).

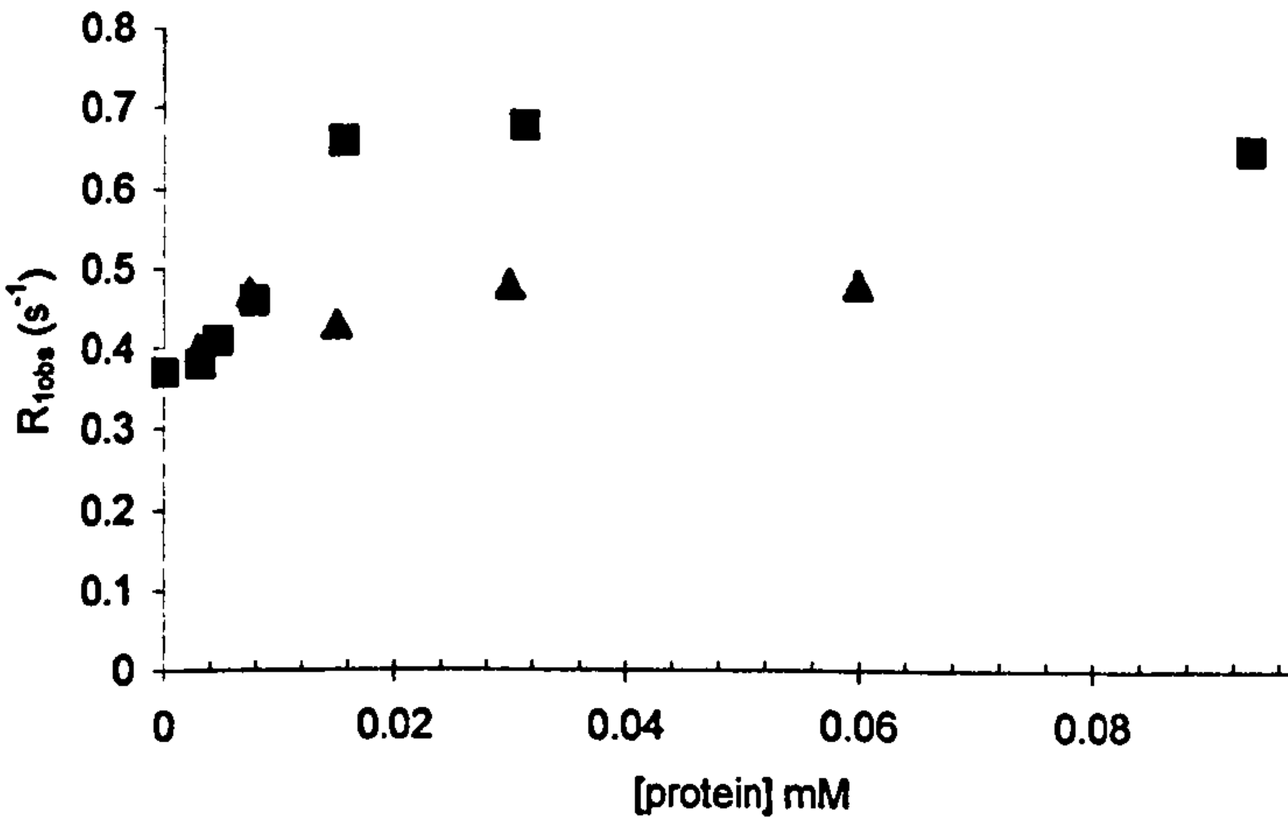

***Figure 4.25** - PRE titration of [Gd·**6**]$^-$ -γ-folate with FBP (squares) and with BSA (triangles) in phosphate buffer solution pH = 7.0, 65 MHz, 293 K.*

The anionic complex [Gd·**6**]$^-$-γ-folate exhibits a clear and significant PRE effect (*ca.* 80% increase) in the presence of FBP, compared to that observed in the presence of the control bovine serum albumin (BSA). This result has demonstrated that the FBP is capable of recognizing specifically the anionic complex. In this case the shorter water residence lifetime τ_M, of the gadolinium complex may be responsible for the observed increase in the relaxation rate. Thus [Gd·**6**]$^-$-γ-folate is a particularly interesting candidate as an MRI targeted contrast agent.

4.7. Conclusion

Two different practicable synthetic routes to allow the regioselective coupling of folic acid to a gadolinium chelate have been developed, using the model system [Gd·**9**]. The relaxometric properties of both the α and γ isomers and their affinity for the specific folate binding protein (FBP) have been fully investigated. The results have shown a very weak interaction between the complexes and the protein and no appreciable difference in affinity between the two isomers has been observed.

In vitro studies to further investigate the affinity of these complexes for the cell surface receptors are currently *en route* at Guerbet s.a.

The anionic complex [Gd·**6**]$^-$ has been synthesized and coupled regioselectively to folic acid. Due to its optimal intrinsic relaxometric properties (*i.e.* faster water exchange, enhanced relaxivity), it represents a better candidate as a targeted MRI contrast agent. Its affinity for the folate binding proteins has been explored and compared to the unspecific bovine serum albumin. The results have clearly demonstrated that the receptor protein FBP is capable of recognizing the anionic complex [Gd·**6**]$^-$-γ-folate, with a significant enhancement of relaxivity in the bound form.

4.8. References

[1] Powell, H. D.; Ni Dhubhghainn, O. M.; Pubanz, D.; Helm, L.; Lebedev, Y.; Schlaepfer, W.; Merbach, A. E. *J. Am. Chem. Soc.* **1996**, *118*, 9333.

[2] Toth, E.; Vauthey, S.; Pubanz, D.; Merbach, A. E. *Inorg. Chem.* **1996**, *35*, 3375.

[3] Toth, E.; Pubanz, D.; Vauthey, S.; Helm, L.; Merbach, A. E. *Chem. Eur. J.* **1996**, *2*, 1607.

[4] Merbach, A. E.; Toth, E. *The Chemistry of Contrast Agents in Medical Magnetic Resonance Imaging*; Wiley: New York, 2001.

[5] Caravan, P.; Ellison, J.; McMurry, T. J.; Lauffer, R. B. *Chem. Rev.* **1999**, *99*, 2293.

[6] Woods, M.; Aime, S.; Botta, M.; Howard, J. A. K.; Moloney, J. M.; Navet, M.; Parker, D.; Port, M.; Rousseaux, O. *J. Am. Chem. Soc.* **2000**, *122*, 9781.

[7] Harvison, P. J.; Kalman, T. I. *J. Med. Chem.* **1992**, *35*, 1227.

[8] Temple, C. J.; Rose, J. D.; Montgomery, J. A. *J. Org. Chem.* **1981**, *46*, 3666.

[9] Martinelli, J. E.; Chaykovsky, M.; Kisliuk, R. L.; Gaumont, Y.; Gittelman, G. *J. Med. Chem.* **1979**, *22*, 869.

[10] Goldman, P.; Levy, C. C. *Proc. Nat. Acad. Sci. USA* **1967**, *58*, 1299.

[11] Platzek, J.; Raduchel, B.; Schmitt-Willich, H.; Graske, K. D. *Process for the production of metal-complex carbodylic acid amides*, 1997.

[12] Weingand, F.; Wacker, A. *Chem. Ber.* **1949**, *82*, 25.

[13] Yanouank, J.; Lebris, N.; Le Gall, G.; Clement, J. C.; Handel, H.; Des Abbayes, H. *J. Chem. Soc., Chem. Comm.* **1991**, *31*, 206.

[14] Atkins, T. J. US 4, 085, 106, 1978.

[15] Hell, C. *Ber. Dtsch. Chem. Ges.* **1881**, *14*, 891.

[16] Zelinsky, N. *Ibid.* **1887**, *20*, 2026.

[17] Volhard *Justus Liebigs Ann. Chem.* **1887**, *242*, 141.

[18] Watson, H. B. *Chem. Rev.* **1930**, *7*, 180.

[19] Hillwood, H. J. *Ibid.* **1962**, *62*, 99.

[20] Harpp, D. N.; Bao, L. Q.; Black, C. J.; Gleason, J. G.; Smith, R. A. *J. Org. Chem.* **1975**, *40*, 3420.

[21] Bunzli, J.-C. G.; Choppin, G. R. *Lanthanide Probes in Life, Chemical and Earth Sciences*; Elsevier: AMsterdam, 1989.

[22] Aime, S.; Barge, A.; Bruce, J. I.; Botta, M.; Howard, J. A. K.; Moloney, J. M.; Parker, D.; De Sousa, A. S.; Woods, M. *J. Am. Chem. Soc.* **1999**, *121*, 5672.

[23] Hoeft, S.; Roth, K. *Chem. Ber.* **1993**, *126*, 869.

[24] Aime, S.; Botta, M.; Ermondi, g. *Inorg. Chem.* **1992**, *31*, 4291.

[25] Jacques, V.; Desreux, J. F. *Inorg. Chem.* **1994**, *33*, 4048.

[26] Clarkson, I. M.; Beeby, A.; Bruce, J. I.; Govenlock, L. J.; Lowe, M. P.; Mathieu, C. E.; Parker, D.; Senenayake, K. *New J. Chem.* **2000**, *24*, 377.

[27] Beeby, A.; Clarkson, I. M.; Dickins, R. S.; Faulkner, S.; Parker, D.; Royle, L.; De Sousa, A. S.; Williams, J. A. G.; Woods, M. *J. Chem. Soc., Perkin Trans. 2* **1999**, 493.

[28] Anelli, P. L.; Calabi, L.; Dehaen, C.; Fedeli, F.; Losi, P.; Murru, M.; Ruggeri, F. *Gazz. Chim. It.* **1996**, *126*, 89.

[29] Woods, M.; Bruce, J. I. *J. Am. Chem. Soc.* **1999**.

[30] Swift, T.; Connick, R. E. *J. Chem. Phys.* **1962**, *37*, 307.

[31] Swift, T. J.; Connick, R. E. *J. Chem. Phys.* **1964**, *41*, 2553.

[32] Aime, S.; Botta, M.; Fasano, M. *Chem. Eur. J.* **1997**, *3*, 1499.

[33] Aime, S.; Barge, A.; Botta, M.; Parker, D.; De Sousa, A. S. *Angew. Chem. Int. Ed. Engl.* **1998**, *37*, 2673.

[34] Batsanov, A. S.; Beeby, A.; Bruce, J. I.; Howard, J. A. K.; Kenwright, A. M.; Parker, D. *Chem. Comm.* **1999**, 1011.

[35] Wright, J. D.; Boudinot, F. D.; Ujhelyi, M. R. *Clin. Pharmacokinet.* **1996**, *30*, 445.

[36] Wedeking, P.; Kumar, K.; Tweedle, M. F. *Magn. Res. Imag.* **1992**, *10*, 641.

[37] Aime, S.; Botta, M.; Fasano, M.; Terreno, E. *Chem. Soc. Rev.* **1998**, *27*.

[38] Peters, T. J. *All about Albumin: Biochemistry, Genetics and Medical Applications*; Academic Press: San Diego, 1996.

[39] Aime, S.; Botta, M.; Fasano, M.; Terreno, E.; Geninatti Crich, S. *J. Biol. Inorg. Chem.* **1996**, *1*, 312.

Pages missing in the original

5.1. Experimental procedures

5.1.1. Materials and solvents

Folic acid dihydrate 97%, benzyl bromide 98%, benzoyl chloride 98%, caesium carbonate anhydrous 99%, dimethyl sulfoxide anhydrous, diisopropylamine 99%, benzyl alchool, tetrafluoroboric acid diethyl ether complex 65%, sodium sulphate anhydrous, 1,4-diaminobutane, N-bromosuccinimide 99%, N-hydroxy succinimide 99%, 1,(3-dimithylaminopropyl)-3-ethyl carbodiimide hydrochloride 99%, 5-amino valeric acid 97%, acetyl chloride, potassium hydroxide, thionyl chloride, sodium thiosulphate, sodium hydrogen carbonate, lithium hydroxide, gadolinium (III) chloride hexahydrate, europium chloride hexahydrate, potassium iodade, chloroacetic acid, palladium hydroxide over carbon, protease (from Rhizopus species type XVIII), pteroic acid, α-benzyl ester of gluatamic acid, trifluoroacetic acid, hydrazine were purchased from Aldrich and were used without further purification.

All the solvents used were dried over the appropriate drying agent: dichloromethane, acetonitrile and triethylamine over calcium hydride; tetrahydrofuran and diethyl ether over sodium with benzophenone as indicator; methanol and ethanol from the corresponding magnesium alkoxide. N,N-Dimethylformamide and dimethylsulfoxide were used directly from the "sure-seal" bottles. Water was purified by the Purite TM system.

5.1.2. Chromatography

Column chromatography was carried out using "gravity" silica (Merck) or neutral alumina (Merck). Cation exchange chromatography was performed using Dowex 50W strong ion-exchange resin, which was pretreated with 3M HCl. Thin layer chromatography was carried out on neutral alumina plates (Merck) or on silica plates (Merck) and visualized by iodine or UV irradiation. Gel filtration chromatography was performed using Sephadex G25 or G10. The resin was swallowed in water, stirring for three hours at room temperature.

Analytical HPLC chromatograms were recorded on a *Varian* liquid chromatography system. The components include a *Varian 9010 Solvent Delivery System*, a *Varian 9065 Polychrom*, and a PC station. A *Hypersil* 5μm ODS 20cm 4.6 mm column was used. The flow was regulated at 1.0 ml/min, and the wavelength of the

detector at 254 nm. The mobile phase was composed by acetonitrile (A) and water + 0.1% of TFA (B); the following linear gradient was used:
t = 0 min, A% = 10, B% = 90; t = 10 min, A% = 30, B% = 70; t = 20 min, A% = 50, B% = 50.

Semi preparative HPLC chromatograms were performed on a *Varian* liquid chromatography system. The components include a Varian 9010 Solvent Delivery System, a Varian 9065 Polychrom, and a PC station. *A* semi-preparative *Dynamax-60A C18* reversed phase column was used. The flow was fixed at10 ml/min and the wavelength of the UV-detector was regulated at 254 nm. The mobile phase was composed by acetonitrile (A) and purite water + 0.1% of TFA (B); the following linear gradient was used: t = 0 min, A% = 10, B% = 90; t = 10 min, A% = 30, B% = 70; t = 20 min, A% = 50, B% = 50.

5.1.3. Characterisation and measurements

^{1}H and ^{13}C spectra were recorded using a *Bruker AC 250* spectrometer operating at 250.13 and 62.9 MHz respectively, *Varian Gemini 200* operating at 200 and 50 MHz respectively, *Varian VXR* operating at 200 MHz or a *Varian VXR* 400 operating at 399.96 and 100.58 respectively. Variable temperature ^{1}H NMR studies were performed on a Varian VXR 400, a JEOL EX-90 and a JEOL EX-400 instrument. Signals are reported in *ppm* to higher frequency of TMS, indicating the relative integral, the multiplicity (*s* singlet, *d* doublet, *t* triplet, *q* quadruplet, *m* multiplet), and the coupling constants J (Hz).

The longitudinal water proton relaxation rates were measured either using a Stelar Spinmaster spectrometer (Mede, Pavia, Italy) operating at 0.5 T, or a modified Varian VXR instrument tuned to 65.6 MHz, by means of the standard inversion-recovery technique (16 experiments, 2 scans). A typical 90^0 pulse width was 3.5 μs and the reproducibility of the T_1 data was ± 0.5%. The temperature was controlled with a Stelar VTC-91 air-flow heater equipped with a copper constant thermocouple (uncertainty of ± 0.1 ^{0}C). The concentration of the complex was typically 0.1-0.4 mM. It was measured accurately by digesting the complex in HNO_3 5M for a period of time between few hours and few days. The relaxation rate of the digested solution was measured and the concentration calculated from the equations 2.5-2.7 in Chapter Two (R_{1d} = 0.40 s^{-1}; r_{1p} (Gd^{3+}) = 12.66 $mM^{-1}s^{-1}$.

The proton $1/T_1$ NMRD profiles were measured on the Koenig-Brown field-cycling relaxometer over a continuum of magnetic field strength from 0.00024 to 1.2 T (corresponding to 0.01–50 MHz proton Larmor frequency). The relaxometer works under computer control with an absolute uncertainty in $1/T_1$ of ± 1%.

Variable temperature ^{17}O NMR measurements were recorded on a JEOL EX-90 (2.1 T) spectrometer equipped with a 5 mm probe, by using a D_2O external lock. Solution containing 2.6% of ^{17}O isotope (Yeda, Israel) were used. The observed transverse relaxation rates were calculated from the signal width at half-height.

Electrospray mass spectra were acquired using a VG Platform (II) instrument, with water, methanol or acetonitrile as a carrier solvent, typically with a cone voltage of 60 V and a source temperature of 110 ^{0}C. Accurate masses were determined at the EPSRC National MS Service at Swansea.

Infrared spectra were recorded on a Perkin-Elmer 1600 FT spectrometer using GRAMS-Analyst softwere; the solids were incorporated into KBr disks.

Melting points were determined on a Reichert Kofler Block.

Elemental analyses were determined on a Carlo Erba 1106. The calculated percentages are indicated between brackets.

Luminescence pH titration were carried out in a background of constant ionic strength (I = 0.1 NaCl, 295 K) or in an anionic background. Solution were made basic by addition of 1M NaOH and titrated to acidic pH using small aliquots (typically 0.5 μL) of 1M or 0.1 M HCl. Excitation wavelengths of 397 nm were used to obtain emission spectra. Excitation and emission slits were 2-5 and 1nm band-pass, respectively. Points were recorded at 1nm intervals with a 0.25 s integration time. The pH was measured with a Jenway 3320 pH meter calibrated with pH 4, 7 and 10 buffer solution.

Excited state lifetime measurements for europium complexes were made on the Instrument SA Fluorolog. Lifetimes were measured by excitation of the sample by a short pulse of light (397 nm) followed by monitoring the integrated intensity of light (594 or 619 nm) emitted during a fixed gate time or delay time. The obtained decay curves were fitted to a simple mono-exponential decay curve using Microsoft Excel.

5.2. Chapter Two experimental

5.2.1. 1,4,7-Tris-([4'methoxycarbonyl]-1'methoxycarboylbutyl)-1,4,7,10-tetraazacyclododecane (24)

1,4,7,10 Tetraazacyclododecane (cyclen) **(22)** (1.37 g; 7.95 mmol), sodium hydrogen carbonate (2.0 g; 23.8 mmol) and few 4 Å molecular sieves were suspended in dry acetonitrile (15 ml). A solution of dimethyl α-bromo adipate **(23)** (6.03 g; 23.84 mmol) in acetonitrile (5 ml) was slowly added over one hour under argon. At the end of the addition the temperature was raised to 75 ^{0}C and the suspension was stirred under argon for 48 hours. The mixture was then cooled, filtered and the solvent removed under reduced pressure. The dark oil was taken up in DCM (25ml) and washed with water (5x25 ml). The organic layer was recovered, dried over potassium carbonate and evaporated to yield a pale yellow oil (5.60 g). It was purified by column chromatography over silica, eluting first with DCM/THF 7:3 (v/v) and then adding 3% of methanol and 0.5% of ammonia solution. A pale brown oil was obtained (1.62 g; 30%).

R_f = 0.34 (SiO_2; THF:DCM:MeOH:NH_3 6:3:0.5:0.5).

ESMS (+) m/z = 689 $(M+H)^+$.

^{1}H NMR ($CDCl_3$; 300 MHz; δ): 1.60-1.85 (18H, br, CH_2); 2.35-2.60 (16H, br, NCH_2); 2.60-3.24 (3H, br, CH); 3.65-3.75 (18H, s, CO_2CH_3).

^{13}C NMR ($CDCl_3$; 200 MHz; δ): 173.5, 170.9 (CO_2), 63.5, 59.0, 51.5, 51.3, 51.0, 46.2, 33.2, 30.0, 21.0 (br, aliphatic C).

IR (thin film) ν_{max}(cm^{-1}): 2919, 2850, 1729 (CO stretching); 1460; 1266; 1178; 918; 825.

5.2.2. 1,4,7-Tris-(4'carboxy-1'carboxybutyl)-1,4,7,10-tetraazacyclododecane (8)

The hexaester **(24)** (0.52 g; 0.75 mmol) was suspended in a 1M lithium hydroxide solution (30 ml). The suspension was heated at 80 ^{0}C for 18 hours. The solution was concentrated to about 5 ml and then passed through a strong cationic exchange resin (Dowex 50 W) eluting with 12% ammonia solution. The fractions were collected and the solvents removed under reduced pressure to yield the ammonium salt as a colourless solid (0.33 g; 73%).

ESMS (-) m/z = 301 $(M-2H)^{2-}$, 603 $(M-H)^-$, 640 $(M-Cl)^-$.

^1H NMR (D_2O; 200 MHz; δ): 1.47-2.74 (34H, br, cyclen ring, CH_2); 3.02 (1H, m, CH); 3.17 (2H, m, CH).

5.2.3. {1,4,7-Tris-(4'carboxy-1'carboxybutyl)-1,4,7,10-tetraazacyclododecane} Gadolinium (27)

To the ligand **(8)** (49 mg; 81 μmol) a solution of gadolinium (III) chloride hexahydrate (30 mg; 81 μmol) in a mixture of water-methanol (2ml; 1:1 v/v) was added. A milky suspension was obtained. The pH was adjusted to 5.5. The mixture was heated at 90 ^0C for 18 hours. The solid in suspension was filtered off, washed with methanol and dried. It was then dissolved in water and the pH was raised to 10.0 by adding a 1M sodium hydroxide solution. The colloidal gadolinium hydroxide, which formed was removed by filtration through a membrane filter. The solution was neutralised and passed through a weakly acidic cationic exchange resin (Amberlite IR-50), eluting with water. The fractions were recovered and freeze-dried to yield a colourless solid (33 mg; 53%).

ESMS (-) m/z = 378 $(M-2H)^{2-}$, 756 $(M-H)^-$.

Elemental Analysis: $C_{26}H_{41}N_4O_{12}Gd \cdot 3H_2O$: C%: 38.53 (38.50); H% 5.26 (5.79); N% 6.89 (6.96).

IR (KBr disc) $\nu_{max}(cm^{-1})$: 3448 (OH), 2935, 2875, 1720 (CO stretching); 1590, 1530, 1483, 1450, 1410, 1390, 1210, 1070, 977, 780.

5.2.4. {1,4,7-Tris-(4'carboxy-1'carboxybutyl)-1,4,7,10-tetraazacyclododecane}Europium (III) (26).

To the ligand **(8)** (15 mg; 25 μmol) a solution of europium (III) chloride hexahydrate (9 mg; 25 μmol) in a mixture of water-methanol (2ml; 1:1 v/v) was added. The pH was adjusted to 5.5. The suspension was heated at 90 ^0C for 18 hours. The solid in suspension was filtered off, washed with methanol and dried. It was then dissolved in water and the pH was raised to 10.0 by adding 1M sodium hydroxide solution. The colloidal europium hydroxide formed was removed by filtration through a membrane filter. The solution was neutralised and passed through a weakly acidic cationic

exchange resin (Amberlite IR-50), eluting with water. The fractions were recovered and then freeze-dried to yield a colourless solid (13 mg; 69%).

ESMS (-) m/z = 375 $(M-2H)^{2-}$, 752 $(M-H)^{-}$.

Elemental Analysis: $C_{26}H_{41}N_4O_{12}Eu \cdot 3H_2O$: C% 38.32 (38.6); H% 5.14 (5.82); N% 6.68 (6.93).

^1H NMR (D_2O; pD 6.0; 200 MHz; δ), (as mixture of diastereoisomers): 46.02 (1H, br s, H_{ax}), 38.23 (1H, br s, H_{ax}), 28.01 (1H, br s, H_{ax}), 21.32 (1H, br s, H_{ax}), 19.91 (1H, br s, H_{ax}), 16.16 (1H, br s, H_{ax}), -2.93, -3.57, -4.10, -5.52, -6.06, -10.99, -19.82, -23.12.

IR (KBr disc) $\nu_{max}(cm^{-1})$: 3445 (OH), 2984, 2925, 1689 (CO stretching); 1598, 1535, 1410, 1315, 1223, 1076, 983, 880.

5.2.5. {1,4,7-Tris-(4'carboxy-1'carboxybutyl)-1,4,7,10-tetraazacyclododecane}Gadolinium (III) – triamide (29)

The gadolinium complex **(27)** (15 mg; 20 μmol) and the amine **(28)** (66 mg; 60 μmol) were dissolved in a mixture of water/dioxane 6:4 (v/v), then EDC (15 mg; 79 μmol) and HOBt (1 mg; 9 μmol) were added. The pH was adjusted to 6.0 and the solution was stirred at room temperature for 24 hours. The mixture was transferred into a flask containing EtOH (50 ml) and the white solid obtained was recovered, washed with more ethanol and dried. The crude was purified by size exclusion chromatography (Sephadex G-25) eluting with water. The fractions were collected and freeze-dried to yield a colourless solid (35 mg; 42%).

Relaxivity (65 MHz, 293 K, in H_2O pH = 7.20) = 27.7 $mM^{-1}s^{-1}$.

5.2.6. {1,4,7,10-Tetrakis-(4'carboxy-1'carboxybutyl)-1,4,7,10-tetraazacyclododecane}Gadolinium (III) – tetraamide (31)

The gadolinium complex **(30)** (10 mg; 11 μmol) was dissolveld in DMSO (0.5 ml) and NHS (8 mg; 67 μmol) was added. The solution was stirred at 50 ^{0}C for three hours. The solution was then cooled and EDC (13 mg; 67 μmol) was added. The solution was stirred overnight at room temperature. The amine **(28)** (50 mg; 44 μmol) was then added and the mixture stirred at room temperature for 24 hours. The mixture was transferred

into a flask containing EtOH (50 ml) and the white solid which formed was recovered, washed with more ethanol and dried under vacuum.

Relaxivity (65 MHz, 293 K, in H_2O pH = 7.20) = 23.4 $mM^{-1}s^{-1}$.

5.3. Chapter Three experimental

5.3.1. α-Monobenzyl-N-{4-[2-amino-4-oxo-3,4-dihydro-pteridin-6-ylmethyl)-amino)-benzoyl}-glutamate (32a) (Method A)

Folic acid dihydrate (3.00 g, 6.29 mmol) **(5)** was slowly dissolved in anhydrous DMSO (150 ml). Caesium carbonate (2.05 g, 6.29 mmol) was added, and after the complete dissolution of the inorganic salt, a solution of benzyl bromide (1.18 g, 6.90 mmol) in DMSO (10 ml) was added drop by drop over thirty minutes. The mixture was stirred at 25 ^{0}C for 48 hours, under argon, in the dark. At the end of this period the mixture was transferred into a flask containing acetonitrile (200 ml) in order to precipitate the products. A yellow solid was obtained; it was separated from the liquid phase by centrifugation and washed with ethyl acetate (3x20 ml). The crude product was purified by column chromatography over silica gel, using isopropanol-chloroform-water-diisopropylamine (60-20-10-10) as eluent. The yellow solid obtained (mixture α-γ 4:1) was washed with dilute hydrochloric acid, and then with ethyl acetate (3x20ml), to yield a yellow solid (1.10 g; 33.0%).

Analytical HPLC: t_r = 21.1 min (α-monoester) and 22.1 min (γ-monoester) (ratio 4:1).
ESMS (-) m/z = 530 (M), 552 $(M+Na)^+$.
^{1}H NMR (d^6DMSO, 300 MHz; δ)*: 1.96 (1H, m, $H_{\beta1}$); 2.01(1H, m, $H_{\beta2}$); 2.28 (2H, t, H_γ), 4.35 (1H, m, H_α); 4.46(2H, d, H_e); 5.09 (2H, s, α-OCH_2); 6. 63 (2H, d, $H_{bb'}$); 6.93 (1H, t, H_d); 7.32 (5H, cm, $CH_2\underline{Ph}$); 7.62 (2H, d, $H_{cc'}$); 8.28 (1H, d, H_a); 9.13 (1H, s, H_f); 10.01 (1H, s, H_h).
*Spectrum of the pure α-benzyl ester obtained by semi-preparative HPLC. See *Figure 5.1* for labels.

5.3.2. γ-Monobenzyl-N-{4-[2-amino-4-oxo-3,4-dihydro-pteridin-6-ylmethyl)-amino)-benzoyl}-glutamate (32b) (Method B)

The reaction was carried out adapting the same conditions used by Albert.[1]

Folic acid **(5)** (1.43 g, 3.00 mmol) and anhydrous sodium sulphate (0.40 g) were suspended in benzyl alcohol (5.6 ml, 54.0 mmol). Then under argon, in the dark, tetrafluoroboric acid diethyl etherate complex 85% (0.6 ml, 4.0 mmol) was added using a syringe and the mixture was stirred at room temperature for 48 hours in the dark. The mixture was diluted with THF (20 ml) and triethylamine (1 ml) was added. The solvent was removed under vacuum, until a yellow slurry was obtained. It was suspended in water (50 ml) and then filtered on a Buchner funnel. The yellow solid was washed with ethyl acetate (3x50 ml), and dried under reduced pressure. The crude product was purified by chromatography column over silica gel, using isopropanol-chloroform-water-diisopropylamine (60-20-10-10) as eluent. A mixture of α-γ esters (ratio 1:2) was obtained.

Analytical HPLC: t_r = 21.1 min (α-monoester) and 22.1 min (γ-monoester) (ratio 1:2).
ESMS (+) m/z = 530 (M), 552 ($M+Na^+$).
^{1}H NMR (d^6DMSO, 300 MHz; δ)*: 1.96 (1H, m, $H_{\beta 1}$); 2.01(1H, m, $H_{\beta 2}$); 2.28 (2H, t, H_γ); 4.04 (1H, m, H_α); 4.46 (2H, d, H_e); 5.04 (2H, s, γ-OCH_2); 6. 63 (2H, d, $H_{bb'}$); 6.93 (1H, t H_d); 7.32 (5H, cm, CH_2Ph); 7.62 (2H, d, $H_{cc'}$); 8.28 (1H, d, H_a); 9.13 (1H, s, H_f); 10.01 (1H, s, H_h).
*Spectrum of the γ-benzyl ester purified by semi preparative HPLC. See *Figure 5.1* for labels.

5.3.3. Dimethyl N-{4-[2-amino-4-oxo-3,4-dihydro-pteridin-6-ylmethyl)-amino)-benzoyl}-glutamate (35c)

Folic acid dihydrate (3.30 g; 6.92 mmol) was suspended in dry methanol (200 ml) and under stirring concentrated hydrochloric acid (0.1 ml) was added. The suspension was refluxed for two hours. In order to precipited the solid, ethyl acetate (300 ml) was added. The resulting yellow compound was treated with more ethyl acetate and dried to yield a yellow powder (3.57 g; 99%).

^{1}H NMR (*d^6DMSO*; 300 MHz; δ)*: 2.02 (2H, m, $H_{\beta\beta'}$); 2.41 (2H, t, H_γ); 3.57 (3H, s, γ-OCH_3); 3.61 (3H, s, α-OCH_3); 4.39 (1H, m, H_α); 4.50 (2H, d, H_e); 6.65 (2H, d, $H_{cc'}$); 7.01 (1H, t, H_d); 7.65 (2H, d, $H_{bb'}$); 8.24 (1H, d, H_a); 8.67 (1H, s, H_f).

ESMS (-) : m/z = 468 $(M-H)^-$.

Analytical HPLC : t_r = 13.2 min.

Elemental analyses $C_{21}H_{23}N_7O_6 \cdot 1/2\ H_2O$: C%: 52.47 (52.72); H%: 5.04 (5.05); N%: 19.30 (20.50).

Mp: > 250 ^{0}C.

*See *Figure 5.1* for labels.

5.3.4. γ-Monomethyl N-{4-[2-amino-4-oxo-3,4-dihydro-pteridin-6-ylmethyl)-amino)-benzoyl}-glutamate (34b)

The dimethyl ester **(33b)** (200 mg; 0.43 mmol) was slowly dissolved in a mixture of phosphate buffer at pH=7.0 and DMSO in ratio 8:2 (v/v; 30 ml). The temperature was maintained at 37 ^{0}C and the enzyme protease (from Rhizopus species Type XVIII Fungal -SIGMA) (400 mg) was added and the suspension was stirred for four days at 37 ^{0}C in the dark. At the end of this period the reaction was stopped, the enzyme and the unreacted diester in suspension were removed by centrifugation. The dark yellow solution was transferred into a flask and acetonitrile (200ml) was added. The solid obtained was recovered, washed with more acetonitrile and dried. Then it was suspended in water (5ml) and the pH was lowered to about 3.0 adding diluted hydrochloric acid. A solid formed which was recovered by centrifugation, washed with acetonitrile and dried to yield a yellow solid (125 mg; 64%).

^{1}H NMR (*d^6DMSO*; 300 MHz; δ)*: 2.02 (2H, m, $H_{\beta\beta'}$); 2.41 (2H, t, H_γ); 3.57 (3H, s, γ-OCH_3); 4.39 (1H, m, H_α); 4.50 (2H, d, H_e); 6.65 (2H, d, $H_{cc'}$); 7.01 (1H, t, H_d); 7.65 (2H, d, $H_{bb'}$); 8.24 (1H, d, H_a); 8.67 (1H, s, H_f).

ESMS (-): m/z = 454 $(M-H)^-$.

Analytical HPLC: t_r = 11.8 min.

$[\alpha]_D^{20} = +14.6$ (c = 0.396 g/100ml in NaOH 0.02M).[2]

Mp: > 250 ^{0}C.

*See *Figure 5.1* for labels.

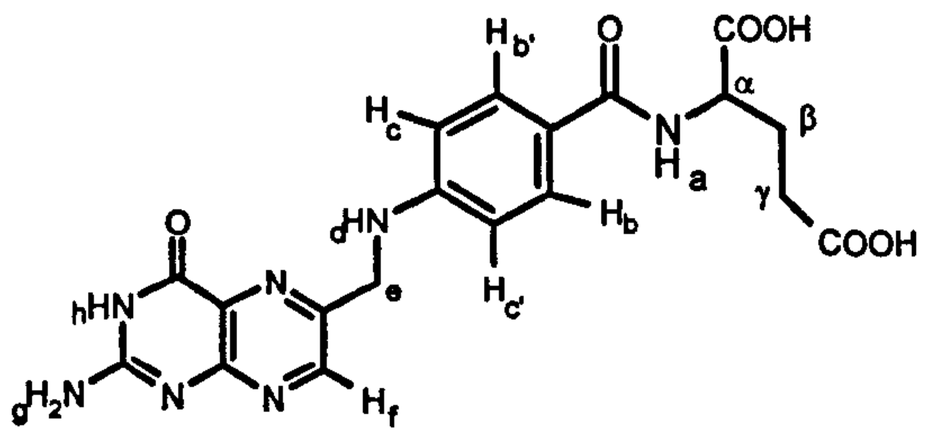

***Figure 5.1** – Labels of the protons of folic acid.*

5.4. Chapter Four experimental

5.4.1. Synthesis of [Ln·9]

5.4.1.1. N-t-butoxycarbonyl-1,4-diaminobutane (40)

Commercially available 1,4-diaminobutane (10.0 g, 113 mmol) was dissolved in dioxane (60 ml) under argon. Then a solution of $(BOC)_2O$ (12.0 g, 55.0 mmol) in dioxane (25 ml) was slowly added over two hours. At the end of the addition the solution was stirred for one hour at room temperature. Then the solution was concentrated to 50 ml, and water (90 ml) was added to precipitate any N,N bis-t-Boc-1,4-diaminobutane. The solid was filtered, and the dioxane was removed under reduced pressure. The aqueous solution was saturated with sodium chloride, extracted with ethyl acetate (5 x 20 ml) and the organic solvent removed under reduced pressure to give an oil. This was taken up into water, acidified to pH=3 with hydrochloric acid, washed with ethyl acetate and the saturated with sodium chloride. The pH was raised to 14 with potassium hydroxide and the aqueous layer extracted with ethyl acetate (5x20 ml). The fractions were combined, dried over potassium carbonate and the solvent removed to yield a pale yellow oil (4.32 g; 20%), which was used directly.

^1H NMR ($CDCl_3$; 300 MHz; δ): 1.19 (2H, t, NH_2); 1.38 (9H, s, $(CH_3)_3$); 1.42 (4H, m, $\underline{(CH_2)_2}CH_2NH_2$); 2.65 (2H, t, $\underline{CH_2}NH_2$); 3.05 (2H, dt, $\underline{CH_2}NH$); 4.35 (1H, br.s, NH).

5.4.1.2. N-(N-t-butoxycarbonyl-1,4-diaminobutyl)-2-chloro acetoamide (38)

Commercially available chloroacetic acid (1.47 g; 15.5 mmol) was dissolved in DCM (70 ml), then HOBt (2.52 g; 18.6 mmol) and EDC (3.57 g; 18.6 mmol) were added and the solution was stirred at room temperature for two hours. After this period a solution of N-t-butoxycarbonyl-1,4-diaminobutane **(40)** (2.93 g; 15.5 mmol) in DCM (20 ml) was added dropwise over thirty minutes, followed by the addition of triethylamine (0.1 ml). The mixture was stirred at room temperature for 18 hours, concentrated to a small volume and water (40 ml) was added. The white solid which formed was filtered off, whereas the emulsion was transferred into a separatory funnel. The organic phase was recovered, washed with water (4x40ml), dried over potassium carbonate, the solvent was evaporated under reduced pressure, to yield a colourless solid (3.28 g; 80%).

^{1}H NMR ($CDCl_3$; 300 MHz; δ): 1.45 (9H, s, $(CH_3)_3$); 1.55 (4H, m, (CH_2CH_2); 3.19 (2H, m, $\underline{(CH_2)}NH^tBoc$); 3.34 (2H, m, $\underline{CH_2}NHCOCH_2Cl$); 4.05 (2H, s, CH_2Cl); 4.60 (1H, br.s, NH^tBoc); 6.62 (1H, br.s, $\underline{NH}COCH_2Cl$).

R_f= 0.76 (SiO_2; DCM:MeOH 9:1).

Elemental analysis $C_{11}H_{21}N_2O_3Cl$: C%: 50.09 (49.90); H%: 8.14 (7.99); N%: 10.54 (10.58).

IR (KBr disc) $\nu_{max}(cm^{-1})$: 3377, 3331 (CONH; NH stretching); 3307, 2980, 2941, 2914 (CH_2 stretching); 1683, 1645 ($COOC(CH_3)_3$ stretching CO); 1544, 1526 (CONH stretching CO); 1366 ($C(CH_3)_3$ stretching); 754 (C-Cl).

Mp : 72-74 ^{0}C.

5.4.1.3. 1,4,7-Tris(tert-butoxycarbonylmethyl)-10-[N-(4-t-butoxycarbonylaminobutyl)carbamoyl]-1,4,7,10-tetraazacyclododecane (37)

The triester **(36)** (1.20 g; 2.33 mmol), caesium carbonate (1.67 g; 5.13 mmol), potassium iodide (0.77 g; 4.66 mmol) and a few 4Å molecular sieves, were suspended in dry acetonitrile (50 ml). Then a solution of **(38)** (1.20 g; 4.66 mmol) in acetonitrile (50 ml) was added by cannula transfer. The mixture was stirred at 80 ^{0}C under argon for 18 hours. After cooling and filtering, the solvent was removed under reduced pressure to yield a colourless solid (2.70 g). The material was purified by chromatography column (SiO_2; THF:DCM:MeOH:NH_3 6:3:0.5:0.5) to yield a colourless solid (1.32 g; 76%).

R_f = 0.45 (SiO_2; THF:DCM:MeOH:NH_3 6:3:0.5:0.5).

ESMS (+) m/z = 765 $(M+Na)^+$.

Elemental analysis: $C_{37}H_{70}N_6O_9 \cdot H_2O$: C%: 58.62 (58.40); H%: 9.20 (9.47); N%: 10.32 (11.00).

^1H NMR ($CDCl_3$; 200 MHz; δ)*: 1.44 (27H, s, ^{t}Bu); 1.53 (4H, m, $H_{d,e}$); 1.64 (9H, s, ^{t}Boc); 2.03-2.96 (cyclen ring); 3.01 (2H, m, H_c); 3.21 (2H, m, H_f); 3.42 (2H, s, H_h).

*See *Figure 5.2* for labels.

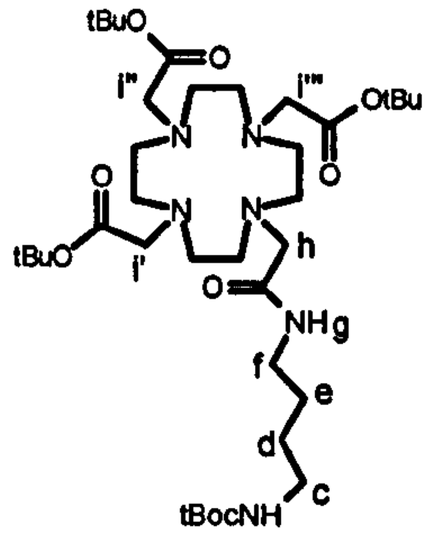

***Figure 5.2** – Labels of the protons of (37).*

5.4.1.4. 1,4,7-Tris(carboxymethyl)-10-[N-aminobutylcarbamoyl]-1,4,7,10-tetraazacyclododecane (9)

The triester **(37)** (1.32 g; 1.78 mmol) was dissolved in DCM (15 ml), then TFA (2.7 ml; 35.6 mmol) was added dropwise using a syringe. The solution was stirred at room temperature for 18 hours. Solvent and the excess TFA were removed under reduced pressure to give a pale yellow oil, which was taken up in DCM (20 ml) and dried. This operation was repeated three times. The oil was taken up in water (20 ml) and washed with DCM (4x20 ml). The aqueous phase was recovered and the water removed under reduced pressure to yield a pale yellow oil (1.50 g; 95%).

R_f = 0.23 (SiO_2; THF:DCM:MeOH:NH_3 6:3:0.5:0.5).

ESMS (+) m/z = 238 $(M+2H)^{2+}$, 475 $(M+H)^+$.

HR-ESMS (+) (m/z): (M+H) calcd for $C_{20}H_{38}N_6O_7$ 475.2880; found 475.2874.

^1H NMR (D_2O; 200 MHz; δ)*: 1.31 (2H, m, H_d); 1.43 (2H, m, H_e); 2.12-3.01 (cyclen ring); 3.02 (2H, m, H_c); 3.30 (2H, m, H_f); 3.54 (2H, s, H_h).

IR (thin film) ν_{max}(cm^{-1}): 3392, 3116 (NH_2 and OH stretching); 1681, 1445, 1204 (CO stretching); 1586 (CONH); 1323; 1136; 1083; 949; 841; 722.

*See *Figure 5.2* for labels.

5.4.1.5. {1,4,7-Tris(carboxymethyl)-10-[N-(4-aminobutyl)carbamoyl]-1,4,7,10-tetraazacyclododecane}-Gadolinium ***[Gd9]***

The amino acid (**9**) (1.67 g; 1.88 mmol) was dissolved in water (30 ml), and gadolinium (III) chloride (0.42 g; 1.13 mmol) was added. The pH was monitored and it was lowered to about 3.0 adding 1M hydrochloric acid solution. The suspension was boiled under reflux for 24 hours. The hot solution was cooled and filtered, then the water was removed under reduced pressure to yield a colourless solid, which was passed through a strong anionic exchange resin, using purite water as eluent (1.20 g; 89%).

R_f = 0.23 (Alumina; DCM:MeOH 8:2).

ESMS (+) m/z = 630 $(M+H)^+$.

Elemental analysis $C_{20}H_{35}N_6O_7Gd \cdot 2H_2O$: C%: 36.07 (36.14); H%: 6.04 (5.94); N%: 14.31 (12.8).

Mp: > 250 ^{0}C.

IR (KBr disc) ν_{max} (cm^{-1}): ~3400; 3115 (broad band; H_2O bound; NH_2 stretching); 2937, 2868 (CH stretching); 1681, 1446, 1203 (C=O stretching), 1586 (CONH), 1323; 1293; 1136; 1083; 949; 841; 800.

5.4.1.6. {1,4,7-Tris(carboxymethyl)-10-[N-(4-aminobutyl)carbamoyl]-1,4,7,10-tetraazacyclododecane}-Europium (III) ***[Eu9]***

The amino acid (**9**) (50 mg; 56 μmol) was dissolved in water (3 ml), and europium (III) chloride hexahydrate (12 mg; 34 μmol) was added. The pH was monitored and it was lowered to about 3.0 adding 1M hydrochloric acid solution. The suspension was boiled under reflux for 24 hours. The hot solution was cooled and filtered, then the water was removed under reduced pressure to yield a colourless solid, which was passed through a strong anionic exchange resin, using purite water as eluent (28 mg; 80%).

R_f = 0.20 (Alumina; DCM:MeOH 8:2).

ESMS (+) m/z = 625 $(M+H)^+$.

Elemental analysis: $C_{20}H_{35}N_6O_7Eu \cdot 2H_2O$: C%: 35.92 (36.3); H%: 5.89 (5.92); N%: 14.31 (12.74).

^{1}H NMR (D_2O; pD = 6.0; 200 MHz; δ), partial assignement: 34.23; 33.21; 32.56; 31.46 (4H, s, H_{ax}); -0.68; -2.02; -2.89; -4.02 (4H, s, $H_{eq'}$); -5.64; -6.20; -6.94; -7.52 (4H, s, H_{eq}); -11.21; -12.52; -15.39; -16.42 (4H, s, $H_{ax'}$).

5.4.2. Synthesis of [Gd·9]-γ-folate conjugate

5.4.2.1. Coupling {1,4,7-Tris(carboxymethyl)-10-[N-(4-aminobutyl)carbamoyl]-1,4,7,10-tetraazacyclododecane}-gadolinium (III) to α-benzyl-N-^{t}Boc glutamate; synthesis of (42)

The gadolinium complex [Gd·**9**] (1.20 g; 1.67 mmol) was dissolved in a mixture of water/dioxane 1:1 (v/v; 100 ml). To the stirred solution α-benzyl-N-^{t}Boc glutamate ester **(35a)** (0.55g; 1.64 mmol) was added. The pH was raised to 6.0 adding a 0.1 M NaOH solution. Then under stirring, EDC (0.52g; 2.71 mmol) and HOBt (24mg; 0.18 mmol) were added. The solution was stirred at room temperature for 20 hours. Solvents were removed under reduced pressure to yield a yellow oil which was purified by chromatography over alumina using DCM/MeOH 8:2 as eluent (1.20 g; 76%).

R_f = 0.30 (Alumina; DCM:MeOH 8:2).

ESMS (+) m/z = 971 $(M+Na)^+$, 497 $(M+2Na)^+$, 475 $(M+2H)^+$.

Analytical HPLC: t_r = 16.5 min.

IR (KBr disc) ν_{max} (cm^{-1}): ~3400 (broad band; H_2O bound); 2870, 2740, (CH_2 straching), 1680 (C=O stretching).

5.4.2.2. Synthesis of (43)

The gadolinium complex **(42)** (0.80 g; 0.84 mmol) was dissolved in a 96% TFA solution in water (10 ml). The solution was stirred for fifteen minutes at room temperature. Solvents were removed under reduced pressure to give an oil, which was taken up in DCM (10 ml) and dried under reduced pressure. This operation was repeated three times with DCM and three times with diethyl ether. The oil was dissolved in water (20 ml) and the solution was washed with diethyl ether (3x20 ml). The aqueous phase was concentered and passed through a strong anionic exchange resin. The fractions were recovered and freeze-dried to yield a colourless solid (0.81 g).

ESMS (+) m/z = 425 $(M+2H)^+$, 447 $(M+2Na)^+$, 849 $(M+H)^+$, 871 $(M+Na)^+$.
Analytical HPLC: t_r = 10.1 min.

*5.4.2.3. Coupling of the complex **(43)** to Pteroic Acid **(44)**. Synthesis of **(45a)**.*

Pteroic acid **(44)** (100 mg; 0.32 mmol) was slowly dissolved in DMSO (50 ml), then EDC (68 mg; 0.35 mmol) and HOBt (4 mg) were added. The mixture was stirred in the dark for three hours at 25 ^{0}C, then a solution of the complex **(43)** (322 mg; 0.38 mmol) in DMSO (5 ml) was added by cannula transfer and 3-4 drops of triethylamine by syringe. The mixture was stirred at 25 ^{0}C for 48 hours; then the yellow solution was transferred into a flask containing acetonitrile (250 ml). The yellow solid obtained was separated from the liquid by centrifugation, washed with acetonitrile (3x20 ml) and dried to yield a yellow solid (250 mg), which was used directly in the next step. Unreacted pteroic acid coprecipitated with the product **(43)** and it was removed in the next step.

ESMS (-) m/z = 311 (Pteroic acid), 570 $(M-2H)^{2-}$, 1141 $(M-H)^-$.
Analytical HPLC: t_r = 8.8 min (Pteroic acid); 13.8 min **(43)**.

*5.4.2.4. Synthesis of **(45b)***

The conjugate complex **(45a)** (250 mg; 0.22 mmol) was dissolved in DMSO (20ml). Then palladium hydroxide over carbon (250 mg) and hydrazine (0.5 ml) were added. The mixture was stirred in the dark at room temperature for 40 hours. The catalyst was filtered over celite; the solvent and the excess hydrazine were removed under reduced pressure to yield a yellow solid. The crude was purified over silica, eluting with iso-propanol: 3.5% ammonia solution (7:3; v/v).

R_f = 0.48 (SiO_2; iso-propanol:NH_3 3.5%).
ESMS (-) m/z = 1050 $(M-H)^-$; 525 $(M-2H)^{2-}$.
Analytical HPLC: t_r = 6.8 min.
Elemental Analysis: $C_{39}H_{52}N_{13}O_{12}Gd \cdot 3H_2O$: C%: 42.12 (42.33), H%: 4.81 (5.24), N%: 16.32 (16.5).
Mp: > 250 ^{0}C.

5.4.3 Synthesis of the [Gd·9]-α-folate conjugate

5.4.3.1. Coupling of folic acid γ-methyl ester to [Gd·9]

The γ methyl ester **(34b)** (150 mg; 0.33 mmol) was dissolved in dry DMSO (4ml), then NHS (57 mg; 0.49 mmol) was added and the mixture was stirred for thirty minutes at 50^0C. After cooling, EDC (94 mg; 0.49 mmol) was added and the solution was stirred for three hours at room temperature. At the end of this period the gadolinium complex [Gd·9] (186 mg; 0.29 mmol) was added together with three drops of triethyamine; the solution was stirred at room temperature for 48 hours. The yellow solution was then transferred into a flask containing ethyl acetate (100 ml), in order to precipitate the crude compound. The solid was recovered by centrifugation, washed with ethyl acetate (3x20ml) and dried to yield a pale yellow solid (480 mg), which was purified by chromatography column over silica, using iso-propanol:ammonia 3.5% (7:3; v/v). The pure compound was obtained as a yellow solid (105 mg; 33%).

R_f = 0.35 (SiO_2; iso-propanol:NH_3 3.5% 8:2).

ESMS (-): m/z = 531 $(M-2H)^{2-}$, 1065 $(M-H)^-$.

Analytical HPLC: t_r = 9.3 min.

Mp: > 250 ^{0}C

5.4.3.2. Hydrolysis of (46a).

The gadolinium complex **(46a)** (100 mg; 94 μmol) was dissolved in a 0.02M NaOH solution (5 ml) and stirred for 24 hours at room temperature. The solution was then neutralized by adding diluted hydrochloric acid and the water solution was removed under reduced pressure to yield a crystalline yellow solid (96 mg; 97%).

ESMS (-): m/z = 524 $(M-H)^{2-}$, 1051 $(M-H)^-$.

Analytical HPLC: 6.2 min

Elemental Analysis: $C_{39}H_{52}N_{13}O_{12}Gd·2H_2O$: C%: 41.89 (42.3), H%: 4.76 (5.24), N%: 15.98 (16.42).

Mp: > 250 ^{0}C.

5.4.4. Synthesis of -[Gd·9]$_2$-α,γ-folate (47)

Folic acid dihydrate **(5)** (20 mg; 0.042 mmol) and NHS (14 mg; 0.13 mmol) were dissolved in dry DMSO (1ml) stirring at 50 ^{0}C for thirty minutes. After cooling of the yellow solution EDC (24 mg; 0.13 mmol) was added and the solution was stirred for three hours at room temperature. At the end of this period the [Gd·**9**] (53 mg; 0.84 mmol) together with one drop of triethylamine were added; the solution was stirred at room temperature for 48 hours. In order to precipitate the crude compound, the yellow solution was then transferred into a flask containing ethyl acetate (100 ml). The solid was recovered by centrifugation, washed with ethyl acetate (3x20ml) and dried, to yield a pale yellow solid (48 mg), which was purified by column chromatography over silica, using iso-propanol:ammonia 3.5% (7:3; v/v). The pure compound was obtained as a yellow solid (22 mg; 32%).

ESMS (-): m/z = 830 $(M-2H)^{2-}$, 1661 $(M-H)^-$.

Analytical HPLC: 12.4 min.

Elemental analysis: $C_{59}H_{85}N_{19}O_{18}Gd_2 \cdot 3H_2O$ C%: 40.95 (41.50); H%: 4.74 (5.33); N%: 14.21 (15.60).

Mp: > 250 ^{0}C.

5.4.5. Synthesis of [Gd·6]

5.4.5.1. N-benzoyl-5-amino pentanoic acid (53)

Commercially available 5-amino pentanoic acid (5.01 g; 42.8 mmol) was dissolved in water (50 ml) and pellets of potassium hydroxide were added to raise the pH to about 10. A solution of benzoyl chloride (7.27 g; 51.7 mmol) in THF (10 ml) was added to the stirred solution. The pH was monitored and some drops of an aqueous solution of potassium hydroxide (1M) were added to keep the pH in the range 8-10. The mixture was stirred for about three hours and the pH was monitored during the whole process. Concentrated hydrochloric acid was added to lower the pH to about 3.0, and the formation of a white precipitate was observed. The white solid obtained was filtered on a Buchner funnel, washed three times with water and dried under vacuum, to yield a colourless solid (8.37 g; 88.%).

R_f = 0.64 (SiO_2; DCM : THF 7:3)

M.p. = 105-106 ^{0}C [3]

^{1}H NMR ($CDCl_3$; 200 MHz; δ): 1.64 (4H, m, CH_2CH_2); 2.34 (2H, t, $\underline{CH_2}COOH$); 3.34 (2H, m, CH_2NH); 6.30 (1H, s, NH); 7.38 (2H, m, H aromatic); 7.68 (2H, d, H aromatic).

5.4.5.2. Methyl 2-bromo-N-benzoyl-5-amino pentanoate (50)

The α bromination was carried out using NBS, following the procedure proposed by Harpp and coworkers.[4]

N-Benzoyl-5-amino pentanoic acid **(53)** (1.32 g; 5.97 mmol) was dissolved in carbon tetrachloride (5 ml). Thionyl chloride (2.84 g; 23.9 mmol) was added slowly. The solution was stirred at 60 ^{0}C for one hour. After this period NBS (1.27 g; 7.16 mmol) and 1-2 drops of hydrobromic acid were added. The mixture was stirred for two hours at 50 ^{0}C. The solvent was removed under vacuum until an orange slurry was obtained. This was dissolved in chloroform and washed with a solution of sodium thiosulphate (50 ml, 2M) in order to reduce the excess bromine. The organic layer was dried over magnesium sulphate and the solvent was removed under vacuum to yield a pale yellow oil. The methyl ester was obtained by treating the oil in dry methanol at room temperature for 24 hours. The solvent was removed under reduced pressure and the solid was purified by column chromatography over silica gel, using ethyl acetate/hexane (1:1) yielding the desired ester as a colourless solid (0.67 g; 36%).

R_f = 0.35 (SiO_2; Ethyl acetate:Hexane 1:1)

M.p. = 60-61 ^{0}C [3]

^{1}H NMR ($CDCl_3$; 200 MHz; δ): 1.74 (2H, m, $\underline{CH_2}CHBr$); 2.04 (2H, m, $\underline{CH2}CH_2NH$); 3.44 (2H, m, $\underline{CH_2}NH$), 3.75 (3H, s, OCH_3), 4.21 (1H, dd, CHBr), 6,43 (1H, s, NH); 7.44 (3H, m, H aromatic); 7.72 (2H, d, H aromatic).

^{13}C NMR ($CDCl_3$; 200 MHz; δ): 26.35 ($\underline{CH_2}CH_2CHBr$); 32.36 ($\underline{CH2}CHBr$); 39.31 ($\underline{CH_2}NH$), 53.22 (OCH_3), 57.04 (CHBr); 127.24-134.64 (C aromatic); 168.18 ($\underline{C}OPh$); 170.41 ($\underline{C}OOCH_3$).

5.4.5.3. 1,4,7-Tris-([3'methoxycarbonyl]-1'methoxycarbonylpropyl]-1,4,7,10-tetraazacyclododecane (49)

1,4,7,10 Tetraazacyclododecane (cyclen) **(22)** (0.80 g; 4.6 mmol) and sodium hydrogen carbonate (1.18 g; 14.0 mmol) were suspended in acetonitrile (5 ml) together with a few 4Å molecular sieves. A solution of dimethyl α-bromoglutarate **(48)** (3.08 g; 12.9 mmol), in acetonitrile (10 ml) was added by cannula transfer under argon and the mixture was stirred at 70 ^{0}C for three days. After this period the mixture was filtered and the solvent was removed under reduced pressure. The residue was taken up in DCM (20 ml) and washed with hydrochloric acid (pH=3). The organic layer was dried over potassium carbonate and the solvent removed. The residue yellow oil was purified by column chromatography, over silica gel. The column was washed with DCM and then with 30% THF in DCM. The product was obtained as a pale yellow oil (0.92 g; 29%) by elution with 5% NH_3, 5% methanol, 30% THF in DCM.

R_f =0.40 (SiO_2; DCM:THF:MeOH:NH_3 6:3:0.5:0.5).

ESMS (+) m/z = 647 $(M+H)^+$.

^{1}H NMR ($CDCl_3$; 200 MHz; δ): 1.72-3.54 (28H, m, cyclen ring and 3xCH_2CH_2); 3.62 (9H, s, 2x$CH_2CO_2\underline{CH_3}$); 3.66 (6H, s, $CHCO_2\underline{CH_3}$); 3.70 (3H, s, $CHCO_2\underline{CH_3}$); 3.89 (2H, dd, $^3J_{H-H}$=6.0 Hz, $^3J_{H-H}$=4.8 Hz, 2xCH); 4.31 (1H, dd overlapping, $^3J_{H-H}$=5.8 Hz, $^3J_{H-H}$=5.8 Hz, CH).

IR (thin film) ν_{max} (cm^{-1}): 3443 (NH); 2953, 2848, 1732, 1745 (C=O stretching), 1453, 1253, 1209, 1169, 919.

5.4.5.4. 1,4,7-Tris-([3'methoxycarbonyl]-1'methoxycarbonylpropyl]-10-([3'methoxycarbonyl]-1'butylamino-N-benzoyl)-1,4,7,10-tetraazacyclododecane (51)

1,4,7-Tris-([3'methoxycarbonyl]-1'methoxycarbonylpropyl]-1,4,7,10-tetraazacyclododecane **(49)** (0.52 g; 0.81 mmol) and caesium carbonate (0.27 g; 0.81 mmol) were added to acetonitrile (10 ml) under argon, in the presence of a few 4 Å molecular sieves. A solution of methyl-2-bromo-N-benzoyl-5-amino pentanoate **(50)** (0.25 g; 0.81 mmol) in acetonitrile (5 ml), was added by cannula transfer and the mixture was stirred under argon at 75 ^{0}C for three days. The residue was cooled, filtered and washed with MeCN (4x20ml). The solvent was removed under reduced pressure,

and the yellow oil was purified by column chromatography over silica gel. The column was washed with DCM 40%, THF 60% and the product was obtained by elution with 5% NH_3, 5% MeOH, 30% DCM in THF. A pale yellow oil was obtained (0.60 g; 84%).

R_f =0.54 (SiO_2; DCM:THF:MeOH:NH_3 6:3:0.5:0.5).

ESMS (+) = 880 $(M+H)^+$, 902.2$(M+Na)^+$.

HR-ESMS (+) (m/z): (M+H) calcd for $C_{42}H_{65}N_5O_{15}$ 880.4555; found 880.4554.

^{1}H NMR ($CDCl_3$; 200 MHz; δ): 1.75-2.85 (32H, m, cyclen ring, $\underline{CH_2CH_2}CHCOOCH_3$); 3.44 (2H, m, $\underline{CH_2}NH$), 3.60 (9H, s, $CH_2CO_2\underline{CH_3}$); 3.62 (9H, s, $CHCO_2\underline{CH_3}$); 3.75 (3H, s, $CHCO_2\ \underline{CH_3}$); 3.85 (2H, dd, 2xCH); 4.30 (1H, dd, CH); 4.35 (1H, dd, CH); 6.40 (1H, s, NH); 7.45 ppm (3H, m, H aromatic); 7.80 ppm (2H, d, H aromatic).

IR (KBr disc) ν_{max} (cm^{-1}): 2952, 2846 (CH_2 stretching); 1681, 1437, 1203 (C=O stretching), 1731 (CONH), 1461; 1537; 1257; 1120; 985.

5.4.5.5. 1,4,7-Tris-([3'carboxy]-1'carboxypropyl]-10-([3'carboxy]-1'propylamino)-1,4,7,10-tetraazacyclododecane (6)

1,4,7-Tris-([3'methoxycarboxy]-1'methoxycarbonylpropyl]-10-([3'methoxycarbonyl]-1'propylamino-N-benzoyl)-1,4,7,10-tetraazacyclododecane **(51)** (0.60 g; 0.68 mmol) was suspended in lithium hydroxide solution (20ml; 1M) and stirred at 100 ^{0}C for 24 hours. The mixture was cooled, filtered and the water removed under reduced pressure. The solid was dissolved in water (5 ml) and passed through a Dowex 50W cationic exchange resin in strong acid form, eluting with 12 % ammonia solution, to yield a colourless solid (0.47 g; 98%).

The solid (0.47 g; 0.66 mmol) was dissolved in hydrochloric acid (15 ml; 6M) and stirred at 100 ^{0}C for 24 hours. The solution was then cooled and washed with ethyl acetate (4x30 ml). The aqueous phase was recovered and the pH adjusted to 7.0 by adding sodium hydroxide pellets. Then it was concentrated to about 5 ml and passed throught Dowex 50W cationic exchange resin in a strong acid form, eluting with 12% ammonia solution, to yield a colourless solid (0.37 g; 95%).

^{1}H NMR (D_2O; 200 MHz; δ): 1.70-2.80 (32H, m, cyclen ring, $\underline{CH_2CH_2}CHCOOH$); 3.85 (2H, dd, 2xCH); 4.30 (1H, dd, CH); 4.35 (1H, dd, CH).

5.4.5.6. {1,4,7-Tris-([3'carboxy]-1'carboxypropyl]-10-([3'carboxy]-1'propylamino)-1,4,7,10-tetraazacyclododecane}-gadolinium ***[Gd·6]***

The ligand **(6)** (0.34 g; 0.50 mmol) was dissolved in water (5ml), then a solution of gadolinium (III) chloride hexahydrate (0.19 g; 0.50 mmol) was added. The pH was adjusted to 5.5 and the mixture was stirred at 100 ^{0}C for 24 hours. The suspension was filtered and the pH was incresed to 10.0 in order to remove the free gadolinium in the form of its insoluble hydroxide. The solid was filtered off throught a membrane filter. The solution was neutralized and freeze-dried. The solid was recrystallized from slightly acidic aqueous solution (pH 5.0) and was isolated as a mixture of diastereoisomers (0.31 g; 76%).

ESMS (-) m/z = 414 $(M-2H)^{2-}$, 831 $(M-H)^-$, 852 $(M-Cl)^-$

IR (KBr disc) ν_{max} (cm^{-1}): ~3400 (OH and NH_2 stretching), 2952, 2846 (CH_2 stretching); 1605, 1383, (C=O stretching), 1087; 987.

5.4.5.7. {1,4,7-Tris-([3'carboxy]-1'carboxypropyl]-10-([3'carboxy]-1'propylamino)-1,4,7,10-tetraazacyclododecane}-europium (III) ***[Eu6]***

The ligand **(6)** (46 mg; 68 μmol) was dissolved in water (1ml), then a solution of europium (III) chloride hexahydrate (25 mg; 68 μmol) was added. The pH was adjusted to 5.5 and the mixture was stirred at 100 ^{0}C for 24 hours. The suspension was filtered and the pH was increased to 10.0, in order to remove the free europium in the form of its insoluble hydroxide. The solid was filtered off throught a membrane filter. The solution was neutralized and freeze-dried. The solid was recrystallized from slightly acidic aqueous solution (pH 5.0) and was isolated as a mixture of diastereoisomers (30 mg; 54%).

ESMS (-) m/z = 412 $(M-2H)^{2-}$, 825 $(M-H)^-$, 860 $(M-Cl)^-$.

IR (KBr disc) ν_{max} (cm^{-1}): ~3400 (OH and NH_2 stretching), 2952, 2846 (CH_2 stretching); 1605, 1383, (C=O stretching), 1087; 987.

^{1}H NMR (D_2O; pD = 6.0; 200 MHz; δ) partial assignment: 39.5-41.2 (s, H_{ax} isomer (M)); 20.0-28.1 (s, H_{ax} isomer (m)); 8.1, 6.4, -6.0; -7.9, -9.2; -11.3, -15.1; -17.7; -26.9; -27.3; -28.6.

5.4.5.8. {1,4,7-Tris-([3'methoxycarboxy]-1'carboxypropyl]-10-([3'methoxycarboxy]-1'propylamino)-1,4,7,10-tetraazacyclododecane}-gadolinium (III) ***(54)***

The gadolinium complex [Gd·**6**]$^-$ (80 mg; 96 μmol) was suspended in dry methanol (5 ml), then two drops of hydrochloric acid were added. The suspension was stirred at 70 ^{0}C for one hour. The solution was cooled and the solvent removed under reduced pressure to yield a colourless solid (81 mg; 96%).

ESMS (-) m/z = 872 $(M-H)^-$.

Elemental analysis $C_{31}H_{49}N_5O_{14}Gd$: C%: 41.63 (42.66); H% 5.11 (5.62); N% 7.67 (8.03).

5.4.6. Synthesis of the [Gd·6]$^-$-γ-folate conjugate

5.4.6.1. Coupling of the α-benzyl ester of folic acid to [Gd·6]$^-$

The α-benzyl ester of folic acid (mix α-γ ratio 4:1) (21 mg; 40 μmol) was dissolved in dry DMSO (1.5 ml). The temperature was raised to 50 ^{0}C and NHS (7 mg; 59 μmol) was added. The solution was stirred for 3 hours, then it was cooled to 0 ^{0}C and EDC (11 mg; 59 μmol) was added. The mixture was stirred overnight at room temperature, and the tri-methyl ester **(54)** (52 mg; 59 μmol) was added with two drops of triethylamine. The mixture was stirred for another 24 hours at room temperature and then the yellow solution was transferred into a flask containing acetonitrile (50 ml). The solid obtained was recovered, washed with more solvent and dried. The crude material was purified by column chromatography over silica gel, eluting with iso-propanol-ammonia 3.5%, 8:2 (v/v), to yield a yellow solid (24 mg; 44%).

R_f = 0.56 (SiO_2; isopropanol:NH_3 3.5% 8:2).

ESMS (-) m/z = 691 $(M-2H)^{2-}$, 1385 $(M-H)^-$.

Analytical HPLC: 6.3 min.

5.4.6.2. Hydrolysis of (56a)

The tri-methylester **(56a)** (24 mg; 17 μmol) was dissolved in sodium hydroxide solution (10 ml; 0.02 M). The pH was adjusted to 9.0 and the solution was stirred at room temperature for 24 hours. The solution was neutralized and washed with DCM (3x10 ml). The aqueous phase was recovered and freeze-dried to yield a yellow solid (19 mg; 90%).

R_f = 0.15 (SiO_2; isopropanol:NH_3 3.5% 8:2).

ESMS (-) m/z = 626 $(M-2H)^{2-}$, 1253 $(M-H)^-$.

Analytical HPLC: t_r = 3.14 min.

Elemental analysis: $C_{47}H_{60}N_{12}O_{19}Gd \cdot 2H_2O$ C%: 42.12 (43.74); H%: 4.84 (5.00); N%: 12.86 (13.03).

Mp: > 250 ^{0}C

5.5 References

[1] Albert, R.; Danklmaier, J.; Honig, H.; Kandolf, H. *Synthesis* 1987, *7*, 635.

[2] Weingand, F.; Wacker, A. *Chem. Ber.* 1949, *82*, 25.

[3] Schniepp, M.; Marvel, J. *J. Am. Chem. Soc.* 1935, *57*, 1557.

[4] Harpp, D. N.; Bao, L. Q.; Black, C. J.; Gleason, J. G.; Smith, R. A. *J. Org. Chem.* 1975, *40*, 3420.

Conferences attended

StereoChemistry at Sheffield

University of Sheffield 8th December 1998

Macrocycles 2000

University of St Andrews 2nd-7th July 2000

10th International Conference on Bioinorganic Chemistry

Convention Center Florence 26th 31st Agust 2001